CO-COMBUSTION OF BIOMASS FUELS WITH COAL IN A FLUIDISED BED COMBUSTOR

A thesis submitted by

Wan Azlina Wan Ab Karim Ghani

To The University of Sheffield
For the degree of Doctor of Philosophy

Department of Chemical and Process Engineering
The University of Sheffield
Sheffield, United Kingdom

May 2005

SUMMARY

Co-combustion of biomass with coal has been investigated in a 0.15 m diameter and 2.3 m high fluidised bed combustor under various fluidisation and operating conditions. Biomass materials investigated were chicken waste, rice husk, palm kernel shells and fibres, refuse derived fuel and wood wastes. These were selected because they are produced in large quantities particularly in the Far East.

The carbon combustion efficiency was profoundly influenced by the operating and fluidising parameters in the decreased following order: fuel properties (particle size and density), coal mass fraction, fluidising velocity, excess air and bed temperature. The smaller particle size and lower particle density of the fuels (i.e. coal/chicken waste, coal/rice husk and coal/wood powder), the higher carbon combustion efficiency obtained in the range of 86-90%, 83-88%, 87-92%, respectively. The carbon combustion efficiency increases in the range of 3% to 20% as the coal fraction increased from 0% to 70%, under various fluidisation and operating conditions. Also, the carbon combustion efficiency increases with increasing excess air from 30-50% in the range of 5 – 12 % at 50% coal mass fraction in the biomass mixture. However, further increased of excess air to 70% will reduced the carbon combustion efficiency. Relatively, increasing fluidising velocity contributed to a greater particle elutriation rate than the carbon to CO conversion rate and hence increased the unburned carbon. Furthermore, the bed temperature had insignificant influence of carbon combustion efficiency among the biomass fuels. Depending upon excess air ranges, fluctuations of CO emissions between 200 - 1500 ppm were observed when coal added to almost all biomass mixtures.

In ash analyses, the percentages of unburned carbon were found to have increased in the range 3 to 30% of the ash content with the increases of coal fraction in the coal/ biomass mixture. Furthermore, no fouling, ash deposition and bed agglomeration was observed during the combustion runs for all tests due to lower operating bed temperature applied. Lastly, a simple model was developed to predict the amount of combustion in the freeboard.

This study demonstrated the capability of co-firing biomass with coal and also demonstrated the capability to be burnt efficiently in existing coal-fired boilers with minimum modification.

This thesis was dedicated to my husband

Azil Bahari and our precious jewel, Faris Erhan

who are the most valuable treasures of my life.

ACKNOWLEDGEMENT

The present research work would not have been achieved without the trust and financial support from the University Putra Malaysia on behalf of Malaysia Ministry of Science, Technology and Environment (MOSTE). For these reasons, I profoundly thank them for supporting me during my studies.

I also wish to express my gratitude to my supervisor, Dr. K.R. Cliffe for his encouragement, supervision and valuable suggestions throughout this investigation. Thanks to all technical staffs of the Chemical and Processing Engineering Department, The University of Sheffield, especially Mr. C. Wright, Mr. A.L. Lumby and Mr. R.V. Stacey for their assistant in the experimental work. Also not forgotten to all the members of Combustion and Incineration Group (CIG), University of Sheffield, U.K for their help and support throughout the research. Lastly, thank to associate professor Dr. Khudzir Ismail from University of Technology MARA for providing the materials for my research work.

Finally, I also wish to acknowledge family whom I admire the most for their continuous supports which was vital throughout the completion of the thesis.

CONTENTS

LIST OF TABLES

LIST OF FIGURES

NOMENCLATURE

EU	*European Union*
DOE	*Department of Environmental*
EIA	*Energy Information Administration*
EPRI	*Energy and Power Research Institute*
ASEAN	*Association of South East Asian Nations*
De NOx	*Devolatilisation of Nitrogen oxides*
DTG	*Derivative of thermogram (rate of weight loss), % / min*
TDH	*Transport disengaging height, m*
FBC	*Fluidised Bed Combustor*
BFBC	*Bubbling Fluidised Bed Combustor*
AFBC	*Atmospheric Fluidised Bed Combustor*
CFBC	*Cycle Fluidised Bed Combustor*
CHP	*Combined Heat and Power Plant*
PC	*Pulverised Coal*
RH	*Rice husk*
MSW	*Municipal solid waste*
RDF	*Refuse derived fuel*
REF	*Recovered fuel*
PEF	*Processed engineered fuel*
PDF	*Packaging derived fuel*
TGA	*Thermogravimetric Analysis*

u_t	*Velocity of fall, m/s*
g	*Acceleration of gravity, m/s^2*
d	*Diameter of particle , m*
F_g	*Gas (propane) flow rate, kg/h*
F_c	*Coal feedrate, kg/h*
F_w	*Wood feederate, kg/h*
F_{a1}	*Main air feedrate, kg/h*
F_{a2}	*Secondary air feedrate, kg/h*
F_{aNET}	*Total air feedrate, kg/h*
HHV_g	*Calorific value of propane, MJ/kg*
HHV_c	*Calorific value of coal, MJ/kg*
HHV_w	*Calorific value of wood, MJ/kg*
C_{pg}	*Heat capacity of propane, KJ/kg K*
C_{pc}	*Heat capacity of coal, KJ/kg K*
C_{pw}	*Heat capacity of wood, KJ/kg K*
Cpair	*Heat capacity of air, KJ/kg K*
$T_i(z)$	*Initial temperature at z_{th} position, °C*
T_o	*Ambient temperature, °C*
T(z)	*Temperature at z_{th} position, °C*
T(w)	*Wall temperature, °C*
dz	*Difference in height, m*
R_o	*Outer radius of insulation, m*
R_i	*Inside radius of insulation, m*

k_{Kw}	*Thermal conductivity, W/m^2K*
h_o	*Convective heat transfer, W/m^2K*
Q_B	*Percentage of heat transferred to Bed, %*
Q_{FB}	*Percentages of heat transferred to Freeboard, %*
Ar	*Arhenius number*
Re_p	*Reynolds number of particles*

Greek symbols

ρ_p	*particles density, kg/m3*
ρ_g	*air density, kg/m^3*
μ	*viscosity of air, kg/m.s*

CHAPTER 1

INTRODUCTION

1.1 Background

Production of energy and reduction of waste are major concerns for government, industry and power companies in the world. Co-combustion of biomass in pulverized coal-fired power plants is a cost-effective strategy to combine energy production and waste reduction in an environmentally sound way. This is the result of the combination of several factors:

- ✓ disposal of wastes with a certain heating value is likely to be forbidden now or in the near future;
- ✓ governments and communities require a reduction of carbon dioxide emissions and translate that wish into financial mechanisms like tax credits, special tariffs etc.;
- ✓ Modern coal-fired power stations have a great potential in accepting solid fuels with diverging qualities and converting these in a very clean manner.

Electricity plays a key role in these plans as it combines high efficiency of power production with low environmental impact regarding transport and end-use of energy. By decreasing the use of fossil fuels in favour of energy sources of a sustainable nature an additional contribution can be made. From the biomass perspective, co-firing with coal offers the opportunity to use larger scale plants with higher efficiency. Using coal as part of a fuel mix allows operators to be able to compensate for variations in the fuel mix and stabilise combustion as a consequence of fuel variation. From a coal perspective, the use of biomass or wastes offers the potential to use cheaper fuels. This is especially the case in some Scandinavian countries where coal is heavily taxed. There are also potential global and local environmental benefits if coal is replaced with biomass fuels which do not release fossil-derived carbon dioxide (CO_2) and lower other pollutants emissions such as nitrogen oxides (NO_X) and sulphur dioxide (SO_2) due to lower temperature combustion [1].

Currently, biomass energy ranks fourth in the world as an energy resource, providing approximately 13% of the world's energy needs (see Figure 1.1). Biomass is the most important source of energy in developing nations, providing 35% of their energy demand and 11% of the world's total primary energy supply in 2000 [2]. In developed countries, biomass energy use is also substantial. In the USA, for example, biomass contributes to about 4% of their primary energy whereas in the European Union such as Sweden and Finland, biomass contributes between 16 and 18% to the annual energy consumption [3]. Biomass resources such as wood and agricultural residues are abundant in most countries especially developing countries (i.e. Asia) and have strong potential as fuels for green power generation. In practice, about half of the agricultural residues are utilised for energy generation which contributes 20% of the primary energy demand industries. The role of biomass is presently limited in power development, but opportunities exist for increasing its share. It is estimated that by 2050 biomass could provide nearly 38% of the world's direct fuel use and 17% of the world's electricity [3].

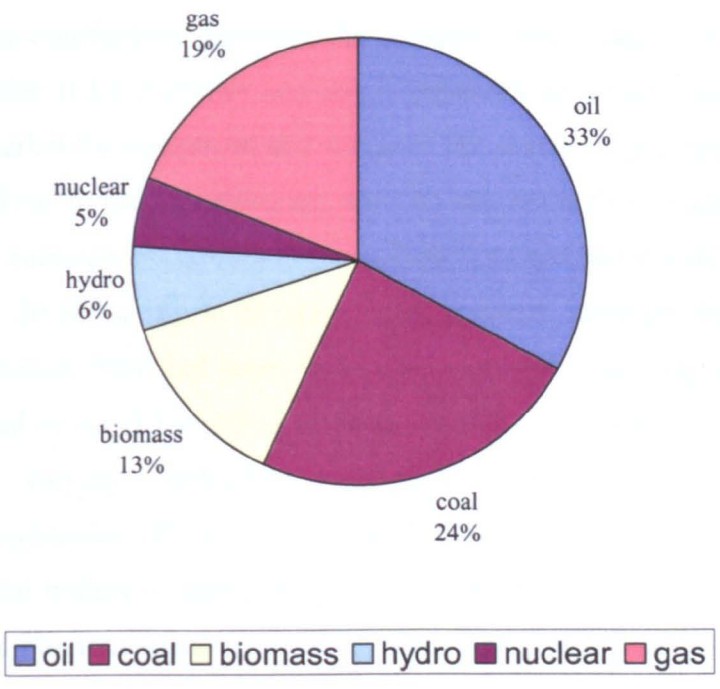

Figure 1.1 World energy consumption 1997 [3]

Co-combustion of biomass and coal has been demonstrated in several fuel plants in Europe and the United States. The main reasons for the growing international interest in utilising renewable fuel are in line with the statements in the European Union (EU) Commission in its Renewable Energy White Paper [4]. This paper has set a target to double the use of renewable energy (80% from biomass fuel) from 6% to 12% of the EU's consumption by the year 2010. Table 1.1 summarises selected previous, existing and planned biomass co-combustion in USA [5]. Also, The Department of Environment (DOE) reference case estimate of biomass use for power generation given by the Energy Information Administration (EIA) is 1.5% of coal-based electricity by the year 2020 [6]. The Energy and Power Research Institute (EPRI) has estimated that 2.29% of coal generation could be displaced at a net cost of $22.62 per metric ton of carbon above the cost of coal, using biomass priced under $0.96/MM Btu [7]. The eventual potential biomass co-combustion where the fuel is available may be considerably larger, since the thermal input from biomass co-combustion is also benefited by the value of tradable emissions credits under US caps on SO_2 and NO_x emissions.

Significant co-combustion potential for biomass and waste materials exists in all European Union (EU) countries and this is mirrored on a worldwide basis, creating a significant market for equipment and services. For instance, in Finland, large quantities of biomass from forest industries are used as the main fuel in grate-firing, bubbling fluidised bed combustors (BFBC) or circulating fluidised bed (CFBC) boilers within the range of 5 to 20 MW_{th} [8]. In Sweden, forest residues, sawdust, demolition wood and other waste wood, fibre and paper sludge is commonly used together with a smaller portion of coal or oil (15 to 30%) in district heating or Combined Heat Power (CHP) plants using varying combustion technologies (grate firing, BFBC, CFBC and pulverised combustion (PC)) [9]. Furthermore, in Austria, co-combustion is used by small industrial boilers located mainly in the pulp and paper industry which generally use their own biomass wastes (e.g., black liquor, bark) [10]. In the Netherlands waste wood is the main supplementary biomass feedstock used in coal-fired PC power plants. In Germany, sewage sludge is the most important co-fired biomass in lignite or coal-fired pc power plants [11].

Table 1.1: Previous, existing or planned biomass co-combustion application [5]

Utility, Plant, Name, Location	Co-fired fuels	Total(Net) Plant Size	Boiler Technology
I/S Midkraft Energy Co. Studrupvaeket, Denmark(Overgrad, 1999)	Coal/straw	150MW_e	Pulverised Coal
Tacoma Public Utilities-Light division steam Plant No. 2 Tacoma, Washington	Coal/RDF/wood residues	2 x 25 MW_e	Bubbling Fluidised Bed
GPU Genco Shawville Station Johnston, Pennsylvania	Coal/wood residues	130 MW_e and 190MW_e	Pulverized Coal
IES Utilities Inc. Sixth Steet (1) and Ottumwa (2) station Marshal, Iowa	1) Coal/agricultural residues 2) Coal/switchgrass	1) 3 units, 6-15 MW_e 2) 714 MW_e	1) Pulverized coal 2) Pulverized coal
Madison Gas & Electric Blount Street station Madison, Wisconsin	Coal/switchgrass	50 MW_e	Pulverized coal
Niagara Mohawk Power Corp., Dunkirk Station, Dunkirk, New York	Coal/wood residues and coal/energy crops (willow)	91 MW_e	Pulverized coal
EPON Central Gelderland Netherlands	Coal/wood residues (demolition)	602 MW_e	Pulverized coal
New York State Electric & Gas, Hickling (1) and Jennison (2) Stations Big Flats and Bainbridge, New York	Coal/ wood residues and coal/tires	1) 37.5 MW_e 2) 37.5 MW_e	1) Stoker 2) Stoker
Northern States Power Bay Front Station Ashland, Wisconsin	Coal/wood residues (forest)	2 x 17 MW_e	Stoker

Note: *the capacity supported by the supplementary fuel will be a fraction of the total capacity shown in this stable, normally in the range of 1 to 10% of the total capacity.

In ASEAN, the potential of biomass for power generation is promising: about 50,000 MW for all biomass resources in Indonesia; approximately 3,000 MW in Thailand; about 1,117 MW in the palm oil industry of Malaysia; about 60-90 MW from bagasse and 352 MW from rice hulls in the Philippines; and 250 MW from bagasse in Vietnam. About 920 MW in installed capacity could be expected from over 19 million tons of residues in the ASEAN wood industry. Much of this potential could be developed through cogeneration [12].

Among these technologies, fluidised bed combustion (FBC) technology has already prove highly efficient, economic and environmentally sound combustion method for a wide variety of fuels in comparison conventional combustors. Hence, with the current demands in electricity and with the recent developments in biomass energy, co-combustion of biomass with coal must be recognised as one of the most important sources of energy for the foreseeable future.

1.2 State of Problem

Although there are many potential benefits associated with co-combustion, there are several combustion related concerns associated with the co-combustion of coal and biomass. Utilisation of solid biomass fuels and wastes sets new demands for boiler process control and boiler design, as well as for combustion technologies, fuel blend control and fuel handling systems. For example, the different mineral matter composition (high alkali levels) and mode of occurrence (mostly mobile forms) in biomass results in concerns over enhanced fouling and slagging of pulverized coal boilers, particularly when firing agricultural residues or herbaceous materials. The economics of co-combustion in pulverized coal boilers are closely tied to the biomass preparation costs (i.e. drying and milling), so an improved understanding of the effect of biomass particle size and moisture content on combustor performance is needed (i.e. in the areas of flame stability, flame shape, and carbon burnout).

Thus, this research was carried out with the objective to characterise biomass properties that affect the co-combustion of biomass with coal, in particular biomass that is available in large quantities in Malaysia.

1.3 Scopes and Objectives of the Research

This research focuses on using biomass samples (rice husk, palm kernel and fibre, animal waste, refused derived fuel and wood waste) in a 10 kW_{th} Fluidised Bed Combustor. The biomass samples for this research were from Malaysia and the United Kingdom. The biomass fuels (rice husks, palm kernels and fibres) are widely abundant as wastes in rice milling and oil palm processing plants in Malaysia and their low bulk density contributes to a landfill problem. Refuse derived fuel (RDF), animal and wood wastes also creates environmental problems such as de-biodegradable and odour problems. Some of this fuel especially wood and RDF also contributes to hazardous material such as heavy metals and dioxins and furans.

This study concentrates on co-firing of the biomass fuels stated above with coal in a FBC in terms of efficiency and emissions to assess the potential advantages offered by a fluidised bed combustor over conventional methods of burning. The influence of various combustor operation parameters and fuel properties on combustion efficiency and CO emissions is determined.

The main objectives of this research are:

1. To investigate the combustion of major biomass materials in a FBC and to compare the combustion efficiency with co-combustion with coal.

2. To identify the major properties of biomass fuel which control the combustion efficiency and CO emissions (i.e. particle size, density and volatility as measured by Thermogravimetric Analyser (TGA)).

3. To develop a simple mathematical model which will give the amounts of material burning in the bed and the freeboard using the temperature profiles as data.

CHAPTER 2

LITERATURE REVIEW

This chapter presents a review of the co-combustion studies of biomass fuels with coal in a fluidised bed technology. The focus is on the fuels, properties and combustion characteristics of biomass in Bubbling Fluidised Bed combustors and Circulating Fluidised Bed Combustors that may contribute some technical problems due to their large variations in fuel properties. Section 2.1 presents an overview of available biomass fuels including their sources, properties and handling properties and technology options for co-combustion that to be implemented. Fluidised bed combustion systems, their advantages and disadvantages and the impact of alternate fuels on their design are briefly discussed in section 2.2. In view of the fundamental combustion studies associated with the mechanisms of biomass combustion in fluidised bed combustors, combustion of many alternative fuels issues and fluidised bed combustor modelling are briefly reviewed in section 2.3.

2.1 Biomass As a Potential Renewable Fuels

Biomass offers important advantages as a combustion feedstock due to the high volatility of the fuel and the high reactivity of both fuel and the resulting char [13]. However, it should be noticed that in comparison with coals, biomass contains much less carbon and more oxygen and consequently has a lower heating value. Furthermore, biomass fuels are considered environmentally friendly due to there being no net increases in CO_2 from biomass burning. Most biomass fuels have very little or no sulphur. Therefore co-firing of coal and biomass can also reduce net SO_2 emissions. This is particularly desirable when co-firing with high sulphur coals. Typically, woody biomass contains very little nitrogen on a mass basis as compared to coal. In addition, most of the fuel nitrogen in biomass is converted to NH radicals (mainly ammonia, NH_3) during combustion. The ammonia reduces NO to molecular nitrogen (essentially providing an in situ thermal $DeNO_x$ source). Hence, it was expected that during co-combustion of biomass with coal could also result in lower NO_x and SO_2 emission levels [13, 14, 15].

In practice, combustion of these fuels has been proven difficult to achieve. The limitations were primarily due to relying on biomass as the sole source of fuel and it is known that biomass fuels have low calorific value and highly variable physical properties. The high moisture (i.e. olive oil waste) and ash contents (i.e. rice husk) in biomass fuels can cause ignition and combustion problems. The melting point of the dissolved ash can also be low (i.e. straw) which causes fouling and slagging problems due to the lower heating values of biomass accompanied by flame stability problems. Also, high chlorine contents compared to most coals which are found in certain biomass types, such as straw, may result in corrosion. Thus, it is anticipated that blending biomass with higher quality coal will reduce the flame stability problems, as well as minimising the corrosion and fouling effects of biomass. [13].

2.1.1 Biomass Sources

For the context of this discussion, biomass is used to describe waste products and agricultural wastes. Waste products include wood waste material (i.e. sawdust, wood chips, etc), livestock waste (i.e. sewage sludge, manure, etc.), refuse derived fuels and crop residues (i.e. rice husks, oil palm kernel and fibre, etc.)[13].

(a) Wood Derived Fuel

Wood fuel resources available for co-combustion are diverse: sawdust, demolition wood, recycled wood, bark, logging residue chips, or even more refined biomass fuels, such as pellets. Wood fuel derived energy is particularly important in the developing countries. As can be seen in table 2.1, Asia, Africa and Latin America account for over 75% of global consumption of wood energy [16].

Table 2.1: Wood energy production 2001 in million cubic metres [16]

Region	Production	Region	Production
Africa	534	Latin America	270
Asia	753	Middle east	42
Australia	13	North America	74
East Europe	69	West Europe	30

Relatively, wood powder is one of the wood wastes that are mainly used for power generation. This fuel is produced from raw materials such as sawdust, shavings and bark. In order to produce a fuel with the best combustion and handling properties, the raw material is crushed, dried and fine milled. In Sweden, processed wood powder fuel is mainly used in large district heating plants (10–75 MW) that earlier used coal powder [17, 18]. However, unlike coal, wood is a fibrous solid that cannot easily be reduced in size. Fuel preparation systems specifically designed for wood waste and burners optimised for this fuel are needed. Co-firing of wood and coal has been demonstrated in several pulverised fuel plants in Europe and the United States. The results have been promising and boiler efficiencies have not suffered considerably. However, the maximum share of wood in the fuel blend has been small, only about 5-10% [19].

(b) Livestock Wastes

Farm livestock manure is a major source of biogas, produced through small scale anaerobic digesters and used for heating and cooking in Asia, particularly in rural China and India. Large centralised anaerobic digestion systems using livestock manure, food and domestic waste are installed in West Europe, Australia and the USA [16]. However, anaerobic digestions contributed to environmental problems such as water and soil pollution due to methane release from the stock [19].

One of the problems associated with using poultry waste as a combustible fuel lies with difficulties involved in their preparation which includes separation, size reduction, handling and feeding to the combustor. The highly irregular shapes of particles and high moisture content which is usually associated with these fuels lead to difficulties in system selection that could adequately handle them to be supplied to any type of combustor [20]. Waste from the poultry industry includes a mixture of excreta (manure), bedding material or litter (i.e. wood shavings or straw), waste feed, dead birds, broken eggs and feathers removed from poultry houses. Its nature is heterogeneous and both content and composition can vary widely.

In addition, the presence of Potassium (K) in the resultant ash is very much a function of what type bedding material is used. Usually K being very high if straw is used, reaching to 4–6%. On the other hand, the use of wood shavings reduces the level of K considerably, being below at 1.5%. For these reasons, poultry litter is quite different from other biomass fuels or coal. Also the moisture content can reach well over 30% that could present problems in both feeding and in maintaining sustainable combustion [20].

(c) Refuse Derived Fuels (RDF)

Refuse derived fuels cover a wide range of waste materials which have been processed to fulfilled guideline, regulatory or industry specifications mainly to achieve a high calorific value. Waste derived fuels include residues from MSW recycling, industrial/trade waste, sewage sludge, industrial hazardous waste, biomass waste, etc. The term Refuse Derived Fuel usually refers to the segregated high calorific fraction of processed MSW. Other terms are used for MSW derived fuels such as Recovered Fuel (REF), Packaging Derived Fuel (PDF), Paper and Plastic Fraction (PPF) and Processed Engineered Fuel (PEF) [21].

It is argued that RDF co-incineration in industrial processes has several advantages such as saving non-renewable resources by substituting fossil fuels in high-demand energy processes. However there are concerns over the discrepancies between the controls applied on dedicated incineration and co-incineration plants and the argument that it encourages their removal from the material recovery/re-use cycle, thereby going against the waste hierarchy which rates waste prevention or minimisation and recycling as being preferable to energy recovery and disposal. On the other hand, some argue that using RDF in industrial processes compared with bulk incineration has a flexibility advantage as to optimise economic performances; incinerators must be fed with a constant throughput of waste which could in certain cases hinder the development of prevention or recycling initiatives. Also, there is a lack of environmental assessment information about these practices and the economics driving the production and utilisation of RDF are also unclear [22].

Power generation from refuse derived fuel is one of the promising technologies for the utilization of municipal solid waste. Large scale plants utilising up to 300,000 tonnes of MSW are primarily to be found in Europe. These plants generate power for district heating and/ or power into the grid. Generating capacity can be up to 2 MW per plant. In Japan, about $51x10^6$ tons of municipal wastes are generated annually and, among them, about 77% are incinerated to reduce their volume [23]. Recently dioxin emission has been identified as a social problem and the emission limit of less than 0.1 ng/m^3 was set for newly built incinerators. Therefore small scale incineration plants less than 100 tons/day could not be built as they could not meet these emission limits.

(d) Crop Residues

Crop or agricultural residues are the most widely used: cereal straw, rice husks, sugar cane bagasse & palm oil residues which are abundant in many regions and cause a land-fill problem due to their low bulk density. The amount of residues produced from bagasse, rice hulls, palm oil waste and wood waste in five ASEAN countries, namely: Indonesia, Malaysia, Philippines, Thailand, and Vietnam are about 107.55 million tonnes. Of this total, bagasse accounted for 32%, palm oil waste 27%, rice hulls 23%, and wood waste 18% [12].

Rice is cultivated in more than 75 countries in the world. The rice husk is the outer cover of the rice grain and on average it accounts for 20% of the paddy produced, on a weight basis. The worldwide annual husk output is about 80 million tonnes with an annual potential energy of 1.2 x 109 GJ corresponding to a heating value of 13-16 MJ/kg [24]. The total number of rice mills in some countries is very large; there are about 92,000 rice mills in India, 60,000 mills in Indonesia, and 40,000 mills in Thailand. Rice husk biomass is renewable in nature and is less polluting due to its low sulphur and heavy metal content. However, rice husk ash contains more than 95% silica which could contribute to ash related problems in boiler such as bed agglomeration, fouling and deposition on super heater tubes.

Malaysia and Indonesia are the largest producers of palm oil products. The EC-ASEAN COGEN estimated that a total of 42 million tonnes of Fresh Fruit Bunches (FFB) were produced in year 2000 [12]. The complete operational process and products of the palm oil industry is shown in Figure 2.1. FFB contain approximately 21% palm oil and 6-7 % palm kernel. The waste together with fibre and shells amounts to 42 % of the FFB, and would translate to a total waste volume of over 17 million tonnes of waste. For low pressure systems with an assumed energy conversion rate of 2.5 kg of palm oil waste material per kW, potentially over 7,000 GW could be generated. There are more than a hundred palm oil processing mills in the two countries. As such, a lot of savings can be done by using the fibre and shell from the processing wastes as an alternative fuel for electricity generation for this industry [25]. Currently the majority of this waste is either landfill or burnt in open fires.

Bagasse is the matted cellulose fiber residue from sugar cane that has been processed in a sugar mill. Previously, bagasse was burned as a means of solid waste disposal. However, as the cost of fuel oil, natural gas, and electricity has increased, bagasse has come to be regarded as a fuel rather than refuse. Bagasse is a fuel of varying composition, consistency, and heating value. These characteristics depend on the climate, type of soil upon which the cane is grown, variety of cane, harvesting method, amount of cane washing, and the efficiency of the milling plant. In general, bagasse has a heating value between 7 and 9 MJ/kg on a wet, as-fired basis. Most bagasse has a moisture content between 45 and 55 percent by weight. Sugar cane is a large grass with a bamboo-like stalk that grows 2.44 to 4.57 m tall. Only the stalk contains sufficient sucrose for processing into sugar. All other parts of the sugar cane (i.e. leaves, top growth, and roots) are termed "trash". The three most common methods of harvesting are hand cutting, machine cutting, and mechanical raking. The cane that is delivered to a particular sugar mill will vary in trash and dirt content depending on the harvesting method and weather conditions. Inside the mill, cane preparation for extraction usually involves washing the cane to remove trash and dirt, chopping, and then crushing. Juice is extracted in the milling portion of the plant by passing the chopped and crushed cane through a series of grooved rolls. The cane remaining after milling is bagasse [26].

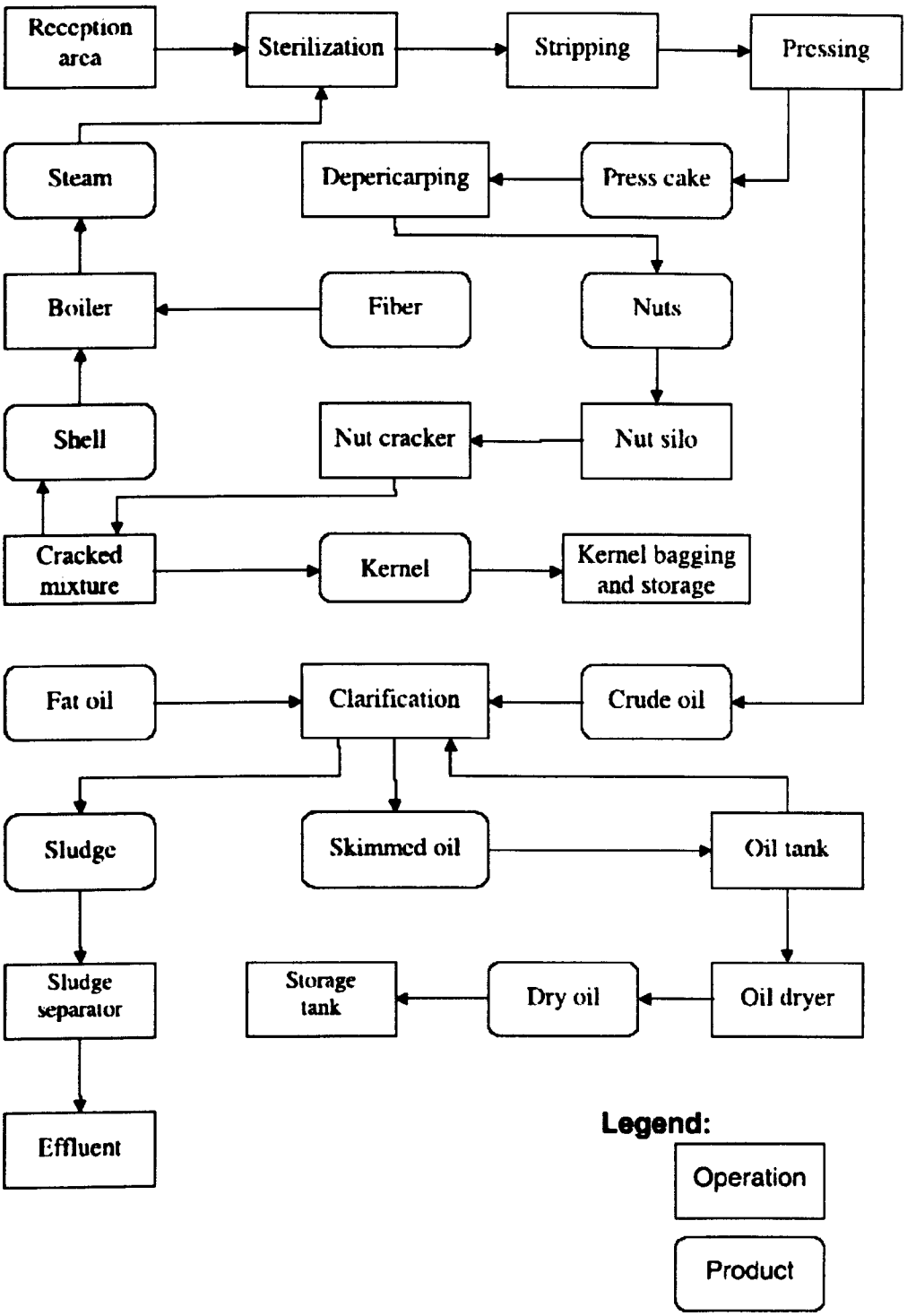

Figure 2.1 Process operation and product of palm oil mill

2.1.2 Fuel Properties

The typical properties differences between coal and biomass are indicated by the proximate and ultimate analyses (Table 2.2). The volatile matter in biomass is generally close to 80%, whereas in coal it is around 30%. Wood and woody materials tend to be low in ash content while the agricultural materials can have high ash contents. It is difficult to establish a representative biomass due to large property variations, but ten examples are included here for comparison. The composition variations among biomass fuels are larger than among different coals, but as a class biomass has substantially more oxygen and less carbon than coal. Less obviously, nitrogen, chlorine, and ash vary significantly among biomass fuels. These components are directly related to NO_x emissions, corrosion, and ash deposition. The wood and woody materials tend to be low in nitrogen and ash content while the agricultural materials can have high nitrogen and ash contents. Furthermore, one important difference between coal and biomass is the net calorific value. Biomass fuels often have high moisture content, which results in relatively low net calorific value [26].

The inorganic properties of coal also differ significantly from biomass (Table 2.2). Inorganic components in coal vary by rank and geographic region. As a class, coal has more aluminium, iron, and titanium than biomass. Biomass has more silica, potassium, and sometimes sodium than coal. The significant effect some of these materials (silica, potassium and sodium) on combustor design (particularly FBC) will be discussed detail in section 2.2.3.

Furthermore, significant differences in physical properties between biomass and coal give rise to several interesting combustion issues (see Table 2.3). For example, the difficulty in reducing biomass to a small size compared to coal makes it a more difficult fuel to combust in a fluidised bed combustor. Furthermore, biomass is also much less dense, which leads to more rapid burnout. Finally, biomass particles have slightly less residence time in the bed because they are elutriated from the bed. These effects combine to allow larger biomass particles to be consumed in the boiler than would be possible for coal [15].

Table 2.2: Composition and heating values of selected coal and biomass

	Bituminous Coal[26]	Rice Husk[27]	Palm kernel Shell[25]	Palm Fibre[25]	Refuse Derived Fuel (RDF)[21]	Chicken litter[20]	Wood waste[27]	Sunflower husks [28]	Cotton Husk[28]	Coffee Husk[28]	Coconut shell[28]
Proximate analysis (% as received)											
Fixed carbon	53.6	14.22	21.73	18.9	9.9	3.2	9.8	19.9	16.9	20.0	22.0
Volatile matter	34	63.52	69.47	69.7	77.8	68	81.7	69.1	73.0	64.6	70.5
Moisture	7.5	4.0	5.6	3.0	4.0	5.0	8.1	9.1	6.9	11.4	4.4
Ash	4.9	18.26	3.2	8.4	8.3	24.8	0.4	1.9	3.2	0.9	3.1
Ultimate analysis (%dry basis)											
Carbon	87.52	38.83	45.61	51.5	45.9	28.17	50.7	51.4	50.4	43.9	51.2
Hydrogen	4.26	4.15	6.23	6.6	6.8	3.64	5.9	5.0	8.4	6.3	5.6
Nitrogen	1.55	35.47	37.46	1.5	1.1	3.78	0.2	0.6	1.4	6.3	0.0
Oxygen	1.25	0.52	1.73	40.1	33.7	34.43	43.1	43.0	39.8	32.1	43.1
Sulphur	0.75	0.05	0	0.3	0	0.55	0.04	0.0	0.0	3.1	0.1
Chlorine	0.16	0.12	n.m	n.m	<0.01	0.63	n.m	n.m	n.m	n.m	n.m

Elemental composition (%)											
SiO_2	37.24	91.42	n.m	63.2	n.m	n.m	12.8	17.8	10.8	13.5	69.3
Al_2O_3	23.73	0.78	n.m	4.5	n.m	n.m	4.1	6.4	1.9	2.2	6.4
TiO_2	1.12	0.02	n.m	0.2	n.m	n.m	n.m	0.2	0.0	n.m	0.01
Fe_2O_3	16.83	0.14	n.m	3.9	n.m	n.m	5.2	9.4	4.0	3.7	1.6
CaO	7.53	3.21	n.m	n.m	n.m	n.m	45.2	14.5	1.3	3.9	8.8
MgO	2.36	<0.01	n.m	3.8	n.m	n.m	0.9	14.6	20.7	10.7	2.5
Na_2O	0.81	0.21	n.m	0.8	n.m	n.m	0.6	8.5	7.5	4.0	1.6
K_2O	1.81	3.71	n.m	9.0	n.m	n.m	0.5	6.8	1.7	n.m	0.01
SO_3	6.67	0.72	n.m	2.8	n.m	n.m	n.m	0.1	1.3	0.4	4.8
P_2O_5	0.10	0.43	n.m	2.8	n.m	n.m	2.1	21.1	49.6	38.1	8.8
Higher heating value (MJ/kg)	35.01	15.84	18	15.43	18.64	10.62	18.41	n.m	n.m	n.m	n.m

n.m = not measured

Table 2.3: Physical properties and dry heating values of biomass and coal [15]

Property	Biomass	Coal
Fuel density (kg/m^3)	~500	~ 1300
Particle size	~3 mm	~100 μm

2.1.3 Fuel Handling and Preparation Prior Feeding

The supplementary fuels of interest in a particular co-combustion project are mostly produced and generated within economical transport distance from the area where they are grown. The preparation of these materials for use as a fuel is governed by the fuel characteristics and by the combustion technology being used and its associated fuel feed mechanisms. Biomass fuels and wastes generally can be cut, chopped or crushed (bark, straw, grass etc.), chipped (wood, trimmings, etc.) or ground (wood) for use in a fluidised bed combustor. These techniques are often well proven, but can represent a considerable capital and/or operating cost to the project [19].

For instance, to be able to burn MSW in a fluidised bed combustor commonly used for coal, it will be necessary to homogenise the material by sorting and by size reduction by cutting or chipping. Some of the main problems of using MSW as a feedstock have been variability, biological and chemical instability, and poor fuel characteristics. An improved method for turning MSW into an environmentally safe and economical fuel has been developed [23]. Recyclable metals, glass and some plastics are mechanically and manually separated from the waste. The remaining (combustible) fraction is combined with a calcium hydroxide binding additive, and formed into cylindrical pellets. These pellets are dense and odourless, can be stored for up to three years without significant biological or chemical degradation, and are easily transported. These pellets have been successfully combined with coal in existing BFBC combustors [21].

However, certain fuels must be prepared in small sizes and have low moisture content for complete combustion although this condition will complicate handling and storage due to their low bulk density (i.e. wood powder). Particles generally need to be less than 3 mm to completely combust. Larger sizes, high moisture contents (greater than 40%) and high particle density all significantly increase the time required to completely combust the particles and may increase fly ash carbon content [19].

Moreover, the fibrous material of palm fibre (PF) causes the particles to stick to each other and contribute to the segregation problem during combustion tests which does not occur for other biomass fuels. In this respect, an attempt has been made by Husain *et al.* [29] to convert these residues into higher density solid fuel. The palm shell and fibre (initially less than 200 kg/m^3) was densified into briquettes of diameter 40, 50 and 60 mm under moderate pressures of 5 - 13.5 MPa in a hydraulic press with densities between 1100 and 1200 kg/m^3. The briquette properties have found to have a higher calorific value (17 MJ/kg) with good resistance to mechanical disintegration, and will withstand wetting.

Similarly the above densification method has been applied to paper and plastics waste to reduce area for storage and to improve in situ handling and feeding [30]. The two most common methods for densifying waste paper and plastics are cubing and pelletising. Boavida *et al.* [30] have claimed that this densification technique not only improves the integrity of the fuel but also potentially increases their heating value. In general the fuel cubes contain relatively small amounts of plastics, particularly rigid plastics, in order to maintain fuel integrity. Also, heated dies have been added to both cubes and pelletisers to improve the integrity of the fuel and allow higher moisture and plastics contents in the fuel feed stocks. While typical dies allow up to 20% moisture, heated dies will allow up to 35% moisture while maintaining relatively good fuel integrity. Without heated dies, plastics content of process engineered fuel will generally be kept below 10% by volume. Heated dies may allow plastics content to reach up to 75% by volume, thus potentially increasing the process engineered fuel heating value significantly.

2.2 Fluidised Bed Combustion Technology (FBC)

Fluidised bed combustors are usually classified as either bubbling or circulating beds. The distinction depends on gas velocity and bed particle size (Figure 2.2). In fluidised beds, the gas is blown through a bed of solid particles. As the velocity of the fluidising air is increased above the minimum fluidisation velocity, the bed particles are lifted up from the fluid grate. Typically, the bed consists of an "inert" material such as sand and/or ash, the fuel particles, and a sorbent such as limestone, if needed, to adsorb SO_2. The presence of a large amount of bed material in FBC combustors compared with the mass of the fuel (98% versus 2%) is beneficial especially in the burning of low-grade fuels. The large heat capacity of the bed material stabilises the fluctuations in energy output associated with the variations in fuel properties.

The first biomass fuel-fired fluidised bed boilers in the world were based on bubbling bed technology and were delivered to the Finnish pulp and paper industry [30]. Initially the boilers were small in size, about 10–50 MW_{th} (thermal effect). Today, atmospheric bubbling fluidised bed combustion (BFBC) is considered commercial up to 150 MW_e (approximately 340 MW_{th}) and circulating fluidised bed combustion (CFBC) up to 400–600 MW_e (approximately 900–1350 MW_{th}) [31,32]. The BFBC and CFBC combustion systems are illustrated schematically in Figure 2.3. The choice between BFBC and CFBC technology is largely linked to the choice of fuels. BFBC, much simpler and cheaper technology, has been favoured for plants exclusively fuelled with biomass or similar low-grade fuels containing high volatile substances. Enhanced CFBC design, on the other hand, may be competitive even in smaller biomass-fired plants. In either case, the low operating temperature of fluidised bed boilers means the effectively no thermal nitrogen oxides (NOx) are formed. Also, because of the low sulphur content of biomass, sulphur emissions control is not required.

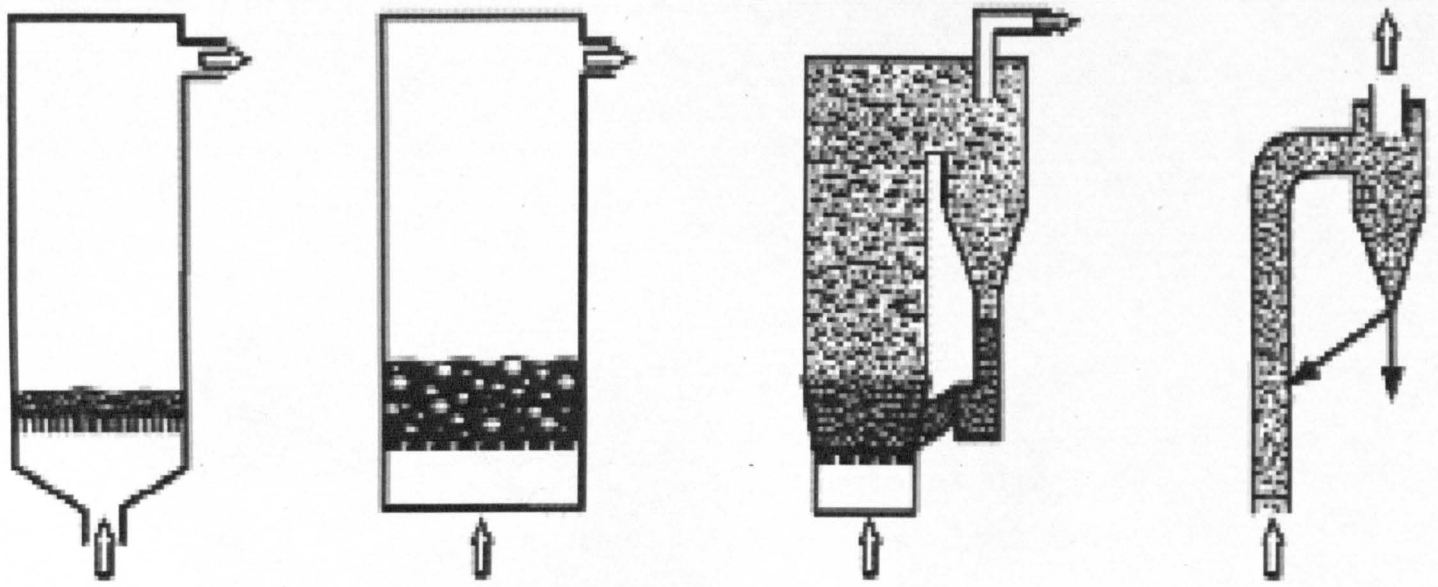

Figure 2.2 Classification of fluidised bed systems [31]

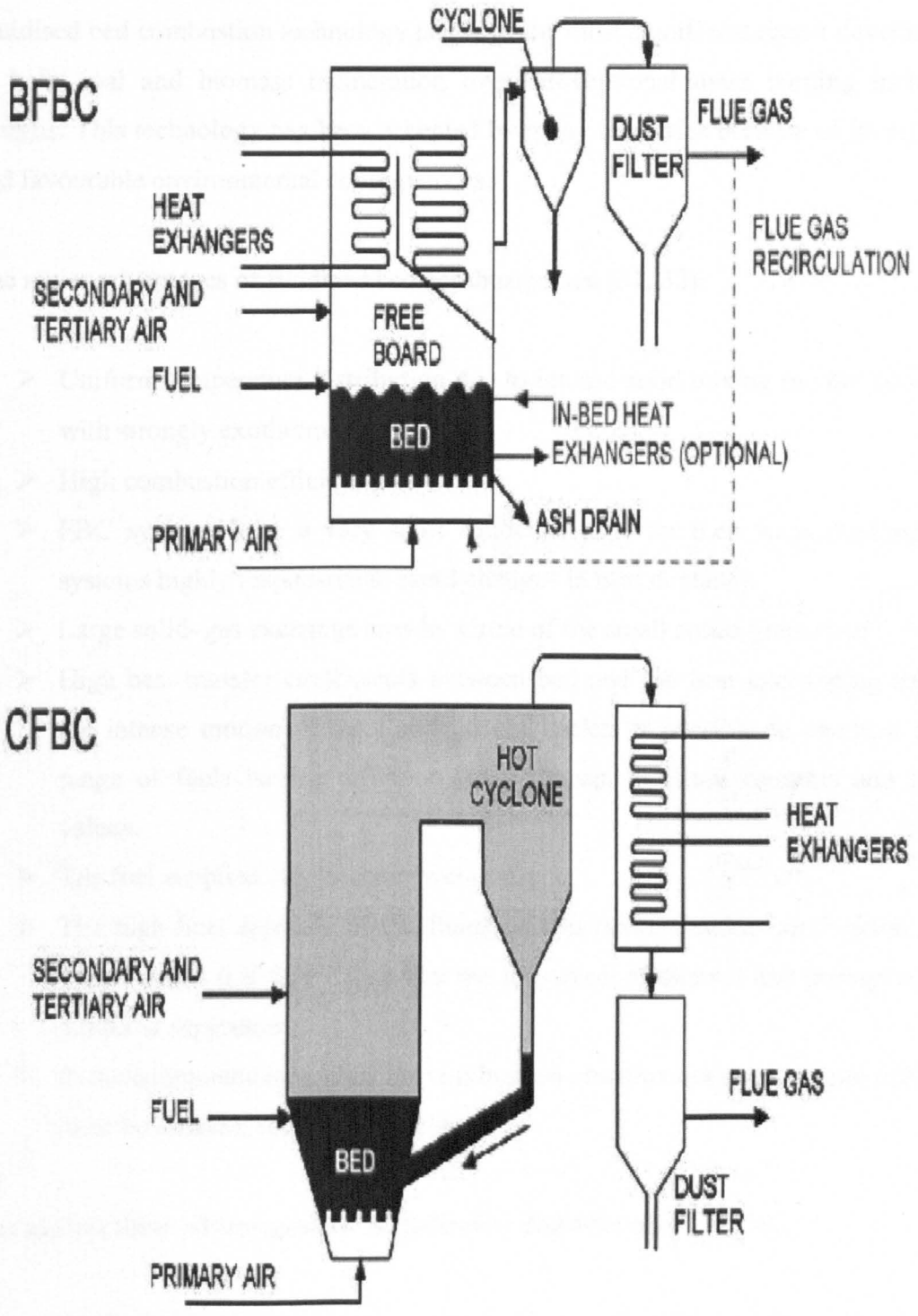

Figure 2.3 Schematic diagrams of the primary fluidised bed combustion Systems [31]

2.2.1 Advantages and Disadvantages of FBC

Fluidised bed combustion technology is one of the most significant recent developments in both coal and biomass incineration over conventional mass burning incinerator designs. This technology has been accepted by many industries because of its economic and favourable environmental consequences.

The major advantages of fluidized bed combustors are [31, 32]:

- Uniform temperature distribution due to intense solid mixing (no hot spots even with strongly exothermic reactions);
- High combustion efficiencies
- FBC systems have a very short residence time for their fuels (making these systems highly responsive to rapid changes in heat demand).
- Large solid–gas exchange area by virtue of the small solids grain size;
- High heat-transfer coefficients between bed and the heat exchanging surfaces; the intense motion of the fluidized bed makes it possible to combust a wide range of fuels having different sizes, shapes, moisture contents and heating values.
- The fuel supplied can be either wet or dry
- The high heat capacity of the fluidized bed permits stable combustion at low temperatures (i.e. 850°C), so that the formation of thermal and prompt nitrogen oxides is suppressed;
- Reduced maintenance since the combustion chamber does not contain grates that must be cleaned, repaired or replaced.

Sets against these advantages are the following disadvantages [33, 34]:

- Solid separation equipment required because of solids entrained by fluidizing gas resulting in a high dust load in the flue gas;
- Possibility of defluidisation due to agglomeration of solids;

2.2.2 Feeding Method

2.2.2.1 In-bed Feeding System

In-bed feed systems usually convey fuel pneumatically into the bed and the fuel flows co-current with the primary air. This system is more complex that the other types of feed system (over-bed). Current design practice requires a feed point per 1 to 2 m^2 distributor area, which corresponds to one feed point per 1.5 to 3 MW_{th} capacities [35]. Also, it is important to ensure uniform volatile matter distribution throughout the bed. Failure to do so may develop fuel rich regions in the bed which in turn carry a risk of corrosion for heat exchanger tubes immersed in the bed [35]. As they flow co-currently with the primary combustion air and the combustion products, particle entrainment and system blockage is more likely to occur. Relatively, a higher CO emission than over-bed feeding (about 1000-1500 ppm) were observed by Armesto *et al.* [36] during combustion of rice husk in a 30 kW FBC. Peel and Santos [37] have suggested that satisfactory combustion (uniform bed temperature and high combustion efficiency) for lower particle density fuels (i.e. bagasse, sawdust and the rice husks) could only be achieved with under-bed feeding.

2.2.2.2 Over-bed Feeding System

Over-bed feed systems include conventional spreader feeders, air swept feeder/mills or gravity feeders. These systems are less prone to blockages and simpler to construct and maintain [31]. For over-bed feeding, fresh fuel is introduced at the top of the bed and the fuel flow is counter-current to the primary air. The air supply is divided between primary combustion air, which introduced at the bottom of the bed, and secondary air, introduced above the bed with the fuel feed. However, large particle sizes of coal (> 5 mm) with burning times sufficiently long to penetrate the bed are usually used, preferably without fines below 1 mm. These particles are liable to suffer attrition that causes flaking off very small carbonaceous particles (<0.1 mm) due to long residence time [35]. However, more uniform heat distribution is obtained using this method due to continuing reaction as the gases rise through the bed of fuel. Larger particle size (> 5 mm) and higher particle density fuel (>200 kg/m^3) are normally recommended using this method.

2.2.3 Biomass Fuel Characteristics and Impact on Design and Performance

The EPRI (Electric Power Research Institute) has reported on alternative fuel firing (biomass fuels) in an atmospheric fluidised bed combustion boiler showing that biomass fuels behaviour in fluidised bed combustor can be fundamentally different from coal. Depending on the fuel properties and their variability with time, the biomass fuel can place different demands on design of combustor and auxiliary systems. Table 2.4 presents a summary of key parameters and their effects on fluidised bed combustion boiler design and performance [38].

2.2.3.1 Fuel composition and compositional variations

Several fluidised bed combustion design and performance factors can be determined from comparison and evaluation of the following fuel data:

- Proximate analysis of the fuel (percent volatiles, ash and moisture)
- Ultimate analysis of the combustibles fractions (C., H, N, O, S, etc)
- Heating value

The higher the ash and moisture content of the fuels the lower the bed temperature due to the heat required to evaporate the fuel moisture, heat up the ash and heat up the combustion air. When the ash or moisture are sufficiently high (>10%), fluidised bed temperature cannot always be maintained at or near the feed point for effective combustion and emission control without the use of a supplement such as coal or propane.

Table 2.4: Key biomass fuel parameters and their impact on design and performance [38]

Fuel properties	Impact of performance	Design areas affected
1. Basic fuel composition ➢ % combustibles, ash and moisture ➢ Ultimate analysis ➢ Heating values	➢ Combustor plan area heat release rate ➢ Auto thermal combustion limit ➢ Flowrates of air, ash and flue gas ➢ Boiler efficiency	➢ Combustor/ backpass surfacing ➢ Fuel preparation and blending requirements ➢ Supplemental fuel requirements ➢ Combustor temperature control methodology ➢ Design margins for air, gas and material handling
2. Particle mixing and combustion characteristics ➢ % moisture ➢ Particle size ➢ Particle density ➢ Volatile matter/fixed carbon ratio ➢ Oxygen/fixed carbon ratio	➢ Particle heat-up and drying time ➢ Devolatilisation and volatile combustion time ➢ Char combustion time ➢ Particle mixing and segregation ➢ Combustion stability	➢ Excess air requirements and injection locations ➢ Fuel sizing/blending requirements ➢ Fuel feed distribution requirements ➢ Combustor gas residence time ➢ Combustion control philosophy
3. Ash and non-combustible impurities ➢ Ash ➢ Ash product size ➢ Chemical composition ➢ Physical composition	➢ Melting/vaporisation temperature ➢ Low melting point compound formation ➢ Bed material grain size (FBC)	➢ Convection pass design and material selection ➢ Bed media size and poultry control ➢ Air distributors and bed left down system design ➢ Particulate control system design
4. Volatile impurities and pollutants ➢ Sulphur ➢ Nitrogen ➢ Chlorine/fluorine ➢ Heavy metals	➢ NOx, SO_2, HCl emissions ➢ Dioxins/furans formation ➢ Vaporised trace metals	➢ In combustor versus post combustion clean up ➢ Sorbent selection and injection rates ➢ Solid waste handling and disposal

2.2.3.2 Particle Mixing and Combustion Characteristics

Many of the biomass fuels characteristics are quite different to those of coal and the ability to burn these fuels in a particular installation will depend on their individual properties and the flexibility of the combustion system. The volatile matter content of biomass fuels is usually at least twice as high as for coal. This means that more combustion will occur in the upper region of the combustor since volatiles are released and so the combustion rate is greater than the fixed carbon combustion rate. This will affect the vertical combustor temperature profile [14].

Furthermore in the case of overbed feeding in particular the pattern for char and volatiles burn-out is further affected by the fraction of fuel particles that are carried immediately out of the bed (or never reach the bed) because their terminal velocities are less than the upward gas velocity (function of particle size, shape and density). In addition, when the fuel moisture, size, and composition vary over time (i.e. RDF), the rate of drying, devolatilisation, and volatile combustion that occur in the bed or lower combustor are also not uniform. Also, there are periods of time when local regions of the combustor are running fuel rich against fuel lean due to the speed at which the burning volatiles consume available oxygen. This resulted in variations in the quantity of unburned volatiles (i.e. CO) leaving the combustor [14].

2.2.3.3 Ash and Non-combustible Impurities

Though fluidised bed combustion temperatures are typically below the point where coal ash softening or melting occurs, some biomass fuels (i.e. MSW) contain varying quantities of glass and aluminium that can become molten at or below typical operating temperatures (800-900°C). In addition, alkali constituents in some biomass fuels and papers sludge are conductive tend to form low melting point compounds. These molten materials can lead to bed agglomeration and fouling of the combustor walls and air/fuel penetrations. Alkaline compounds of potassium and sodium in biomass ash have very low melting temperatures. Potassium and sodium oxides can also form eutectics with silica and other constituents. This lowers the ash softening point from 1087°C to 768°C.

Also, deposits on heat recovery tubes of an FBC boiler can occur with many biomass fuels, due to either the carryover of molten or semi-molten ash particles from the bed or condensation of alkali salts that were vaporised during combustion. These deposits can lead to fouling of the tube, and/or if sulphur or chlorine is present in the tube deposit, and subsequent corrosion, particularly when higher steam pressures and temperatures are used [14]. Details on bed agglomeration and deposition experiences during combustion in FBC will be discussed later in section 2.4.4.1.

2.2.3.4 Volatiles Impurities and Pollutants

Co-combusting biomass fuels with coal typically increase the scope of potential flue gas emissions and control requirements. However, since some biomass fuels (i.e. mostly agricultural residue) can contain lower levels of nitrogen and sulphur than most coals, co-combustion can effectively reduce NO_x and SO_2 emissions upon combustion. The chlorides present in most alternative fuels evolve as vapours, i.e. HCl, during combustion due to their high volatility. Organically bound chlorine (from plastics and vinyls in MSW or automobile wastes) can contribute to the formation of chlorinated organic compounds such as dioxins and furans. Also some biomass fuels (i.e. MSW) typically contain sufficient levels of certain heavy metals (i.e. cadmium, lead, zinc, mercury and arsenic) to cause greater environmental problems than burning coal [13]. They can leave the stack as vapours or solids, and can concentrate in the fly ash, which increases potential for triggering hazardous waste disposal requirements. With the exceptions of mercury that remains as a vapour at stack temperatures, effective particulate control (by fabric filters or electrostatic precipitators) is considered essential for controlling stack emissions of most metals [14].

2.2.4 Combustion Studies

Fluidized bed combustion of alternative solid fuels (including biomass) are attractive as a result of the constantly increasing price of fossil fuels, the presence of high quantities of wastes to be disposed of and global warming issues. Extensive experimental investigation has been carried out to date on the feasibility and performance of different biomass fuels FB combustion such as rice husk [24, 39, 40, 41], animal waste [20, 30, 42], MSW [43, 44] and RDF [23] that will discussed detail in the next following section. In whatever form biomass residues are fired (loose, baled, briquettes, pellets), a deeper understanding of the combustion mechanisms is required in order to achieve high combustion efficiency and to effectively design and operate the combustion systems. The combustion properties and their effect on combustion mechanisms are all important information required to understand the combustion characteristics of biomass residues and their co-combustion with coal in FBC.

2.2.4.1 Combustion Mechanisms

As discussed previously in section 2.1.2, biomass fuels have different physical and chemical characteristics from coals, so that the combustion behaviour of these two kinds of fuels in a FBC varies from one to another. However, in general when a single coal or biomass particle enters a fluidised bed furnace, then three phenomena occur, namely [13]:

(i) Heating up and drying – the fuel particle temperature will rise to its ignition temperature and beyond.

(ii) Devolatilisation (pyrolysis) – for a short period of time (<10 second), volatile matter will be evolved and can be burnt at or beyond the particle.

(iii) Char oxidation – the remaining solid combustible matter (mostly carbon), will be oxidised relatively slowly with the evolution of heat until only incombustible ash remains.

The temperatures at which devolatilisation and char combustion start, the composition of the devolatilisation products and the effect of physical and chemical properties of fuels on the overall combustion process, are all important information required to understand the combustion characteristics of biomass or coal fuels. This section discusses some of these issues. Also, it is expected that blending of biomass with coal will compensate each other during combustion.

2.2.4.1.1 Drying

The drying process is the phenomenon occurs during removal of moisture of the fuel in FBC. The evaporation of the surface moisture is not likely to affect the coal combustion directly, although the feeding of the paste or slurry can cause agglomeration in the fluidised bed. The temperature normally reduces to a level where combustion cannot be supported. In contrast, in biomass combustion this factor is of significant importance and in some instances may dominate the combustion process [28]. Inherent moisture of biomass or low rank coals may be as high as 40% or more and its evaporation may occur in conjunction with shrinkage, resulting in some processes such as devolatilisation and ignition by retarding the release of volatiles and their ignition. In addition, the loss of water can also be associated with significant morphological changes in the low rank coals or biomass fuels [13].

The influence of ignition retarding by high moisture content is shown in Figure 2.4 by Suskankraisorn *et al.* [43] during combustion of high moisture content MSW in a 0.15-m diameter and 2.3-m high fluidised bed combustor. The temperatures were plotted against the height of combustor at different moisture content, 5, 10, 15, and 20%. Considering 5% moisture content the temperatures above the bed surface were higher than those within the bed. Since 65% of the simulated MSW is volatile matter, it was expected that the volatile matter be released as the simulated MSW entered the combustor and tended to burn above the bed or along the height of the combustor. The highest freeboard temperature was 850 °C while the bed temperature was around 640 °C giving a 200°C difference. At 10 and 15% moisture content the bed temperatures were increased to 750 and 710 °C, respectively. Increased moisture content in the simulated MSW increases the devolatilisation time of the simulated MSW giving more time for

the simulated MSW to go into the bed and burn in it. The bed temperature at 15% moisture content was lower than that at 10% moisture content because of the higher moisture content. The 20% moisture content gave the lowest bed temperature, 600°C, and showed the variation in the bed temperatures. The freeboard temperature was 50°C higher than the bed temperature implying the simulated MSW was burnt above the bed surface. Increasing the moisture content the simulated MSW was formed into a lump that could effect to the quality of fluidisation. The simulated MSW could be floated and burnt over the bed surface [43].

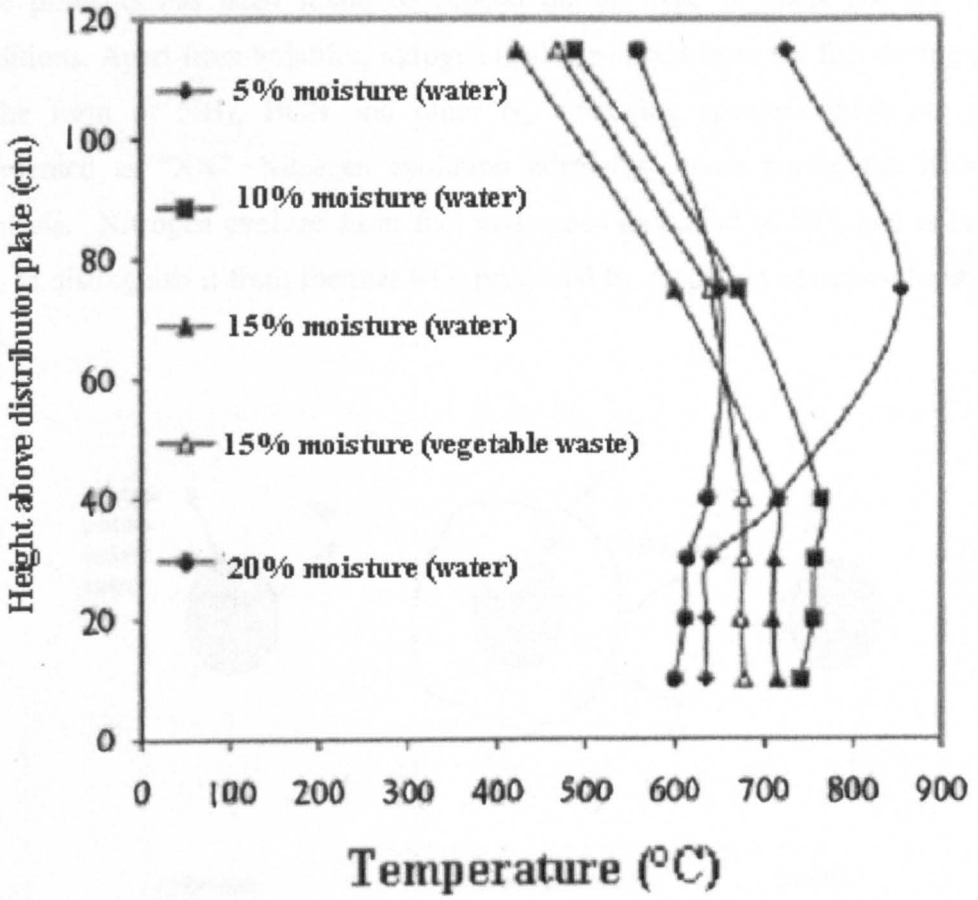

Figure 2.4 Temperature profile of simulated MSW at different moisture content [43]

2.2.4.1.2 Devolatilisation (Pyrolysis)

Devolatilisation (pyrolysis) is a thermal decomposition process where the large and heavy molecules of organic matter in the solid fuel particle break up or crack, followed by the evolution of lower molecular weight species known as volatiles [28].

Figure 2.5 shows a schematic representation of the various physical mechanisms important in the pyrolysis and combustion of coal. Pyrolysis products range from lighter volatiles (CH_4, C_2H_4, C_2H_6, CO, CO_2, H_2, H_2O, etc) to heavier tars. The quantity of these products has been found to depend on the type of fuels and the operation conditions. Apart from volatiles, nitrogen is also evolved from the fuel during pyrolysis in the form of NH_3, HCN and other N_2-containing species which are generally represented as "XN". Nitrogen evolution normally occurs during the later part of pyrolysis. Nitrogen evolved from fuel undergoes oxidation to NO_x and is called fuel NO_x to distinguish it from thermal NO_x produced by oxidation of atmospheric nitrogen [13].

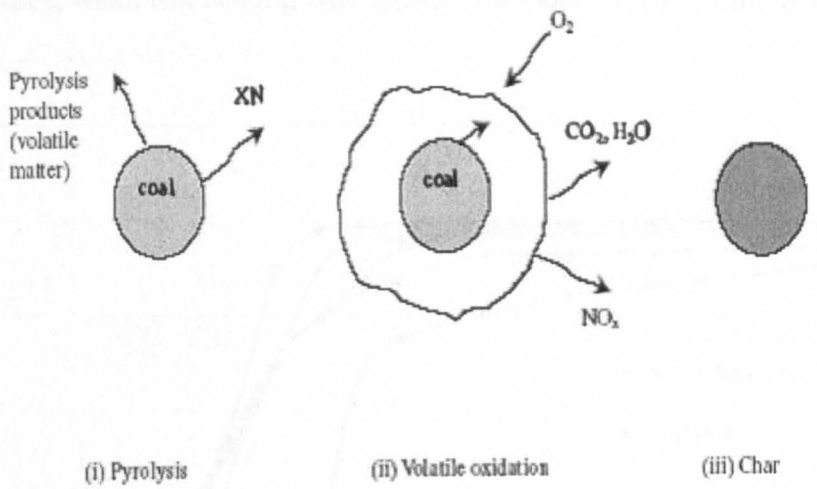

Figure 2.5 Schematic of coal combustion mechanisms [13].

The temperature at which devolatilisation occurs depends on the fuel type and the heating rate which was determined by thermoanalytical techniques, in particular thermogravimetric analysis (TGA) and derivative thermogravimetry (DTG). Figure 2.6 shows a graph of temperature of weight loss for biomass fuels (wood chips, rice husk, palm kernel shell, palm fibre) and coal (see Table 2.4 for the compositions)[13, 28, 45] determined using a thermogravimetric analyser. Typically, the devolatilisation of the biomass fuels starts (upon completion of drying) at low temperatures of 160–200°C. Around 200°C, the devolatilisation is rapid and significant weight loss is recorded whereas above 500-600°C, the weight remains more or less constant which indicates the completion of combustion process (volatiles and char). For bituminous coal, pyrolysis occur at about 350–400°C. A constant weight loss is observed at temperature higher than 650°C for heating rate <100°C/s [28]. Therefore, it is possible to draw a conclusion about the temperature at which the combustion of the volatiles takes place and it can be concluded that the low temperature of devolatilisation and combustion appears to be a characteristic of biomass fuels. In addition, heating rate also affects the thermal decomposition characteristics. The lateral shift in the DTG profiles to higher temperatures, when fast heating was applied, for example 10°C/min to 100°C/min [46].

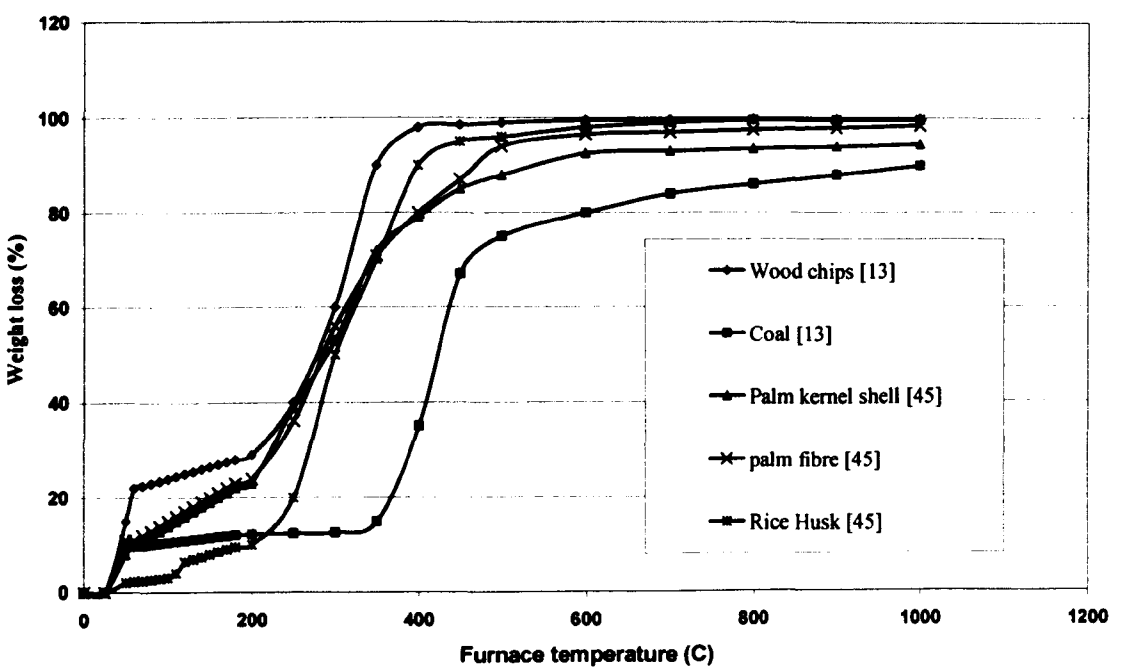

Figure 2.6 Temperature resolved weight loss analysis of wood chips, palm kernel shell and palm fibre, rice husk and coal.

Combustion of the volatiles has been claimed would be the dominant step during the combustion of biomass [13, 28]. In this respect, Kaeferstein *et al.* [47] investigated the combustion process of biomass (wood and straw) during batch experiments in a bubbling fluidized bed using oxygen concentration profiles measured directly over the bed with solid electrolyte sensor probes. They observed that for the combustion of the biomass, there was a rapid consumption of oxygen, which took place in one phase. Whereas, for coal, the oxygen consumption profile exhibited two regions characterizing a short phase for volatile combustion and a long char combustion phase. The combustion of the biomass was almost complete after the completion of volatile combustion. Analysis of heat distribution during the combustion of wood chips and straw showed that over 67% of their calorific values were released through the combustion of the volatiles. Consequently, it may therefore be expected that during biomass combustion significant combustion and heat release would take place near the point where the particles devolatilised.

In spite of volatiles combustion, Cooke *et al.* [48] have observed the floating and sinking behaviour of fuel particles during the combustion particles of coal and biomass samples of RDF and fibre fuels (which contains non-recyclable printed paper, board, packaging material, plastics (but excluding PVC) and fibrous waste) in the fluidized bed of silica sand (previously sieved to be between 300 and 355 mm) which was housed in a cylindrical, quartz tube (internal diameter: 160 mm). Once released, the volatiles were observed to undergo oxidation within the gas film surrounding the particle. The particles during these stages tend to float on top of the bed and then sink after releasing all the water and volatiles. Volatiles were found to disengage from the solid as jets. This phenomenon observed during fluidised bed combustion was mainly governed by (1) sand motions, (2) variations superficial velocities and (3) fuel properties.

The sand could be on top of the particle allowing the fuel to reach the bed's surface after releasing water and volatiles. After all the vapours have been released, the sand fell down into the bed (especially near the walls) and carried the char particles downwards to the bottom of the bed. A coal particle floated on top of the bed during devolatilisation, but the remaining, less dense char particle sank and circulated around

the bed during its combustion. By comparison, particles of RDF and fibre fuels floated on the sand during the entire period of their burning due to less or no char burning in the bed. Furthermore, variations in superficial velocities have also caused the floating effect. The increasing fluidising velocity through the distributor plate helps to maintain the fuel particles to be in the upper part of the bed. Those solid fuels with high volatile/fixed carbon ratios require large particles with low surface/mass ratio. This means that fuel with high volatiles content (60%) need to be heavier or have specific gravity high enough to devolatilise inside of the bed instead of on the surface to achieve good heat recovery rates with the in-bed tubes or at least to sustain the operating temperature of the bed.

Another important factor, which must be considered during the devolatilisation process, is fragmentation or segregation of volatiles. The fuels might break into 2 to 5 pieces due to internal particle gas pressures that occur during the production of the volatiles gases. For example, particles of fibre fuel changed shape during devolatilisation [48]. They expanded to give a very much greater external surface area and also fragmented (broke into pieces). These smaller pieces are elutriated from the bed and either completes the burning in the freeboard or is carried out of the rig incompletely burnt. The degree or combustion depends mainly on fluidising velocity and freeboard temperature.

Relatively, the devolatilisation time in general increases with increasing particle size, and moisture content. However, it decreases with increasing heating rate, oxygen concentration, fluidising velocity and bed temperature [49]. The almost cylindrical particles of RDF had a devolatilisation time independent of their length but being largely dependent by their diameter. The larger diameter contributed to a longer devolatilisation time due to the smaller surface area per unit volume. Also, higher moisture content (>15%) needs longer devolatilisation time upon drying and evaporation of water content in the fuel [43]. Increasing fluidising velocity not only offered better mixing of the fuel or fuel blends but also should increase oxygen supply and heat transfer providing the bed temperature is maintained. Thus, it can reduce the devolatilisation time of fuel in the overall combustion by bringing up some of the fuel particles to above the bed surface.

2.2.4.1.3 Char Oxidation

After devolatilisation, the skeletal char remaining is essentially fixed carbon. The fuel particle structure changes and the material left are the char and its associated mineral matter. The char then burns and the mineral matter is transformed into ash, slag and fine particles in various proportions. The mass transfer of oxygen from the bed to the particle's exterior controls the combustion of the remaining char in coal. The char oxidation reactions proceed largely by the carbon molecule reactivity at the surface of particle with oxygen producing CO.

The main factors to be considered during this process are the diameter of the fuel particle (surface/volume ratio), the oxygen availability in the combustion environment and the temperature due to the influence in the kinetics of char oxidation surface reactions and the inability of oxygen to penetrate into pore structures of the fuel particle at high temperatures (i.e mass transfer). Moisture is another parameter that influences the process as it facilitates CO oxidation in the gas phase but at the same time inhibits the overall char oxidation. Furthermore, the biomass chars contain high levels of oxygen and low levels of hydrogen compared to coal. In addition, the structural disorder may also lead to higher reactivity of biomass in the late stages of combustion since more edge carbon (which is more reactive) is available [28].

2.2.4.1.4 Burn out time

The burn-out time of volatiles and char of different materials in a FBC has been studied by Cooke *et al.* [48] by measuring the concentration of CO and CO_2 in the flue gas. Figure 2.7 shows a similar profile for the three different materials (of identical mass); Coal (30 mm diameter), fibre fuel (cubes with sides of 25–30 mm) and RDF (15mm in diameter and 30–50mm in length). The figure clearly shows the difference of the devolatilisation and char burning process of these fuels. The larger peak registered by the fibre fuel during devolatilisation is due to the higher volatile content. This shows the importance of the form of the fuel content. In the fibre fuel its carbon is concentrated in the volatile matter whereas in coal it is concentrated in the char form. This is due to the molecular weight of the fuel. Thus, with a much smaller fraction of carbon in the char,

the burn-out times for the waste fuels (fibre fuels and RDF, 13 min) are considerably smaller compared to coal (40 min). Importantly, the char burn-out is not dependent of the original mass (or size) of the fuel.

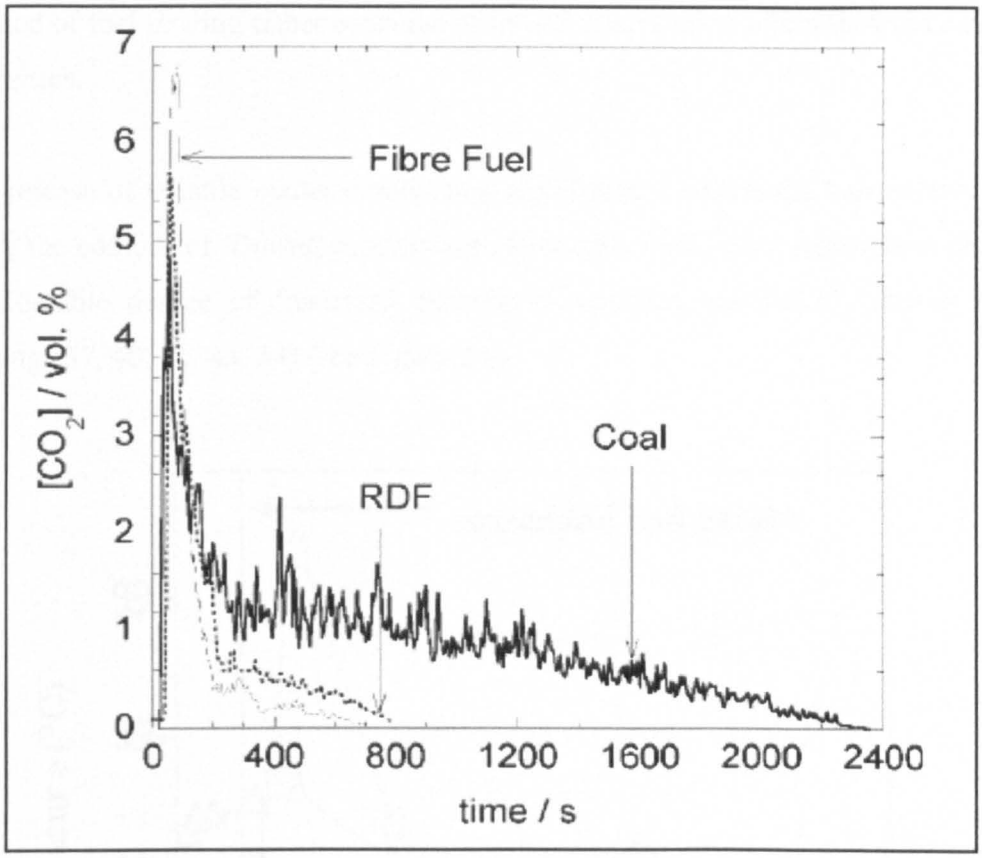

Figure 2.7 CO_2 concentrations during the combustion of fibre fuel, RDF and coal [48]

A comparison of pyrolysis, ignition and combustion of coal and biomass particles reveals the following:

1. Pyrolysis starts earlier for biomass fuels compared to coal fuels.

2. The fractional heat contribution by volatile matter in biomass is of the order of, 70% compared to, 30% for coal.

3. Burn out time for biomass is much less than coal due to the lower fixed carbon ratio.

2.2.4.2 Combustion Issues

2.2.4.2.1 Temperature Profile

The temperature profiles observed for biomass combustion are mainly governed by method of fuel feeding either over-bed or in-bed, distribution of combustion air and fuel properties.

The release of volatile matter combustion significantly affects the heat release profiles along the combustor. During combustion of biomass fuels, most researchers observed a considerable degree of freeboard burning of volatiles, particularly during over-bed feeding [37, 40, 41, 43, 44] (see Figure 2.8).

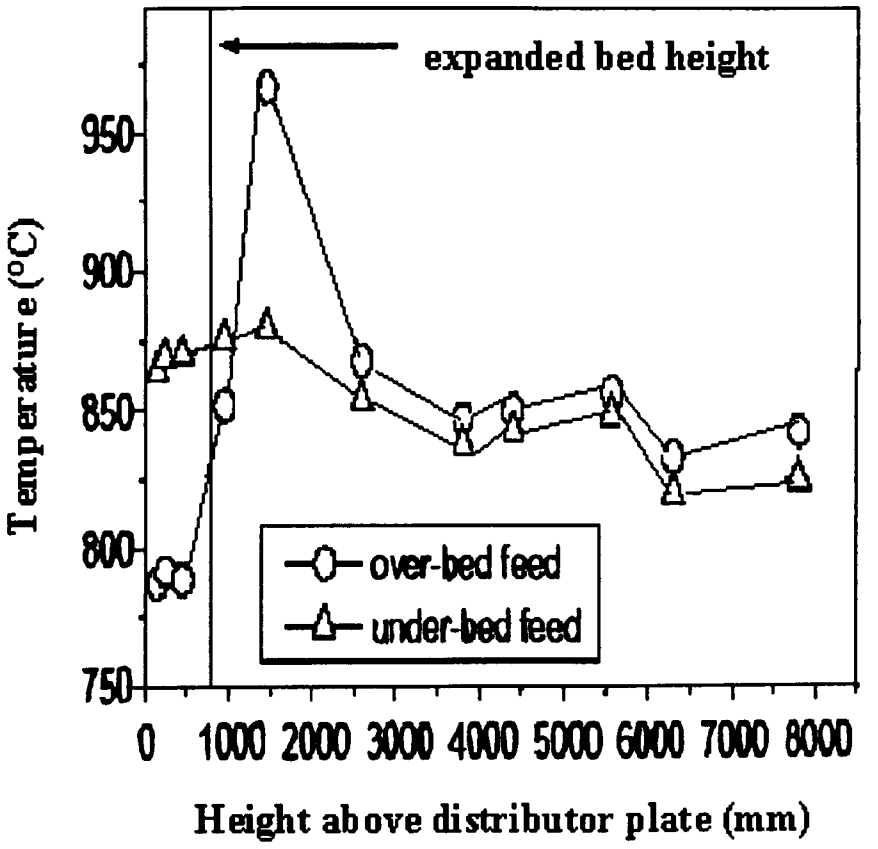

Figure 2.8 Temperature profiles in FBC combustor during combustion of biomass (over-bed feed: 1100 mm, in bed feed: 380 mm above distributor) [28]

Relatively, the distribution of combustion air also plays an important role for biomass combustion in a FBC system. Kuprianov and Pemchart [41] have carried out an experimental study on combustion of three distinct biomass fuels (sawdust (0.8 x 0.8mm) , rice husk (2.4 x 8 mm) and pre-dried sugar cane bagasse) in a single fluidized-bed combustor with a conical bed using silica sand as the inert bed material with over-bed feeding. The FBC comprised of two parts: (1) a conical section of 1 m height with the cone angle of 20°, and (2) a cylindrical section of 0.9 m inner diameter and 2 m height. They observed that varying excess air for a fixed load, the bed temperatures remained almost unchanged in the fluidised bed combustor using silica sand as the inert bed material. However, in the freeboard region the temperatures were found to have a tendency to increase for higher excess air. When excess air varied from about 20% to 100% in the tests with maximum fuel feed rate, the temperature at the combustor top (2.75 m height) increased by 60–80°C for firing rice husk and bagasse, whereas it increased by 160°C for firing sawdust. Similar observations were made by Armesto *et al.* [50] during combustion of rice husk in a 30 kW atmospheric FBC with in-bed feeding. Both suggested that the higher excess air contributes to higher fluidising velocities that will move the combustion zone to the freeboard. Also, higher fluidising velocity increases settling time for biomass to reach the bed and most combustion will be complete before the biomass reaches the bed surface.

Additionally, the moisture content is very high in the case olive oil waste and chicken litter (40-60%) which will also affect the temperature profile. High moisture contents have been found to increase the devolatilisation time and increased the burning inside the bed region. Also high water content, more than 20% can result in agglomeration, which promotes a poor fluidisation regime and at the same time reducing the bed temperature [43, 44]. In the case of co-combustion, most researchers found that the bed temperature decreased almost linearly with increasing fraction of biomass in the coal - biomass mixtures [49, 50, 51]. In fact, the higher the fraction of MSW, the higher freeboard temperature due to higher volatiles and lower fixed carbon in the MSW; thus, less fuel particles are burned in the bed [51]. This observation is in agreement with that of Cliffe and Patumsawad [52] who investigated the co-combustion of coal with waste from the production of olive oil, which contains high volatile matter.

Furthermore, Boavida *et al.*[30] have investigated the variation of temperature profile as a function of time during the combustion of coal with plastic wastes. It was observed that as the amount of waste was increased in the mixture supplied (fluffy plastics waste), the tendency of variations in the temperature profile become more pronounced. When just the coal was burned, the temperature was almost constant as shown in Figure 2.9(a). The addition of waste by 20% in weight was found to cause only a little disturbance in the bed temperature whereas a large variation in the freeboard as shown in Figure 2.9 (b). The thermocouples (T10 –T14) measured in the graphs denoted the bed temperature at 130, 550, 1100, 1600 and 4900 mm above distributor plate. This could be due to the fact that addition of plastic waste increased the amount volatiles released and most of which appeared to burn in the freeboard. The degree of combustion was claimed to be dependent on both the rate of the release of volatiles and the success of the subsequent mixing between volatiles and air, thus giving rise to oscillations in temperature along the freeboard height.

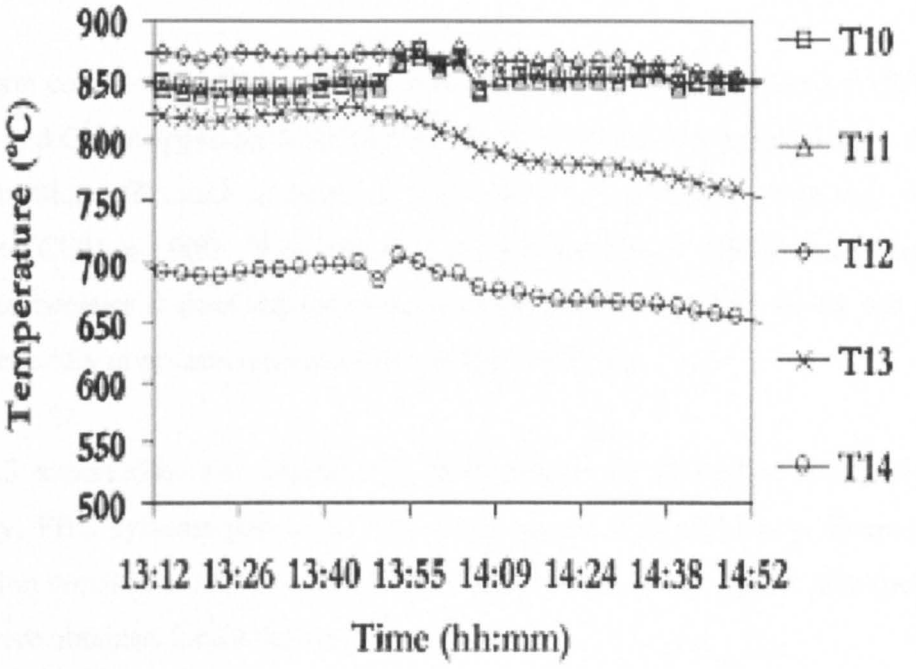

(a)

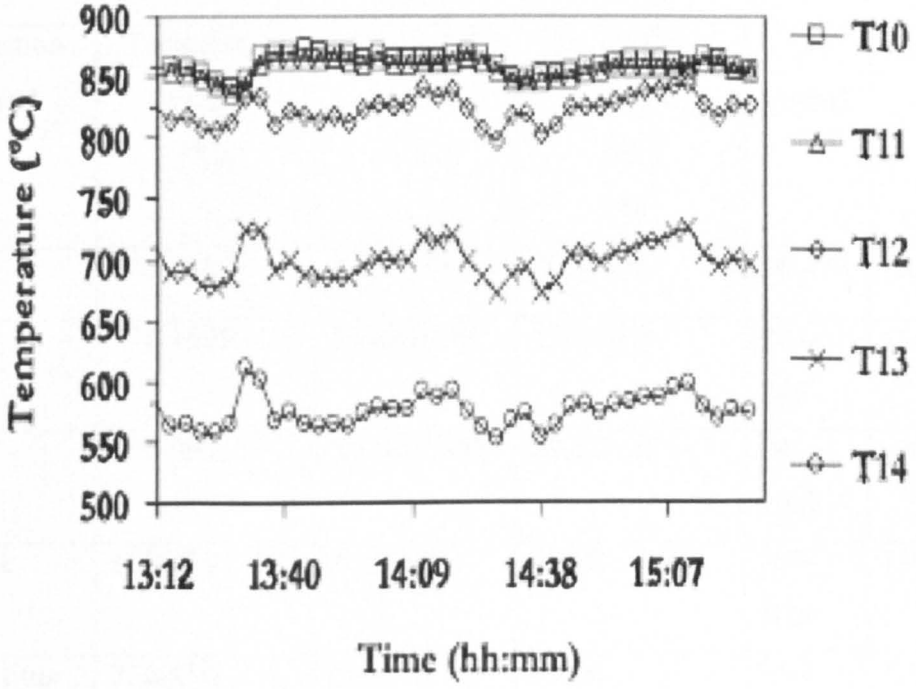

(b)

Figure 2.9 Temperature profile inside the combustor as the function of time when (a) coal and (b) mixture of 80% coal and 20% plastic waste was burned: Tbed = 850°C and 50% of excess air [30].

2.2.4.2.2 Combustion Efficiency

The carbon combustion efficiency of a system has been expressed as $\eta_C = (B/C) \times 100$ where B and C (see appendix B for derivation) [53]. Some of the authors have evaluated the combustion efficiency in terms of CO and CO_2 emissions, where $\eta_{CE} = [CO_2] / \{[CO_2] + [CO]\} \times 100\%$. However, this second method of calculation is considered inaccurate because it does not take into account unburned carbon in the ash products and so generally gives much higher combustion efficiency.

Table 2.5 summarises the combustion performance of alternative fuels in a FBC. Generally, FBC systems proved to have high combustion efficiency. Even when the combustion conditions are quite different between the tests for a particular fuel, similar values were obtained for all the cases.

Table 2.5 Combustion performances of alternative fuels in a FBC

Combustion material	Temperature range (°C)	Fractional excess air	Combustion efficiency (E2) (%)	CO (ppm)	References
Propane	366-843	0.746 -2.06	99.8-100	26-443	[53]
Wood	778-1099	0.102-0.649	85.0-98.9	205-345	[54]
RDF	800-963	0.174-0.803	80.1-91.8	34-1088	[24,55, 56]
Rice husk	650-800	0.30-0.95	81-98	200-5000	[39, 40,50]
Chicken litter	750-850	0.5-0.92	80-90	350-540	[20, 30]
Palm kernel/fibre	800-900	0.30-1.00	> 88	400-2000	[44]

In general, combustion efficiency is mainly governed by interaction between operating conditions (i.e. bed and freeboard temperature, excess air and secondary air) and fuel properties.

Armesto *et al.* [50] has stated that the bed temperature has an effect on combustion efficiency, which improves from 97% to 98% as bed temperature increased from 840 to 880°C. Also, they found that the efficiency increased with decreasing fluidising velocity. They claimed that when fluidisation velocity increased above 1.0 m/s, the combustion efficiency decreased. This behaviour was attributed to an increase in the elutriation of unburned carbon. On the contrary, Suthum [44] found that the combustion efficiency increased from 88% to 92% with increasing excess air (in relation with increasing fluidising velocity) up to 30% during combustion of oil palm waste in a 10 kW FBC with over-bed feeding. Saxena *et.al.* [53] also reported similar results. It was suggested that there is an optimum balance between the carbon to CO conversion rate and increased elutriation with high excess air.

Fahlstedt *et.al.* [57] carried out a series of tests on co-firing wood chips, olive pit and palm nut shell with coal in 1MW FBC facility. It was noted that the co-combustion had a slightly higher carbon combustion efficiency based on flue gas emissions (97.2 - 98.1%) than coal-only combustion (97.1%). The reason is likely due to the higher volatile matter content of the biomass fuels. Increased volatile matter will also increase the fuel reactivity and hence reduce the unburned carbon. This result agreed with Van Door et al. [58] who co-combusted of coal and wood, straw and sewage sludge in a fluidised bed combustor. In contrast, a decrease in combustion efficiency was obtained by Armesto *et al.* [50] and Suksankraison *et al.* [51] during co-combustion of Lignite-olive waste and Lignite-MSW mixture, respectively, even though the volatility of the fuel used quite similar (60-70% VM). The decrease was mainly attributed to a drop in the bed temperature. Since most fixed carbon generally burns in the bed while the volatile gas burns in the freeboard, there is insufficient chance for CO conversion to CO_2. CO formed in the freeboard will have less time to convert to CO_2 than that formed in bed. As the freeboard temperature is maintained at a higher value, devolatilisation

occurred rapidly and produced more volatile gases. As the biomass fraction increased, the reduced fixed carbon gives more chance for the volatiles to escape combustion. Additionally, the influence of excess air is also significant during co-combustion. Suksankraisorn *et al.* [51] found that for the case of secondary air, SA =0.2, at 0% waste, the efficiency decreased about 10-12% as the excess air increased from 40% to 100%. At 40% waste, the efficiency decreased about 5-10%. This trend was similar to that observed by most other researchers during co-combustion of various types of biomass with coal [50, 53]. As mentioned earlier, at high excess air, the particle elutriation rate is greater than the carbon to CO_2 conversion rate. Hence, it was expected that higher unburned would be carbon collected in the ash. Secondary air was found to have only a slight effect on carbon combustion efficiency. Since the change in proportion of secondary air affects the stoichiometry in the bed at the same time, a potential gain in combustion efficiency above the bed may be negated by a lower efficiency in the freeboard due to a lower temperature [52]. Also, secondary air does not alter the velocity in the bed but only alters the velocity in the freeboard.

2.2.4.2.3 CO Emissions

Significant fluctuations of CO emissions were reported during co-combustion of biomass in a FBC. The value of the CO concentration in the flue gas has been found to depend on the type of fuel, fuel properties (volatility, particle size and density) and the operating conditions (bed and freeboard temperature, excess air, secondary air). In addition to the expected immediate ignition and the high volatile matter contents, the volatiles consist mainly of the combustibles (CO, H_2, C_xH_y). These factors together indicate that the combustion of the volatiles would be the dominant step during the biomass combustion. At higher temperatures, the combustibles (CO, H_2, CH_4) accounted for more than 70–80% of the gas components [28]. Most researchers have made these observations during combustion of oil palm shell and fibre, and rice husk [44, 50].

Saxena *et al.* [55] found that the hydrodynamic activity in the bed is related to the solid mixing and gas-solids contacting and these in turn are directly related to CO emissions. Higher bed temperature seems to provide optimum conditions for rapid devolatilisation

and hence increased conversion CO to CO_2. They found that in the turbulent regime, the carbon utilisation efficiency reached a maximum and a further increase in the fluidisation velocity had an insignificant influence on the bed hydrodynamics and hence CO emissions. Similarly, as most of the biomass combustion was observed to take place in the freeboard, the supply of oxygen to this zone in amounts sufficient to achieve satisfactory combustion had to be ensured. It was verified by Abelha *et al.* [20] during combustion of chicken litter in a 0.3 m diameter x 5 m high FBC that if all the air was introduced as fluidising air, the level of CO was high and there were fluctuations which suggested that the mixing of air with fuel was always efficient. Furthermore, Sami *et al.* [13] found that if the level of CO was within acceptable limits, then approximately 10% excess air and a temperature of 650°C provided optimum conditions for the combustion of manure in a fluidised bed unit. However, there was a significant improvement in CO emissions, particularly when the air to the freeboard was introduced at different heights (air staging). The CO levels were brought down to about 60 mg/N m^3 at 11%O_2 in the flue gases, which is very close to what is permitted by EU directives; 50 mg/N m^3 at 11% O_2.

Additionally, Guilin *et al.* [23] have discussed the relation between the air ratio and the CO concentration in product gas at a bed temperature of 775°C without secondary air injection during combustion of two different RDF fuels in a 0.3 m x 0.3 m and 2.73 m high bubbling type Fluidized bed combustor with overbed feeding. The diameters of the two RDF fuels (RDF-A and RDF-B) were both 15 mm, and the lengths were 25 mm and 40 mm, respectively. Fuel ratios (the ratio of fixed carbon to volatile matter) were 0.178 and 0.054, which were significantly different from each other but with similar CV (20 and 18 MJ/Kg, respectively). In addition, the compressive strength of RDF-A and RDF-B were 1.39 MPa and 3.32 MPa, respectively. For RDF-B, the results indicated that the CO concentration (about several ppm) slightly decreased with an increase of air ratio (ratio of primary air to secondary air). However, for RDF-A, the air ratio strongly affects CO concentrations when air ratios increase from 1.4 to 2.4. The CO concentration decreased rapidly from several hundreds of ppm to less than 100 ppm. Since the density and strength of RDF-A was much lower than RDF-B, RDF-A was easily broken down into small fragments and the entrained fragments were burnt in the

freeboard. However, since the reaction rate of RDF- A was slower than that of RDF-B, part of the combustible gas/solid in RDF-A did not have enough time to react and exited from the combustor and unburned. However, the results indicate that when the secondary air was used, the CO concentrations for both RDF-A and RDF-B were decreased (see Figure 2.10).

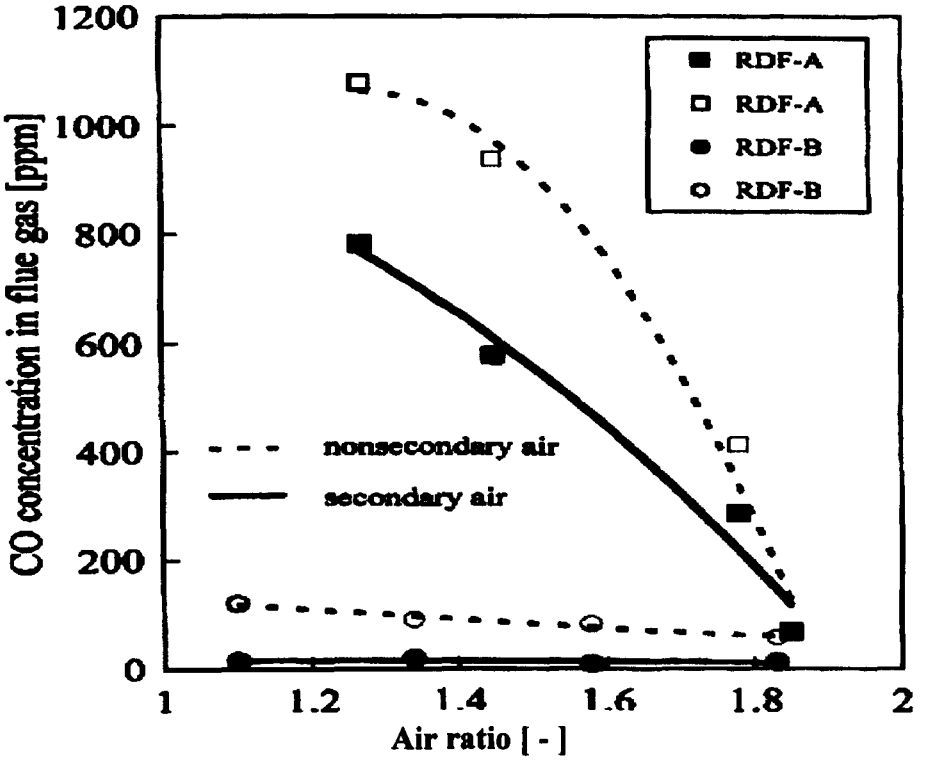

Figure 2.10 Effect of secondary air injection on CO concentration in flue gas at bed temperature 800°C [23]

The trends observed during single fuel combustion are reflected also in co-combustion: in the practically important cases with moderate amounts of biomass (an energy fraction of less than 25%) the properties of the base fuels dominate the emission obtained. Suksankraisorn *et al.* [51] reported that for 100% lignite combustion, CO drops significantly as excess air increases due to the increased CO to CO_2 conversion. However, with co-combustion of MSW with lignite, the emission of CO is relatively insensitive to changes in excess air and waste fraction, which further strengthen the argument that co-combustion is dominated by the combustion of the volatiles in the freeboard zone (see Figure 2.11). Furthermore, the increase of secondary to total air ratio beyond 0.1 causes an increase in CO due to the reduced in bed excess air, particularly at low waste fraction.

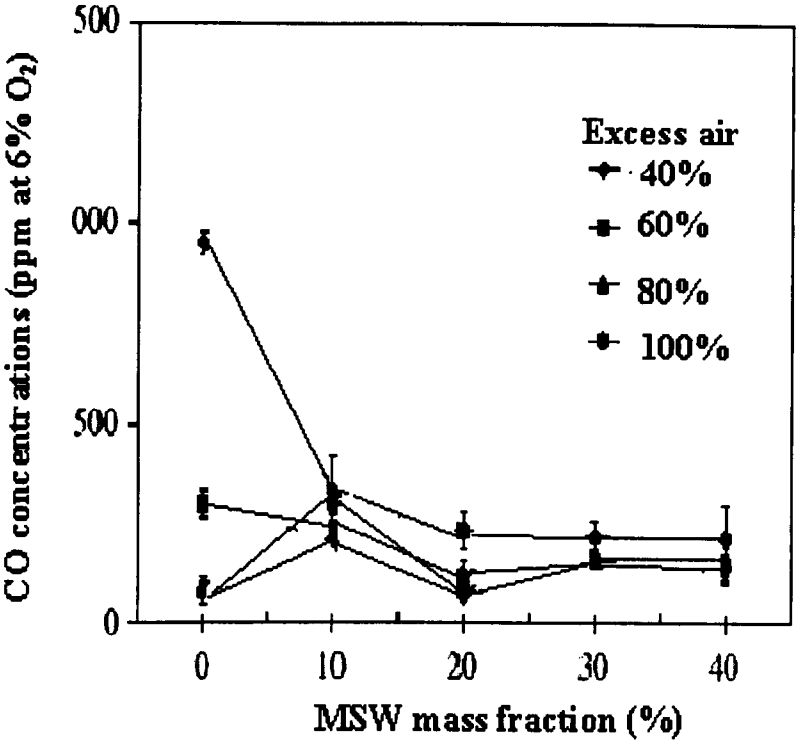

Figure 2.11 CO emission as a function of MSW mass fraction and excess air at SA=0.2 during co-combustion lignite-MSW mixture [51]

In contrast, in the work of Desroches-Durcane [59], CO concentration was almost constant for coal mass fraction less than 30% but it increased steadily with an increase fraction of coal during co-combustion of simulated French MSW with coal in a 25 kW CFB. This was due to the significant difference of moisture content between MSW used (Suksankraisorn MSW (60%) and MSW (35%)) as well as in the fixed carbon content between bituminous coal (70%) and lignites (35%). The higher CO emission was observed as coal mass fraction higher than 30% caused by additional CO production from char combustion and HCl formation that inhibit the CO oxidation. Leckner and Karlson [54] also observed similar results during the co-combustion of bituminous coal with wood in a pilot scale 12 MW CFB.

2.2.4.2.4 Ash Related Problems

As stated previously, the feasibility of FBC technologies has been widely demonstrated for the combustion of a variety of fuels. Moreover, the environmental benefits associated with these technologies are well established. As a drawback, severe problems of agglomeration in the bed as well as fouling and slagging may sometimes occur, especially during combustion of biomass fuels. As already mentioned in section 2.1, some biomass fuels especially agricultural residues have high contents of alkali oxides and salts, the low melting points of which may lead to various problems during combustion.

a) Bed Agglomeration

Agglomeration of the bed material is defined as a gathering of particles into clusters that are larger than the original bed particles. Often the same phenomenon is described by the term 'bed sintering'. Agglomeration of the bed material decreases heat transfer in the bed and the quality of fluidisation, leading to poor combustion efficiency and loss of control of the bed operational parameters. In the worst case, agglomeration may result in total de-fluidisation of the bed and unscheduled plant shutdowns [60].

The "coating" behaviour of bed particles is regularly detected when firing biomass in a fluidized bed, especially when quartz sand is used as bed material [61]. The ash layer covering the bed particle includes mainly non-volatile ash elements. The quartz core below the "ash coating" reacts with alkalis (K and Na) released during combustion. It consists mainly of SiO_2, the melting point of which is around 1450°C [28]. Thus, this should not be a problem in a FBC since the bed temperature usually ranges between 800-900°C. The biomass ash however builds a "new" bed material by depositing on the bed particles. Inorganic mixtures formed in bed do not melt at a certain temperature but have a wide temperature range where both the solid phase and the liquid phase are present. Alkali silicates for example have a low melting point and may cause sintering or agglomeration of bed. A pure potassium oxide has the first melting temperature at 742°C within the range of K_2O between 0.25 and 0.5 [28].

Wether *et al.* [28] encountered the problems of sintering and agglomeration during the combustion of coffee husks in a 150 mm diameter fluidized bed combustor. The test plant had previously been used to burn various coals, sewage sludge and wood chips without any agglomeration problems. Similar observations were reported by Bapat *et al.* [62] during the firing of sunflower husks, cotton husks, soya husks and coconut shell with silica sand as bed material (see Table 2.3 for composition). All the materials resulted in bed agglomeration within 4–6 h of operation.

Also, some agricultural residues have low contents of K_2O and can be burnt in fluidized bed without agglomeration problems. For example, Preto *et al.* [40] reported successful burning of rice husks in a pilot scale fluidized bed plant (cross-section 380 mm x 406 mm, total height 4.8 m) without experiencing any agglomeration. The rice husks produced a very fine ash, which was easily carried out from the bed and was subsequently separated from the flue gas by cyclone. It has been shown experimentally that rice husks have a melting point much higher than the normal operating temperatures found in a fluidized bed. Moreover, Liu et al. [63] placed rice husk samples in crucibles and heated for 2 h in an electric furnace at 950, 1000 and 1050°C, respectively. The result showed that the rice husk did not agglomerate or slag. The ash fusion point of the rice husk was found to be above 1500°C.

In addition, appropriate fuel mixing can significantly reduce agglomeration tendencies. Co-combustion with coal has sometimes been suggested to help [19]. Results obtained by Miles *et al.* [64] and Ergudenler and Ghaly [65], however, imply that both the silica-rich bed material and silica-containing fuels may participate in the bed agglomeration process through the formation of low melting alkali silicates.

b) Slagging and fouling

Slagging and fouling of combustor surfaces is a major issue that has played an important role in the design and operation of combustion equipment. Slagging can be defined as the deposition of fly ash on the heat transfer surface and refractory in the furnace volume primarily subjected to radiant heat transfer. Fouling is defined as deposition in the heat recovery section of the steam generator subject mainly to convective heat exchange by fly ash quenched to a temperature below its melting point. Slagging and fouling reduces heat transfer and causes corrosion and erosion problems, which reduce the lifetime of the equipment. The degree of slagging and fouling varies throughout the boiler depending namely on: (1) local gas temperature, (2) gas velocities, (3) tube orientation, and (4) fuel composition [19].

The main factors that contribute to fouling are caused by inorganic materials in the fuel. Biomass ash contains a larger amount of alkalines compared with coal ash. This is particularly true for some agricultural residues and new tree growth. The chemical composition of ash, such as alkali metal, phosphorous, chlorine, silicon, aluminium and calcium content, as well as the chemical composition of the compounds, affect ash melting behaviour. Alkaline metals compounds are easily vaporised during combustion. In biomass fuels, a major proportion of inorganic material is in the form of salts or bound in the organic matter, but for example in coal, a large proportion of inorganic substances are bound in silicates, which are more stable. Additionally, chlorine-rich deposits induce hot corrosion of heat transfer surfaces. Although slagging and fouling may be detected quite quickly, corrosion progresses slowly over a longer period and may also occur without any associated slagging or fouling [13].

Muthukrishnan *et al.* [65] have encountered the problems of fouling and slagging during the commissioning of a 10 MW fluidized bed combustion plant firing 100% rice stalk in baled forms. The rice stalk had an alkaline (K_2O+ Na_2O) content of 7.2 wt%. The resulting high flue gas temperatures (>1000°C) softened the ash and led to ash deposition on the convection superheater tubes in the flue gas path. The deposition rate was so high that in less than 12 h of operation the space between the convection superheater tubes was completely bridged with ash and the flue gas could not pass

through it. In contrast, there was no deposition on the furnace walls and roof tubes where the surface temperatures were lower because of the water/steam mixture in the tubes. A similar experience has also been reported on straw fired hot water boilers in Denmark where their capacity ranged from 1 to 10 MW. Miles *et al.* [63] have suggested that above 0.17 kg alkali/GJ fouling is probable and above 0.34 kg/GJ, fouling is virtually certain to occur in a combined heat and power (CHP) plant. The alkali index (in kg/GJ) i.e. for almond hulls is 1.75, for rice straw 1.6, for wheat straw 1.1 and for rice hulls 1.0. This indicates that fouling should occur for rice hulls in most operations. For comparison, the alkali index of a typical bituminous coal is 0.07 kg/GJ. This alkali index may be useful to give an indication as to whether ash problems occur. It should be noticed that ash melting points measured in the laboratory or indices calculated from the ash composition are far from being sufficient to predict the ash behaviour in a large-scale plant.

However, according to present knowledge, control of the rate of deposit formation in biomass combustion is associated with the reactions between compound that contain chlorine, sulphur, aluminium and alkaline substances. High-risk chlorine compounds are of the type NaCl or KCl. These alkaline chlorides can, however, react with sulphur and aluminium silicate compounds releasing HCl [19].

$$2KCl + SO_2 + \tfrac{1}{2} O_2 + H_2O \rightarrow K_2SO_4 + 2HCl \quad (2.1)$$

$$Al_2O_3 \cdot 2SiO_2 + 2KCl + H_2O \rightarrow K_2O \cdot Al_2O_3 \cdot 2SiO_2 + 2HCl \quad (2.2)$$

The S/Cl ratio in the feedstock has often been shown to affect Cl deposition and corrosion. In addition to aluminium silicate reactions, one parameter that has been often referred to is the sulphur-to-chlorine atomic ratio (S/Cl) in fuels or fuel blends. It has been suggested that if the S/Cl ratio of fuel is less than two, there is a high risk of superheater corrosion. When the ratio is at least four, the blend could be regarded as non-corrosive. According to recent studies AlSi/Cl ratio can even dominate over the S/Cl ratio. This phenomenon was illustrated in Figure 2.12 [19].

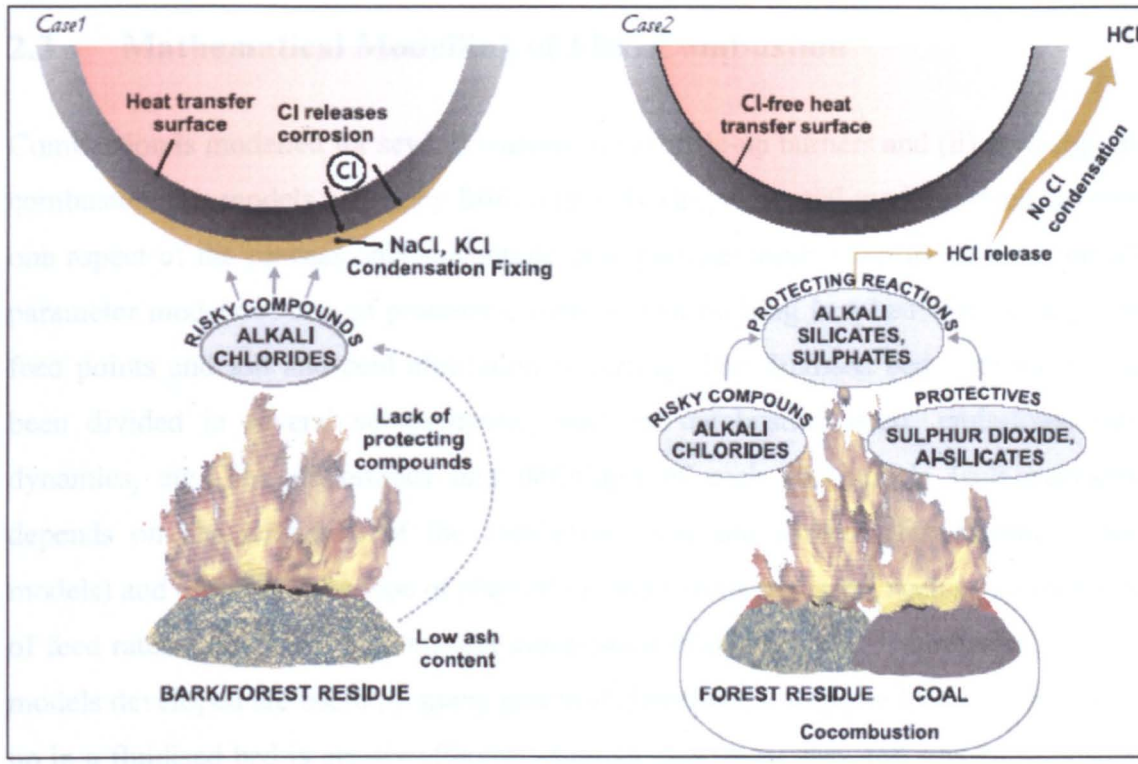

Figure 2.12 The phenomenon of ash deposition on the heat transfer surfaces during combustion of single biomass and co-combustion with coal.

In Case 1, bark or forest residue is combusted alone. The ash of these fuels has high alkaline metal content. When this is associated with high chlorine content, which is often the case, these elements react to form alkali chlorides. This, in turn, induces corrosion rates after deposition of these substances on the heat transfer surfaces. In Case 2, sulphur and aluminium silicates from coal ash are able to form alkali silicates and alkali sulphates. Now chlorine is released as HCl in flue gases and alkali metals are bound in compounds that have a high melting point and no corroding effect. A different approach has been made by Baxter [67] who addressed ash deposition and corrosion problems during coal and biomass combustion in his developed mechanistic model which was mainly controlled by biomass fuel combustion. As well as types of inorganic material in the fuel blend, the combustion conditions such as temperature and fluidising velocity has been identified as the major mechanisms of ash deposition. Baxter [67] has concluded that as compared to deposits from coal combustion, the strength of biomass combustion deposits will be higher, with smooth deposits surfaces and little deposit porosity. This means that the deposits from biomass combustion may be hard to remove.

2.3 Mathematical Modelling of FBC Combustion

Combustion is modelled for several reasons; (i) to scale-up burners and (ii) to design the combustor. The models used vary from relatively simple, partial models which describe one aspect of the process only, i.e. single char particle combustion models, to lumped parameter models of sets of processes, such as coal burning in a bed with several coal feed points and ash and coal elutriation occurring. The fluidised bed combustion has been divided in several sub-processes, such as combustion itself, emissions, fluid dynamics, etc. The importance and definition of each sub-models (sub-processes) depends on characteristics of the combustor, fuel and sorbent (for emissions sub-models) and especially the type of predictions and results expected, such as optimisation of feed rates, pollutant emissions and combustion efficiency, etc. The relatively simple models developed are useful in many practical situations. For example, the carbon hold-up in a fluidised bed is greatly affected when air flow rates vary and several trends can be predicted, indicating excess air level, the maximum particle temperature which relates to sintering and the bed temperature. The algebraic simplicity of the simple models can, in many cases, more than make up for their mechanistic limitations. Mano and Reitsma have proposed a complete framework of a FBC modelling (see Figure 2.13)[68].

A number of FBC models have been developed. Most of the mathematical modelling for combustion in fluidised beds is based on the two-phase theory, which only takes into account the solid-free bubble and the emulsion phase (where the solid are mixed). The three-phase model has included the drag of particles within the wake (third phase) of the moving bubbles. There are several discrepancies between the models, especially in the hydrodynamic and kinetic sub-models. Related to this, Adanez and Abanades [69] have carried out a sensitivity analysis on the modelling of the combustion of lignite in a fluidised bed. They found that although some sub-models describe processes in the bubbling bed more realistically than others, they do not improve the quality of some results and only complicate the solution of the model. Their evaluation of the sensitivity analysis results is shown in Table 2.6.

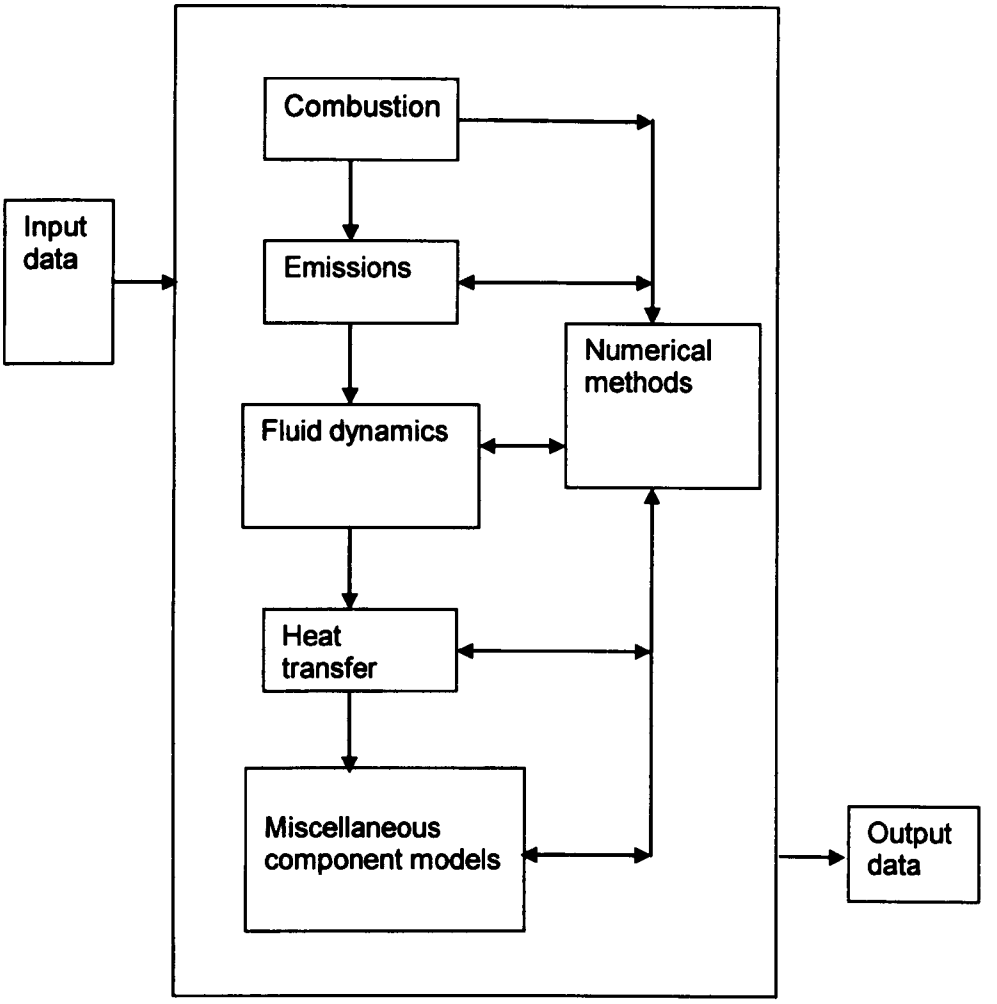

Figure 2.13 General framework of a FBC model [68]

Table 2.6 Sensitivity analysis of the combustion efficiency in a FBC [69]

Low impact	High impact
✓ Equations to calculate the heat and oxygen transfer coefficient around the particle ✓ Place and kinetics of the devolatilisation as long as it occurs inside of the bed.	✓ Reactivity of the coal used ✓ Value of the elutriation constant considered ✓ The type of bubbles in the bed which determine the oxygen transfer between phases.

For the purpose of the simulation, most of the researches have distributed the FBC into three sections: the bed (dense phase), the splashing region (emulsion phase) and the freeboard (dilute phase) [69]. Accordingly, the splashing zone has been considered well stirred as regards both the gas and the solid phases. Furthermore it is assumed that afterburning of volatiles by passing the bed is completed within this region. Plug flow pattern applies to the freeboard section, where only fines post-combustion take places.

Scala and Salatino [70] have carried out a simple lumped-parameter model of the FBC modelling work based on the fluid dynamics in the bed and on the two-phase fluidisation theory to model the combustion of high volatile solid fuels. The combustor was divided into three sections: the dense bed, the splashing region and the freeboard. A general diagram of the material balance is presented in Figure 2.14(A), which is based only on the fixed carbon, volatile matter and oxygen in each combustor section during combustion of a solid fuel, taking into account fuel particle fragmentation and attrition, volatile matter segregation as well as post-combustion of both carbon fines and volatiles escaping the bed. The study was complemented by a simplified thermal balance on the splashing zone taking into account volatiles and elutriated fines post-combustion and radiative and convective heat fluxes to the bed and freeboard (see Figure 2.14(B)). Results from calculations with either low or high volatile solid fuels indicate that low volatile bituminous coal combustion takes place essentially in the bed mostly via coarse char particles combustion, while high-volatile biomass fuel combustion occurs to a comparable extent both in the bed and in the splashing region of the combustor.

A more complex model to describe the hydrodynamic behaviour of the bubbling fluidised bed using a three phase model has been developed by Marias *et al.* [71]. The third phase considered in this model is a film between the bubble (fuel lean) and the emulsion (fuel rich) phases that helps to describe the diffusion phenomena occurring inside of a fluidised bed. This model in particular, focussed on the formation of SO_x and NO_x emissions.

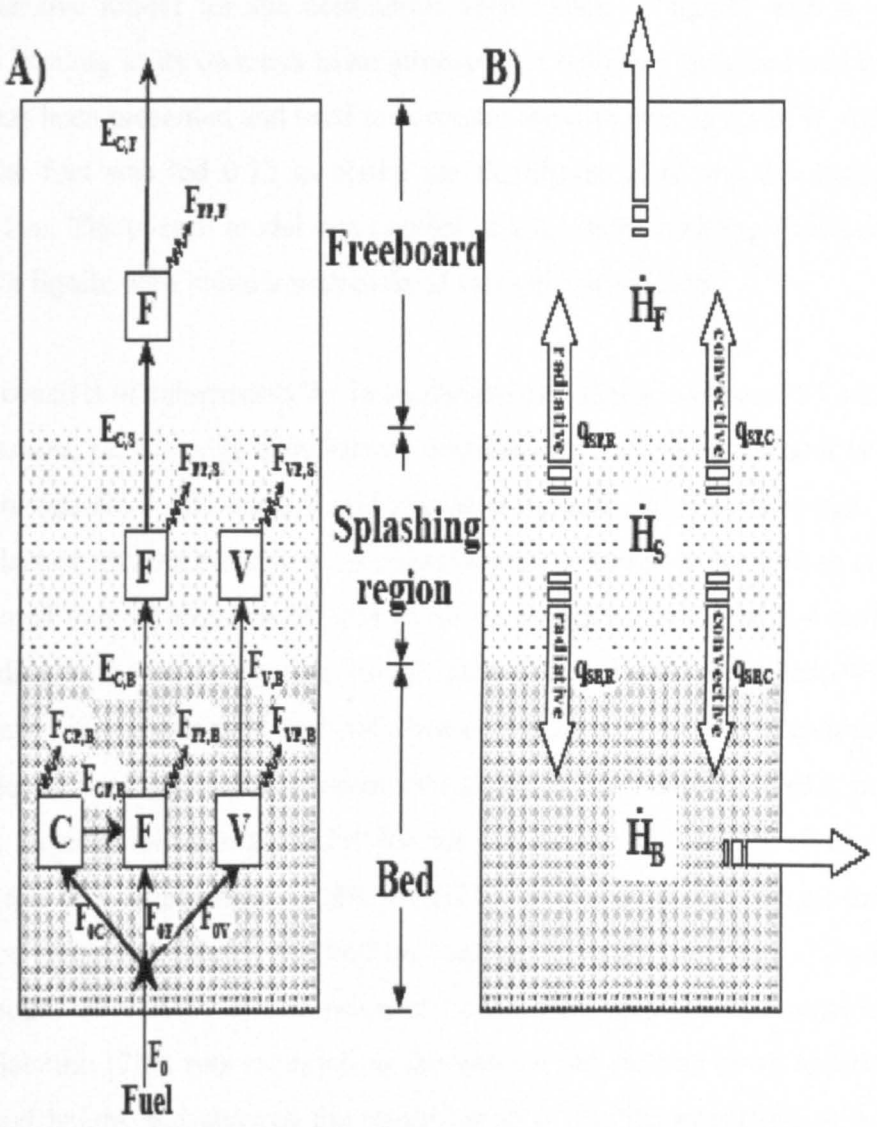

Figure 2.14 Scheme representing material balances on combustibles (A) and fluxes (B) in the various combustor sections [70]

Nomenclature of Figure 2.14

$F_{xy,z}$ = mass flow rate from the x^{th} phase to the y^{th} phase in the z^{th} section
$E_{xy,z}$ = unburned fixed carbon escaping the z^{th} reactor section
Fuel phases:
0 = raw fuel
V = volatile matter
F = Fine char particles
P = combustion products (H_20 and CO_2)
$q_{SF,R}$: heat flux from splashing region to the freeboard; radiative heat transfer mechanism
$q_{SB,R}$: heat flux from splashing region to the freeboard; radiative heat transfer mechanism
$q_{SF,C}$: heat flux from splashing region to the freeboard; convective heat transfer mechanism
$q_{SB,C}$: heat flux from splashing region to the freeboard; convective heat transfer mechanism

A comprehensive model for the continuous combustion of lignite with a wide size distribution burning in its own ash in an atmospheric bubbling fluidised bed combustor (ABFBC) has been presented and used to correlate the data from a 0.3 MW ABFBC test rig [72]. The fuel was fed 0.22 m above the distributor plate and the expanded bed height was 1 m. The overall model was applied to a 0.3 MW bubbling fluidised bed test rig fired with lignite with volatile matter/fixed carbon ratio of 2.16.

The model consists of sub-models for hydrodynamics, volatiles release and combustion, char combustion, particle size distribution, entrainment and elutriation and is based on conservation equations for energy and chemical species. It was assumed that fuel particles splashed into the freeboard de-volatilise and fell back to the bed as char. Also, it was assumed that combustion of char particles elutriated from the bed surface took place according to the shrinking-core model and was kinetically controlled. With regard to heat transfer, it was assumed that both bed and freeboard operate non-adiabatically, and all modes of heat transfer were taken into account. The volatiles release model was based on a particle movement model for the estimation of portion of the volatiles released in the bed. Application of this model led to the release of 9% of the volatile matter to the freeboard despite the bottom feeding of lignite particles. This indicated that the amount of volatile matter released in the freeboard (as discussed earlier by Scala and Salatino [70]) was expected to increase as the feeding point approaches the expanded bed height and showed the significance of the incorporation of a volatiles release model into the system model particularly for high volatile coals. Figure 2.15 illustrates the comparison between the predicted and measured temperatures along the combustor for the experiment under consideration. Predicted profiles and the measured values are found to be in reasonable agreement. The fall in the gas temperature toward the exit is due to the presence of a cooler in the top of the reactor. Predicted mixed mean and measured concentrations of O_2, CO_2 and CO along the combustor are compared in Figure 2.16. As depicted in the figure, predicted gas concentration profiles follow the same trend as measurements in both bed and freeboard sections of the combustor. A decrease in oxygen and increase in carbon dioxide concentration occurs but with a lower slope in the freeboard section indicating the combustion of volatiles in the freeboard.

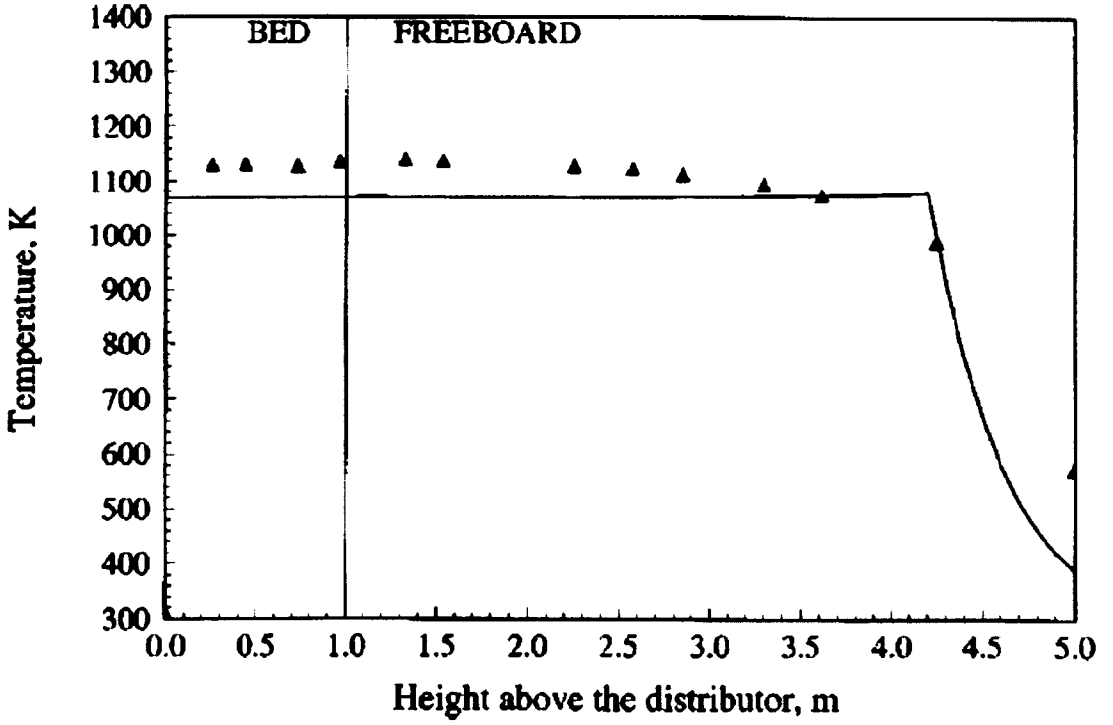

Figure 2.15 Measured (▼) and predicted temperature profiles [72]

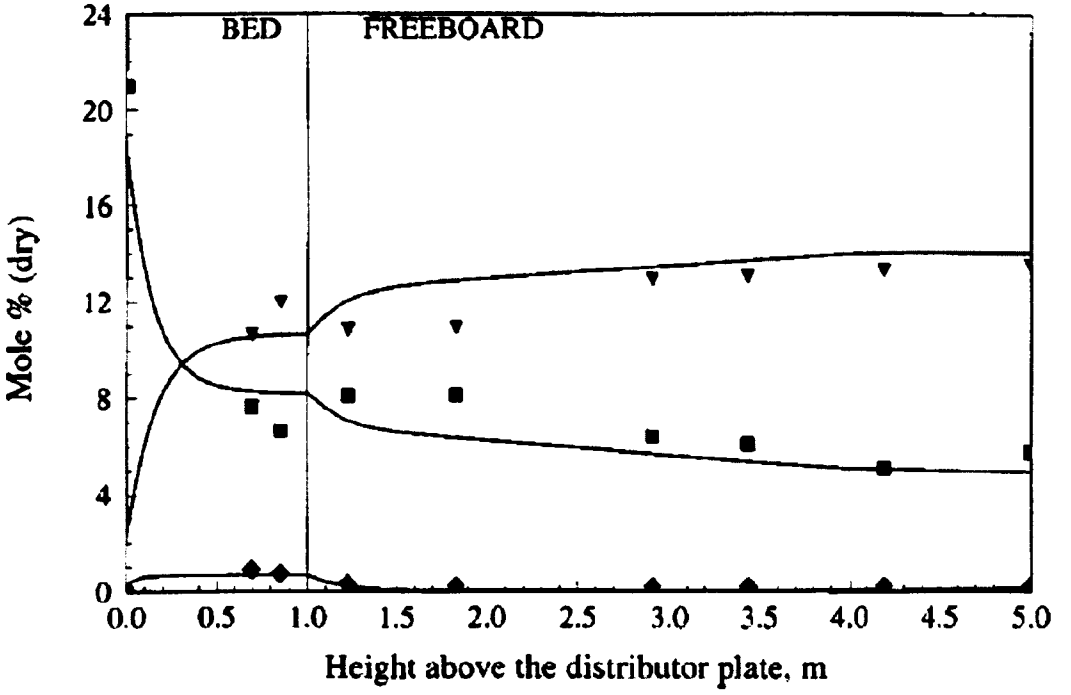

Figure 2.16 Measured .O_2 : ■, CO_2 : ▼, CO: ♦. and predicted mixed mean concentration profiles [72]

2.4 SUMMARY

The following summary can be drawn concerning fluidised bed combustion of coal and solid fuels:

- Co-combustion of biomass with coal offers significant advantages over single fuel combustion by reducing fuel costs, atmospheric pollutants (CO_2, NO_x and SO_2) and offers a method of disposing of high moisture content waste

- Biomass in general has lower calorific value, bulk density, carbon content but higher volatile matter content and oxygen content compared to coal.

- Combustion in a FBC undergoes three main processes (drying, devolatilisation and char combustion) and their characteristics are mainly governed by physical (particle size and density), chemical (C, H, O, N, S), thermal (calorific value) and mineral properties (K, Na, Si, etc).

- Combustion of the volatiles will be the dominant step during the combustion of agricultural residues and related biomass. A considerable degree of freeboard burning of volatiles was observed particularly during over bed feeding. Fluidising velocity (superficial velocity), secondary air (air staging), particle size, particle density and moisture content are other important parameters that affect the temperature profile during co-combustion.

- Low particle density fuels such as straw and rice husk are suitable for in-bed feeding while over-bed feeding is more suitable for high particle density fuel such as coal, palm kernel shell and other nut shells. This is related to de-volatilisation time and to reduce fragmentation or segregation problems during feeding. Also a more uniform temperature distribution occurs during over-bed feeding compared to in-bed feeding due to efficient heat transfer from the combustion process.

- Single biomass combustion efficiency has been improved up to approximately 10-15% with co-combustion. An increase in co-combustion efficiency is likely due to

the higher volatile matter content of the biomass fuels and the high carbon content of coal. The high volatile matter content of the biomass can compensate each other during co-combustion and provide a better combustion process than individual fuels, providing the bed temperature is maintained in the region of 800-900°C. Also, the combustion efficiency increases with increased excess air up to 80% and when air staging is applied. Also efficiency can be increased with moisture content up to a maximum value of 15%. However, there is a lack of information regarding the relationship of fuel particle size and density on combustion efficiency.

- Significant fluctuations of CO emissions occur during the co-combustion of biomass with coal. CO emissions increase as the biomass mass fraction increases due to high volatiles concentration but this value is reduced with increasing fluidising velocity or air staging. However, there are some reports those CO emissions increase as the mixing ratio of coal to biomass increases (>30%) because of CO oxidation to CO_2 is inhibited by char combustion and HCl formation.

- The presence of very high contents of potassium oxide gives low melting temperatures of the ashes and result in bed agglomeration in fluidized bed as well as fouling, slagging and corrosion of the heat transfer surfaces. A pure potassium silicate has a melting temperature at 742°C. Miles et al. [64] have suggested that above 0.17 kg alkali/GJ fouling is probable and above 0.34 kg/GJ fouling is virtually certain to occur. Co-combustion of biomass with coal reduced this effect.

- In modelling, the development of models of co-combustion (i.e. in relating experimental results with predictions results) is still in an early stage. To date, there only one model available has been validated experimentally [72].

CHAPTER 3

EXPERIMENTAL APPARATUS AND METHODOLOGY

3.1 Experimental Rig

A sketch of the experimental fluidized bed is shown in Figure 3.1. The combustor was 0.15 m diameter and 2.3 m high allowing bed depths up to 0.3 m with 2 m in freeboard height and consisted of sand with an average diameter of 850 μm. Fluidising air was introduced at the base of the bed through a nozzle distributor and used as both fluidisation and combustion air. Fuel was fed pneumatically to the bed surface from a sealed hopper through an inclined feeding pipe and the flow rate was controlled by a screw feeder. Entrained bed materials and fly ash were captured by the hot cyclone and they were collected in a separate catch pot. On-line gas analysers continuously monitored the oxygen, carbon monoxide, and carbon dioxide concentrations in the flue gas. Temperatures along the combustor were monitored continuously by using thermocouples.

The experimental rig consisted of the following parts:

3.1.1 Combustor

The combustor body was made of 1 cm thick 306 stainless steel. The combustor vessel was 0.15 m diameter and 2.3 m high, including 0.3 m high bed of sand (average size of 850μm) and 2 m freeboard. The freeboard vessel was insulated with Kaowool insulation. A pair of opposite openings at a height of 0.10 m above the bed section was made, one that houses the pilot burner for start-up operation and the other one as a view port. There were three ports for temperature monitoring in the bed and another five ports in the freeboard. Detail design of the combustor is presented in appendix A-1.

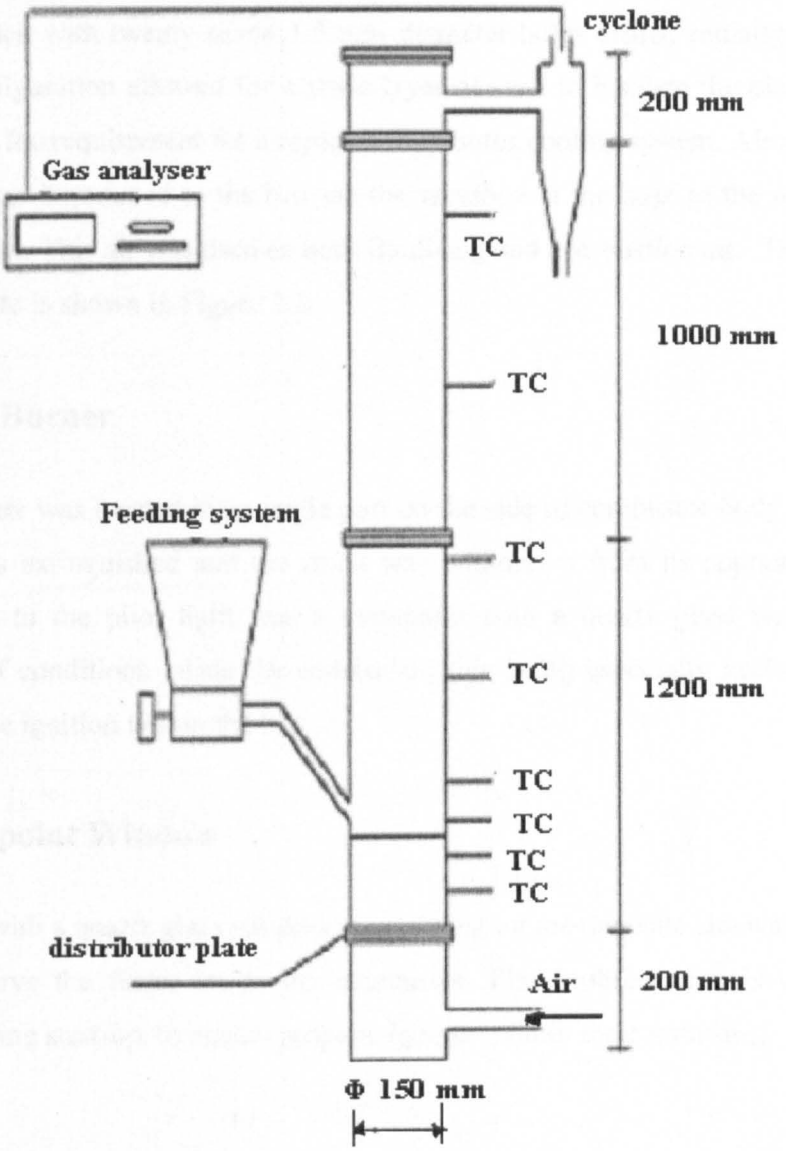

Figure 3.1 Diagram of experimental rig

3.1.2 Distributor Plate

The distributor plate was a 10cm thick stainless steel plate with nineteen 6cm high capped standpipes, each with twenty seven 1.5 mm diameter holes drilled radially just below the top. This configuration allowed for a static layer of sand to insulate the plate from the hot bed removing the requirement for a separate distributor cooling system. Air supplied from a compressor was introduced to the bed via the windbox at the base of the unit through the distributor plate. This air was used as both fluidising and combustion air. The layout of the distributor plate is shown in Figure 3.2.

3.1.3 Pilot Burner

The pilot burner was located in an angle port on the side of combustor body. After start- up the flame was extinguished and the torch was withdrawn from its support tube. On the opposite wall to the pilot light was a viewpoint with a quartz glass window allowing observation of conditions inside the combustor, this being especially useful at start-up to ensure propane ignition within the bed.

3.1.4 Viewpoint Window

A viewpoint with a quartz glass window was located on the opposite sidewall to the pilot in order to observe the flame inside the combustor. Flame observation is very important, especially during start-up, to ensure propane ignition within the combustor.

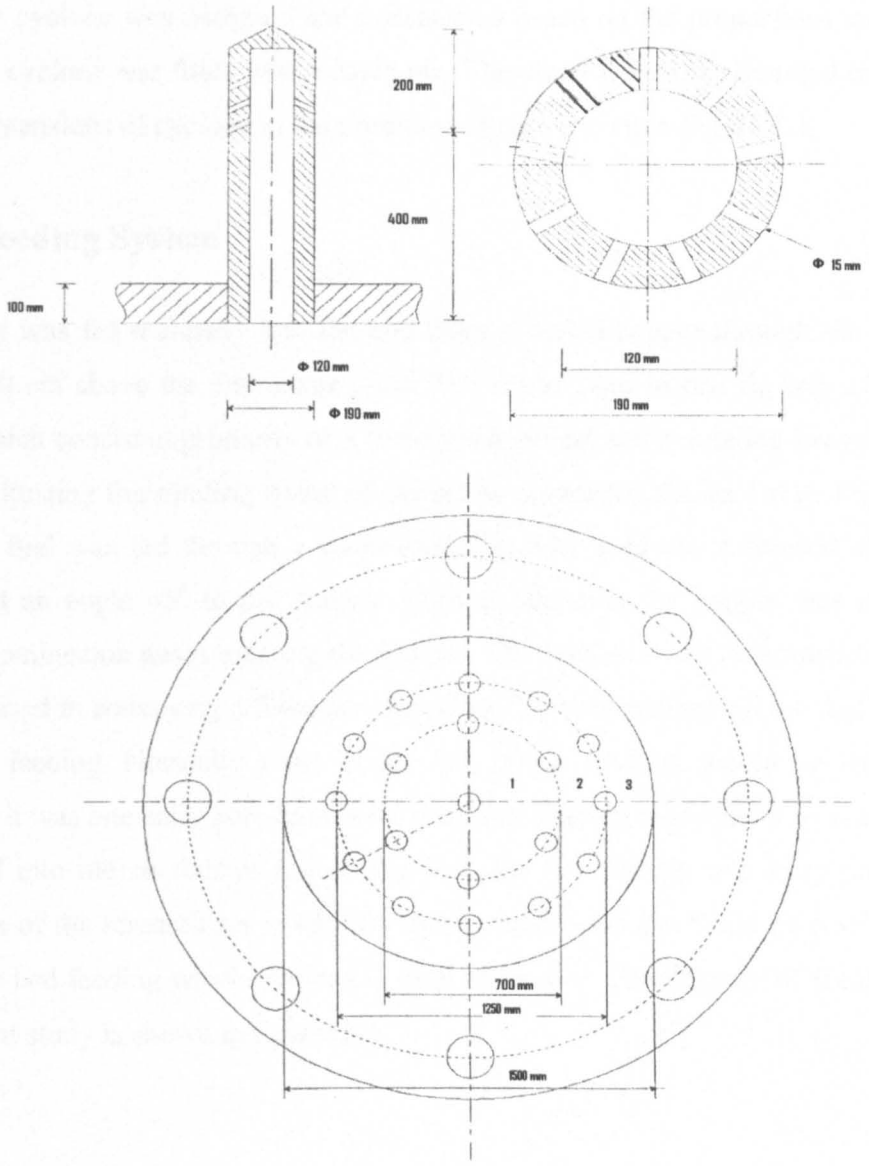

Figure 3.2 Layout of distributor plate

3.1.5 Particulate Collector (cyclone)

A cyclone was used to capture the bed materials elutriated and fly ash. The cyclone used in this research was constructed from stainless steel and was 0.10 m diameter and 0.40 m high. The cyclone was designed and constructed based on the proportions stated by Perry [73]. The cyclone was fitted with a catch pot. The detail design is presented in appendix A-2. The dimensions of cyclone in the present study are shown in Figure 3.3.

3.1.6 Feeding System

Solid fuel was fed manually into the bed from a sealed hopper through the screw feeder located 70 cm above the distributor plate. The feeder used in this rig was a K-tron Soder feeder which consisted primarily of a fixed pitch helical screw rotating beneath the hopper outlet. Adjusting the rotating speed of the screw controlled the feed rate. From the screw pipe, the fuel was fed through a water-cooled gravity feed chute situated above the bed surface at an angle 45° to the vertical. During operation the hopper was pressurised to prevent combustion gases entering the hopper. The feed rate was determined by observing the time used in conveying a fixed amount of fuel. In this research all the fuel was fed with over-bed feeding. Normally some of the less dense biomass should be fed in the bed. However it was one entry port considered desirable that the feed should be premixed before being fed into the combustor and so the fuel was fed through one entry port. The main objectives of the research are to identify the biomass fuels that could be co-fired with coal with over-bed feeding which resulted in high efficiency. The diagram of feeding system in the present study is shown in Figure 3.4.

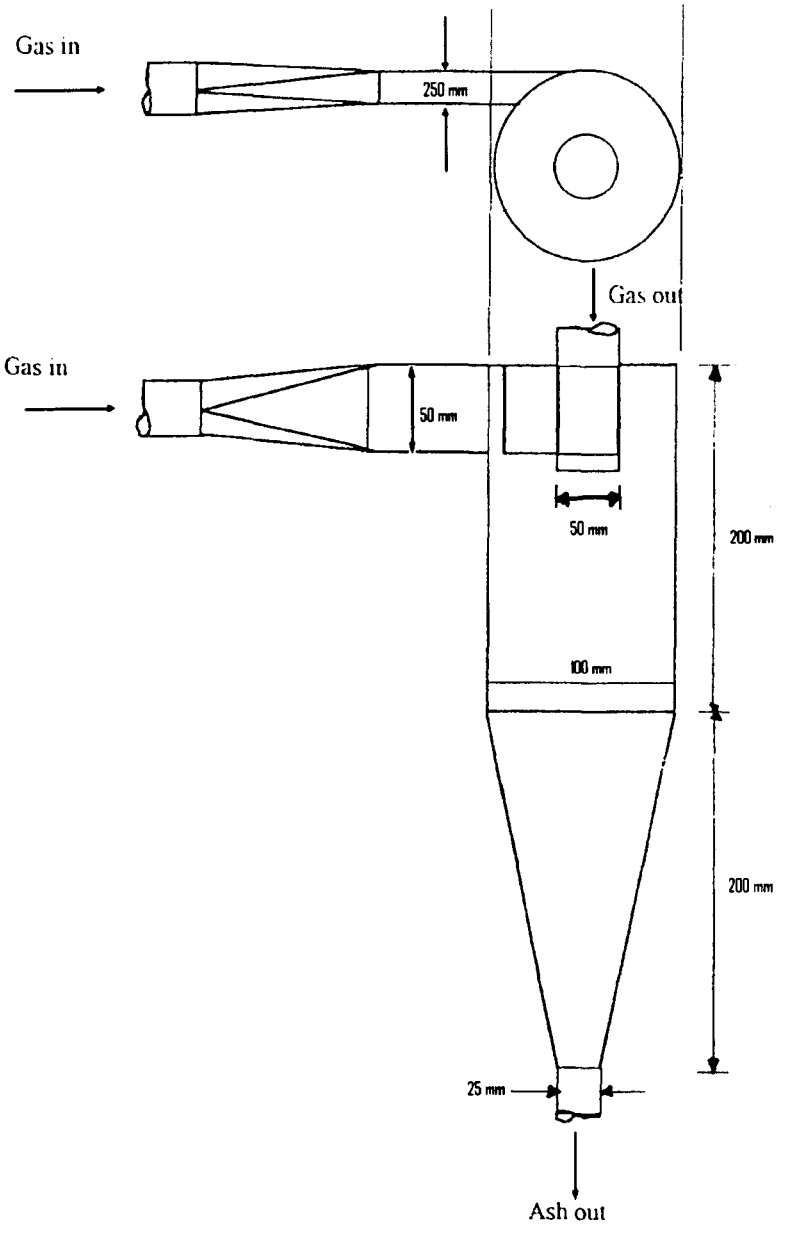

Figure 3.3. Layout of cyclone

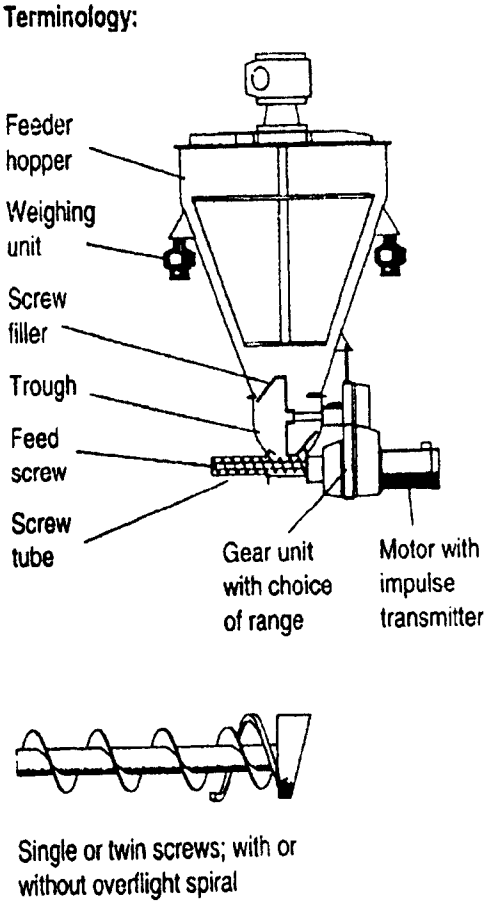

Figure 3.4 A diagram of feeding system

3.1.7 Measuring Facilities

a) Thermocouples

Bed and freeboard temperatures were measured at 8 different heights above the distributor plate by means of sheathed Ni-Cr/Ni-Al thermocouples Type K 1.5 mm diameter and 20 cm long. The thermocouples were located at 10, 20, 30, 40, 75, 115, 155, and 195 cm above the distributor plate and the temperatures were displayed on a computer via 8 channel temperature measurement board (PC 73C-T). The thermocouples were calibrated according to BS EN 60584.1 Part 4: 1996.

b) Gas Analyser

Combustion gas samples were obtained from a sampling port located at the cyclone exit and analysed by on-line gas analysers. Gas analysers are susceptible to dust and water vapor thus the gas sample had to be cleaned and dried. The gas sample was passed through a glass wool filter, a water-cooled heat exchanger, and a drier consisting of magnesium oxide granules before entering the on-line gas analysers. The gas analysers used are as listed in Table 3.1.

Table 3.1 Lists of the analysers used in the experiment

Gas	Range	Type
O_2	0 - 20%	Xentra 4904 B1 continuous emissions analyser
CO	0 - 2500 ppm	Xentra 4904 B1 continuous emissions analyser
CO	0 – 20%	Non-dispersive infrared absorption spectrometer analyser

i) CO and O_2 Analysers

CO and O_2 were measured using a Servomex International Limited, Xentra 4904 B1 continuous emissions analyser supplied. The measurement ranges of O_2 and CO were 0-20% and 0-2500 ppmv, respectively.

ii) CO_2 Analysers

CO_2 was measured by using a non-dispersive infrared absorption spectrometry analyser manufactured by the Analytical Development Company Limited (ADC). The measurement range of CO_2 was 0-15 % with repeatability of 0.5%. Prior to experimental start up, the gas analysers were subjected to calibration procedures whereby the individual gas with certain amount of concentration was purged into the analyser. The selected concentrations for calibration purposes were given in Table 3.2 below.

Table 3.2 Calibration gas concentrations

Analyser	Calibration gas concentrations
O_2/CO	21%(air) and 2400 ppm
CO_2	6.1%

3.2 Operational Procedure

In this section, a step-by-step description of the FBC performance is outlined for a typical experimental run. Experimental trials were performed for various fuel types, fluidization conditions, excess air, bed temperature and feed rate.

3.2.1 Fuel preparation and characterisation

The biomass fuels (rice husk, palm kernel shell and fibre) used in the experimental tests was delivered from different Malaysian mill companies. These materials are produced in large quantities in the Far East and are widely abundant as wastes, coupled with their low bulk density results in a landfill problem, which has been mentioned earlier in chapter 1. Other fuels such as chicken manure, refuse derived fuels, and wood wastes were obtained from the United Kingdom and Denmark. These materials were used due to their high potential to be converted into energy as well as minimised environmental problems created by them. Before commencing any test, the samples to be handled were screened to a particle size as listed in Table 3.3. By this stage, the fuel had been previously dried at room temperature for up to two days. For co-combustion runs feed mixtures were prepared by mixing the appropriate amount of each in a bucket.

Table 3.3 Fuel particle size for combustion testing

Fuel	Particle size (mm)
Coal	1.4 and 4.8 mm
Chicken pellets	3 mm diameter and 10 mm length
Refused derived fuel	10 mm diameter and 21.5 mm length
Palm kernel shell	2 - 6 mm
Palm fibre	Ground into <1mm length
Rice Husk	0.8-1.0 mm long (cylindrical shape and flaky nature)
Wood pellets	1.0 mm diameter and 2-5 mm length

The characteristics of the fuels measured including calorific value, proximate and ultimate analyses are significant for the combustion tests. The calorific values of fuels were determined by using a bomb calorimeter. According to this method, 1 gram of sample was burned in oxygen under standardised conditions inside a bomb. The heat released was transferred into the water jacket surrounding the bomb and a thermometer measured the temperature rise of the water. The amount of heat released was then calculated to give the calorific value of the sample. The proximate and ultimate analyses of the fuels tested were determined experimentally following the methods described in British Standard 1016 [74], the results are presented in Table 4.1.

3.2.2 Feeder Calibration

Before the experimental run, a feeder calibration test was made for each sample to determine their feedrate. About 3 kg of sample was placed in the feed hopper for each experiment. The feeder was started and the weight of sample discharged from the feeder was determined as a function of time. The cumulative weight delivered from the feeder was measured at 2.5 minutes intervals. The average feedrate, F_{avg}, was calculated from the cumulative weight delivered during specific time intervals and then the procedure was repeated.

3.2.3 Combustion Start Up

This gas was fed directly into the distributor plate from the compressed bottle and mixed with air in the nozzles, providing a combustible mixture at the nozzle exit. To ignite the propane-air mixture, inside the combustor, a natural gas-fired pilot burner was used. The propane gas was used as an auxiliary fuel to raise the bed temperature to a designated temperature, normally above the ignition temperature of the solid fuels burned in the combustor. When the bed temperature reached the designated temperatures, the solid fuel was fed to sustain the combustion.

Below are the steps that were followed to start the combustor for each experimental run:

1. All water lines and extract fan were turn on.
2. The pilot burner was removed and tested for starting several times; it was then replaced in the bed at the correct depth.
3. The fluidising air, flowrate at 420 l/min was turned on to unblock the bed for 5 minutes.
4. The fluidising air flowrate reduced to zero.
5. The pilot burner was lit up and a visual check was made.
6. The ball valve for propane was opened and slowly increased until it was ignited in the bed.
7. The fluidising air and propane were increased together until the minimum fluidising level of air was reached. Flowrates of air and propane were normally 400 l/min and 16 l/min respectively.
8. The temperatures in the bed (thermocouple number 5, 6 and 7) were monitored.
9. The Air/propane flowrates were maintained at the values in 7 until all these three thermocouples read the same temperature.
10. The air/propane flowrates were reduced as the bed temperature increased.
11. The air/propane flowrates were increased if the lowest thermocouple temperature (no. 8) started to fall with respect to the top one (no. 7).
12. The air/propane was reduced until the minimum amounts were found to keep bed at required temperature.
13. The ball valve was immediately turned off if the flame went out in the bed; the bed was purged with air and step 5 was repeated.
14. A visual check was made on the flame using a sight glass and mirror.
15. When the bed temperature reached the desired temperature (ignition temperature of solid fuel), the solid fuel was fed at an increasing rate and the propane flow rate was decreased.
16. The propane flow rate was continued to be decreased to zero and the solid fuel feed rate was increased to the desired rate.

3.2.4 Collection of Data

Flue gas concentration and combustion chamber temperature were monitored continuously. Once steady state conditions had been reached, temperature and gas concentrations were recorded.

A fly ash sample was collected from the catchpot after finishing the combustion run. The fly ash sample was then weighed and analysed to determine the total amount of unburned carbon of the fuels in the test.

Finally, after the completion of experimental run, the system was shut down following the procedure outlined below.

3.2.5 Shut-down

After collecting the desired data, the following steps were taken to stop the system:

1) Feeding solid fuel was stopped.
2) Flowrate of cooling water was increased.
3) The fluidising air was increased.
4) The fluidising air and the cooling water were turned off when the bed temperature reduced to about 100°C.
5) All measuring facilities and safety valves were turned off.

3.3 Ash Analysis

3.3.1 Unburned Carbon

The carbon analysis was determined experimentally following the methods described in British Standard 1016 [74]. The results are presented in Table 4.15-4.20 in chapter 4.

3.3.2 Ash Deposits

An ash deposits probe was inserted into the combustor at 70 cm above the distributor plate. The objective was to investigate whether the high alkali content of the biomass fuel would result in low melting point ash which would deposit on surfaces. The ash deposit probe for this study is shown in Figure 3.5.

3.3.3 Particle Size Distribution

The particle size of the material in the catch pot was determined using a Malvern particle size analyser [75]. About 10g sample were inputted into the sampling port and the size distribution in the range 0 – 2400 μm were calculated.

3.4 TGA Analyses

TGA of biomass fuels were carried out using a Pyris Perkin Elmer Thermogravimetric Analyser. A sample approximately 20 mg was placed in the alumina crucible and heated to 950°C at heating rates 10 and 100°C min^{-1} using nitrogen as the purge gas. The apparatus provides for the continuous measurement of sample weight as a function of temperature and electronic differentiation of the weight signal gave the rate of weight loss.

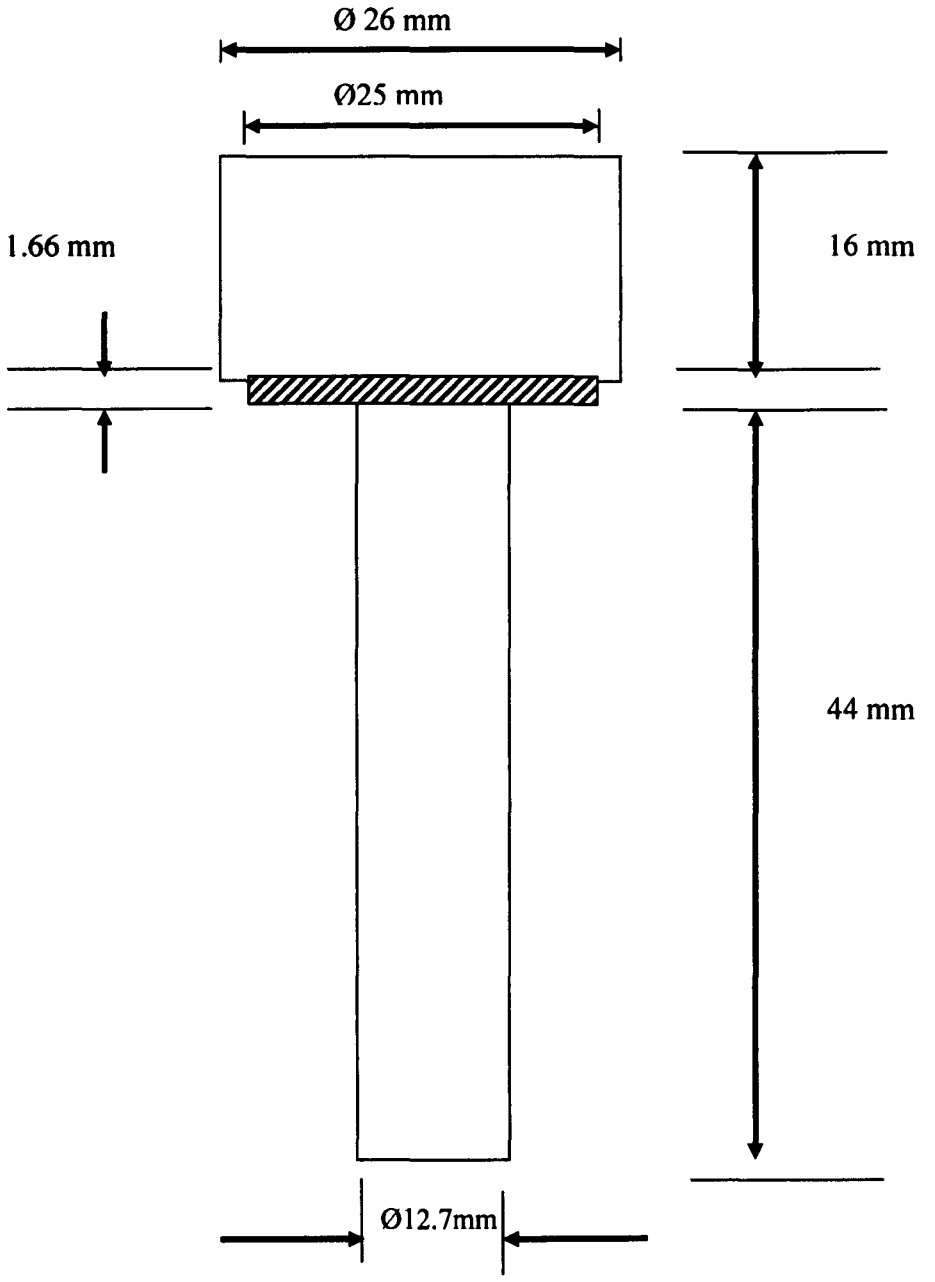

Figure 3.5 Ash deposit probe design

3.5 Combustion Calculation

3.5.1 CO Efficiency

Combustion efficiency is defined as the percentage carbon utilisation in the combustion process. A very common method for calculation of the combustion efficiency is computed from the following relation:

$$E1\ (\%) = \frac{\%CO_2 \text{ in flue gas x } 100\%}{(\%CO_2 + \%CO) \text{ in flue gas}} \qquad (3.1)$$

This efficiency calculation procedure is based on knowledge of flue gas composition only and assumes that there are no carbon losses and carbon composition presented in the feed is converted completely to carbon monoxide and carbon dioxide only. However, in the FBC, the majority of carbon loss is unburned carbon that is blown out of the combustor with the fly ash. Consequently, the combustion efficiency calculated by employing this procedure will be inaccurate.

3.5.2 Carbon Utilisation Efficiency

Saxena *et al.* [55] have developed a procedure to calculate the combustion efficiency based on the carbon balance and so accounts for material elutriated from the bed. The efficiency equation is given below.

$$E2\ (\%) = (B + \text{unburned carbon in ash})/C \text{ X } 100\% \qquad (3.2)$$

where B and C are the mass fractions of burnt and total carbon in the fuel, respectively. B can be calculated by knowing flue gas composition, fractional excess air, and the ultimate analyses of fuel. Details regarding this calculation are given in Appendix B-6.

CHAPTER 4

RESULTS AND DISCUSSION

This chapter presents a series of experimental results that were gathered co-combusting of coal with biomass in the fluidised bed combustor. The influences of fuel properties such as particle size, particle density and volatility as well as influences of operating parameters such as excess air, fluidising velocity on axial temperature profile, the combustion efficiencies and CO emissions are discussed. In addition, TGA analyses of the raw fuel which was used to study their heating profile during combustion is also included. Finally, the present experimental data is compared with other data based on a theoretical model.

4.1 Fuel Characteristics

Table 4.1 presents a summary of the properties of fuels used in this study. This table shows that the biomass fuels (chicken waste, rice husk, palm kernel shell, refuse derived fuel and wood pellets) have a lower calorific value (14-22 MJ/kg) than bituminous coal (31.1 MJ/kg) on a dry basis. The volatile matter of biomass fuels (60-75%) are almost twice than that of bituminous coal (38%) which indicates that the biomass fuels are easier to ignite and burn than coal. The ash content varies from one biomass to another. For example, the ash content of the palm kernel shell and wood pellets are low, 1.01 and 0.40 wt% on a dry basis, respectively. However, high ash content of chicken waste (24.70 wt%), rice husk (20.61 wt%) and refused derived fuel (18.92 wt%) is high compared to an average bituminous coal (2.80 wt%). For the combustion of biomass fuels with high ash contents, consideration must be given to incorporate efficient ash removal equipment from the flue gas to eliminate or reduce particulate pollution, just like in the case of coal combustion.

Table 4.1: Fuel properties of the studied fuels

Fuel Type	Propane	Coal	Chicken manure	Rice Husk	Palm Kernel	Refused Derived Fuel	palm fibre	Wood pellets
Proximate Analysis (% dry basis)								
Fixed carbon	0	58.87	9.00	15.02	18.56	9.70	16.80	17.90
Volatile matter	0	38.15	65.00	60.68	72.47	67.61	72.80	81.70
Ash	0	2.98	26.00	24.30	8.97	22.69	10.40	0.40
Ultimate Analysis (%as received)								
Carbon	82	75.4	34.7	34.9	45.6	39.7	47.2	50.2
Hydrogen	18	5.0	4.3	5.5	6.2	5.8	6.0	6.1
Oxygen	0	9.3	29.5	38.9	37.5	27.2	35.5	33.6
Nitrogen	0	0.9	1.9	0.1	1.7	0.8	1.4	0.12
Sulphur	0	0.7	0.0	0.0	0.0	0.4	0.3	0.01
Ash	0	2.80	24.70	20.61	1.01	18.92	8.4	1.9
moisture	0	5.9	5.0	3.7	8.0	3.3	1.2	8.1
Calorific value (MJ/kg) (as received)	50.5	31.1	12.9	13.5	18.0	12.3	14.3	17.2
Particle Size (mm)	none	1.4-4.8 mm	3 mm diameter x 10mm length	0.8 - 1.0 mm (cylindrical shape, non-granular and flaky nature)	3 mm diameter and 2 - 6 mm length	10 mm diameter x 21.5 mm length	< 1mm Diameter and 1.5 cm length	7 mm diameter x 10.5 mm length
Particle density (kg/m^3)	0.58 at 1KPa and 25 C	1200	646	98	435	410	104	490
state	gas	solid	solid	solid	solid	solid	solid	solid

From the ultimate analysis in Table 4.1, it shows that the carbon composition of biomass fuels are lower than that of bituminous coal, 14-46% compared to 80% on a dry basis. This low carbon contents results in the low heating value compared to coal. In contrast, the oxygen content in biomass fuels were higher than that of bituminous coal, 15-40% compared to 10% on a dry basis. Other components (hydrogen, nitrogen, and sulphur) are only slightly different. Those parameters stated above have an influence on the stoichiometric air requirement.

Furthermore, most biomass fuels have a larger particle size and lower particle density in comparison to bituminous coal. As can be seen in Table 4.1, the particle density of biomass fuels are less than half the of particle density of bituminous coal. The low particle size and particle density of biomass fuels complicates its processing, transportation, storage and firing process especially the feeding system.

4.2 Operating Conditions

In this experiment, baseline data was first obtained for single combustion of 100% British bituminous coal. Also, single combustion of other biomass fuels was carried out to investigate their combustion characteristics in comparison to coal during the co-combustion study. Co-combustion tests at biomass fractions of 30%, 50%, and 70% were performed. For each biomass fraction, excess air was varied from 30% to 70% at 20% intervals. For each excess air condition, air staging combustion was applied where the total secondary air is maintained at 65 l/min (about 10-20% to total air ratio). The solids fed included British bituminous coal (size 1.4 – 4 mm) and seven biomass fuels (as stated above). Also, co-combustion studies of burning the bituminous coal with the biomass fuels were carried out. In order to study the impact of fuel property changes (volatiles, ash, and combustibles), heat input was fixed at the design value of the experimental rig i.e. 10 kW. The combustion tests were operated in the bed temperature range of 700-950 °C and the superficial velocity range of 0.63 – 1.12 m/s. The operating conditions and flue gas analysis results are presented in Tables 4.2-4.8.

Table 4.2: Results for co-combustion of coal with chicken waste at feeder air flow rate of 65 l/min.

Fuel mixture (coal : chicken waste) (%)	Feed rate, (kg/hr)	Superficial gas velocity (m/s)	Main air flow rate, (l/min)	Total air flow rate, (l/min)	Excess air (%)	Bed Temperature (°C)	Freeboard Temperature (°C)	[CO_2] stack (%)	[CO] stack (ppm)	[O_2] stack (%)	Combustion Efficiency E1 (%)	Combustion Efficiency E2 (%)
0 : 100	3.0	0.67	190	255	30	841	591	13.0	504	5.0	99.61	80.74
0 : 100	3.0	0.81	230	295	50	837	617	12.5	354	7.1	99.70	83.35
0 : 100	3.0	0.94	270	335	70	826	677	10.0	295	8.7	99.69	82.55
30 : 70	2.47	0.83	240	305	32	896	700	12.5	405	6.0	99.97	80.18
30 : 70	2.47	0.98	275	340	50	880	686	11.5	425	6.5	99.63	85.85
30 : 70	2.47	1.12	300	365	72	855	689	9.0	307	8.1	99.66	81.73
50 : 50	2.10	0.78	210	275	28	904	645	13.0	328	6.5	99.75	85.94
50 : 50	2.10	0.93	250	315	47	893	695	12.0	304	7.3	99.74	89.42
50 : 50	2.10	1.08	300	365	70	860	614	10.0	365	8.2	99.64	86.91
70 : 30	1.78	0.76	205	270	31	913	711	13.0	314	4.5	99.84	88.34
70 : 30	1.78	0.91	250	315	52	904	673	11.5	331	5.0	99.71	91.58
70 : 30	1.78	1.03	290	355	72	857	667	10.0	352	6.9	99.65	90.39
100 : 0	1.20	0.67	175	240	30	934	613	13.0	223	5.5	99.82	90.25
100 : 0	1.20	0.80	210	275	50	938	608	12.0	157	7.8	99.87	95.68
100 : 0	1.20	0.91	240	305	71	926	594	10.5	120	9.2	99.89	96.22

Table 4.3: Results for co-combustion of coal with rice husk at feeder air flow rate of 65 l/min.

Fuel mixture (coal : rice husk) (%)	Feed rate, (kg/hr)	Super ficial gas velocity, (m/s)	Main air flow rate, (l/min)	Total air flow rate, (l/min)	Excess air (%)	Bed Temperature (°C)	Freeboard Temperature (°C)	[CO_2] stack (%)	[CO] stack (ppm)	[O_2] stack (%)	Combustion Efficiency (E1) (%)	Combustion Efficiency (E2) (%)
0 : 100	2.97	0.56	185	250	31	733	682	11.5	543	5.3	99.53	66.62
0 : 100	2.97	0.67	225	290	52	721	674	10.5	685	7.1	99.35	71.71
0 : 100	2.97	0.75	265	330	73	700	621	9.5	768	8.4	99.20	74.71
30 : 70	2.44	0.83	225	290	31	896	845	12.5	406	7.3	99.68	85.33
30 : 70	2.44	1.00	275	340	53	880	826	11.0	396	9.3	99.64	78.60
30 : 70	2.44	1.03	315	380	71	767	751	10.0	452	10.3	99.55	80.48
50 : 50	2.10	0.85	235	300	31	892	803	13.0	333	6.5	99.74	83.24
50 : 50	2.10	1.01	275	340	49	888	806	12.0	270	8.3	99.78	87.66
50 : 50	2.10	1.19	325	390	71	865	810	10.0	220	9.1	99.73	84.23
70 : 30	1.73	0.81	225	290	33	900	761	13.	420	5.4	99.83	86.07
70 : 30	1.73	0.98	265	330	51	893	788	12.0	630	6.7	99.48	91.40
70 : 30	1.73	1.09	305	370	69	860	810	10.0	430	7.5	99.57	85.48
100 : 0	1.20	0.67	175	240	30	934	613	13.0	223	5.5	99.82	90.25
100 : 0	1.20	0.80	210	275	50	938	608	12.0	157	7.8	99.87	95.68
100 : 0	1.20	0.91	240	305	71	926	594	10.5	120	9.2	99.89	96.22

Table 4.4: Results of co-combustion of coal with palm kernel shell at feeder air flow rate of 65 l/min.

Fuel mixture (coal : palm kernel shell) (%)	Feed rate, (kg/hr)	Super ficial gas velocity, (m/s)	Main air flow rate, (l/min)	Total air flow rate, (l/min)	Excess air (%)	Bed temperature (°C)	Freeboard temperature (°C)	[CO_2] stack (%)	[CO] stack (ppm)	[O_2] stack (%)	Combustion efficiency (E1) (%)	Combustion efficiency (E2) (%)
0 : 100	1.97	0.59	175	240	35	889	795	12.0	496	9.4	99.59	80.67
0 : 100	1.97	0.68	205	270	51	876	778	11.5	571	10.3	99.51	87.89
0 : 100	1.97	0.81	245	310	74	874	773	9.5	679	5.8	99.29	84.29
30 : 70	1.74	0.74	210	275	30	884	715	12.0	431	6.2	99.64	80.73
30 : 70	1.74	0.87	250	315	49	882	711	11.5	479	7.9	99.59	89.15
30 : 70	1.74	1.03	295	360	71	878	689	9.5	543	9.0	99.43	84.85
50 : 50	1.59	0.65	189	254	32	903	664	12.0	516	5.9	99.57	89.86
50 : 50	1.59	0.78	229	294	53	882	671	11.5	608	6.4	99.47	92.82
50 : 50	1.59	0.85	265	330	71	870	674	10.0	868	7.2	99.14	91.36
100 : 0	1.20	0.67	175	240	30	934	613	13.0	223	5.5	99.82	90.25
100 : 0	1.20	0.80	210	275	50	938	608	12.0	157	7.8	99.87	95.68
100 : 0	1.20	0.91	240	305	71	926	594	10.5	120	9.2	99.89	96.22

Table 4.5: Results of co-combustion of coal with palm fibre at feeder air flow rate of 65 l/min.

Fuel mixture (coal : palm fibre) (%)	Feed rate (kg/hr)	Superficial gas velocity (m/s)	Main air flow rate (l/min)	Total air flow rate (l/min)	Excess air (%)	Bed temperature (°C)	Freeboard temperature (°C)	[CO_2] stack (%)	[CO] stack (ppm)	[O_2] stack (%)	Combustion efficiency (E1) (%)	Combustion efficiency (E2) (%)
100 : 0	1.20	0.67	175	240	30	934	613	13.0	223	5.5	99.82	90.25
100 : 0	1.20	0.80	210	275	50	938	608	12.0	157	7.8	99.87	95.68
100 : 0	1.20	0.91	240	305	71	926	594	10.5	120	9.2	99.89	96.22
90 : 10	1.28	0.63	180	245	31	851	638	12.0	961	6.6	99.24	76.59
90 : 10	1.28	0.76	215	280	50	840	646	11.0	1102	7.6	99.09	81.83
90 : 10	1.28	0.88	255	320	71	839	651	9.5	1123	8.4	98.73	81.40
80 : 20	1.36	0.62	183	248	31	799	654	11.0	639	6.1	99.42	72.96
80 : 20	1.36	0.74	220	285	51	792	656	10.5	651	6.5	99.38	80.57
80 : 20	1.36	0.85	255	320	69	780	656	10.0	743	6.4	99.18	78.04
70 : 30	1.44	0.54	185	250	32	665	678	10.0	1128	6.9	98.88	69.39
70 : 30	1.44	0.67	220	285	50	651	630	9.0	1300	6.6	98.58	71.87
70 : 30	1.44	0.72	260	325	70	629	629	8.0	1257	6.9	98.54	73.33

Table 4.6: Results of co-combustion of coal with refuse derived fuel at feeder air flow rate of 65 l/min.

Fuel mixture (coal : refuse derived fuel) (%)	Feed rate, (kg/hr)	Superficial gas velocity (m/s)	Main air flow rate (l/min)	Total air flow rate (l/min)	Excess air (%)	Bed temperature (°C)	Freeboard temperature (°C)	[CO_2] stack (%)	[CO] stack (ppm)	[O_2] stack (%)	Combustion efficiency (E1) (%)	Combustion efficiency (E2) (%)
0:100	2.74	1.19	335	400	31	815	620	11.5	720	5.8	99.40	80.78
0:100	2.74	1.40	395	460	51	780	633	10	496	6.1	99.53	85.35
0:100	2.74	1.61	455	520	71	720	577	9.0	535	6.8	99.41	81.34
30 : 70	2.34	0.97	275	340	31	837	660	12.0	997	6.8	99.18	80.56
30 : 70	2.34	1.12	325	390	50	807	682	11.0	1106	7.1	99.0	85.73
30 : 70	2.34	1.30	385	450	73	787	667	9.0	1763	8.3	98.08	82.15
50 : 50	2.10	0.84	240	305	61	838	765	12.0	716	7.3	99.41	81.23
50 : 50	2.10	1.02	290	355	52	839	732	11.0	1346	9.2	98.76	87.91
50 : 50	2.10	1.16	335	400	71	811	726	9.5	1578	11.1	98.37	86.17
70 : 30	1.69	0.79	220	285	32	859	809	12.5	1320	8.9	98.96	86.85
70 : 30	1.69	0.94	260	325	50	865	789	11.5	1560	10.6	98.66	91.85
70 : 30	1.69	1.10	305	317	71	870	815	9.5	2437	11.0	97.50	87.88
100 : 0	1.20	0.67	175	240	30	934	613	13.0	223	5.5	99.82	90.25
100 : 0	1.20	0.80	210	275	50	938	608	12.0	157	7.8	99.87	95.68
100 : 0	1.20	0.91	240	305	71	926	594	10.5	120	9.2	99.89	96.22

Table 4.7: Results of co-combustion of coal with wood pellets at feeder air flow rate of 65 l/min.

Fuel mixture (coal : wood pellets) (%)	Feed rate (kg/hr)	Superficial gas velocity (m/s)	Main air flow rate, (l/min)	Total air flow rate (l/min)	Excess air (%)	Bed temperature (°C)	Freeboard temperature (°C)	[CO_2] stack (%)	[CO] stack (ppm)	[O_2] stack (%)	Combustion efficiency (E1) (%)	Combustion efficiency (E2) (%)
0:100	1.91	0.55	160	225	32	820	456	12.5	287	5.0	99.77	82.95
0:100	1.91	0.66	190	255	50	819	474	11.0	256	7.6	99.77	83.25
0:100	1.91	0.75	225	290	70	786	455	10.0	221	8.2	99.78	85.40
30 : 70	1.68	0.63	175	240	31	847	510	11.0	189	6.2	99.83	84.46
30 : 70	1.68	0.76	210	275	51	846	519	10.0	188	6.8	99.81	88.54
30 : 70	1.68	0.88	245	310	70	843	523	9.0	190	7.2	99.80	90.30
50 : 50	1.55	0.64	180	245	30	861	440	12.5	183	5.8	99.85	85.31
50 : 50	1.55	0.77	215	280	50	860	442	11.5	184	6.2	99.84	90.30
50 : 50	1.55	0.91	255	320	70	857	449	10.0	178	7.0	99.82	90.27
70 : 30	1.33	0.63	170	235	31	897	463	13.0	196	5.9	99.84	90.74
70 : 30	1.33	0.76	205	205	52	895	467	12.0	194	6.1	99.84	92.11
70 : 30	1.33	0.89	240	240	71	892	471	10.0	192	6.5	99.80	91.71
100 : 0	1.20	0.67	175	240	30	934	613	13.0	223	5.5	99.82	90.25
100 : 0	1.20	0.80	210	275	50	938	608	12.0	157	7.8	99.87	95.68
100 : 0	1.20	0.91	240	305	71	926	594	10.5	120	9.2	99.89	96.22

Table 4.8: Results of co-combustion of coal with wood powder at feeder air flow rate of 65 l/min.

Fuel mixture (coal : wood pellets) (%)	Feed rate (kg/hr)	Superficial gas velocity (m/s)	Main air flow rate, (l/min)	Total air flow rate (l/min)	Excess air (%)	Bed temperature (°C)	Freeboard temperature (°C)	[CO_2] stack (%)	[CO] stack (ppm)	[O_2] stack (%)	Combustion efficiency (E1) (%)	Combustion efficiency (E2) (%)
0:100	2.91	0.94	275	340	31	818	781	12.5	211	6.2	99.75	82.11
0:100	2.91	1.11	325	390	50	809	767	11.0	221	8.4	99.73	87.27
0:100	2.91	1.26	375	440	70	807	762	9.5	231	9.4	99.66	86.27
50 : 50	2.51	1.34	375	440	31	860	840	11.5	513	9.2	99.81	87.14
50 : 50	2.51	1.57	440	505	50	858	812	10.5	310	9.4	99.79	91.64
50 : 50	2.51	1.83	510	575	71	855	800	9.5	340	11.5	99.76	90.07
100 : 0	1.20	0.67	175	240	30	934	613	13.0	223	5.5	99.82	90.25
100 : 0	1.20	0.80	210	275	50	938	608	12.0	157	7.8	99.87	95.68
100 : 0	1.20	0.91	240	305	71	926	594	10.5	120	9.2	99.89	96.22

4.3 Experimental Observations

Visual observation of the behaviour of both coal and biomass combustion throughout the experimental programme is given below. Also, the fuels combustion characteristics were evaluated based on their axial temperature profiles and were compared with heating profiles obtained using thermogravimetric analysis (TGA).

4.3.1 Temperature Profile

When fuel (biomass or biomass/coal mixtures) was fed onto the bed (over bed feeding), there was initially observed a strong flame in the freeboard. Thereafter occasional flames would appear on the surface of the bed. This apparently corresponds to the arrival of the fuels undergoing devolatilization near the surface and indicates that a considerable degree of freeboard combustion had occurred. The bed temperature remained constant for sometime after the flame in the freeboard had disappeared indicating further combustion of char in the bed. A similar phenomenon was also observed by Preto *et al.* [40] during the combustion of rice husk in a rectangular 380 x 406 mm fluidised bed, by Peel and Santos [37] during the combustion of sawdust, bagasse, rice husks, wood chips and corn cobs in a 200 mm diameter fluidised bed and Abelha *et al.* [20] during co-combustion of lignite with chicken waste in a 30 kW FBC as mentioned earlier in section 2.2.4.2.1. In addition, for the case of the refuse derived fuel, clear and visible blue flames were observed on the surface of the bed indicating the presence of plastic components in the samples as suggested by Cozzani *et al.* [21] and Guilin *et al.*[23].

The phenomenon of this behaviour was evaluated based on their axial temperature profiles of FBC. Figures 4.1 – 4.9 illustrates the axial temperature distributions along the bed height for different single and co-combustion experiments at 50% excess air and constant secondary air (SA) at 65 l/min.

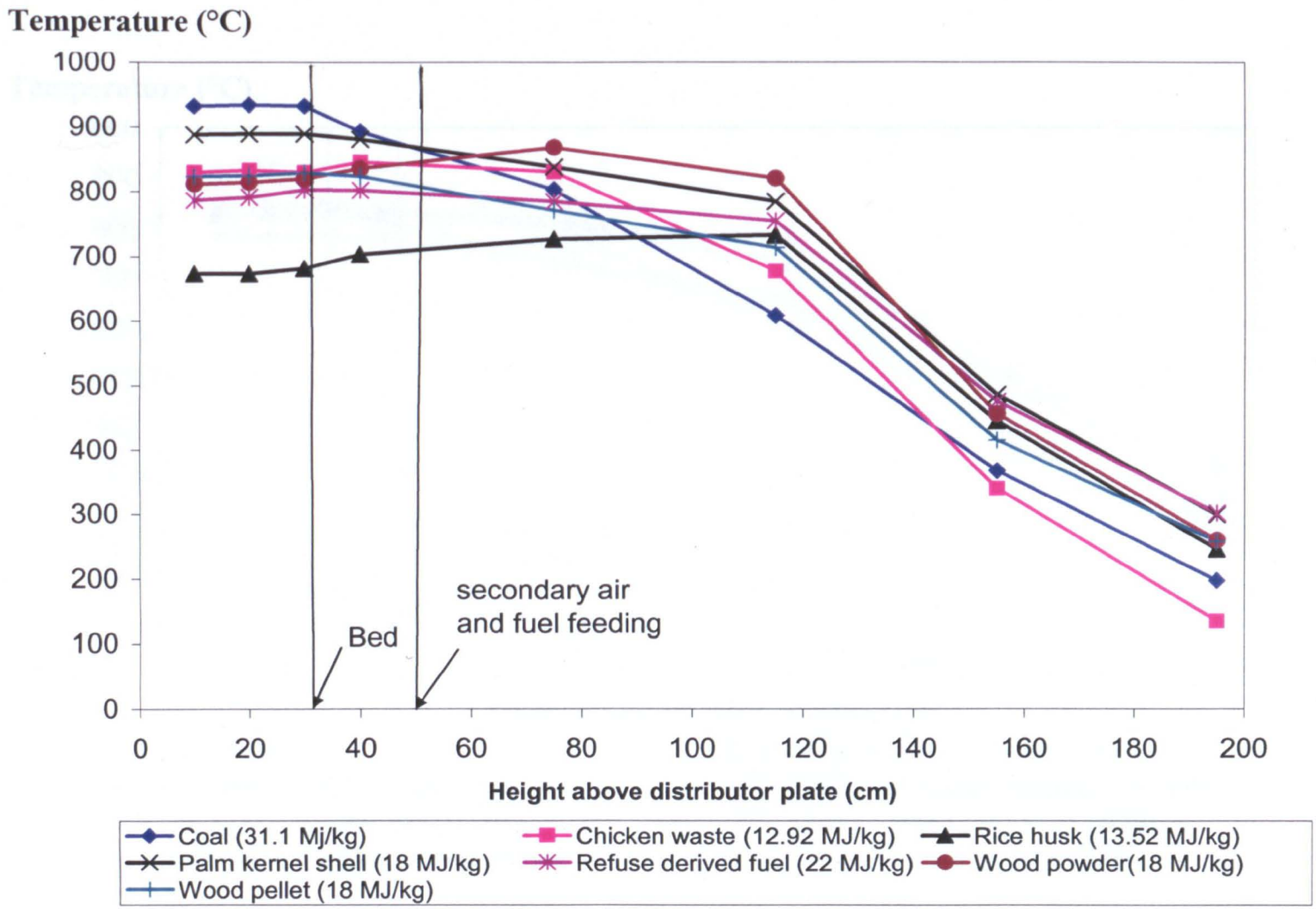

Figure 4.1 Axial temperature profile for coal and different biomass combustion in the case of excess air = 50% and secondary air = 10%

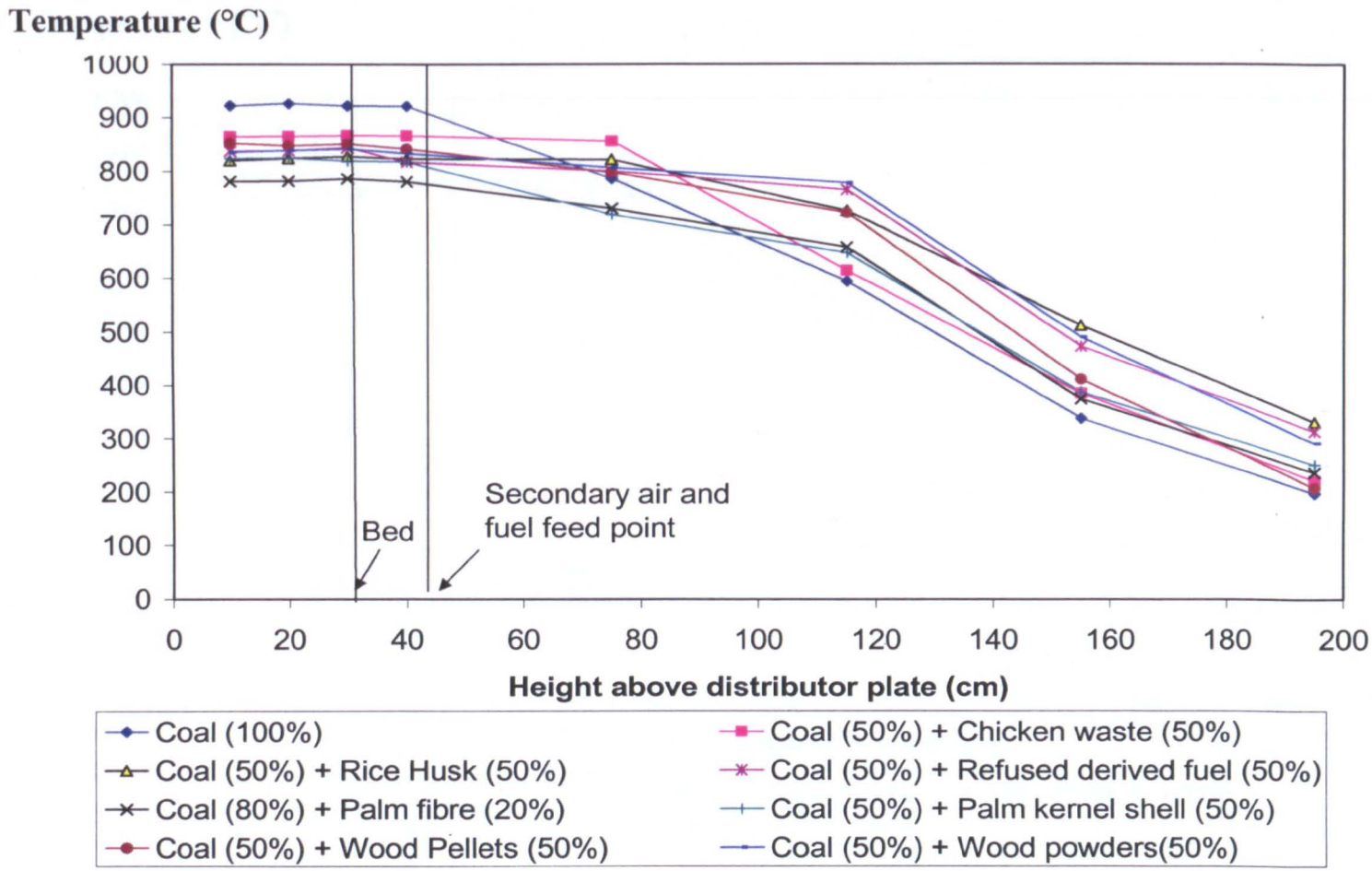

Figure 4.2 Axial temperature profile for co-combustion of coal with biomass combustion in the case of excess air = 50% and secondary air = 10%

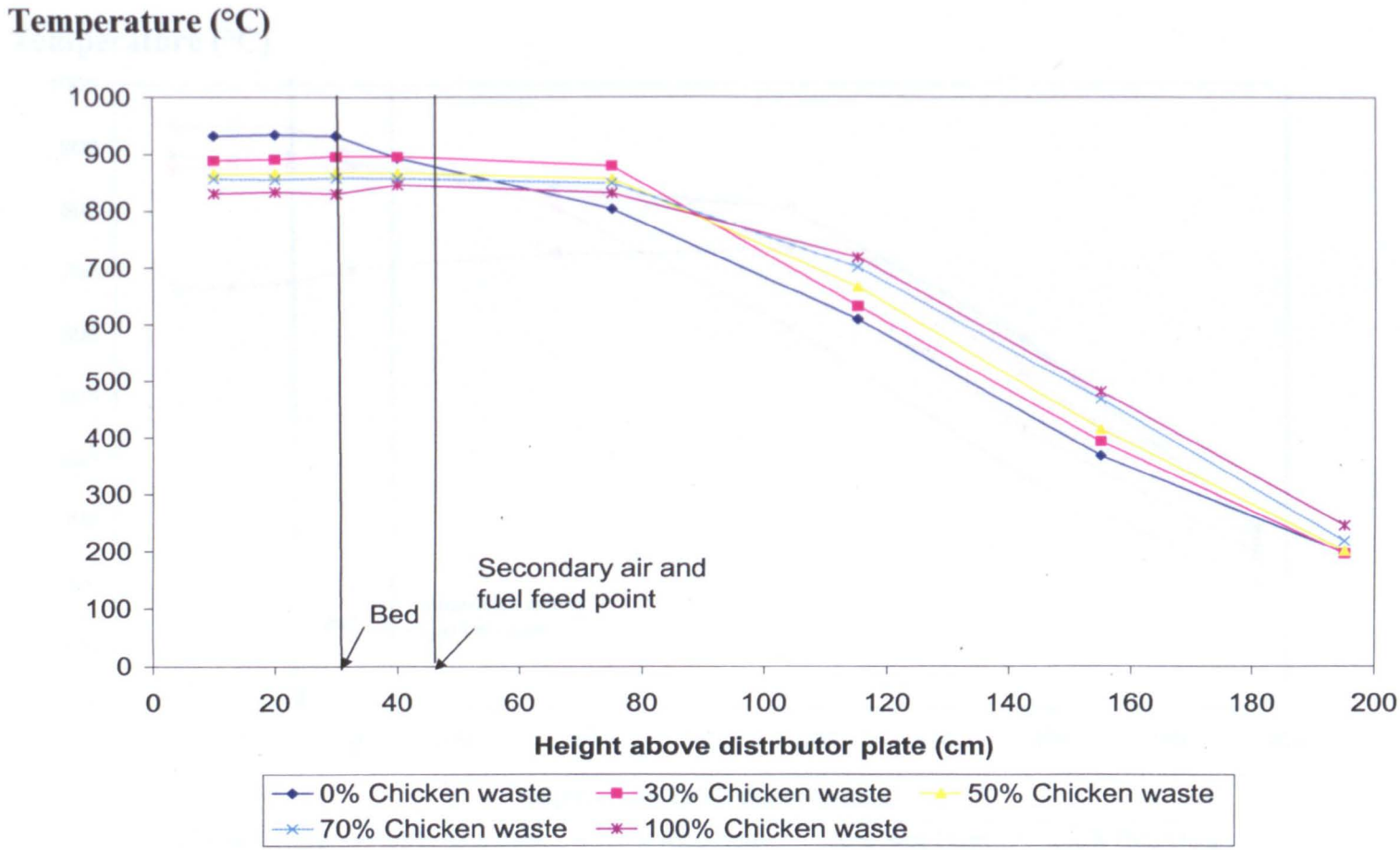

Figure 4.3 Axial temperature profile for co-combustion of coal with chicken waste combustion in the case of excess air = 50% and secondary air = 10%

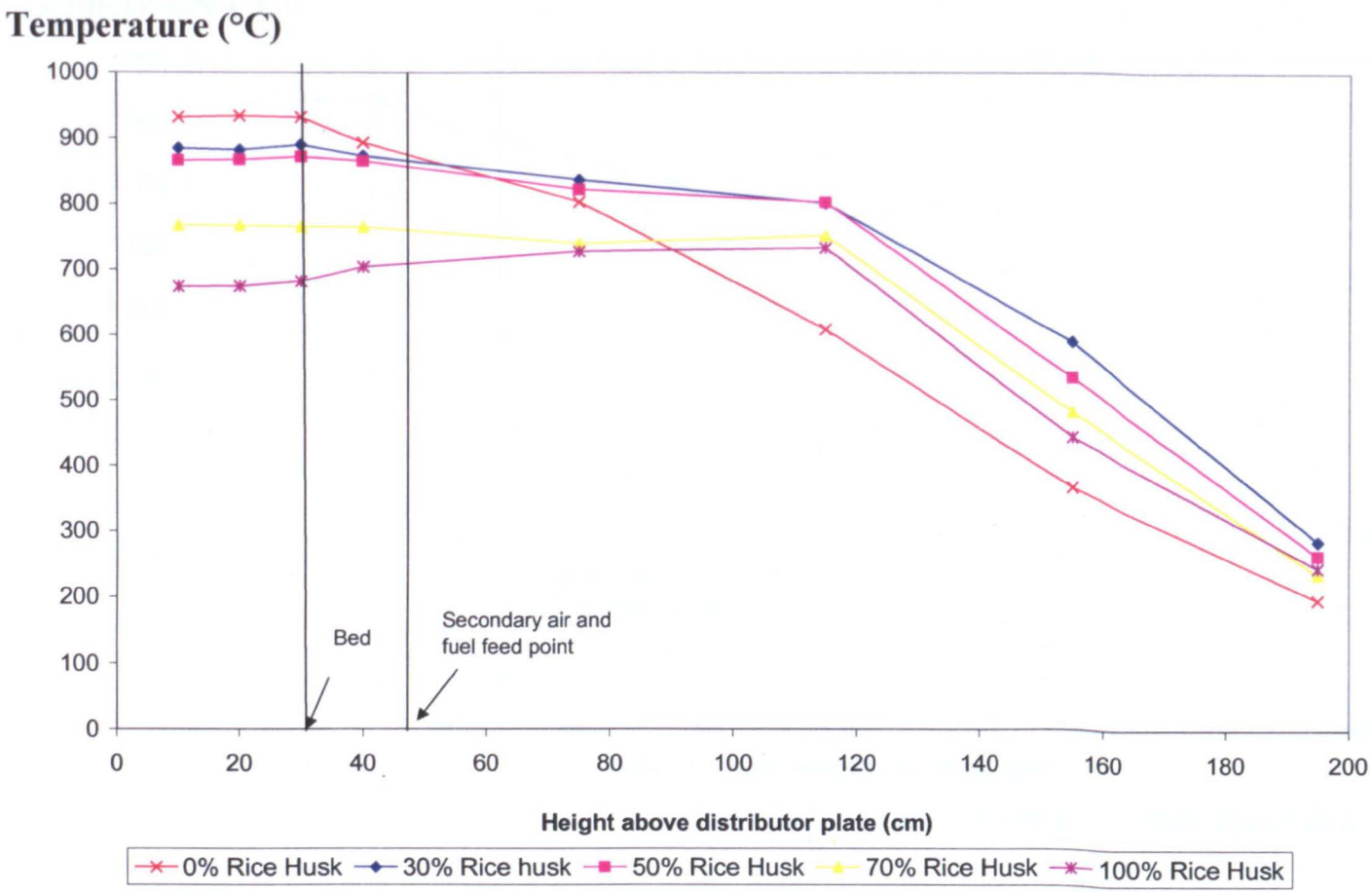

Figure 4.4 Axial temperature profile for co-combustion of coal with rice husk combustion in the case of excess air = 50% and secondary air = 10%

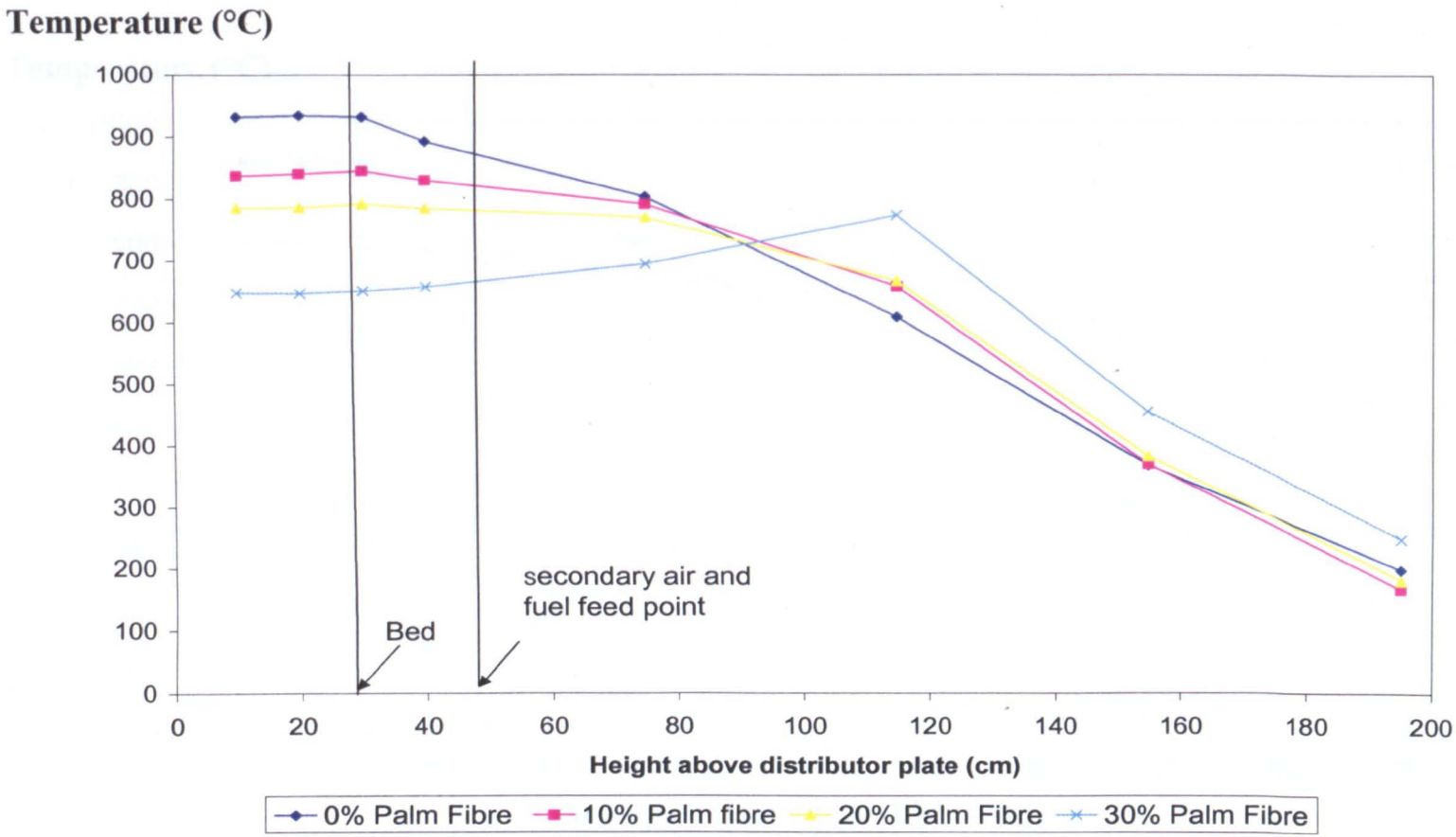

Figure 4.5 Axial temperature profile for co-combustion of coal with palm fibre combustion in the case of excess air = 50% and secondary air = 10%

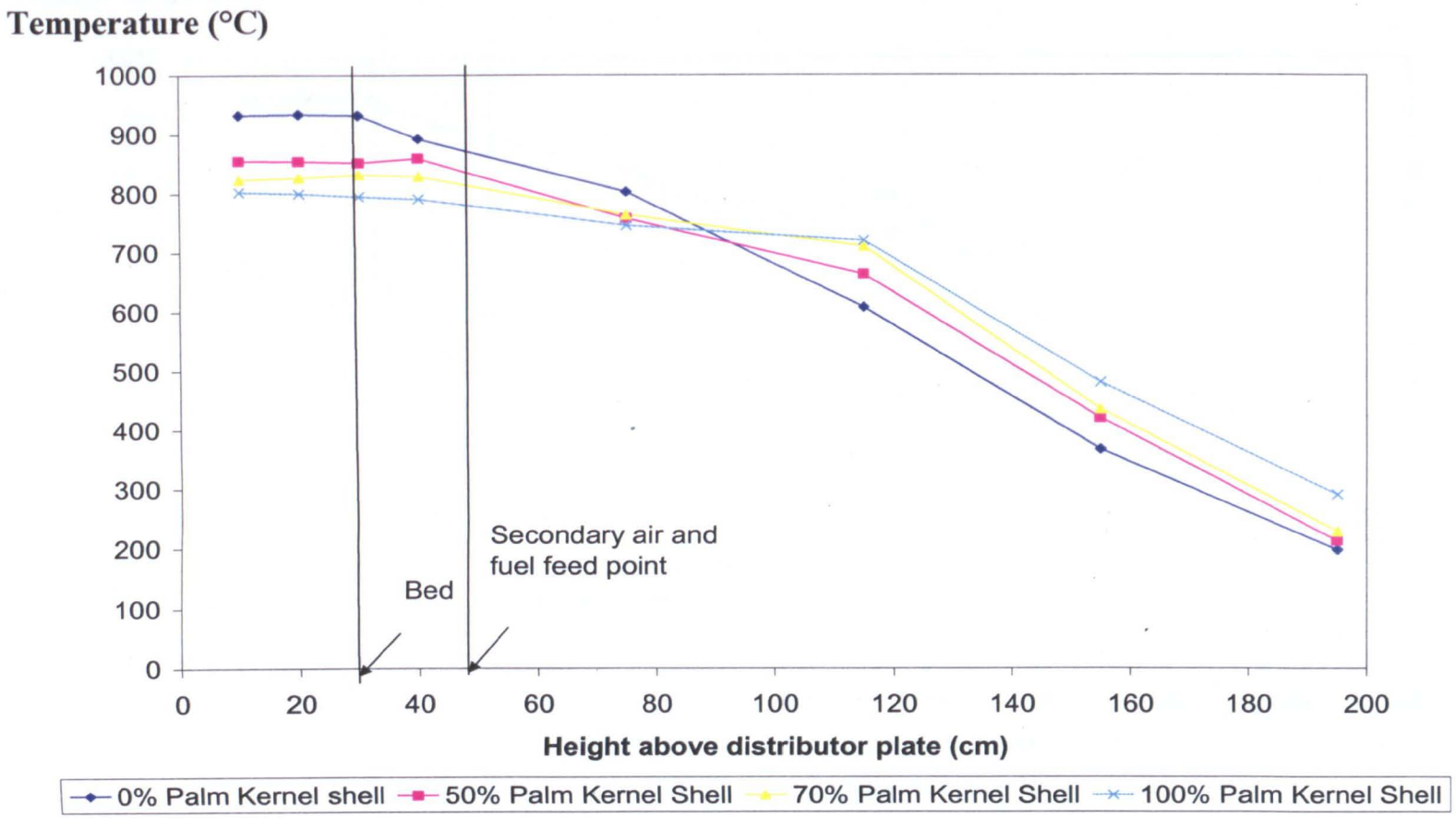

Figure 4.6 Axial temperature profile for co-combustion of coal with palm kernel shell combustion in the case of excess air = 50% and secondary air = 10%

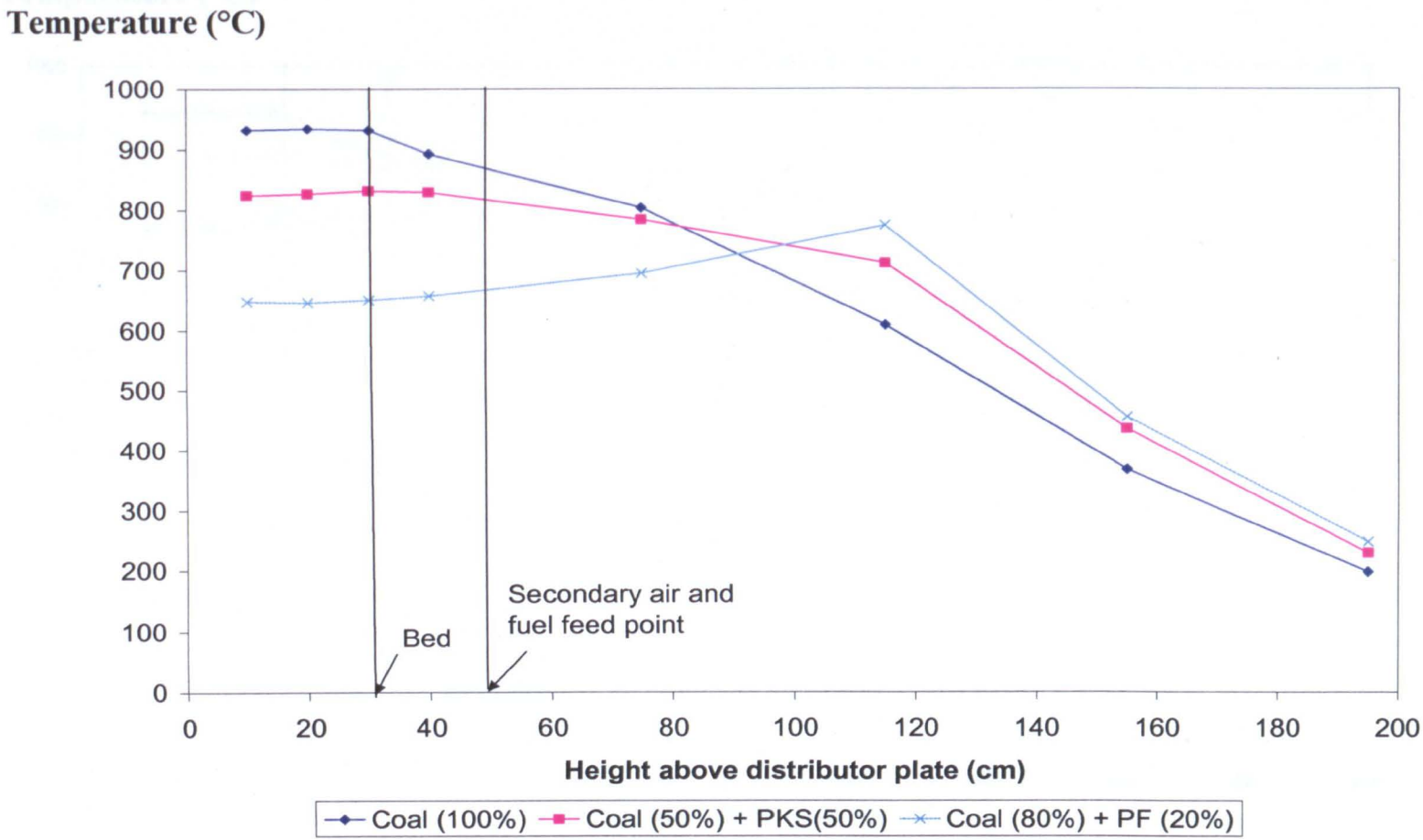

Figure 4.7 Axial temperature profile for co-combustion of coal with palm fibre and palm kernel shell combustion in the case of excess air = 50% and secondary air = 10%

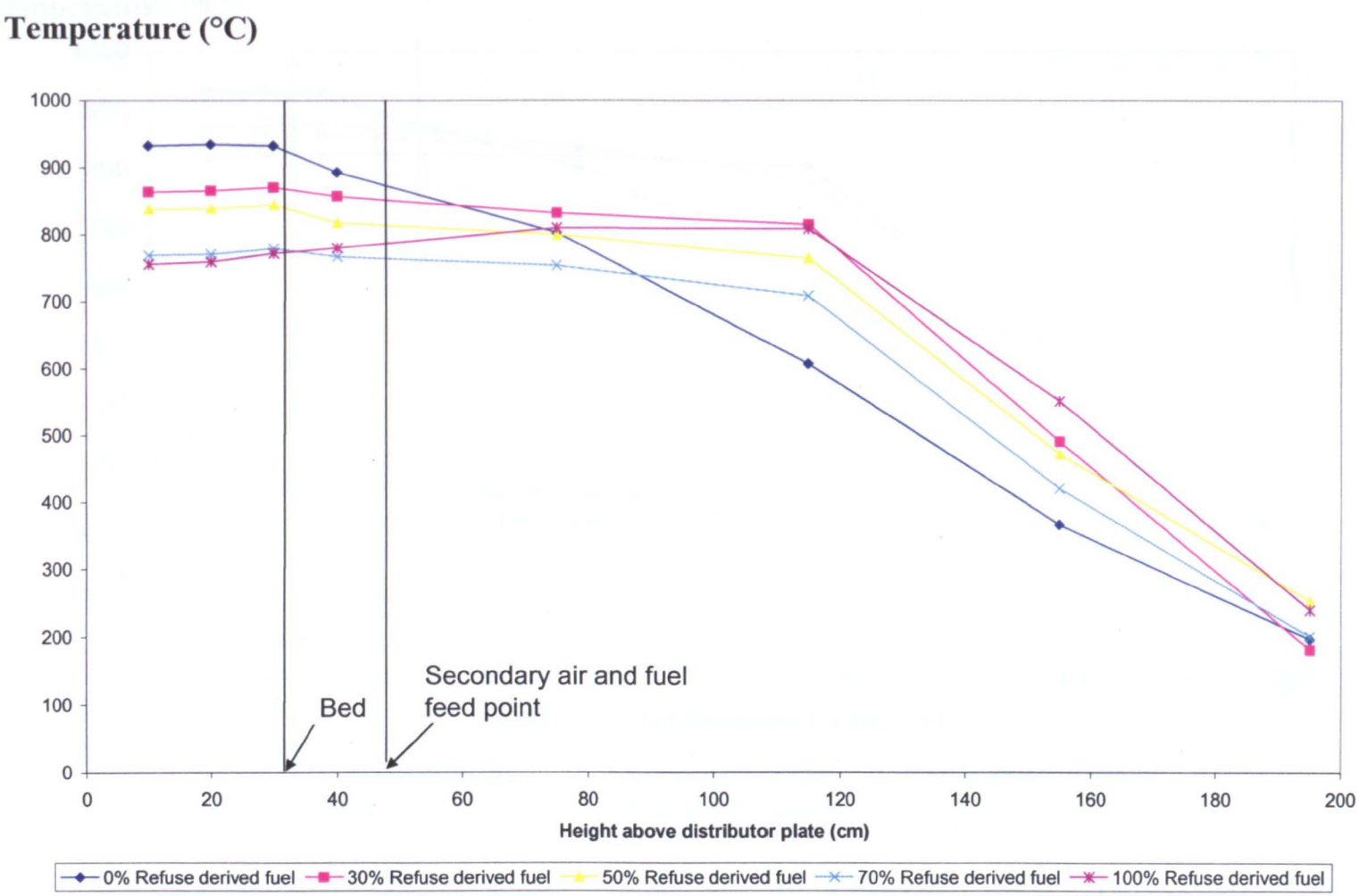

Figure 4.8 Axial temperature profile for co-combustion of coal with refuse derived fuel combustion in the case of excess air = 50% and secondary air = 10%

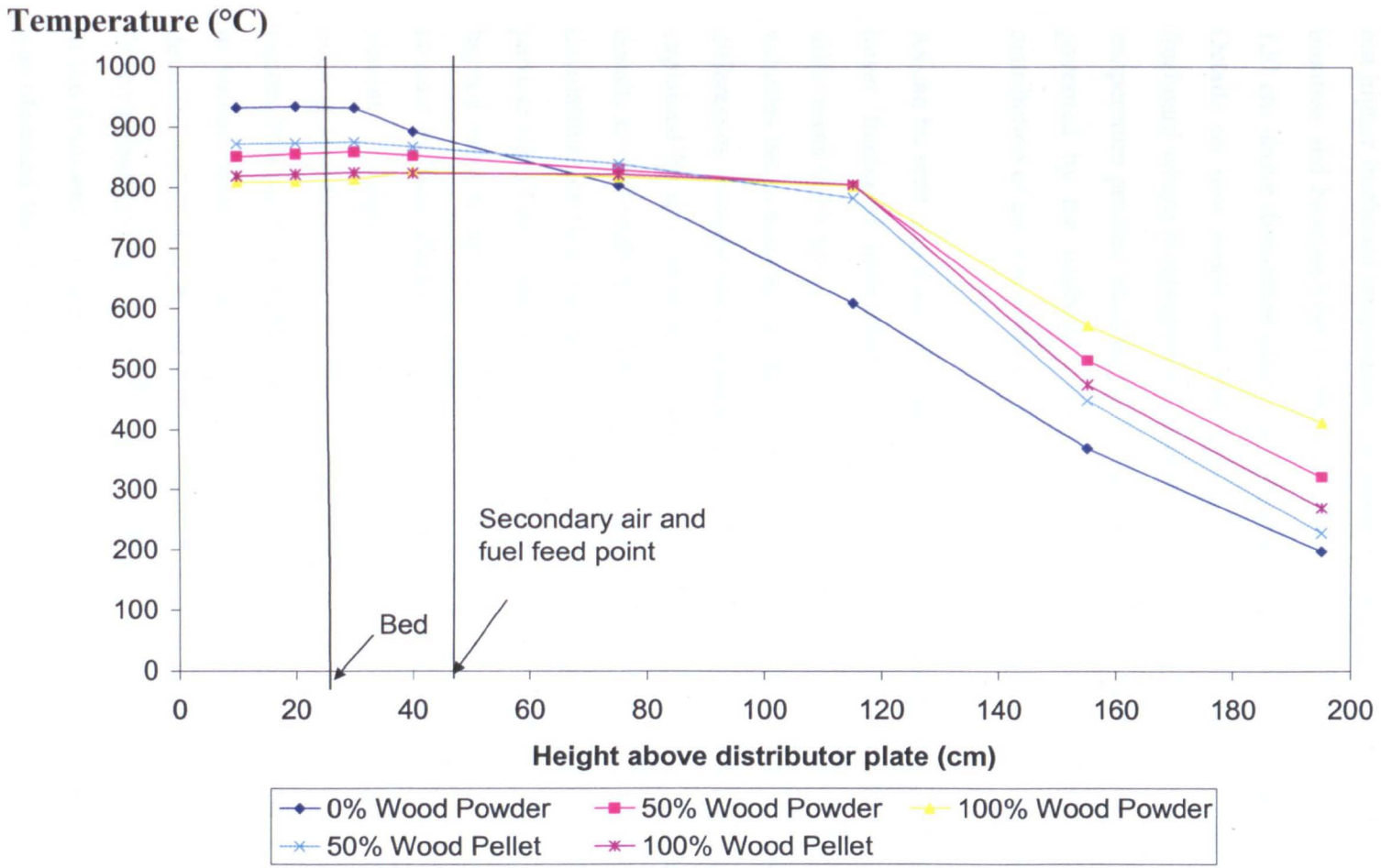

Figure 4.9 Axial temperature profile for co-combustion of coal with wood pellets and wood powder combustion in the case of excess air=50% and secondary air =10%

Generally, in comparison to coal, a lower bed temperature (0-40 cm above distributor plate) but higher freeboard temperature was observed (80-120 cm above the distributor plate) for biomass and biomass/coal combustion. Also in general the temperature starts to fall from 120 cm above distributor plate that indicates that most of the combustion was completed. Details on how much fuel was burned in bed and freeboard as well the point in the freeboard where combustion is completed will be discussed in section 4.6. In general, the temperature profiles obtained for biomass or biomass/coal mixtures combustion are mainly governed by the method of fuel feeding (overbed in this case), fuel properties and distribution of air. The influences of these factors are discussed in the below.

As can be seen previously in Figure 4.1, coal combustion gives higher bed temperature but lower freeboard temperature in comparison to biomass. This is due to significant differences in biomass volatility (as twice) in comparison to coal. Thus, as expected, more volatiles are combusted in the freeboard for biomass fuels. However, there are noticeable differences between the temperature profiles for biomass fuels. These differences can be explained by the variation of their physical properties such as particles size and particle density even though their volatility is similar. These factors contributed to their settling and devolatilisation time during combustion in the FBC. For example, wood pellets with larger particle size (7 mm diameter and 10 mm long) and higher particle density (490 kg/m^3) have burned more in the bed indicated by higher bed temperature in comparison with wood powder (< 1mm diameter and < 10 kg/m^3, respectively) although their volatility is almost similar. The lighter and smaller wood waste mostly kept burning in the freeboard region even at low fluidising velocity (<1 m/s) and was mostly burned before it reached the bed region. This can be explained by the fact that a smaller particle size has a larger surface area to volume ratio. Consequently, this contributed to a lower settling velocity and quicker devolatilisation time. Additionally, similar to wood powder combustion, rice husk and palm fibre combustion also occurred with lower bed temperature. As most of the combustion was in the freeboard, it is considered that was due to the low particle density. A similar result was observed for chicken pellet and refuse derived fuel (particle size as twice of chicken waste) combustion.

Apart from particle size, the plastic material degradation during refuse derived fuels combustion also contributes to greater de-volatilisation time in the freeboard region in comparison to chicken pellets and wood pellets which have a more uniform composition. Thus, the effects of plastic degradation during refuse derived fuels combustion was investigated using themogravimetric analysis in order to find out detail regarding the behaviour of these plastics material behave prior to combustion. The results will be discussed in section 4.3.2. Further some of the refuse derived fuel particles breaks up upon feeding (about 5%) compared with less than 1 % occurred for other pelletised biomass fuels such as chicken manure pellets and wood pellets.

During co-combustion (see Figures 4.2 - 4.9), the bed temperature increases almost linearly with increasing fraction of coal in biomass fuels with an average increase of about 10-20°C for every 20% increased in coal fraction. This is due to differences in fuel particle density between coal and biomass fuels. Biomass fuels with lower density (about half) compared to coal tend to burn in freeboard and coal tends to burn in the bed region. Therefore, the addition of coal in biomass increases the amount of fixed carbon reaching the bed resulting in higher bed temperatures. This observation agrees with the results of Abelha *et al.* [20] and Suksankraisorn *et al.* [51] who investigated the co-firing of coal and chicken litter and co-firing of lignite with municipal solid waste in a FBC, respectively. Moreover, distribution of combustion air also plays an important role for biomass or biomass-contained combustion in a FBC system. It was observed that every 20% increase in excess air reduces the bed temperature to about 10-30 °C on average due to increased heat loss and reduced residence time for the fuel particles (see Tables 4.10-4.15). However, in the freeboard region the temperatures were found to have a tendency to increase with higher excess air (see Tables 4.2-4.8). This is explained by the fact that the higher excess air contributes to higher fluidising velocity [44, 55]. Thus, settling time for biomass to reach the bed will be greater and most combustion will complete before it reaches the bed. The exception is the combustion of palm fibre (see Figure 4.5) where further increases of the palm fibre fractions (more than 30%) leads to instability of the bed temperature (decreased to below 700 °C) and so the combustion process could not be sustained.

4.3.2 Thermogravimetric Analysis (TGA)

Thermogravimetric analysis has been carried out to investigate the pyrolysis behaviour of different biomass raw fuels at typical rates of conventional pyrolysis processes. The results are represented by Thermogram (TG) profiles which plot the weight loss against the temperature and derivative thermogravimetry (DTG) curves which referred to the rate of weight loss. The peak in DTG curves verifies and explains the detail of the temperature profiles obtained for the fuels studied in the FBC.

The TG and DTG curves of the biomass residues and bituminous coal with particle sizes of approximately 250 μm were obtained at a heating rate of 10 °C min^{-1}, are shown in Figures 4.10 and 4.11. As can be observed, TGA and DTG curves are similar except for bituminous coal and the refuse derived fuel. At heating rate of 10 °C min^{-1}, for all the biomass (except refuse derived fuel) the thermal decomposition starts at approximately 200 °C. A major loss of weight follows, where the main devolatilisation occurs with a maximum rate between 300 and 400 °C and is essentially completed by about 450 °C. This is followed by a slow further loss of weight up to the final temperature. The DTG peaks differ in position and height. Taking into consideration that peak height is directly proportional to the reactivity, while the temperature corresponding to peak height is inversely proportional to the reactivity [46], the wood pellet, which has also the highest volatiles content, is the most reactive among the species studied, followed in sequence by palm kernel shell, rice husk, palm fibre, chicken waste, refuse derived fuel and bituminous coal. On the other hand, for the TGA curves of bituminous coal, the decomposition starts at about 350 °C, which is significantly higher than the one corresponding to the biomass samples. The maximum pyrolysis rate occurs at 500 °C, at a level of 3 x 10^{-2} min^{-1} which is 5 - 7 times lower than that of the biomass materials, thus indicating that bituminous coal is less reactive. Decomposition of bituminous coal continues until the end of experiment, indicating that its conversion lasts over a greater temperature interval compared to biomass.

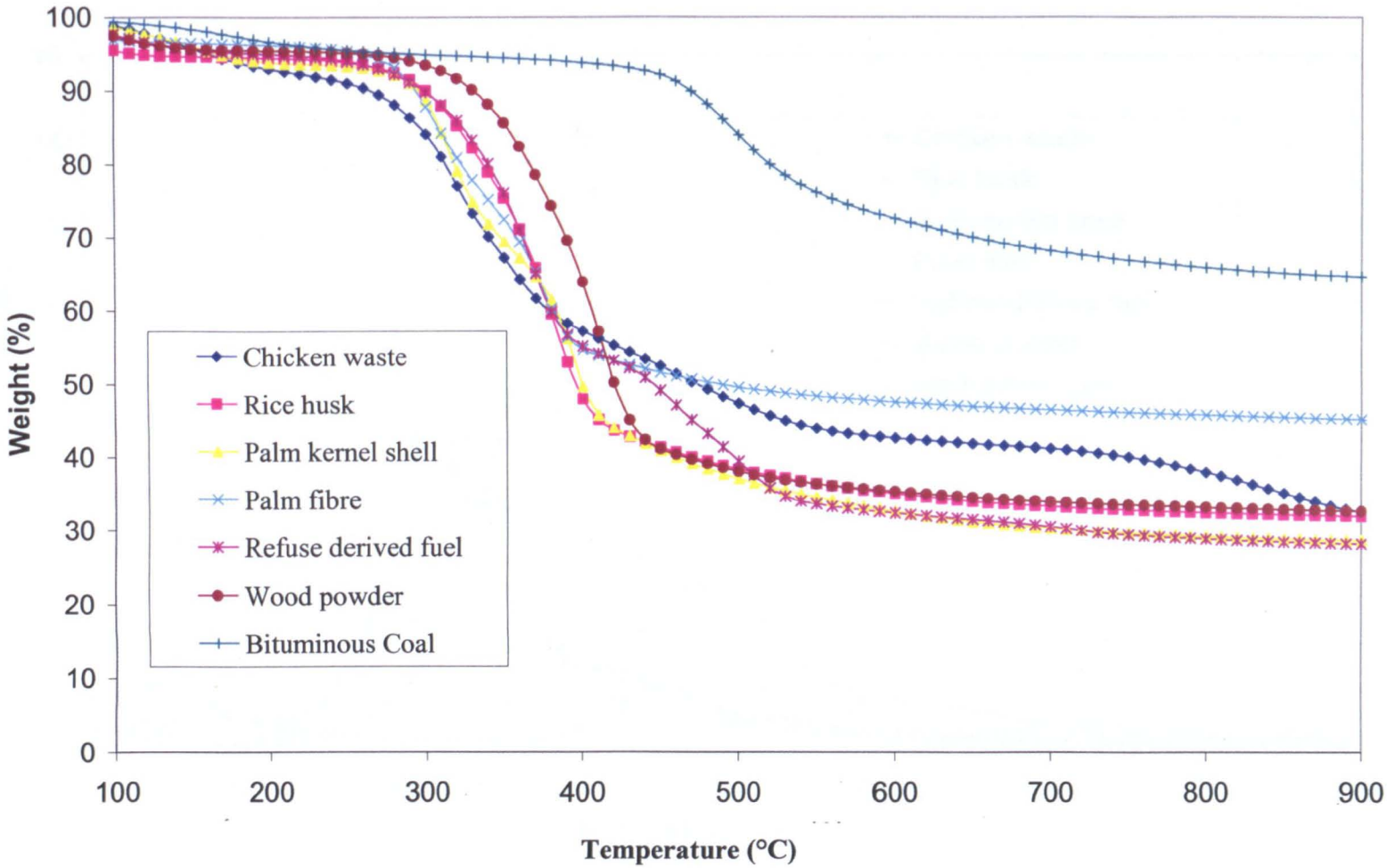

Figure 4.10 Thermogram (TG) profiles of the biomass materials and bituminous coal at heating rate 10°C/s

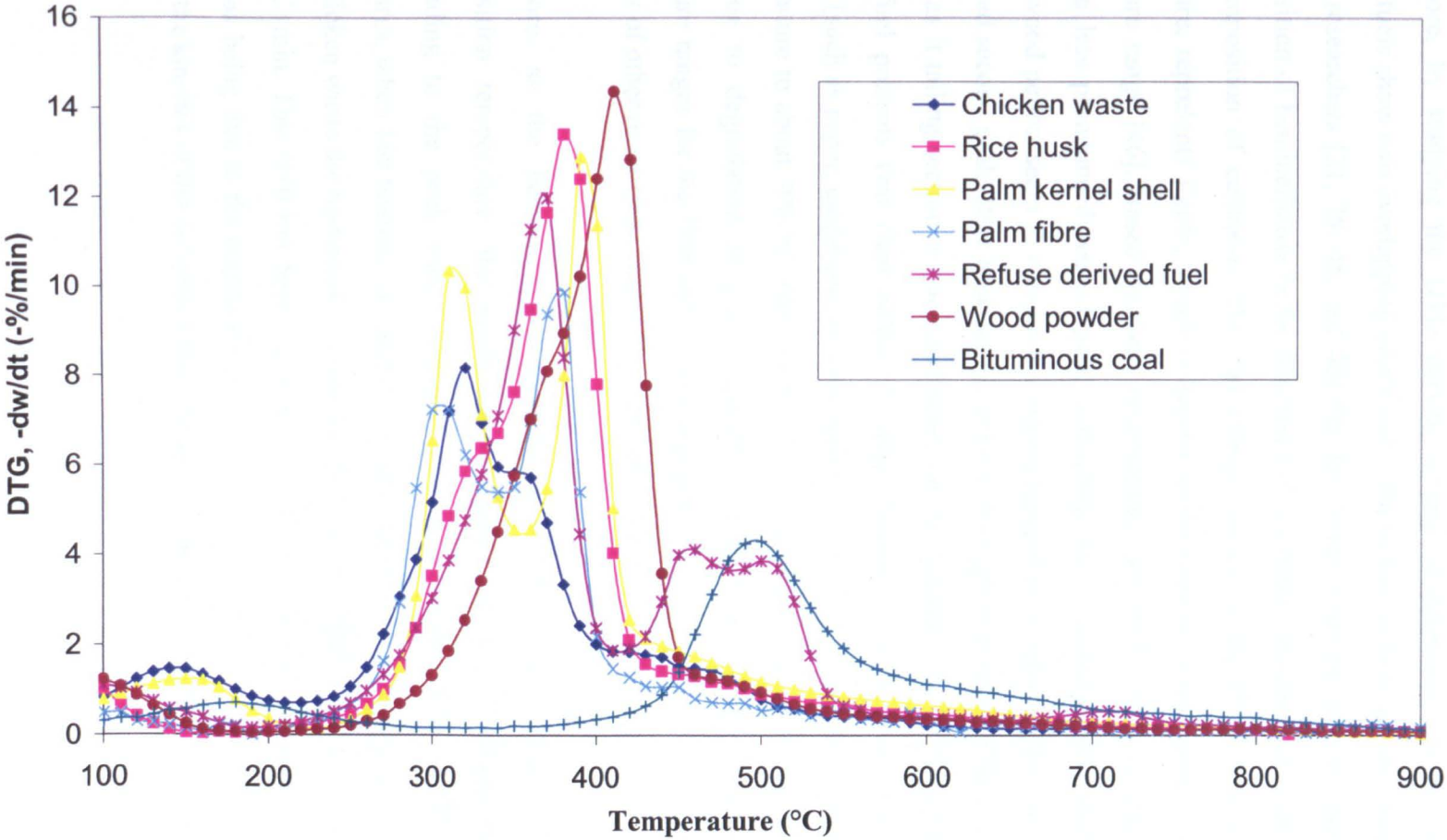

Figure 4.11 DTG profiles of the biomass and bituminous coal at heating rate 10 °C/s

Furthermore, by studying the DTG curves, several observations can be highlighted. Biomass fuels show two overlapping peaks and a flat tailing section. Its have been debated by other researchers [21, 28, 45, and 46] that the lower temperature peak represents the decomposition of hemicellulose in the material and the higher temperature peak represents the decomposition of cellulose. The flat tailing section of the DTG curves at higher temperature, represents lignin, which is known to decompose slowly over a very broad temperature range [46]. Based on these observations, the DTG curve of chicken waste exhibits a less pronounced second peak, indicating that it contains less hemicellulose, whereas wood pellets seem to contain the largest amount of hemicellulose, due to its well pronounced second peak. Rice husk seems to have the highest amount of lignin among the samples, as it tailing section is quite profound. On the contrary, the DTG curve of refuse derived fuel presents two clear peaks. A large fraction of volatiles, mainly cellulosic materials (such as paper, cardboard, etc) are released in the first faster step of the pyrolysis, at temperature to about 300 °C. The second, in a temperature range between 400 and 500 °C, is due to degradation of plastic materials. Qualitative pyrolysis behaviour and temperature ranges for the first and second degradation steps are in good agreement with the results of other researchers in the literature [22, 23, 46].

Furthermore, as the heating rate increased from 10 to 100 °Cmin^{-1}, the initial decomposition temperature, the maximum devolatilisation rate and the temperature corresponding to the peak were increased. The lateral shift in the DTG to higher temperatures, when fast heating was applied, is also shown in Figure 4.12. As an example, for the chicken waste the maximum degradation shifted from 300 °C at 10 C/min to 330 °C at 100 °C /min. This shift has been reported for different types of biomass and has been assigned as being due to the combined effects of the heat transfer at the different heating rates and the kinetics of the decomposition, resulting in delayed decomposition [46].

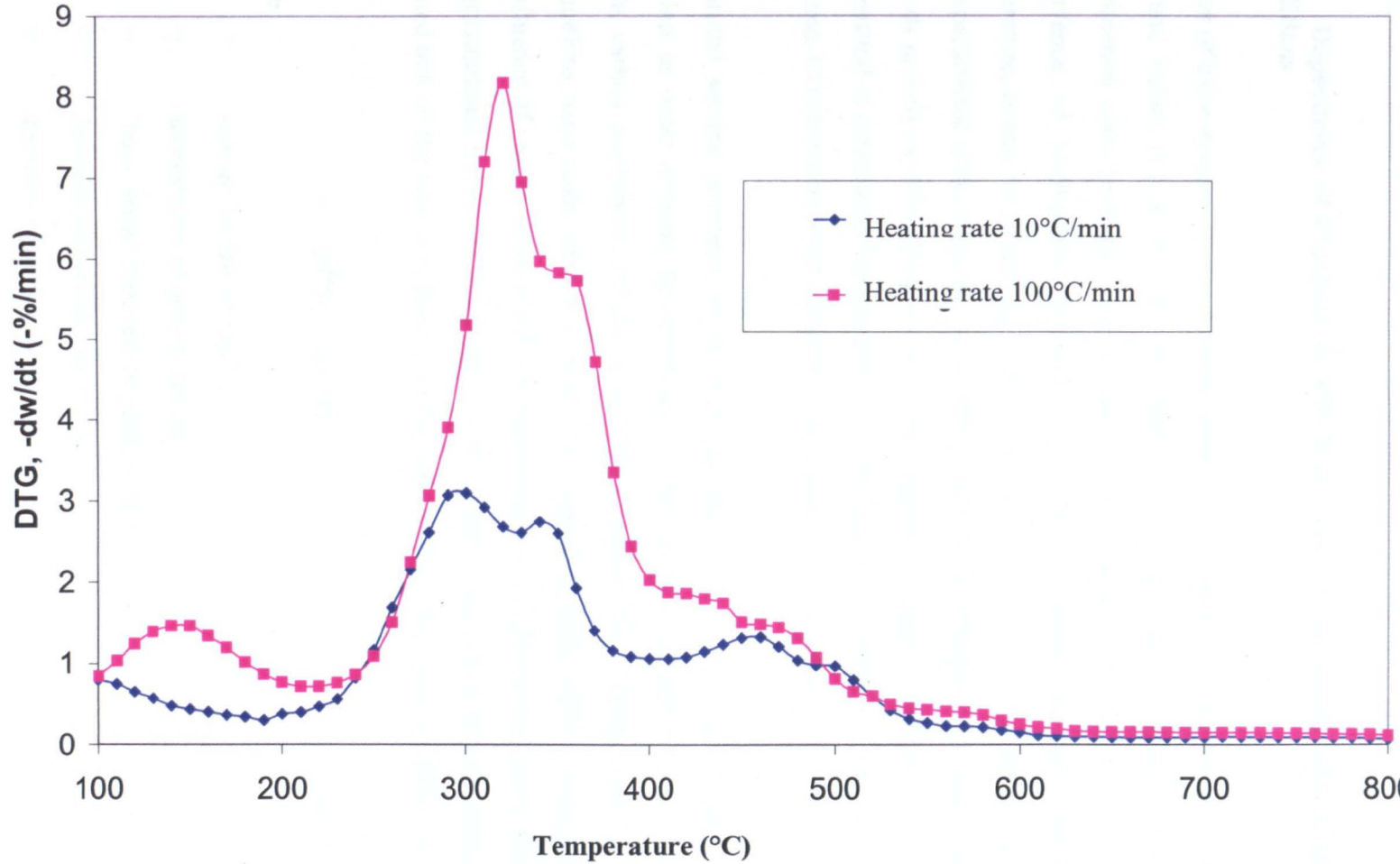

Figure 4.12 Effect of heating rate on the DTG profiles of results of chicken waste

4.4 Dependence of Combustion Efficiency and CO emissions upon Experimental Conditions

The set of experimental results obtained in the current work is presented in Figures 4.13 to 4.35 and Tables D.1 to D.7 (in Appendix D). The operating conditions and individual experimental runs were given previously in the Tables 4.2 - 4.8. In this section, the dependence of combustion efficiency and CO emissions on fuel properties, bed temperature, excess air, fluidising velocity and coal mass fraction are discussed. Based on the experimental data, the combustion efficiencies were calculated by using two different methods namely: a) CO efficiency (E1) and b) modified carbon utilisation efficiency (E2). The method of calculation had been shown in section 3.5 in chapter 3. Also, for comparison purposes, CO emissions in all tests were converted to CO emitted at 6% of O_2 in flue gas.

The initial settling velocities of the fuel particles were also evaluated based on Stokes equation in order to study the influence of fuel particle density effect on temperature profile, carbon combustion efficiency and CO emission. The formula is given in Eq. 4.1. Calculations were made relative to coal. This formula applies when a particle falls under the influence of gravity when it will accelerate until the frictional drag in the fluid balances and gravitational forces. At this point it will continue to fall at a constant velocity. It was assumed that all the Re < 0.1. Results of this calculation were given in Table 4.9.

$$u_t = gd^2(\rho_p - \rho_g)/18\mu \qquad (4.1)$$

where

u_t = velocity of fall (m sec^{-1}),

g = acceleration of gravity (m sec^{-2}),

d = "equivalent" diameter of particle (m),

ρ_p = densities of particle (kg m^{-3}),

ρ_g = densities of air (kg m^{-3}),

μ = viscosity of medium (N sec m^{-2}).

Table 4.9: Differences of particle diameter, particle density and settling velocity ratio of coal and biomass

Fuel	Particle diameter (mm)	Particle density (kg/m^3)	Settling velocity ratio (compared to coal)
Coal	1.4	1200	1
Chicken waste	3	646	2.47
Rice husk	0.8	98	0.03
Palm kernel shell	3	435	1.66
Palm fibre	1	104	0.04
Refused derived fuel	10	410	17.43
Wood pellets	7	490	10.21
Wood powders	1	490	0.21

As can be seen in the Table 4.9, the rate of initial settling velocity is directly proportional to the square of their diameter (relative to coal diameter). The larger the diameter of the fuel particles a higher settling velocity ratio were resulted. For example, the settling velocity ratio for refuse derived fuel is much higher than that of palm fibre which is ten times smaller particle diameter. However it was noticeable that the refuse derived fuel disintegrated on feeding (see section 4.3.1). So the settling velocity ratio is probably overestimated. Also, there was significant difference between settling velocity ratio between wood pellets and wood powder due to large difference in their fuel particle size even though their fuel density is similar. Wood pellets have larger diameter and usually are fed and go through the combustion as their original size. Wood powder, however, was much smaller because they were ground from the wood pellets.

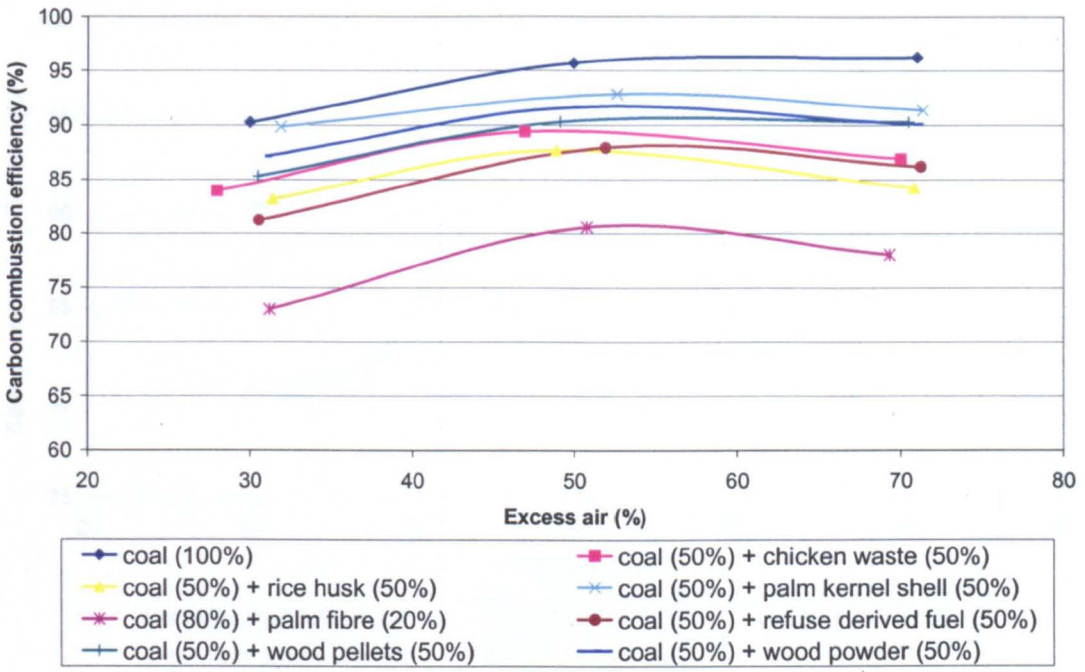

Figure 4.13 Carbon combustion efficiency during co-combustion as a function of excess air.

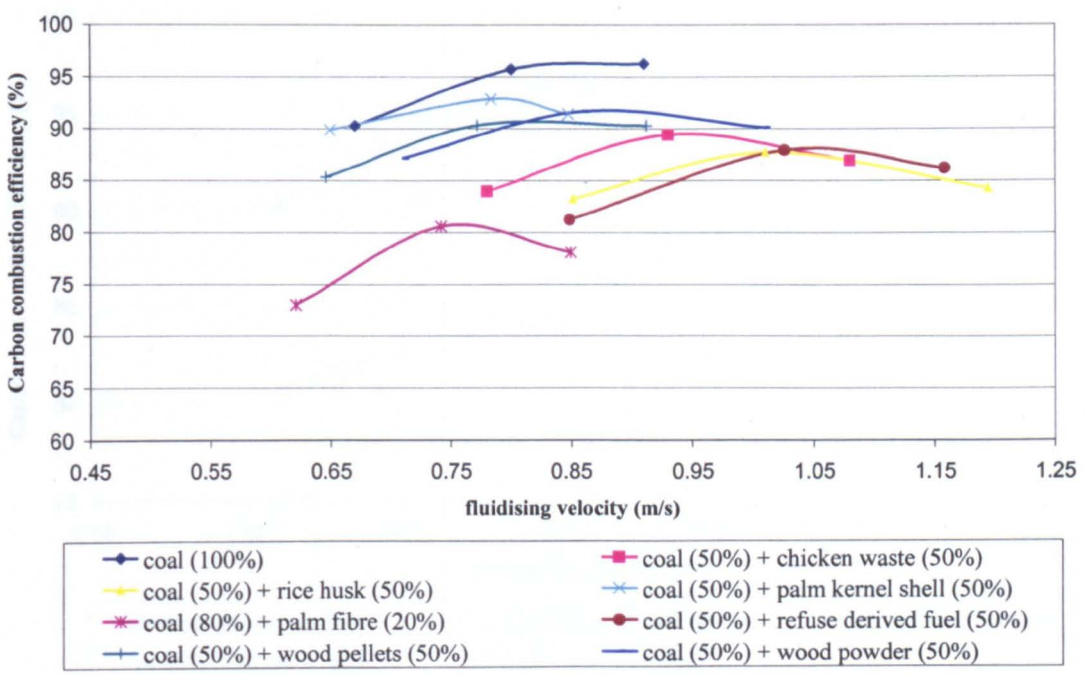

Figure 4.14 Carbon combustion efficiency during co-combustion as a function of fluidising velocity.

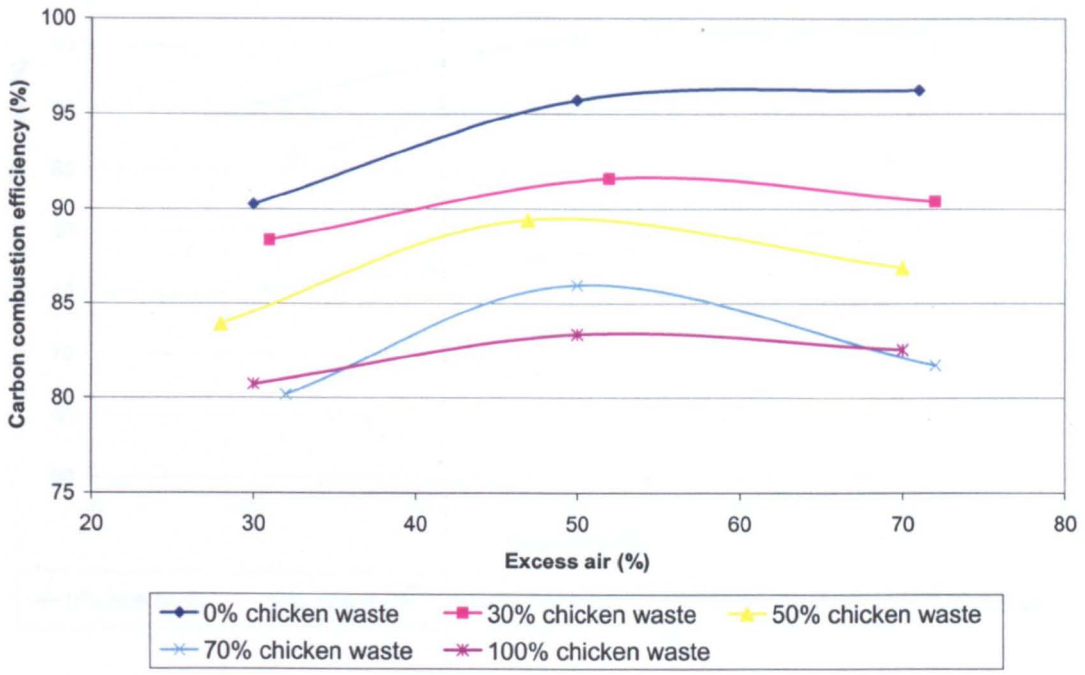

Figure 4.15 Carbon combustion efficiency during co-combustion of coal with chicken waste as a function of excess air.

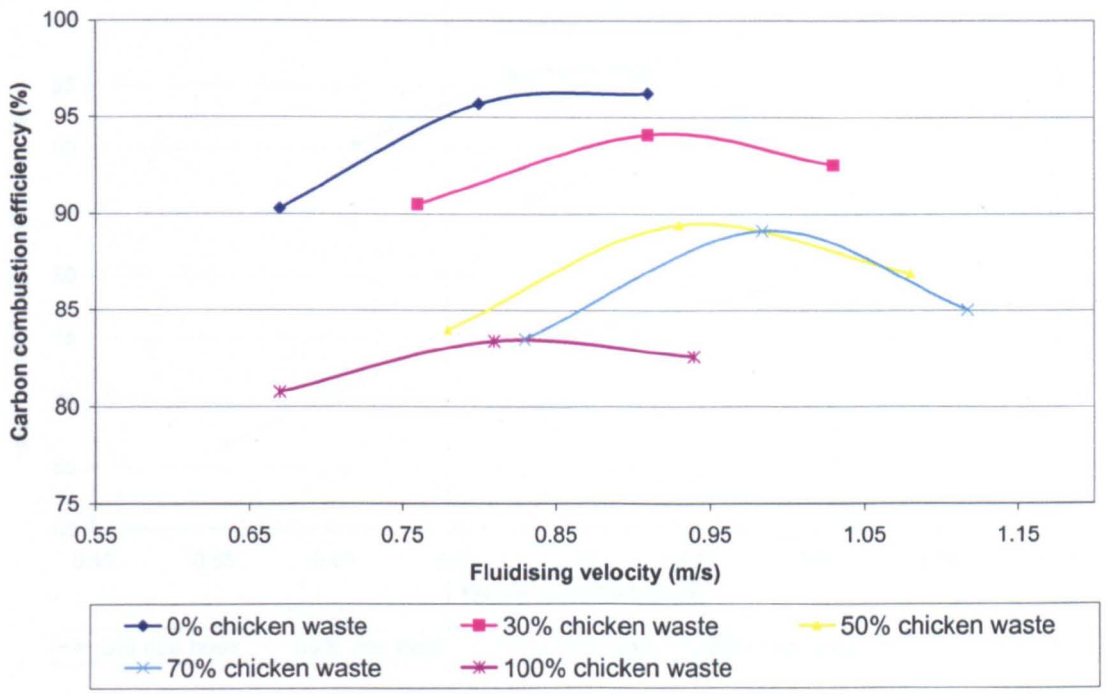

Figure 4.16 Carbon combustion efficiency during co-combustion coal with chicken waste as a function of fluidising velocity.

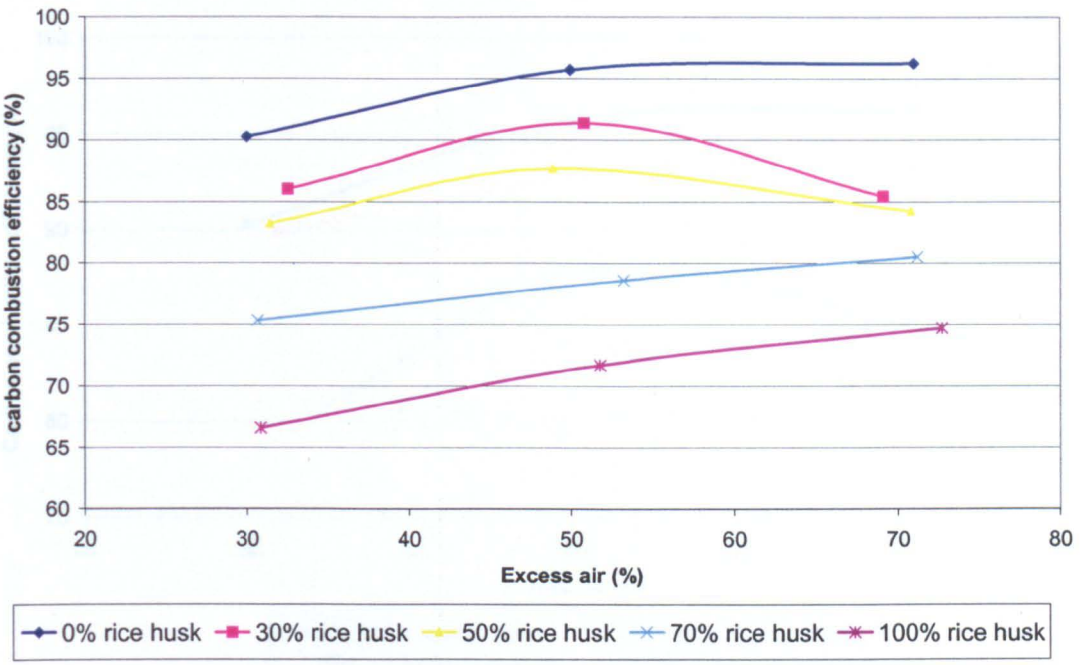

Figure 4.17 Carbon combustion efficiency during co-combustion of coal with rice husk as a function of excess air.

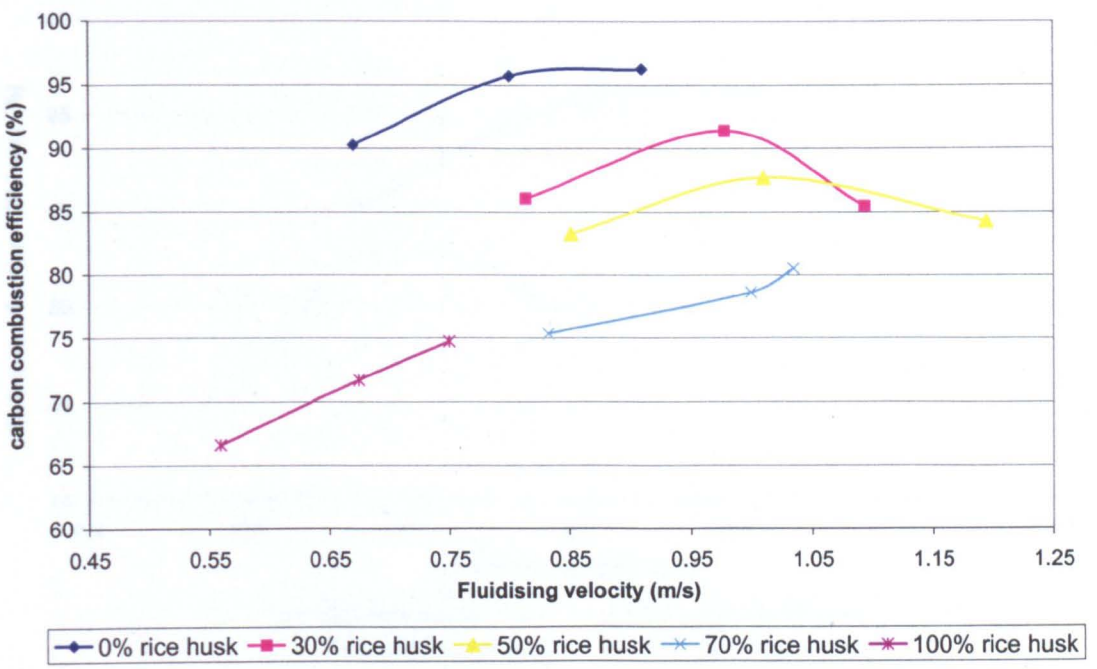

Figure 4.18 Carbon combustion efficiency during co-combustion coal with rice husk as a function of fluidising velocity.

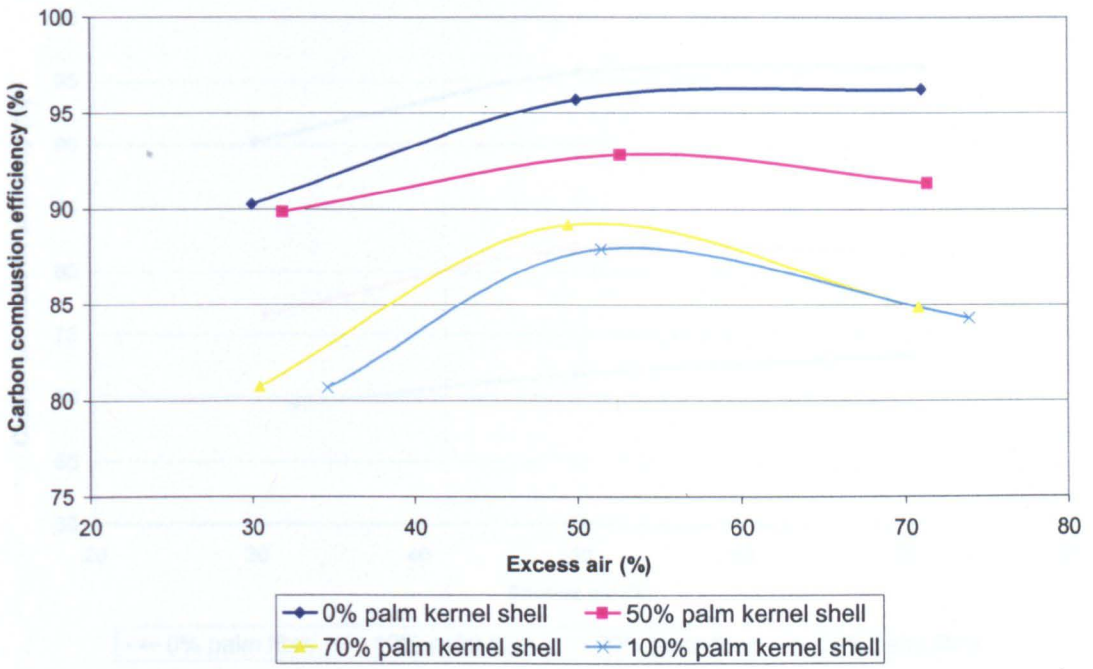

Figure 4.19 Carbon combustion efficiency during co-combustion of coal with palm kernel shell as a function of excess air.

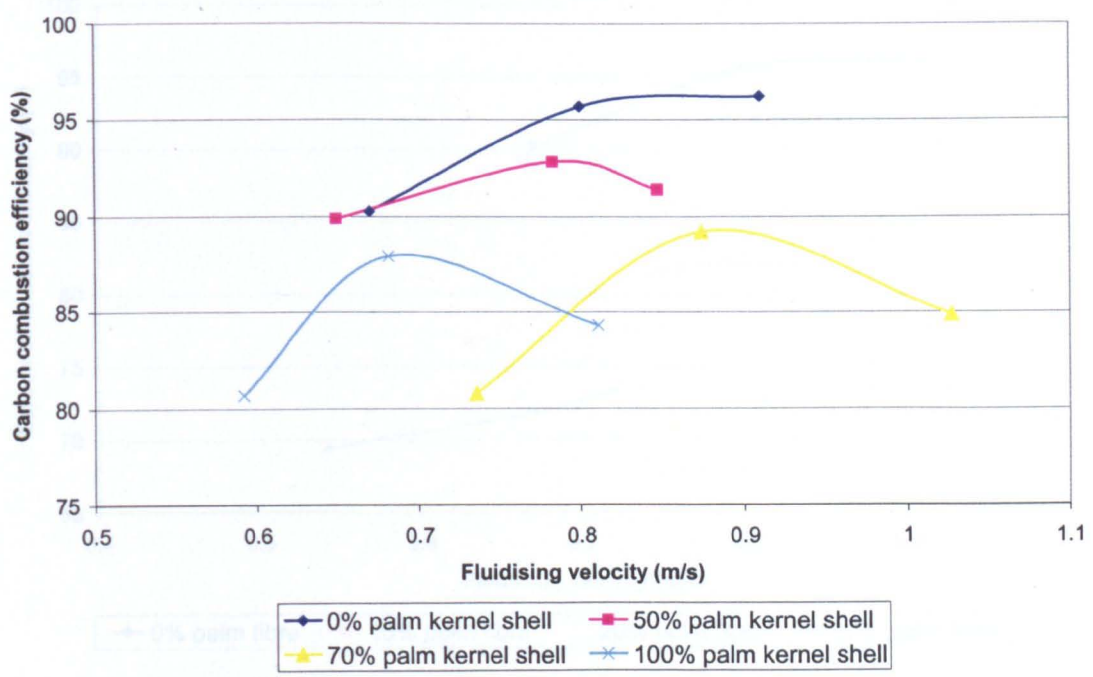

Figure 4.20 Carbon combustion efficiency during co-combustion coal with palm kernel shell as a function of fluidising velocity

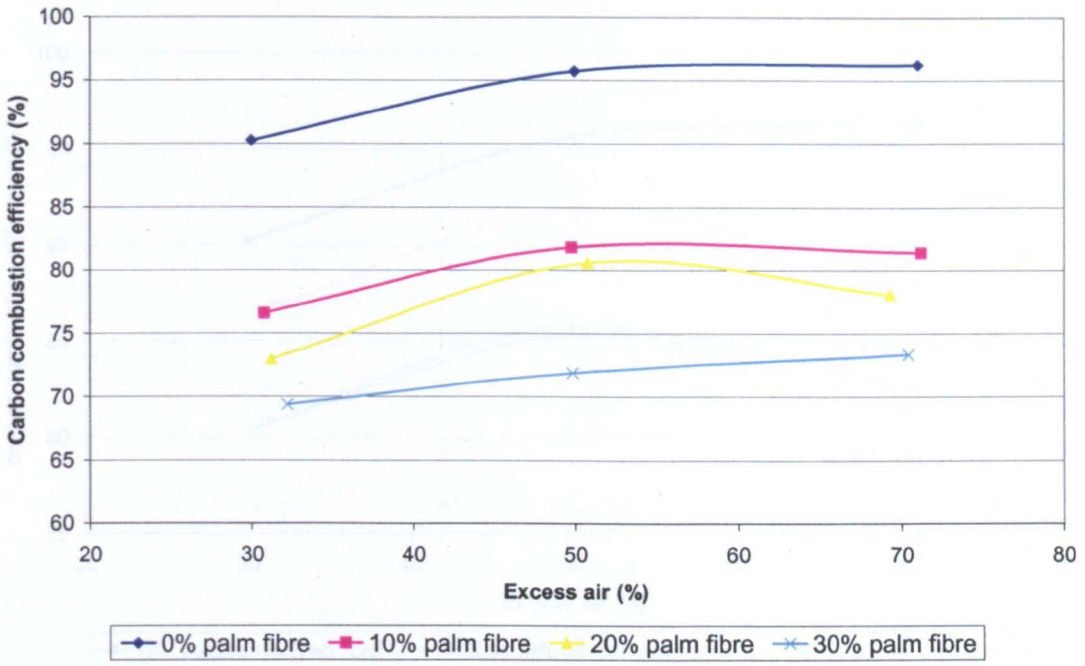

Figure 4.21 Carbon combustion efficiency during co-combustion of coal with palm fibre as a function of excess air.

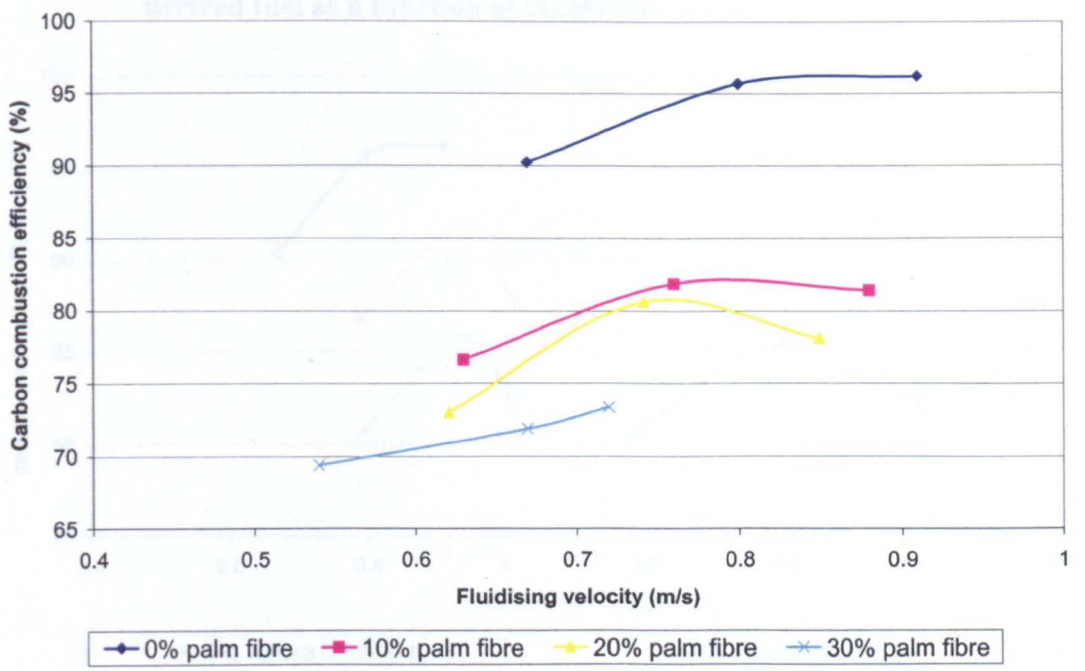

Figure 4.22 Carbon combustion efficiency during co-combustion coal with palm fibre as a function of fluidising velocity.

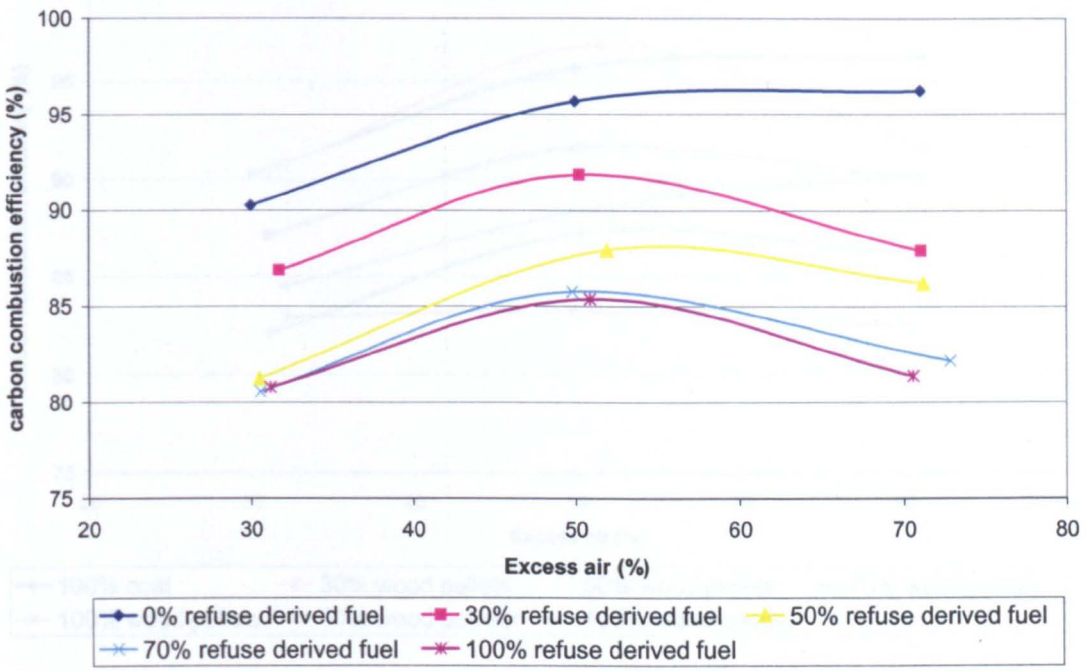

Figure 4.23 Carbon combustion efficiency during co-combustion of coal with refuse derived fuel as a function of excess air.

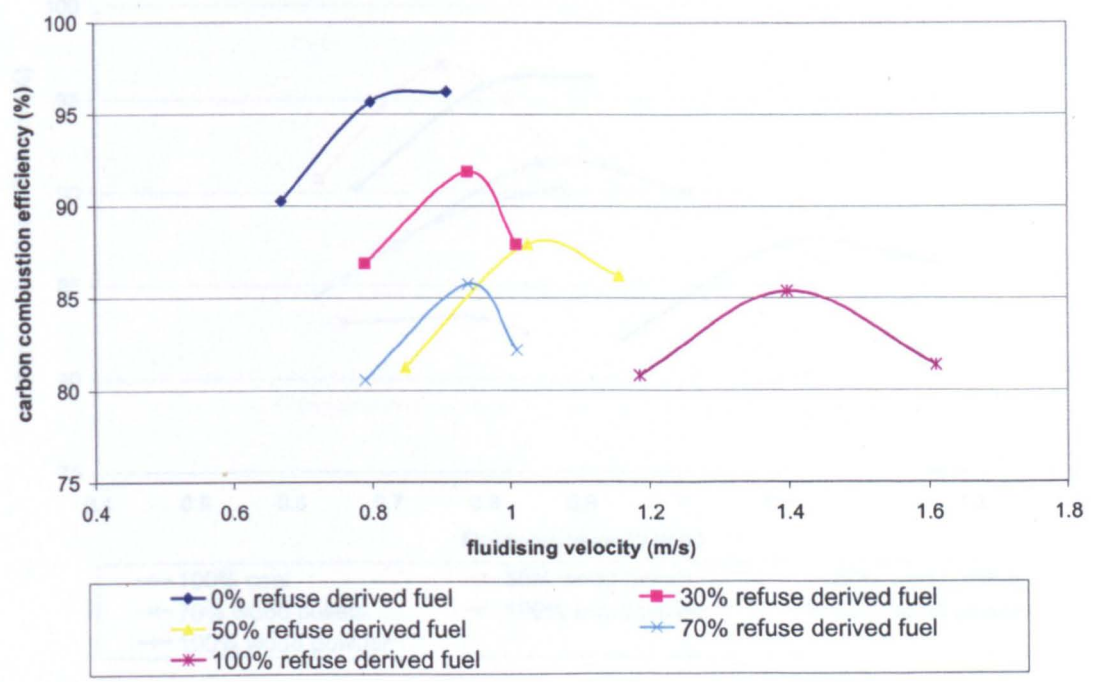

Figure 4.24 Carbon combustion efficiency during co-combustion coal with refuse derived fuel as a function of fluidising velocity.

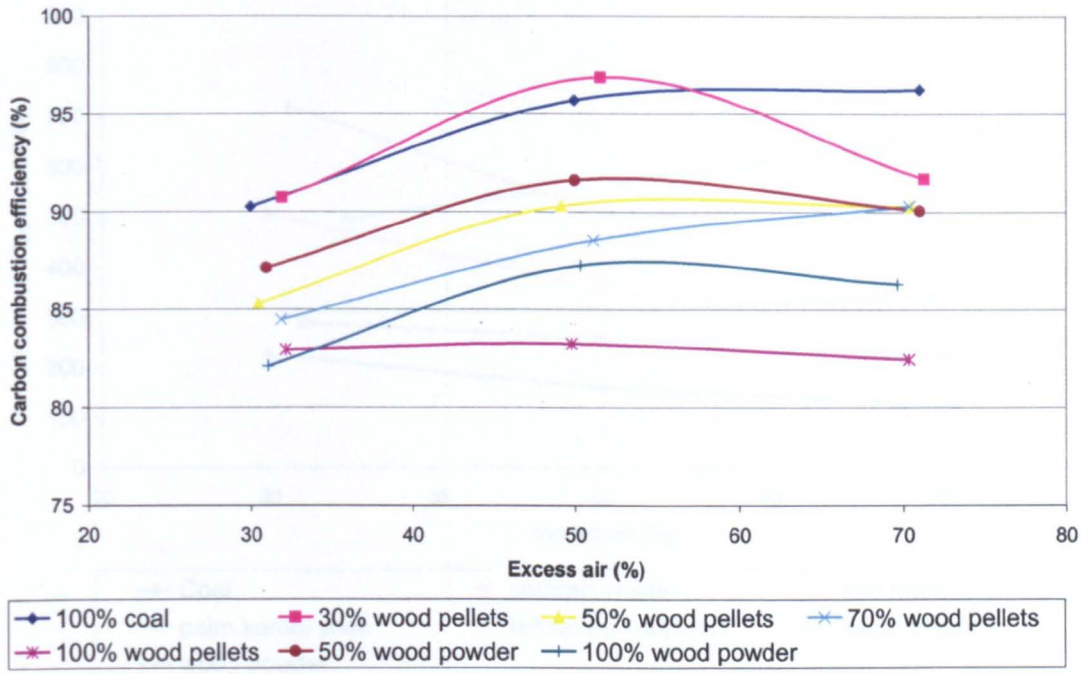

Figure 4.25 Carbon combustion efficiency during co-combustion of coal with wood pellets and wood powder as a function of excess air.

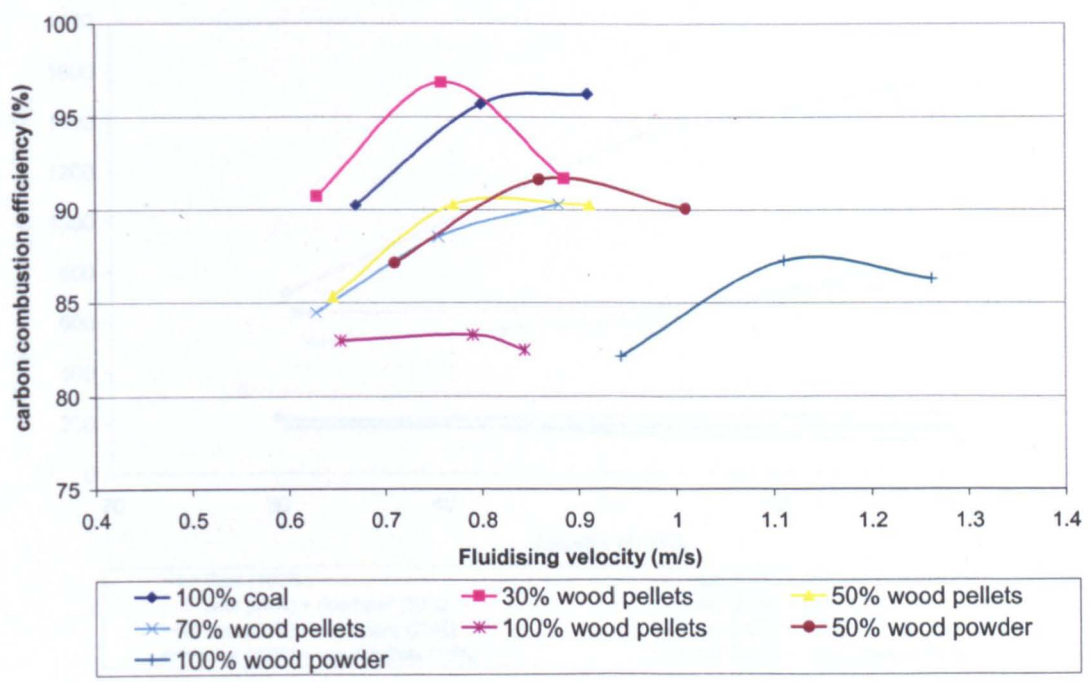

Figure 4.26 Carbon combustion efficiency during co-combustion coal with wood pellets and wood powder as a function of fluidising velocity.

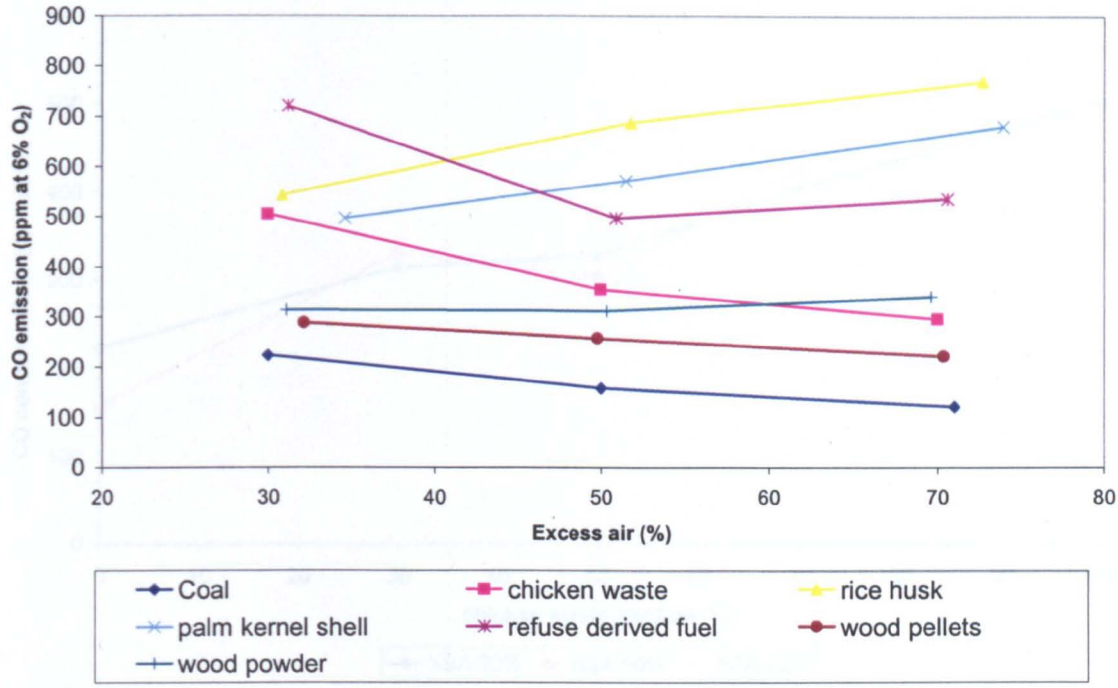

Figure 4.27 CO emissions during single fuel combustion at heat input 10 KW

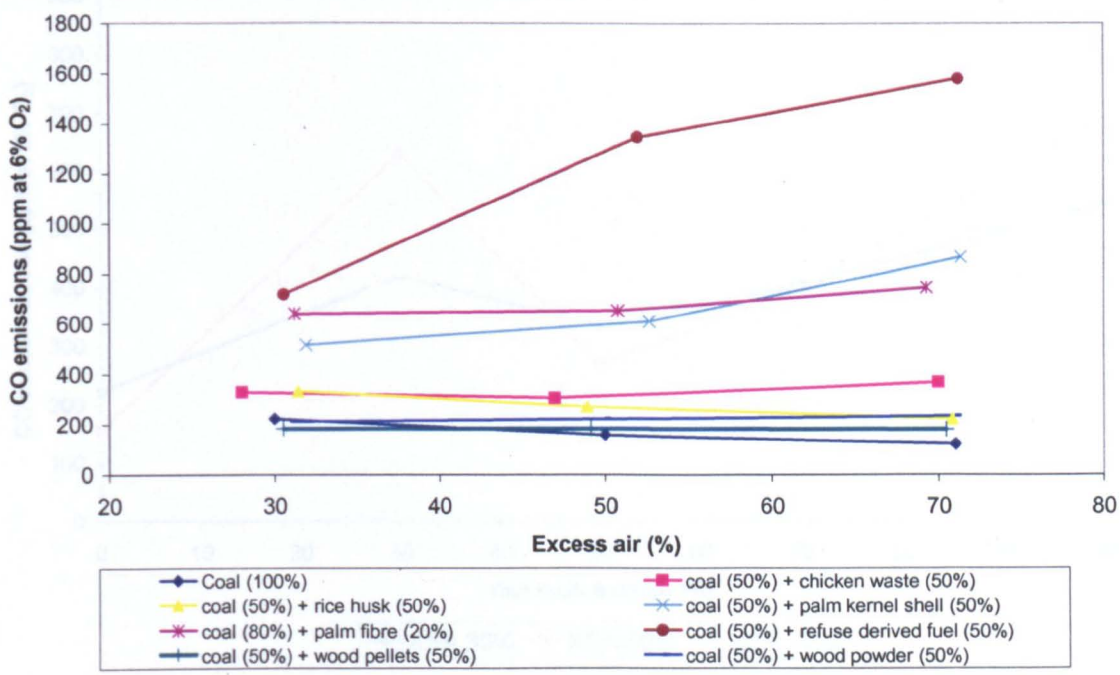

Figure 4.28 CO emissions during co-combustion coal with biomass at heat input 10KW.

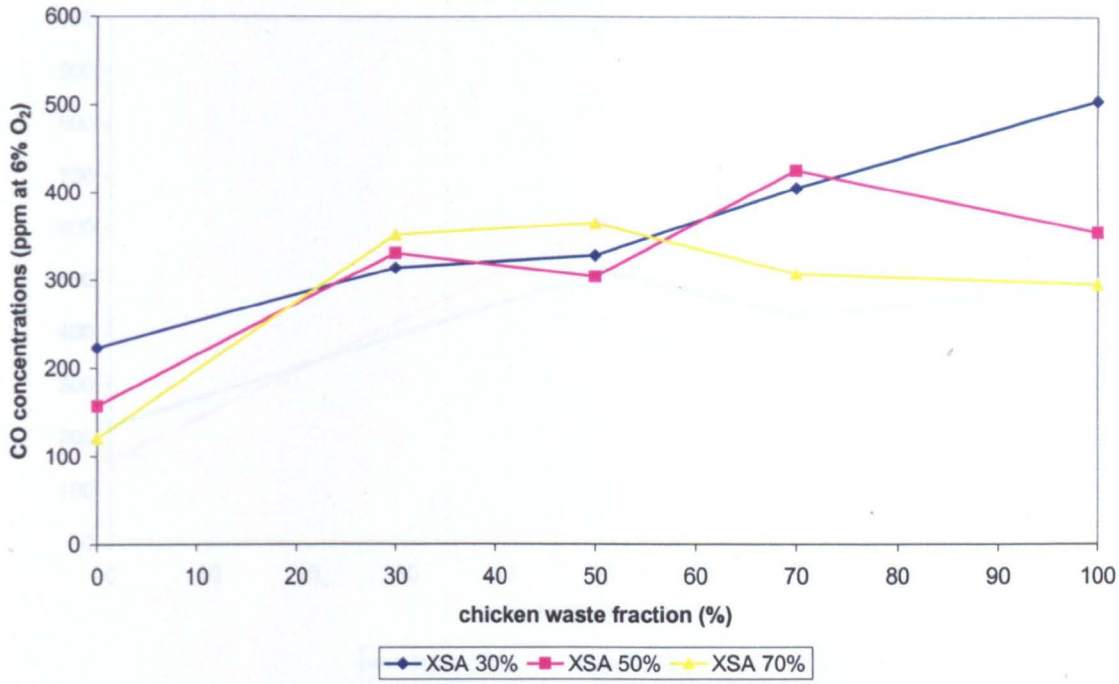

Figure 4.29 CO emissions as a function of excess air and chicken waste fraction at heat input 10 KW.

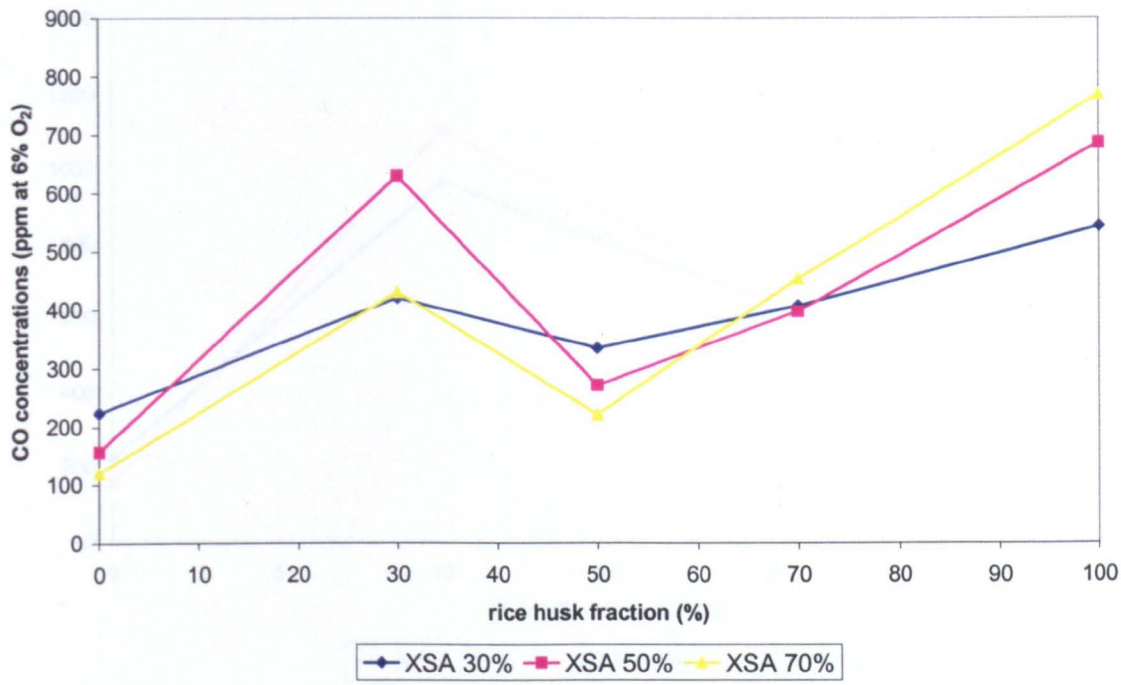

Figure 4.30 CO emissions as a function of excess air and Rice husk fraction combustion at heat input 10KW.

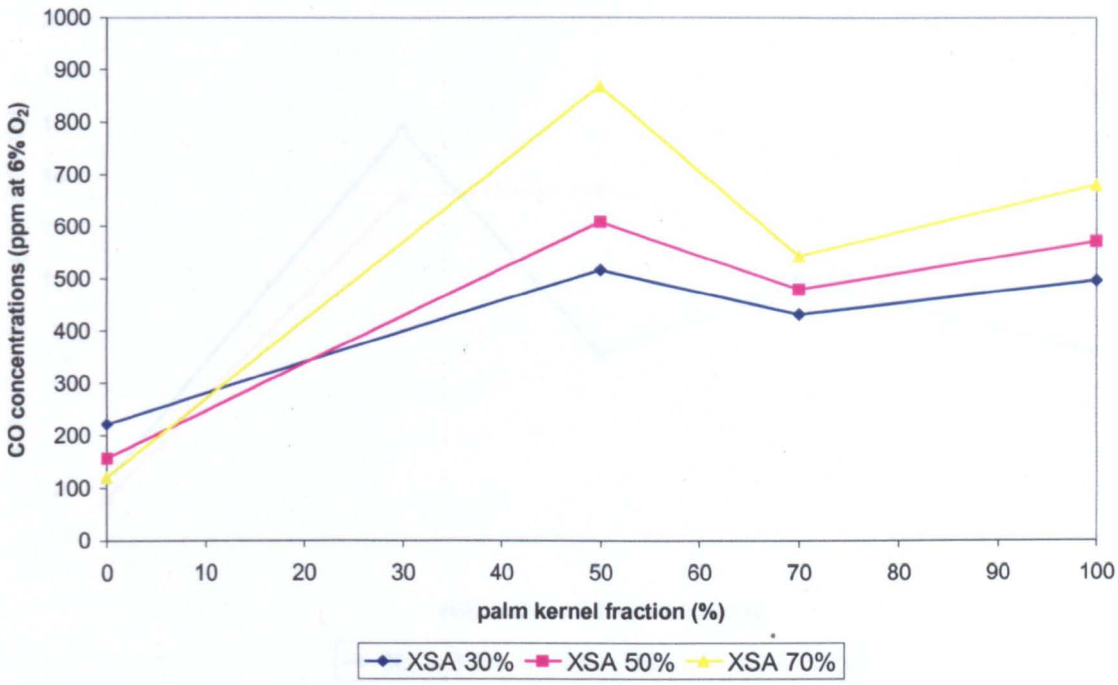

Figure 4.31 CO emissions as a function of excess air and palm kernel shell fraction combustion at heat input 10KW.

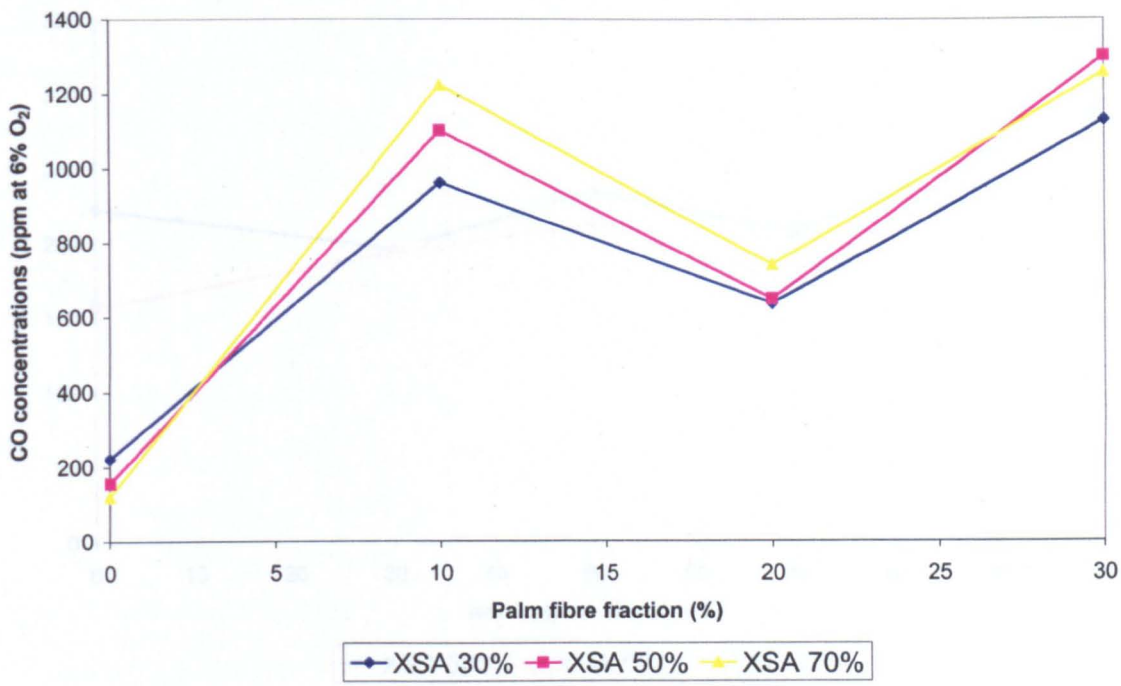

Figure 4.32 CO emissions as a function of excess air and palm fibre fraction combustion at heat input 10KW.

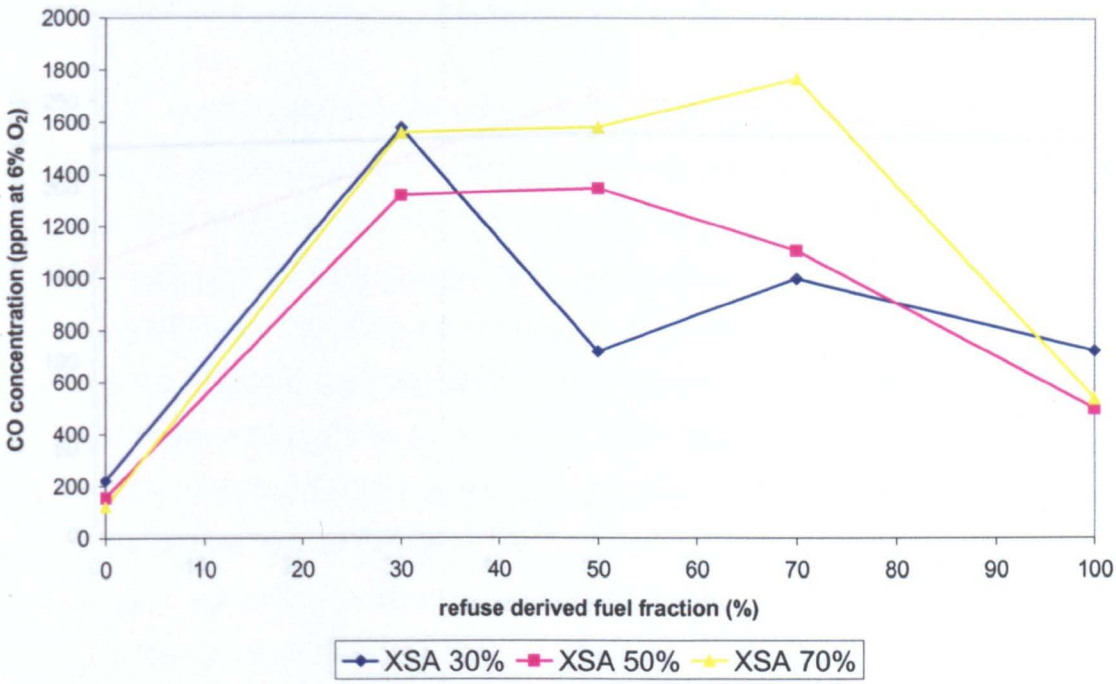

Figure 4.33 CO emissions as a function of excess air and refuse derived fuel fraction combustion at heat input 10KW.

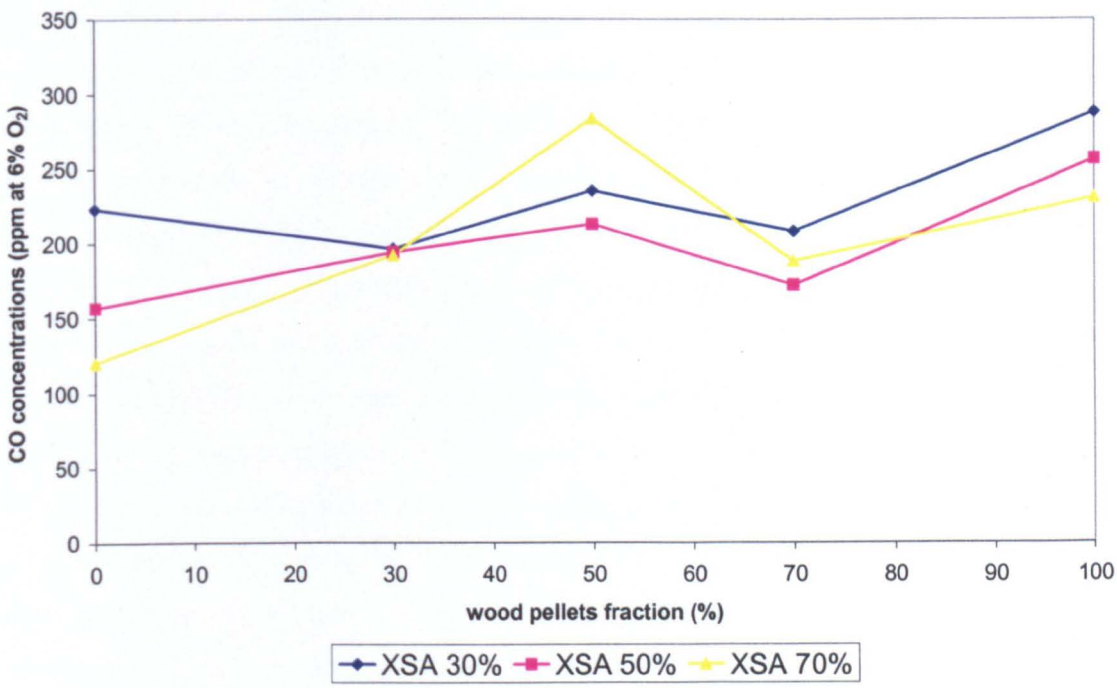

Figure 4.34 CO emissions as a function of excess air and wood pellets fraction combustion at heat input 10KW.

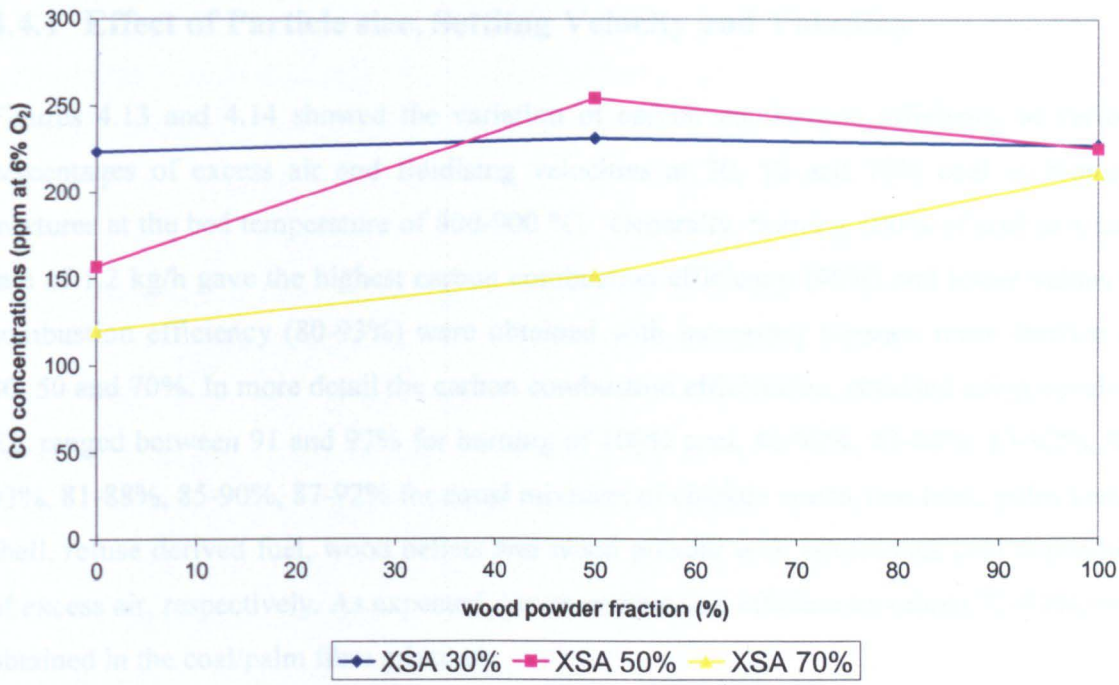

Figure 4.35 CO emissions as a function of excess air and wood powder fraction combustion at heat input 10KW.

4.4.1 Effect of Particle size, Settling Velocity and Volatility

Figures 4.13 and 4.14 showed the variation of carbon combustion efficiency at various percentages of excess air and fluidising velocities at 30, 50 and 70% coal in biomass mixtures at the bed temperature of 800-900 °C. Generally, burning 100% of coal at a feed rate of 1.2 kg/h gave the highest carbon combustion efficiency (96%) and lower values of combustion efficiency (80-93%) were obtained with increasing biomass mass fraction of 30, 50 and 70%. In more detail the carbon combustion efficiencies, obtained using equation E2, ranged between 91 and 97% for burning of 100% coal, 86-90%, 83-88%, 83-92%, 90-93%, 81-88%, 85-90%, 87-92% for equal mixtures of chicken waste, rice husk, palm kernel shell, refuse derived fuel, wood pellets and wood powder with bituminous coal depending of excess air, respectively. As expected, lower combustion efficiencies (about 72-81%) was obtained in the coal/palm fibre mixtures.

Among the biomass fuels, co-combustion of 50% coal with 50% palm kernel shell gave the highest combustion efficiency and the lowest was co-combustion of 80% coal with 20% palm fibre at 50% excess air. Mixtures of coal/palm kernel shell blend that gave the highest combustion efficiency are due to the highest fixed carbon ratio (about 0.32) compares to other biomass fuels. In the case of coal/palm fibre, the combustion efficiency is still the lowest among other fuels even though the coal fraction was 30% higher than other mixtures. The instability indicated by lower bed temperature has retarded its combustion performance. Furthermore, as can be seen in Figures 4.13 and 4.14, the smaller the fuel particle size and the greater settling velocity, the higher carbon combustion efficiency was obtained at optimum conditions (50% excess air). This phenomenon can be seen in the case of coal/rice husk, coal/wood powder and coal/chicken waste compared to combustion of coal/wood pellets or coal/refuse derived fuel. The smaller particle size of rice husk and wood powder gives a rapid and efficient combustion due to the larger surface area to volume ratio. This is verified by higher freeboard temperature (about 200-400°C) which is than refuse derived fuel or wood pellet indicating more combustion in the freeboard region as showed previously in Figure 4.2. This can be explained by the fact that the greater the

settling velocity, more combustion occurred in the freeboard and hence increased the carbon combustion efficiency. However this effect is insignificant for coal/rice husk and coal/palm fibre even though their settling velocities are quite similar. Coal/rice husk tended to compact in the screw feeder resulting in a fluctuating feed rate. Meanwhile, in the case of coal/palm fibre this is due to the segregation problem during coal/palm fibre combustion in the combustor. The palm fibre fuels cannot be fed at constant rate runs resulted due to stickiness of the fibrous material. This problem however was reduced with coal addition to the mixtures. Relatively, the bed temperature appears not to be a major factor in this case where even higher bed temperatures were observed in the case of coal/wood pellets or coal/refuse derived fuel, the carbon combustion efficiency is still higher for smaller particle size fuels. Moreover, this can be explained in terms of their reactivity and devolatilisation time. As can be seen in Figure 4.10, heating profiles of rice husk and wood powder were characterised as highly reactive indicated by the high peak and the low devolatilisation time. In the case of chicken waste, even though the reactivity is lower, the completion time is faster than the refuse derived fuel. Thus, the combustion will be faster than the refuse derived fuel since larger particle size needs a longer devolatilisation time.

Figures 4.27-4.35 show the CO emissions as a function of excess air and biomass mass fraction. In this study, significant fluctuations of CO emissions were recorded ranging between 100 and 2000 ppm for the same conditions. These orders of fluctuation were similar to those observed by Abelha *et al.* [20] and Sami *et al.* [13]. This is due to the slight variations in the feed composition that could give rise to these fluctuations. This effect is reflected in the emissions graph and not in the temperature profiles. Generally, higher CO emissions were observed for single biomass or coal/biomass combustion except in the case of coal/wood pellets in comparison to 100% coal combustion. This can be explained by the fact that higher volatiles combustion is a dominant step during biomass combustion. The higher volatile matter content mainly consists of combustibles (CO, H_2 and CxHy) which accounted 70-80-vol% of the gas components. These results were found in good agreement with other results as discussed earlier in section 2.2.4.2.3.

4.4.2 Effect of Coal Mass Fraction

Generally, the carbon combustion efficiency increases with increasing coal addition in all cases (as previously shown in Figures 4.13-4.26). The maximum carbon combustion efficiency increases range from 3% to 20% as the coal fraction increases from 0% to 70%, depending upon the percentage of excess air. As illustrated previously in Figures 4.15 and 4.16, it can be seen that the average combustion efficiency increases from 85 to 92 % with the amount of coal added from 30 to 70% at 50% of excess air in the case of combustion of coal with chicken waste. In the case of coal/rice husk combustion, the experimental runs gave carbon combustion efficiencies ranging between 91 and 96% for burning of 100% of coal, 86-92%, 83-88%, and 80-83% for 30, 50 and 70% of rice husk mixed with coal, respectively (see Figures 4.17 and 4.18). In the case of palm kernel shell and palm fibre combustion (see Figures 4.19 and 4.20), the carbon combustion efficiencies were between 90-93%, 72-81% for co-combustion of coal with palm kernel shell and palm fibre, respectively. Furthermore, as can be seen in Figures 4.21-4.22 the maximum carbon combustion efficiency decreased from 3% to 6% as the waste fraction increased from 0% to 70% of the refuse derived fuel fraction, depending upon the percentage of excess air. In addition, the efficiency for both wood pellets and wood powders were higher compared to other fuel mixtures which were between 82-95 % (see Figures 4.22 – 4.23). The carbon combustion efficiency generally decreased with increasing mass fractions of wood pellets.

The decrease in combustion efficiency with increasing biomass mass faction is mainly attributed to a drop in the bed temperature as shown in Tables 4.9-4.14 which is caused by reduction of fixed carbon content in the mixture since most fixed carbon generally burns in the bed while the volatile gas burns in the freeboard. Thus there is less chance for fuel C conversion to CO_2 as the chicken waste fraction increased because of the reduced fixed carbon, while there is more chance for the volatiles to escape combustion because of the increased concentration. These results are in general agreement with previously published work [13, 15, 20, 36, and 44]. This also influenced by the synergistic effect of the coal and biomass mixture which enhances the combustion reaction and hence combustion efficiency

as suggested by Suksankraisorn *et al.* [51]. However, the average carbon combustion efficiency obtained in this study (85-90%) is relatively lower than the values obtained by Bhattacharya *et al.*[39](90-95%) and Suksankraisorn *et al.* [51] results (>90%). However, both of them did not take into account any unburned ash collected in the cyclone during in their efficiency calculation.

Significant fluctuations of CO emissions values observed when coal was added into almost all biomass mixtures depending upon excess air (see Figures 4.27-4.35). The addition of coal had no significant influence on CO emissions during all co-combustion cases except at coal (50%) / rice husk (50%) where it tends to be lower than that of the other rice husk fractions (see Figure 4.30). This phenomenon is due to the synergistic effect of coal and rice husk mixture that enhances the fuel reactivity and hence lower the CO emissions. The results however were in contrast with Leckner *et al.* [54] and Desroches-Ducarne *et al.* [59] during co-combustion of coal with municipal solid waste and coal with wood waste, respectively (see section 2.2.4.2.3). They claimed that the CO emissions should increase as the coal mass fraction increased in the mixture due to char combustion and the presence of HCl should inhibit the CO oxidation to CO_2. This can be explained by the significant difference between the FBC and CFBC system used in their experiments. In CFBC combustion systems, the remaining unburned fuel is recycled onto the bed. Thus, as coal increased more char combustion occurred in the bed surface due to the addition of coal from the recycling point and hence the CO emissions increased. However, in FBC systems, there is no recycling of the fuel.

4.4.3 Effect of Excess Air

Despite the fuel properties and coal addition, the percentage of excess air is also believed to influence the combustion performance. Thus, in order to find the optimum condition of each case studied, the percentages of excess air have been varied from 30 to 70%. Figures 4.13 to 4.19 show the carbon combustion efficiency at various excess air levels for all co-combustion runs.

Generally, the carbon combustion efficiency increased with increases of excess air and peaks at 50% excess air. As can be seen in Figure 4.14, in the case of co-combustion of coal and chicken waste, the carbon combustion efficiency increases (about 3-10%) with increasing of excess air up to 50% as well as increasing coal mass fraction from 30 to 70%. However, further increase of the percentage of excess air beyond 70% had reduced the carbon combustion efficiency by about 3-5%. The remaining cases (coal/rice husk, coal/palm kernel shell, coal palm fibre, coal/refuse derived fuel, coal/wood pellets, coal/wood powders) followed a similar trend but with some differences. Their corresponding carbon combustion efficiency increased with excess air from 30-50% was found to be in the range of 5 – 12 % at 50% coal mass fraction in the biomass mixture. With the coal/rice husk, coal/ palm kernel shell and coal/wood powder they showed higher carbon combustion efficiency, while the coal/ refuse derived fuel, coal/palm fibre and coal/wood pellets showed lower combustion efficiencies at 50% excess air (see Figure 4.13).

The increasing of excess air increases the amount of oxygen supplied in order to react with the fuel. This effect can clearly be seen in Figure 4.13-4.19 when the percentage of excess air had increased from 30-50%. This was also observed by Abelha *et al.* [20] during combustion of mixture poultry litter with peat in a 50% poultry litter/coal undertaken in a 5 m height (300 mm bed height) fluidised bed combustor. However, further increase in excess air up to 70% has reduced the carbon combustion efficiency even though the amount of oxygen supplied is higher as excess air levels increased. This can be explained by the

fact that increasing excess air levels not only provides enough oxygen to enhance combustion but also increased the fluidising velocity. As suggested by Suksankraisorn *et al.* [51], this phenomenon will contribute to a greater particle elutriation rate than the carbon to CO conversion rate and hence increases the amount of unburned carbon. The significant effect of fluidising velocity on carbon combustion efficiency will be evaluated in detail in section 4.4.4. Moreover, lower bed temperature observed as the excess air increased has only a minor effect of lowering the carbon combustion efficiency as will be discussed later in section 4.4.5.

The CO emissions results obtained showed only minor dependence on excess air levels in most co-combustion tests. As can be seen in Figure 4.27, for 100% coal, chicken waste, wood pellets and refuse derived fuel combustion, CO drops as excess air increases from 30% to 70% due to the increased CO to CO_2 conversion. Furthermore, increased excess air has reduced residence time for lower particle density fuel burned in the reactor. This argument was also supported by Saxena *et al.* [53] for their paper pellets on combustion, which concluded that in the turbulent regime, further increases in excess air had an insignificant influence on the bed hydrodynamics.

In the case of co-combustion, almost the same trend as single combustion was observed. As can be seen previously in Figure 4.29, the addition of coal to chicken waste reduced CO when the excess air was relatively low (30% and below) but the CO rose when the excess air was relatively high (70% and above). On the contrary, as can be seen in Figures 4.32 and 4.33, the CO emissions were found to increase with the increasing excess air levels in the case of coal/palm kernel shell and coal/palm fibre combustion. However, in the case of coal/rice husk, coal/refuse derived fuel, coal/wood pellets and coal/wood powder combustion, the emission of CO seems relatively insensitive to changes of excess air (see Figures 4.30, 4.33, 4.34 and 4.35).

The decrease of CO levels at low percentages of excess air (30-50%) in the case of coal/rice husk can be explained by the fact that with low excess air, the bed temperature is relatively high (about 900°C) which causes rapid release and ignition of volatiles from chicken waste and higher CO to CO_2 conversion enhances the reactivity of the mixture. In the case of coal/palm kernel shell and coal/palm fibre, the CO values still increase with increases of excess air even though the bed temperature decreased. It should be noted that the lower bed temperatures did not have any detrimental affect on CO emissions because increased turbulence in the bed created by the high air flow rate was more significant than the reduced bed temperature. The insensitive effect with increased excess air in the remaining cases was due to increased segregation problem of fuels in the combustor between the feed point and the bed. If the combustor received a batch with a relatively high amount of fuel pellets, then during the beginning of this burning time there won't be any CO_2 produced since the pellets need to be heated and dried first. While it occurs, the oxygen is not going to be consumed and resulting in a high CO emission values. The same observations were also reported by other researchers during co-combustion coal with some biomass fuels at similar conditions [20, 50, 51, and 52] especially during low feed rates.

4.4.4 Effect of Fluidising Velocity

As mentioned earlier in the previous section, the influences of excess air levels on carbon combustion efficiency and CO emissions are related to the fluidising velocity. The effects of fluidising velocity on carbon combustion efficiency and CO emissions are previously shown in Figures 4.16, 4.18, 4.20, 4.22, 4.24 and 4.27-4.35, respectively.

In general, the carbon combustion efficiency for all cases was increased as the fluidising velocity increases. Since the biomass fuels are characterised by high volatile matter content fuel in comparison to coal, it is expected that the volatiles combustion will take place or be released spontaneously as the biomass fuels entered the combustor and will tend to burn above the bed or along the freeboard area of the combustor. This evidence can be seen in the temperature profiles of biomass or coal/biomass combustion as previously shown in

Figures 4.2 -4.10. Increasing the fluidising velocity increases the turbulence in the bed leading to better solid mixing and gas-solid contacting and so as the amount of carbon in the bed is burnt at higher rate. Consequently, higher carbon burn out obtained leads to a higher carbon combustion efficiency. However, when the combustion is stabilised, increasing fluidising velocity contributed to a greater particle elutriation rate than the carbon to CO conversion rate and hence increased the unburned carbon. This phenomenon can be seen in Figures 4.16, 4.18, 4.20, 4.22, 4.24 where the carbon combustion efficiency is rather decreased when the fluidising velocity increased beyond the optimum value.

Apart from solid mixing, increasing fluidising velocity also influenced the settling time of fuel particle during the combustion process in FBC. Increasing fluidising velocity has brought the lighter fuel particle upward to the freeboard region which is indicated by higher freeboard temperature as shown in Tables 4.2-4.8. Thus, the settling time for the biomass to reach the bed will be greater and a significant portion of the combustion will be completed before the bed is reached. This settling time depends on the fuel particle size and particle density (see Table 4.9). As can be seen in Figures 4.1-4.2, the greater settling time the higher the freeboard temperature due to more volatiles combustion that contributed to higher combustion efficiency provided the bed temperature was maintained within the range of 800-900°C. This effect explained why the higher carbon combustion efficiency was obtained in the case of coal/rice husk and coal/wood powder combustion in comparison to the case of coal/wood pellets or coal/refuse derived fuel combustion. The effect of bed and freeboard temperature on carbon combustion efficiency will be discussed in the following section.

4.4.5 Effect of Bed Temperature

Generally, the bed temperature had only a small influence of carbon combustion efficiency among the biomass fuels (see Tables 4.10 to 4.15). For example, as can be seen in the case of coal/wood powder, the carbon combustion efficiency is still higher (about 3-5%) than that in the case of coal/wood pellets even though the bed temperature is lower (about 50-100°C). In this case, the fuel particle sizes become the main factor on the carbon combustion efficiency which has been explained previously in section 4.4.1.

Tables 4.10 to 4.15 show the dependence of bed temperature on coal mass fraction and various excess air levels obtained during the experimental runs. As can be seen, the bed temperature increased with increased coal mass fraction and also increased with decreased excess air levels. The bed temperature shows a linear dependence on coal addition as well as the carbon combustion efficiency at the same excess air levels. As been mentioned earlier in section 4.4.2, the increased fixed carbon due to increased coal fraction in the coal/biomass mixtures contributed to higher bed temperatures which led to greater carbon combustion efficiency. In contrast, the reduced bed temperature has no significant effect on carbon combustion efficiency as excess air levels increased in all co-combustion cases (see Figure 4.36). This can be explained by the fact that turbulence created by increasing excess air also resulted with increases in fluidising velocity which had a more significant influence than reduced bed temperature as suggested by Saxena *et al.* [55].

Like other factors, the bed temperatures did not have any detrimental affect on CO emissions due to increased turbulence in the bed created by the high air flow rate was more significant than the reduced bed temperature (see Figure 4.37). For instance, in the case of coal/refuse derive fuel the CO emissions are relatively higher (about 500 -700 ppm by difference) compared to the case of coal/palm fibre even though their bed temperatures were higher (about 50°C difference).

Table 4.10: Bed temperature profile (°C) as a function of excess air for different fuel mixtures of coal and chicken waste mass fraction.

Excess air (%)	Coal (100%)	Coal (30%) : Chicken waste (70%)	Coal (50%) : Chicken waste (50%)	Coal (70%) : Chicken waste (30%)	Chicken waste (100%)
30	934	913	904	896	841
50	938	904	893	880	837
70	926	857	860	855	826

Table 4.11 Bed temperature profile (°C) as a function of excess air for different fuel mixtures of coal and rice husk mass fraction.

Excess air (%)	Coal (100%)	Coal (30%) : Rice husk (70%)	Coal (50%) : Rice husk (50%)	Coal (70%) : Rice husk (30%)	Rice husk (100%)
30	934	896	892	900	733
50	938	880	888	893	721
70	926	767	865	860	700

Table 4.12: Bed temperature profile (°C) as a function of excess air for different fuel mixtures of coal and palm fibre mass fraction

Excess air (%)	Coal (100%)	Coal (30%) : Palm Kernel Shell (70%)	Coal (50%) : Palm Kernel Shell (50%)	Palm kernel shell (100%)
30	934	834	853	889
50	938	832	832	876
70	926	828	820	874

Table 4.13: Bed temperature profile (°C) as a function of excess air for different fuel mixtures of coal and palm fibre mass fraction.

Excess air (%)	Coal (100%)	Coal (90%) : Palm fibre (10%)	Coal (80%) : Palm fibre (20%)	Coal (70%) : Palm fibre (30%)
40	934	851	799	665
60	893	845	792	651
80	892	839	780	629

Table 4.14: Bed temperature profile (°C) as a function of excess air for different fuel mixtures of coal and refuse derived fuel mass fraction

Excess air (%)	Coal (100%)	Coal (30%) : Refuse derived fuel (70%)	Coal (50%) : Refuse derived fuel (50%)	Coal (70%) : Refuse derived fuel (30%)	Refuse derived fuel (100%)
3	934	837	838	859	815
5	893	807	839	865	780
7	892	787	811	870	720

Table 4.15: Bed temperature profile (°C) as a function of excess air for different fuel mixtures of coal and wood pellets and wood powders mass fraction

Excess air (%)	Coal (100%)	Coal (30%) : Wood pellets (70%)	Coal (50%) : Wood pellets (50%)	Coal (70%) : Wood pellets (30%)	Wood pellets (100%)	Coal (50%) : Wood powders (50%)	Wood powders (100%)
40	934.0	847	861	897	820	860	768
60	893.0	846	862	898	819	859	779
80	892.0	843	857	893	786	855	757

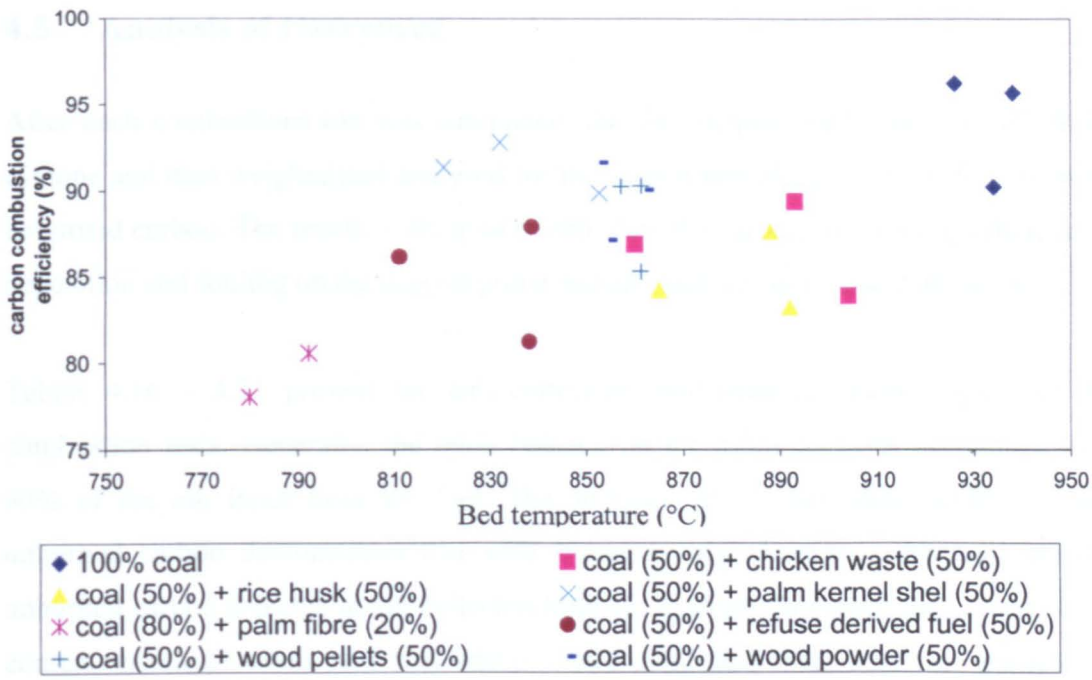

Figure 4.36 The influence of Bed temperature (° C) on carbon combustion efficiency during co-combustion study at 10 kW

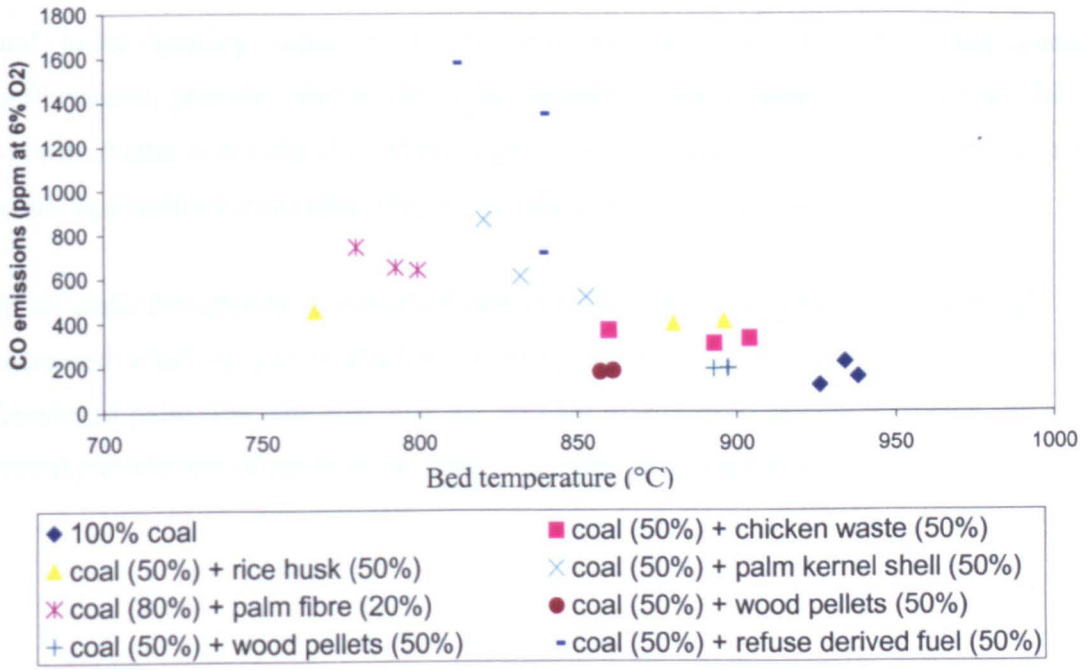

Figure 4.37 The influence of bed temperature (°C) on CO emissions during co-combustion study at 10 kW

4.5 Analysis of Carryover

After each combustions run was completed, the fly ash produced was collected from the cyclone and then weighed and analysed for the carbon percentage in order to determine the unburned carbon. The results were used to calculate the carbon combustion efficiency. Ash deposition and fouling on the deposit probe and any bed ash were also determined.

Tables 4.16 – 4.21 present the ash collection and unburned carbon analyses during combustion tests. Generally, the mass balance on the ashes particles accounted for over 90% of the ash input from the fuel. The analyses of the ash collected in all tests for unburned carbon demonstrates that with biomass only, there was the least amount of unburned carbon detected in ash collected from the cyclone. However, the unburned carbon content increased when coal was added which suggested that some fine particles were elutriated with the fluidising gases. This has been discussed earlier in section 4.4.1-4.4.4. The amount of unburned carbon was, however, quite low, corresponding to about less than 5% of the total carbon input. Such observations seem to suggest that the large particle size and lower heating value of the biomass fuel did not adversely affect combustor performance, probably due to the higher volatile matter content of the biomass fuel. The volatile matter burns rapidly and the higher volatile matter content of the biomass can also result in a highly porous char, thus accelerating the char combustion as well.

In all cases the amount of unburned carbon in the ash increased as the percentages of coal increased which is due to the low volatility of coal. For the biomass materials the low density of palm fibre and rice husk are also led to increased carbon content in the ash. The initial particle size of the biomass does not appear to be significant.

Table 4.16: Ash analyses for single and co-combustion of coal and chicken waste at varies percentage of excess air.

Fuel	Feed (kg/h)	Superficial Velocity (m/s)	Carbon feed (kg/h)	Ash (kg/h)	Carbon in Ash (%)	Efficiency E2 (%)
Coal (100%)	1.20	0.67	0.900	0.039	23.0	90.25
Chicken waste (100%)	3.00	0.67	1.050	0.773	6.0	80.74
Coal (30%) : Chicken waste (70%)	2.47	0.83	1.158	0.477	8.0	80.18
Coal (50%) : Chicken waste (50%)	2.10	0.78	1.156	0.399	9.0	85.94
Coal (70%) : Chicken waste (30%)	1.78	0.76	1.125	0.218	11.0	88.34

Table 4.17: Ash analysis for single and co-combustion of coal and rice husk at varies percentage of excess air

Fuel	Feed (kg/h)	Superficial Velocity (m/s)	Carbon feed (kg/h)	Ash (kg)	Carbon in Ash (%)	Efficiency E2 (%)
Coal (100%)	1.20	0.67	0.900	0.039	23.0	90.25
Rice husk (100%)	2.97	0.56	1.038	0.621	14.5	66.62
Coal (30%) : Rice husk (70%)	2.16	0.99	1.149	0.348	20.9	75.33
Coal (50%) : Rice husk (50%)	1.60	0.85	1.159	0.196	28.7	83.24
Coal (70%) : Rice husk (30%)	1.40	0.81	1.094	0.176	26.6	86.07

Table 4.18: Ash analysis for coal and co-combustion of coal and palm fibre at varies percentage of excess air.

Fuel	Feed (kg/h)	Superficial Velocity (m/s)	Carbon feed (kg/h)	Ash (kg)	Carbon in Ash (%)	Efficiency E2 (%)
Coal (100%)	1.20	0.67	0.900	0.039	23.0	90.25
Coal (90%) : Palm fibre (10%)	2.97	0.63	1.045	0.048	21.9	76.59
Coal (80%) : Palm fibre (20%)	2.16	0.62	0.949	0.051	25.0	72.96
Coal (70%) : Palm fibre (30%)	1.60	0.54	0.857	0.064	27.0	69.39

Table 4.19: Ash analysis for single and co-combustion of coal and palm kernel shell at varies percentage of excess air.

Fuel	Feed (kg/h)	Superficial Velocity (m/s)	Carbon feed (kg/h)	Ash (kg)	Carbon in Ash (%)	Efficiency E2 (%)
Coal (100%)	1.20	0.67	0.900	0.039	23.0	90.25
Palm kernel shell (100%)	1.97	0.59	0.898	0.028	5.0	80.67
Coal (30%) : Palm kernel shell (70%)	1.74	0.74	0.949	0.030	11.7	80.73
Coal (50%) : Palm kernel shell (50%)	1.59	0.65	0.962	0.031	14.9	89.86

Table 4.20: Ash analysis for single and co-combustion of coal and refuse derived fuels at varies percentage of excess air.

Fuel	Feed (kg/h)	Superficial Velocity (m/s)	Carbon feed (kg/h)	Ash (kg)	Carbon in Ash (%)	Efficiency E2 (%)
Coal (100%)	1.20	0.67	0.900	0.039	23.0	90.25
Refuse derived fuel (100%)	2.74	1.19	1.088	0.006	10.1	80.78
Coal (30%) : Refuse derived fuel (70%)	2.34	0.97	1.177	0.045	14.9	80.56
Coal (50%) : Refuse derived fuel (50%)	2.10	0.85	1.204	0.039	17.2	81.23
Coal (70%) : Refuse derived fuel (30%)	1.69	0.79	1.088	0.025	19.5	86.85

Table 4.21: Ash analysis for single and co-combustion of coal and wood pellets and wood powders at varies percentage of excess air.

Fuel	Feed (kg/h)	Superficial Velocity (m/s)	Carbon feed (kg/h)	Ash (kg)	Carbon in Ash (%)	Efficiency E2 (%)
Coal (100%)	1.20	0.67	0.900	0.039	23.0	90.25
Wood pellet (100%)	1.91	0.65	0.959	0.018	3.0	83.25
Wood powders (100%)	2.91	0.84	1.461	0.028	3.0	87.27
Coal (30%) : Wood pellet (70%)	1.68	0.63	0.971	0.020	6.0	84.47
Coal (50%) : Wood pellet(50%)	1.55	0.67	0.973	0.030	10.0	85.31
Coal (70%) : Wood pellet (30%)	1.33	0.68	0.902	0.030	11.7	90.74
Coal (50%) : Wood powder (50%)	2.51	0.71	1.576	0.050	15.4	87.14

Moreover, the percentages of unburned carbon in the ash increased in the range 3 to 15% with the increases of coal fraction in the coal/biomass mixture. This can be explained by the fact that as the coal fraction increased the higher char combustion and less volatile combustion occurred. Volatiles combustion of biomass is relatively higher and faster than char oxidation of the coal particles. Thus, even though the combustion of volatiles was completed, the char particles did not have a residence time long enough for complete combustion. The unburned carbon percentages in total carbon feed however contribute only a small percentage (about 3% difference) on the overall carbon combustion efficiency calculation. Thus, it was observed that the carbon combustion efficiency was still high at higher coal fraction. In contrast, the effect of unburned carbon on combustion efficiency showed significant effect with increasing fluidising velocity at fixed coal/biomass fraction. Figures 4.38 clearly illustrated that the elutriated carbon loss increased as fluidising velocity increased. As a result, the lower carbon combustion efficiency was obtained.

Furthermore, it was found that the bed temperature has no strong influence on carbon loss during the tests. The lower carbon loss was determined at higher bed temperature. For example, higher unburned carbon was determined in the case of coal/rice husk, coal/refuse derived fuel and coal/palm fibre in comparison to coal/palm kernel shell although their bed temperature was similar (see Figure 4.39). Again, as explained earlier this unburned carbon only contributed a small percentage on the overall carbon combustion efficiency.

The performance of the cyclone was analysed by comparing the collection efficiency of the cyclone at any particle size by referring to Figure A-1 (see appendix A) and the particle size distribution of the collected carryover in the cyclone (see Table C-1 –C-17). This calculation was carried out to determine the reliability of the cyclone. This gives an average collection efficiency of 70% with an average particle size of 53.75 μm.

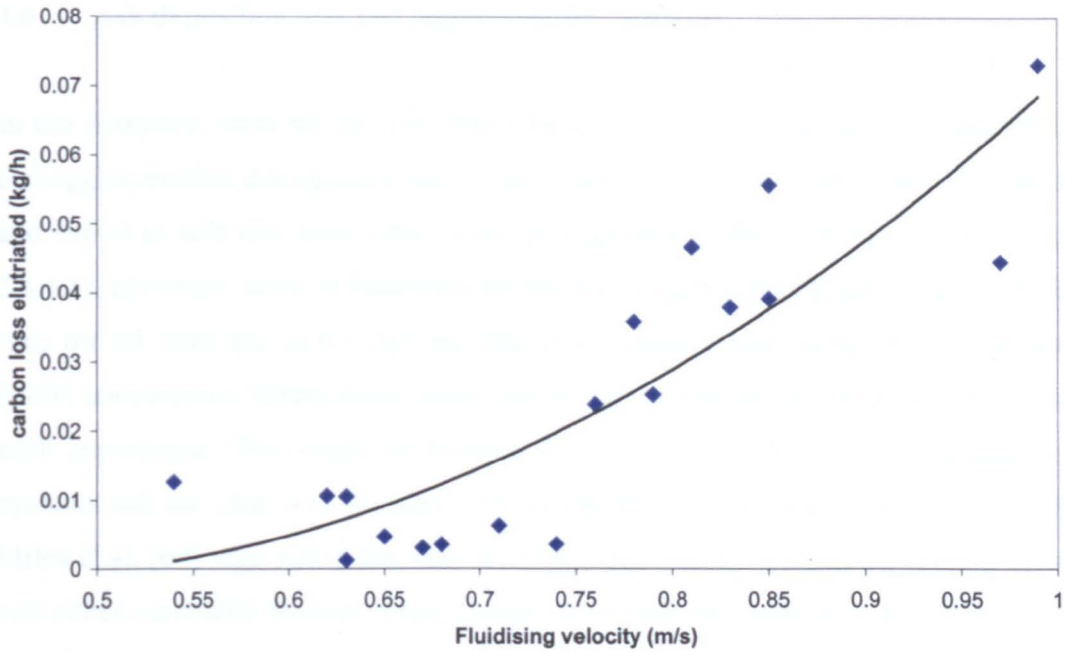

Figure 4.38 The influence of fluidising velocity on carbon loss elutriated during co-combustion runs for all coal/biomass samples.

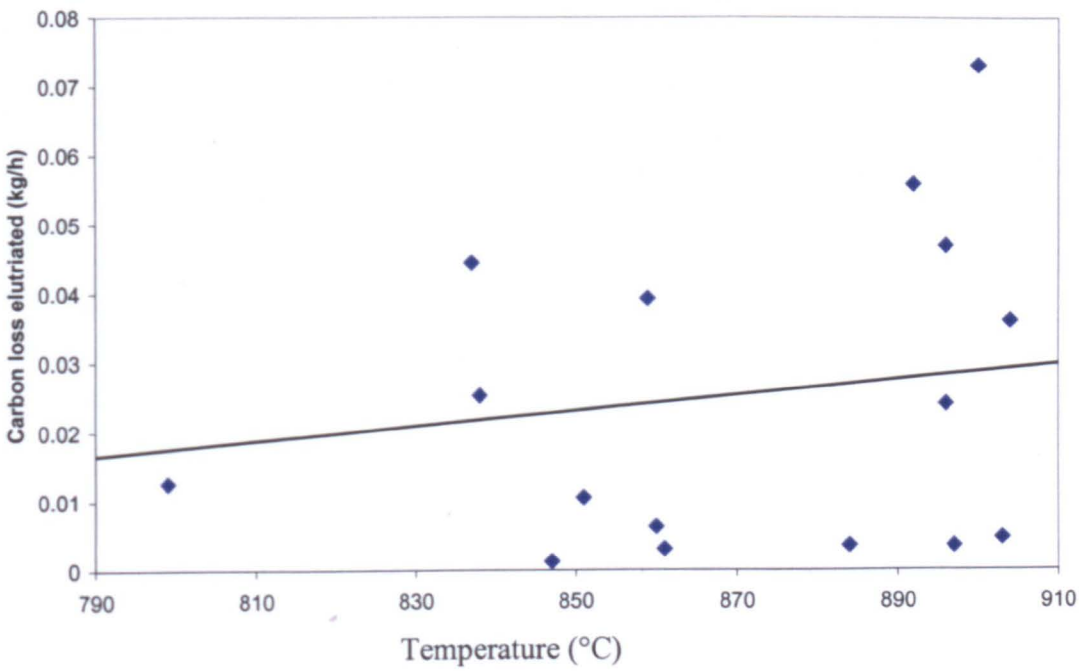

Figure 4.39 The influence of bed temperature (°C) on carbon loss elutriated during co-combustion runs for all coal/biomass samples

4.6 Ash deposition and bed agglomeration analyses

In the literature, most of the researchers have experienced fouling, ash deposition and bed agglomeration during combustion runs using biomass samples (especially rice husk and straw) as sole raw fuels. This is due to high alkali content in the fuels (see section 2.4.4.1). However, none of these phenomena had occurred during the all the combustion runs for all tests due to the bed and freeboard temperatures being lower than the ash fusion temperature. Furthermore, there was almost no bed ash found at the completion of each experiment. This might be because any unburned material was elutriated to the cyclone and the char was complete. These results however are in contrast with those Miles et al. [64] who stated that with an alkali index above 0.34 kg/GJ fouling certainly will occur especially for high alkali content fuels such as rice husk (1.6). It is suggested that the reason that no fouling was observed during the current work was due to the lower operating bed temperature in an FBC (800-900°C) whereas Miles carried out his experiment in a CHP combustor where temperatures greater than 1000°C .

5.0 Theoretical Model

A simple model of an atmospheric bubbling fluidized bed combustor burning gas, low-volatile and high-volatile solid fuel has been developed to relate to the temperature profile in the combustor. Several models for the in-bed and over bed volatiles release have been proposed on the basis of specific experiments carried out on bench-scale reactors exists in the literature. However, none of the models have been used because the models are difficult to use due to the extensive data such as bed and freeboard hydrodynamics, volatiles and char combustion, and char particle size distribution were required to determine the extent of the combustion in the bed or freeboard.

5.1 System Model

The objective of the model is to use temperatures to predict percentages of combustion in various zones. The proposed model was primarily developed and validated for propane combustion where no volatile matter combustion was involved. The propane was fed co-currently with fluidising air from the bottom of the distributor plate with no secondary air. In order to study the evolution of the combustion process along the combustor, the proposed model is based on the conservation equations for energy for both bed and freeboard sections. The proposed model for propane combustion in the fluidised bed is divided into two zones: (1) combustion region (2) Combustion completed. The experimental results were obtained under the operating conditions and model calculations are described in Table 4.22 and table 4.23, respectively. This propane model was carried out to demonstrate that once the temperatures started to fall combustion was complete. As the results show good agreement between the model and the experimental results it was extended to the combustion of solid fuels with secondary air being introduced.

Table 4.22 Operating conditions tested during experimental study used for modelling

Test	Fuel feed rate (kg/hr)	Excess air (%)	Air flow rate (kg/hr)	Tbed (°C)
1	3.0	30	24.1	910
2	3.0	50	33.0	895
3	3.0	70	36.7	815
4	1.20	30	17.4	936
5	1.20	50	19.9	932
6	1.20	70	22.9	922
7	1.91	30	16.3	820
8	1.91	50	18.5	819
9	1.91	70	21.1	786

Table 4.23 Equations of the model

E-1 Energy balance sub-model for propane combustion

Assumptions:
1. Take 100% efficiency of fuel combustion and no secondary air applied.
2. Combustion was complete when the temperatures start to fall.

Input data:

F_g	=	4	$T_i(z\text{-}1)$	=	0
HHV_g	=	50.5	T_o	=	25
F_a	=	36.663	R_o	=	0.225
C_{pa}	=	1.005	R_i	=	0.075
			h_o	=	3
C_{pg}	=	73.6	K_{kw}	=	0.081

Zone 1 – Bed region (0-40 cm)

[Heat generated by propane combustion] = [Heat absorbed by air] + [Heat absorbed by propane to increase to combustion temperature] + [Heat loss through the combustor wall]

$$F_g HHV_g = F_a C_{pa}(T_i(z)-T_i(z\text{-}1)) + F_g C_{pg}(T_i(z) - T_o) + 2\pi dz(T_i(z)-T_o)/[(\ln(R_o/R_i)/K_{kw} + 1/(R_o h_o)] \quad \textbf{(E-1)}$$

$T_i(z)$ were obtained by substituted z from 0 to 40 cm in Eqn (E-1). The balances of the equation given as below:

202000	=	201995.99 , Thus;		
Q_{bed}	=	201995.99 / 202000 x 100	=	99.99%
$Q_{freeboard}$	=	100 - Q_{bed}	=	0.001 %

Zone 2 – Freeboard region (40 cm onwards)
Combustion assumed complete at approximate 40 cm and the energy balance for that zone given as follows;

Heat input – Heat output + Heat generation = 0

$$F_a C_{pa}(dT/dz) + 2\pi/(\ln(R_o/R_i)/K_{kw} + 1/(R_o h_o)\Delta z(T(z)-Tw) = 0 \quad \textbf{(E-2)}$$

$$\text{Let } \lambda = 2\pi/(\ln(R_o/R_i)/K_{kw} + 1/(R_o h_o))/ F_a C_{pa}$$
$$dT/dz + \lambda(T(z) - Tw) = 0$$
$$dT/(T(z) - Tw) = -\lambda dz$$
$$Ln\,(T(z) - Tw) = -\lambda z + Ln\,K$$
$$K = T_0 - Tw$$
$$(T(z) - Tw)/(T_0 - Tw) = EXP(-\lambda z)$$
$$T(z) = (T_0 - Tw) * EXP(-\lambda z) + Tw$$

T(z) was obtained by substituting z in Eqn. (E-2) from 40 cm onwards.

E-2 Energy balance sub-model for coal combustion

Assumptions:

1. Take 90% efficiency for the fuel combustion by taking into account 10% energy loss due to unburned carbon and secondary air applied (at 45 cm above distributor plate).
2. Combustion was complete when the temperatures start to fall (at 80 cm onwards)

Input data: (For case of 50% XSA)

F_c	=	*1.2*	C_{pc}	=	*37*
HHV_c	=	*31.1*	$T_i(z\text{-}1)$	=	*0*
F_{a1}	=	*17.424*	T_o	=	*25*
F_{a2}	=	*4.719*	R_o	=	*0.225*
F_{aNET}	=	*22.143*	R_i	=	*0.075*
C_{pa}	=	*1.005*	h_o	=	*3*
			K_{kw}	=	*0.081*

Zone 1

a) 0 to 40 cm

[Heat generated by propane combustion] = [Heat absorbed by main air] + [Heat absorbed by propane to increase to combustion temperature] + [Heat loss through the combustor wall]

$$F_g HHV_g = F_{a1}C_{pa}(T_i(z)-T_i(z-1)) + F_gC_{pg}(T_i(z) -T_o) + 2\pi dz(T_i(z)-T_o)/[(\ln(R_o/R_i)/K_{kw} + 1/(R_oh_o)] \quad \textbf{(E-3)}$$

a) 40 to 80 cm

[Heat generated by propane combustion] = [Heat absorbed by main air] + [Heat absorbed by propane to increase to combustion temperature] + [Heat absorbed by secondary air] + [Heat loss through the combustor wall]

$$F_cHHV_c = M_aC_{pa}(T_i(z)-T_i(z-1)) + 2\pi dz(T_i(z)-T_o)/[(\ln(R_o/R_i)/K_{kw} + 1/(R_oh_o)] + F_cC_{pc}(T_i(z)-T_o) + F_{a2}C_{pa}(T_i(z)-T_i(z-1)$$
$$= F_{aNET}C_{pa}(T_i(z)-T_i(z-1)) + 2\pi dz(T_i(n)-T_o)/[(\ln(R_o/R_i)/K_{kw} + 1/(R_oh_o)] + M_cC_{pc}(T_i(z) -T_o) \quad \textbf{(E-4)}$$

$T_{i(z)}$ were obtained by substituted z from 0 to 80 cm. The balances of the equation given as below:

37320	=	33363.64 , Thus;		
Q_{bed}	=	33363.64 / 37320 x 100	=	80.46 %
$Q_{freeboard}$	=	100 - Q_{bed}	=	19.54 %

Zone 2 – 80 cm onwards

Input data was substituted in Eqn. (E-2) for z from 80 cm onwards.

E-2 Energy balance sub-model for wood combustion

Assumptions:

1. Take 83% efficiency of fuel combustion by taking into account 17% energy loss due to unburned carbon and secondary air applied (at 45 cm above distributor plate).
2. Combustion was complete when the temperatures start to fall (at 120 cm onwards) due to high volatile combustion.

Input data: (For case of 50% XSA)

F_w	=	*1.91*	C_{pw}	=	*25*
HHV_w	=	*18*	$T_i(z\text{-}1)$	=	*0*
M_a	=	*11.616*	T_o	=	*20*
M_{a2}	=	*4.719*	R_o	=	*0.225*
M_{aNET}	=	*16.335*	R_i	=	*0.075*
C_{pa}	=	*1.005*	h_o	=	*3*
			K_{kw}	=	*0.081*

Zone 1

a) 0-1200 cm

Input data was substituted in Eqn. (E-3) and Eqn. (E-4) for z from 0-40 cm and 45-120 cm, respectively. The balances of the equation given as below:

34380	=	28460.65	, Thus;	
Q_{bed}	=	28460.65/ 34380 x 100	=	71.77%
$Q_{freeboard}$	=	100 - Q_{bed}	=	28.23%

Zone 2 - 85-200 cm

Input data was substituted in Eqn. (E-2) for z from 120 cm onwards.

In order to test the validity of this model, the predicted profiles have been correlated with the experimental data obtained at bed temperature ranging within 800-900°C. Figure 4.40 shows the comparison between predicted profiles and experimental data obtained at the bed temperature equal to 900°C and 100% efficiency. As can be seen, the model predicts satisfactorily the axial temperature profiles along the reactor height. The temperature is unchanged between the zone 0 to 30 mm (bed region) and start to fall afterward till 200 mm indicated that the combustion was completed. Percentages of the combustion split between bed / freeboard predicted by the model was found to be 99.99/0.01. Also, predicted split of the percentages of heat released in bed and freeboard at different bed temperature is shown in Table 4.24. It can be noticed that the higher the bed temperature, the more heat is released in the bed.

During propane combustion, the gas mixture initially burnt on the surface of the bed. Meanwhile the top most layers of sand were heated up, glowing orange, as it was fluidised and then darker, cool sand was drawn up from the lower part of the bed a crackling, popping noised was heard. It was accompanied by increasing agitation of the sand. As the temperature increased, the propane combustion occurred starting at the top surface and then moving downward toward distributor plate. This implied that; 1) heat was released from combustion within the bed and 2) heat was released from the flames at the top of the bed and was conducted into the bed. Thus, it was expected the combustion would occur in the bed [13]. The percentages of the split heat release in Table 4.24. The ratio of heat release in bed, Q_B increased linearly with the bed temperature about 10%.

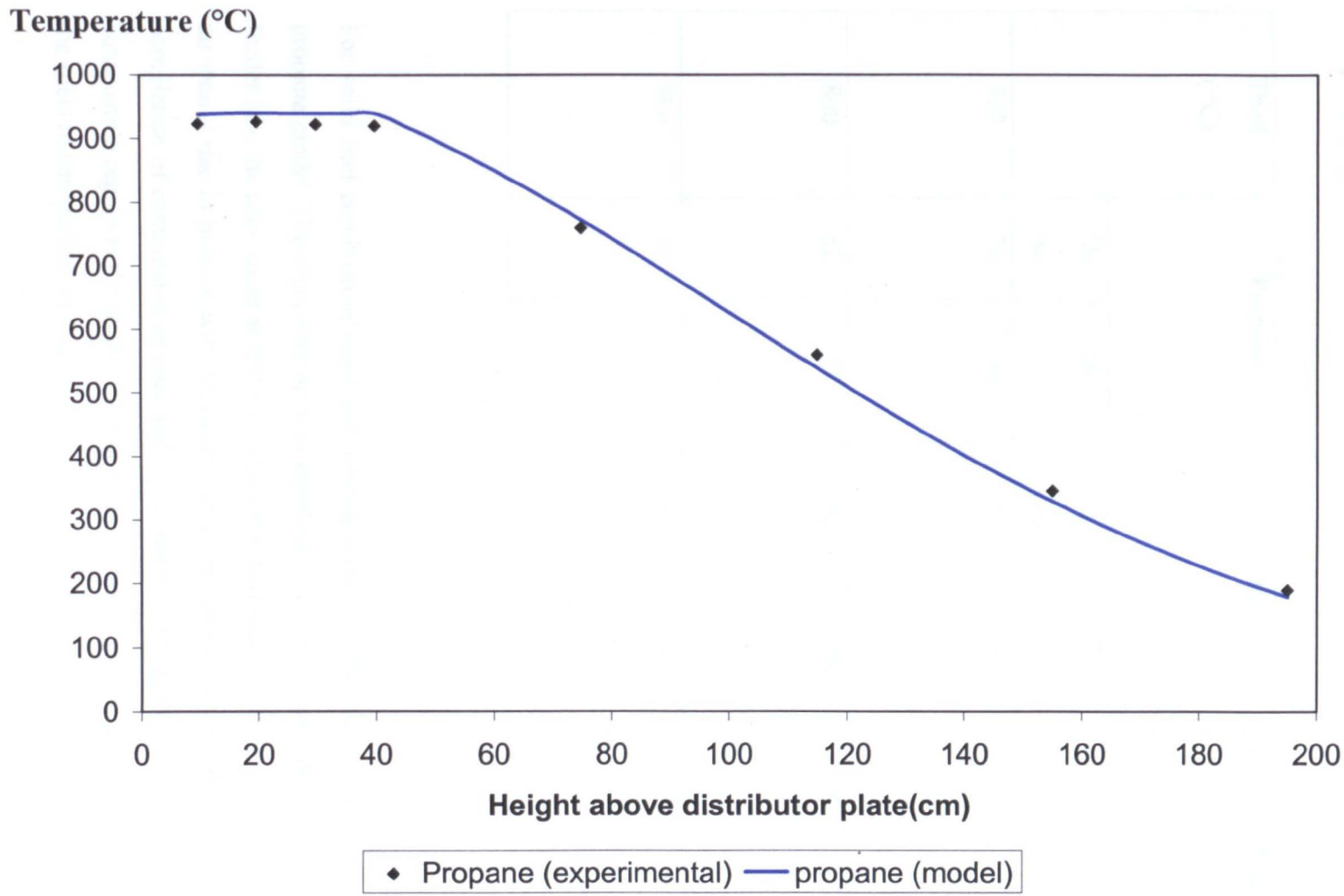

Figure 4.40 Comparison between experimental and modelling results for propane combustion at 50% excess air.

Table 4.24 Predicted values of heat released in bed and freeboard at different bed temperatures.

Tbed (°C)	Propane		Coal		Wood	
	Q_B (%)	Q_{FB} (%)	Q_B (%)	Q_{FB} (%)	Q_B (%)	Q_{FB} (%)
700	70	30	57	43	67	32
800	82	18	72	28	82	18
900	95	5	87	13	96	3

For solid fuel combustion (coal and wood), some modifications have been made on the propane model. The secondary air was supplied co-currently with the solid fuel through the feeder into the combustor at 450 mm above the distributor plate. It was assumed that all the air would rise in parallel with fluidising air in the combustor. Furthermore, in zone 2, the completion of combustion of coal and wood starts at 80 and 120 cm, respectively. Longer combustion region in the freeboard was taken for wood combustion due to high volatility of the fuels in comparison to coal.

Figure 4.41 shows the experimental temperatures profile obtained for coal combustion at 50% excess air fitted well with the modelling calculations. The computations carried out with Tb = 800°C and carbon combustion efficiency of 90%. As can be seen, the temperatures above the bed surface at 30 and 40 mm were found to be more or less than the bed temperature indicating the freeboard combustion had occurred in this region. This explained the difference found with propane combustion where no volatile matter presents. The volatiles combustion in the freeboard region has increased the temperature surround the area. However, it was found that a slight drop of temperature for the modelling curve once secondary air was injected. The addition of secondary air that was supplied co-currently with fuels reduced the temperature around the injected area. The temperature however, starts to fall at about 80 mm distance above distributor plate which indicates that the combustion was complete so only heat loss occurred. It was estimated that the split for the bed and freeboard combustion were 80 and 20%, respectively.

The wood combustion modelling was also carried out to study the influence of high volatile fuels combustion in comparison of coal combustion. The computations carried out with Tb = 800°C and carbon combustion efficiency of 83%. As shown in Figure 4.42, wood combustion model has a similar trend as coal combustion but with longer freeboard combustion. This phenomenon was confirmed experimentally where it was expected from higher volatiles combustion (about twice) in the freeboard compared to coal. Relatively it was confirmed with calculation of amount of heat released in the bed and freeboard combustion, 70 and 30%, respectively. Also, it was found that the combustion was completed about 120 mm above distributor plate due to parallel straight line from the figure onwards. Furthermore, in comparison to coal, a higher combustion efficiency (>80%) could be obtained at a lower bed temperature about 800°C (see Table 4.24).

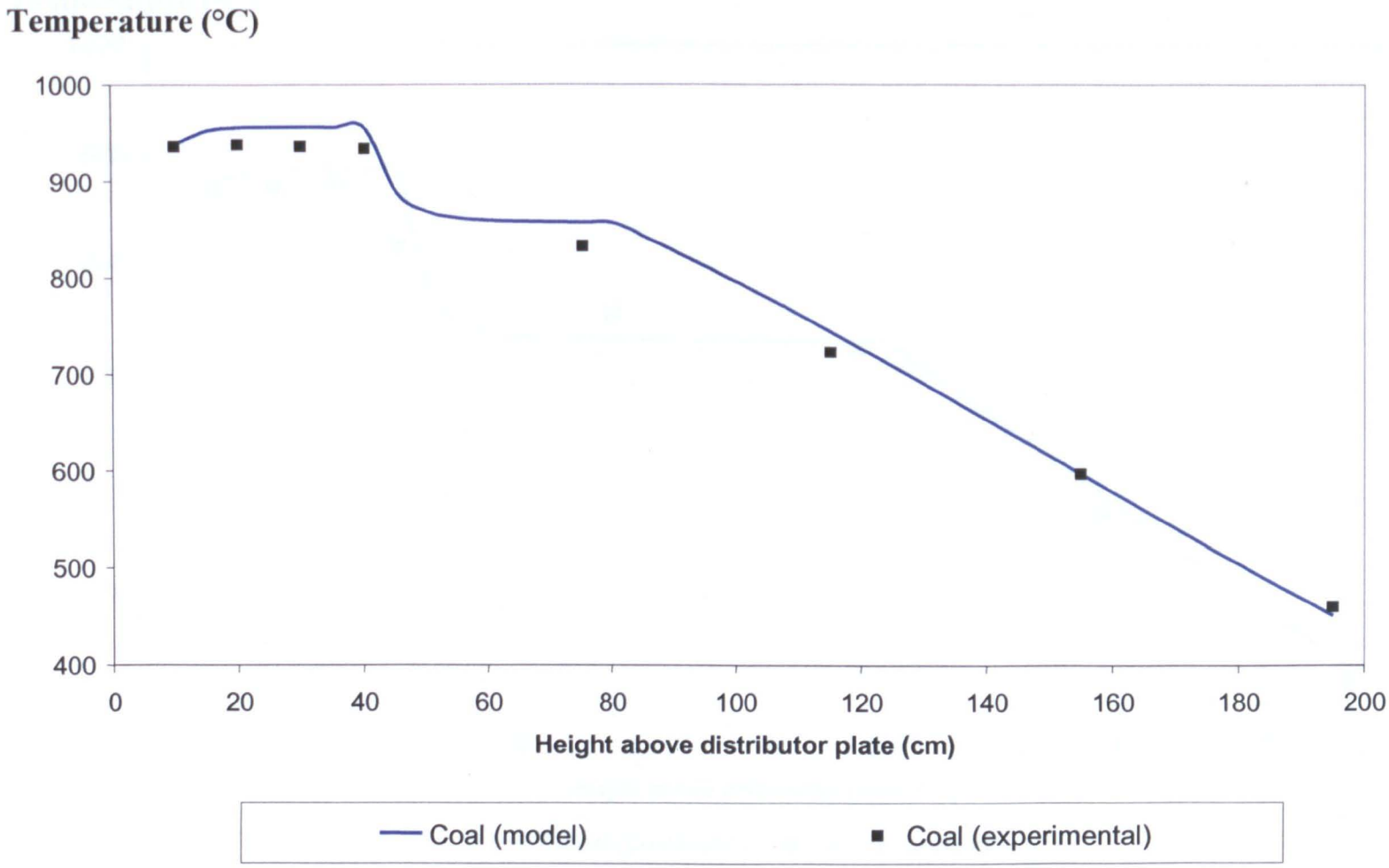

Figure 4.41 Comparison between experimental and modelling results for coal combustion at 50% excess air

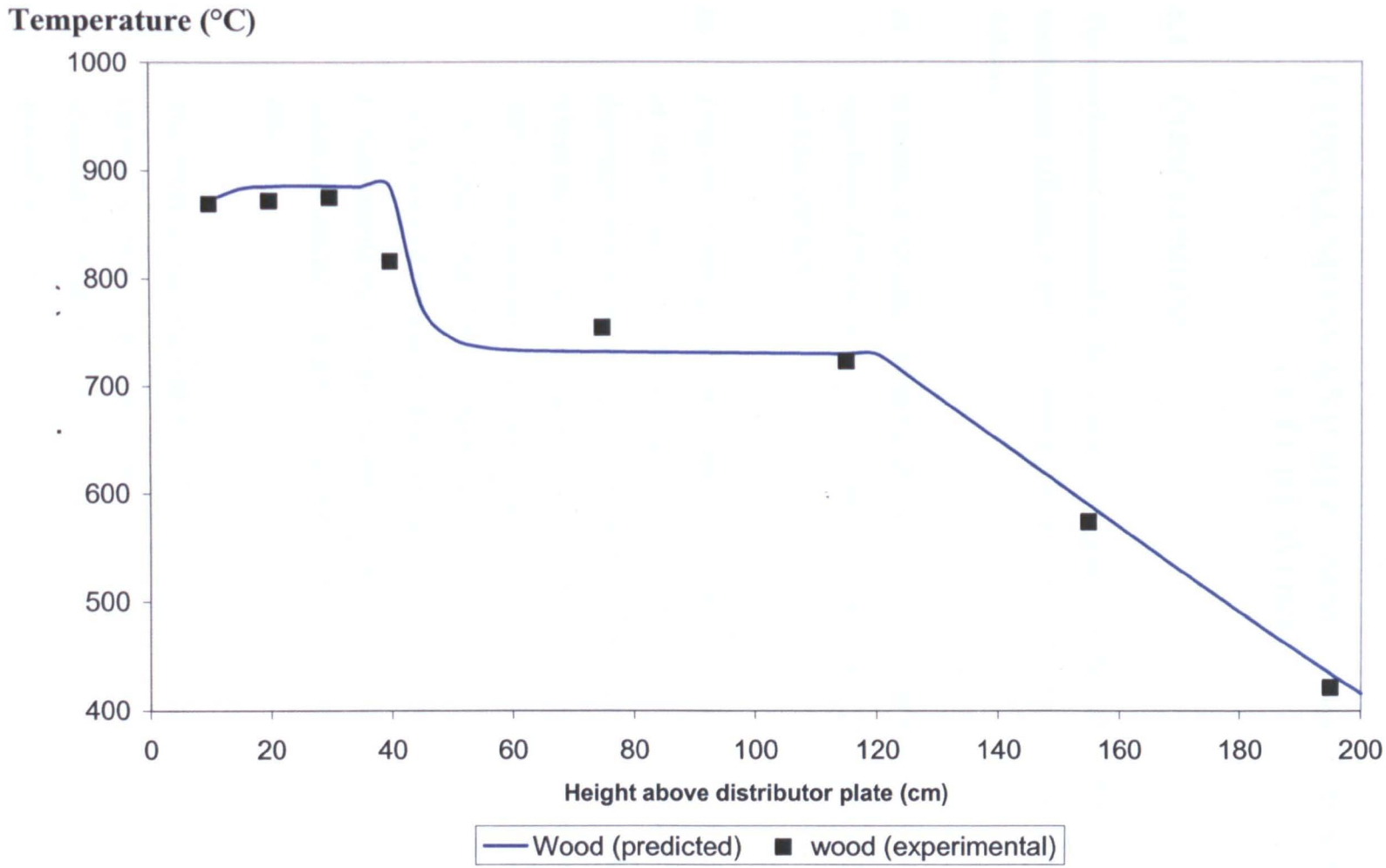

Figure 4.42 Comparison between experimental and modelling results for wood combustion at 50% excess air

CHAPTER 5

CONCLUSIONS AND RECOMMENDATIONS FOR FUTURE WORK

5.1 CONCLUSIONS

The conclusions obtained in the present investigation on the temperature profile, carbon combustion efficiency and CO emissions in a 10 kW FBC can be summarised as follows:

a) Biomass combustion behaves differently in comparison to coal due to the significant difference in volatile matter content and variations of particle size and particle density.

b) From the Thermogravimetric Analysis (TGA) it was found that at a heating rate of 10 °C min^{-1}, for all the biomass (except refuse derived fuel) the thermal decomposition starts at approximately 200°C. A major loss of weight follows, where the main devolatilisation occurs, with a maximum rate between 300 and 400 °C and is essentially completed by about 450 °C. This is followed by a slow further loss of weight up to the final temperature. On the other hand, for the TGA curves of bituminous coal, the decomposition starts at about 350 °C, which is significantly higher than the one corresponding to the biomass samples. This result influenced the temperature profile of co-combustion biomass with coal in FBC.

c) The DTG curves showed that the wood pellet, which has also the highest volatiles content, is the most reactive among the species studied, followed in sequence by palm kernel shell, rice husk, palm fibre, chicken waste, refuse derived fuel and bituminous coal. Furthermore, a lateral shift in the DTG curves was observed as the heating rate increased from 10 to 100°C.

d) The carbon combustion efficiency was influenced by the operating and fluidising parameters in the decrease following order: a) settling velocity; b) coal mass fraction; c) fluidising velocity; d) excess air and e) bed temperature (Tb).

e) The carbon combustion efficiency increased between 3% and 20% as the coal fraction increased from 0% to 70%, under various fluidisation and operating conditions. This demonstrated that it is possible to combust low density material with overbed feeding with the exception of a coal/palm fibre mixture. This was due to their stickiness of the palm fibre resulting in a feeding problem which retarded the combustion performance.

f) Generally, the carbon combustion efficiency increased with increases of excess air and peaks at 50%. The corresponding increasing carbon combustion efficiency with excess air from 30-50% was found to be in the range of 5 – 12 % at 50% coal mass fraction in the biomass mixture. Further increase of excess air to 70% reduced the carbon combustion efficiency.

g) Increasing the fluidising velocity increases the turbulence in the bed leading to better solid mixing and gas-solid contacting and shows as the amount of carbon in the bed is burnt at higher rate. However, when the combustion is stabilised, increasing fluidising velocity contributed to a greater particle elutriation rate than the carbon to CO conversion rate and hence increased the unburned carbon.

h) Apart from solid mixing, increasing fluidising velocity also influenced settling time of fuel particle during the combustion process in FBC. Increasing fluidising velocity brought the lighter fuel particle upward to the freeboard region and completed before they reached the bed surface.

i) The bed temperature had a small effect on carbon combustion efficiency for the biomass fuels. The turbulence created by increasing excess air, related to increases in fluidising velocity, had a greater influence that that due to reducing the bed temperature.

j) Significant fluctuations of CO emissions ranging between 200-1500 ppm were observed when coal was added into almost all biomass mixtures depending upon excess air.

k) The analyses of the ash collected in all tests for unburned carbon demonstrates that with biomass only, there was less unburned carbon detected in the ash collected from the cyclone indicating that the combustion of fixed carbon was almost complete. However, there was some unburned carbon measured when coal was added which suggested that some fine particles were elutriated with the fluidising gases.

l) The percentages of unburned carbon increased in the range 3 to 30% of the ash content with the increases of coal fraction in the coal/biomass mixture. This can be explained by the fact that as the coal fraction increased the higher char combustion and less volatiles combustion occurred. Moreover, the elutriated carbon loss increased as fluidising velocity increased resulting in the lower carbon combustion efficiency. On the contrary, it was found that the bed temperature had no strong influence on carbon loss during the tests.

m) The average of the cyclone collection efficiency is 70% and average particle size was 53.75 μm.

n) Fouling nor agglomeration in the bed was not a problem with any of the biomass fuels burnt even though the fouling index values were above 0.34 kg/GJ, the value proposed by Miles et al [64] at which fouling should occur.

o) The simple theoretical model based on energy balance demonstrates that axial temperature profiles can be used to determine the percentage combustion of each zone.

5.2 RECOMMENDATIONS FOR FUTURE WORK

a) Modify the combustor to:
(i) Compare inbed with overbed feeding of coal/biomass mixtures.
(ii) Investigate the effect of air staging on combustion.
(iii) Study the effect of bed temperature on combustion efficiency by having a cooling coil in the bed instead of using air flowrate.

b) To investigate the release of NOx from coal/biomass mixtures. Although the nitrogen content of biomass is generally low the compounds have a lower molecular weight and are more volatile.

c) Investigate co-firing of coal with a wide range of densified biomass fuels that are currently available.

REFERENCES

1. Makansi, J. 'Co-combustion: burning biomass, fossil fuels together simplifies waste disposal, cut fuel cost', Power, 131(7), 1987, pp. 11-18

2. Hall, D. O, Rossillo-Calle, F and Woods, J, 'Biomass, its importance in balancing CO_2 budgets'. In: gassi G, Collina, A, Zibetta, H, editors. Biomass for energy, industry and environment, 6th E.C Conference, London: Elsevier Science, 1991, pp. 89-96.

3. Hall, D. O., and House, J. I., 'Biomass: A modern and environmentally acceptable fuel', Solar Energy Materials and Solar Cells, 38 (1-4), pp. 521-542.

4. Energy for the Future: Renewable Source of Energy – White Paper for a Community Strategy and Action Plan. COM(97) 599 of 26.11.1997.

5. Tillman, D. A. 'Biomass cofiring: the technology, the experience, the combustion consequences', Biomass and Bioenergy, 19(6), 2000,pp. 365-384.

6. Energy Information Administration, Form EIA-906, "Power Plant Report;" Government Advisory Associates, Resource Recovery Yearbook and Methane Recovery Yearbook; and analysis conducted by the Energy Information Administration, Office of Coal, Nuclear, Electric and Alternate Fuels. URL: http://www.eia.doe.gov/cneaf/solar.renewables/page/trends/table8.html. on 10 – November-2004

7. EPRI (Electronic Power Research Institute) (1985), 'Alternative fuel firing in an atmospheric fluidised bed combustor boiler, EPRI C5-4023, RP 2306-1

8. Saloski, P. Technical constraints of co-combustion –experiences in Finland. In: Proceedings of the workshop on technical constrains in Austria, 1999

9. Kallner, P., Technical constraints of co-combustion –experiences in Sweeden. In:Proceedings of the workshop on technical constrains in Austria, 1999

10. Hammerschmidt, A. Technical constraints of co-combustion –experiences in Sweeden. In:Proceedings of the workshop on technical constrains in Austria, 1999

11. Rosch, C. and Kaltschmitt, M. 'Energy from biomass -do non-technical barriers prevent an increased use?" Biomass and Bioenergy, 16(5),1999, pp. 347-356.

12. Balce, G. R, Tjaroko, T. S. and Zamora, C. G. 'Overview of biomass power generation in Southeast Asia, 2003. http://www.ec-asean-greenippnetwork.net on 10 –November-2004.

13. Sami M, Annamalai K, and Wooldridge M. 'Co-combustion of coal and biomass fuel blends', Progress Energy Combustion Science, 27, 2001, pp.171–214.

14. Gulyurtlu, I., Bordalo, C., Penha, E., and Cabrita, I., European *Co-combustion of coal, biomass and wastes.* In:Bemtgen, J. M., Hein, K. R. G., Minchener, A. J., editors. Combined combustion biomass/sewage sludge and coals, final reports, EC-research project, APAS- contract COAL-CT92-0002, 1995

15. Dermibas, A., 'Combustion characteristics of different biomass fuel,' Progress in energy and combustion science, 30, 2004, pp. 219-230

16. Knight, B. and Westwood, A., 'Global biomass resources for heat and electricity generation and capital expenditure forecasts',

17. Reference plants. Petrokraft. Sweden; 2002.http://www.petrokraft.se/refppes.htm on 10 –November-2004.

18. Reference plants. VTS projects. VTS AB. Sweden; 2002.http://www.vts.nu/projects.htm on 10 –November-2004.

19. European Bioenergy Networks,'Biomass co-firing'. As accessed from: http://eubionet.vtt.fi on 10 –November-2004.

20. Abelbha, P., Gulyurtlu, I., Boavida, D., Seabra Barros, J., Cabrita, I., Leahy, J., Kelleher, B., and Leahy, M, 'combustion of poultry litter in fluidised bed combustor', Fuel, 82, 2003, pp. 687-692

21. Cozzani, V., Nicolella, C., Petarca, L. Rovatti, M. and Tognotti, L., 'A fundamental study on conventional pyrolysis of a Refused-Derived Fuel', Industrial and Engineering Chemistry Research, 34(6), 1995, pp. 2006-2020

22. Gendebian, A., Leavens, A., Blackmore, A., Godley A., Lewin, K, Whitting, K. J., and Davis, R., European Commision; Refused derived fuel, current practice and perspectives, final reports, EC-research project, B4-3040/2000/306517/MAR/E3

23. Guilin, P. Shigeru, A., Shigekatsu, M., Seiichi, D., Yukihisa, F., Motohiro, K and Masataka, Y.,'Combustion of refused derived fuel in a fluidised bed', Waste management, 1, 1998, pp. 509-512

24. Natrajan, R., Nordin, A., and Rao, A. N., 'Overview of combustion and gasification of rice husk in fluidised bed reactors', Biomass and bioenergy, 14,1998, pp.533-546

25. Mahlia, T. M., Abdulmuin, M. Z., Alamsyah, T. M. I., and Mukhlishien, D., ' An alternative energy source from palm wastes industry for Malaysia and Indonesia', Energy conversion and management, 42, 2001, pp. 2109-2118

26. Environmental Protection Agency, EPA-450/3-77-077, "Background Document: Bagasse Combustion in Sugar Mills;" URL:http://www.epa.gov/ttn/chief/ap42/ch01/final/c01s08.pdf - on 1 may 2005)

27. Jenkins, B. M., 'Combustion properties of biomass', Fuel Processing Technology, 54(1-3), 1998, pp.17-46.

28. Werther, J., M. Saenger, et al. 'Combustion of agricultural residues', Progress in Energy and Combustion Science, 26(1), 2000, pp. 1-27.

29. Husain, Z., Zainal, Z. A. and Abdullah, M. Z., 'Analysis of biomass-residue-based cogeneration system in palm oil mills', Biomass and Bioenergy, 24, 2003, pp. 117-124

30. Boavida, D. Abelha, P., Gulyutlu, I. and Cabrita, I., 'Co-combustion of coal and non-recyclable paper and plastic waste in a fluidised bed reactor', Fuel, 82, 2003, pp. 1931-1938.

31. Hupa, M., and Boström, S., Fluidized Bed Combustion; Prospects and Role, Report 91-7, Åbo Akademi University, Åbo/Turku, Finland, 1991. Invited Presentation at the First World Coal Institute Conference: "Coal in the Environment", London, UK, April 3–5,1991.

32. Mutanen, K., Circulating Fluidized Bed Technology in Biomass Combustion—Performance, Advances and Experiences, Proceedings, 2nd Biomass Conference of the Americas: Energy, Environment, Agriculture and Industry, Portland, USA, August 1995, pp. 449–460

33. Atmospheric Fluidized Bed Coal Combustion: Research, development and application (M. Valk, Ed.), Elsevier, The Netherlands, 1995.

34. Basu, P., and Fraser, S.A., Circulating Fluidized Bed Boilers, Butterworth-Heinemann, USA, 1991.

35. Raul G. B-M, Determination of the rate of transfer of volatile matter into the freeboard of a fluidised bed combustor. Ph.D. Thesis. The university of Sheffield, 1993.

36. Armesto, L., Bahillo, A., Veijonen, K., Cabanillas, A. and Otero, J., 'Combustion behaviour of rice husk in a bubbling fluidised bed', Biomass and Bioenergy, 23(3), 2002, pp. 171-179

37. Peel, R.B., and Santos, F. J., 'Fluidised bed combustion of vegetable fuels,' In. proceedings: Fluidised combustion-systems and applications. Institute of energy symposium series 4, 1980, London, UK

38. Howe, W.C and Divilio, R.J., 'Fluidised bed combustion experience with alternative fuels', *Proceedings of strategic benefits of biomass and waste fuels*, EPRI TR-103146, Research project 3295-02, pp. 4-11-4-30

39. Bhattacharya, S.C. and Wu, W., 'Fluidised bed combustion of rice husk for disposal and energy recovery', *Energy from Biomass and Wastes XII*, 1989, 591, p. 601

40. Preto, F., anthony, R., G., Lalk, T. R., and Craig, J.D., 'Combustion trials of rice hulls in a pilot scale fluidised bed', Proc. Int. Conf.Fluidised Bed Combustion., 2,1997, pp.1123-1127.

41. Kuprianov, V. I and Pemchart, W. 'Emissions from a conical FBC fired with a biomass fuel', Applied Energy, 74, 2003, pp. 383–392

42. Kelleheler, B. P., Leahy, J.J, Henihan, A.M, O'Dwyer, T.F, Sutton, D., Leahy, M.J., 'Advances in poultry litter disposal-a review', Bioresource Technology, 83,2002, pp. 27-36

43. Suksankraisorn, K, Patumsawad, S. and Fungtammasan, B., 'Combustion studies of high moisture content waste in a fluidised bed', Waste Management, 23, 2003, pp. 433–439

44. Suthum, P., Co-combustion of high moisture content of MSW with coal in fluidised bed combustor. Ph.D. thesis. The university of Sheffield, 2000

45. Williams, P. T., and Besler, S., 'The pyrolysis of rice husks, the influence of temperature and heating rate on the product composition. In: Grassi, G., Collinna, A., Zibetta, H., editors. Biomass for energy, industry and environment, 6th E.C. Conference, London; Elsevier Applied Science, 1991, pp. 752-75

46. Vamvuka, D., Kakarasb,E., Kastanakia,E. and Grammelis, P. 'Pyrolysis characteristics and kinetics of biomass residuals mixtures with lignite', Fuel, 82 2003, pp. 1949–1960

47. Kaferstein, P., Gohla, M, Teper, H., Reimer, H., 'Fluidisation: combustion and emissions behavior of biomass in fluidised bed combustion units. In: Preto FDS, editor. Proceedings of the 14th international conference on fluidised bed combustion, Vancouver, Canada, New York:ASME, 1997, pp. 15-27

48. Cooke, R.B, Goodson, J and Hayhurst, A. N., 'The combustion of solid wastes as studied in fluidised bed', Trans IChemE, Vol 81, Part B, May 2003, pp. 156-166

49. IEA Clean Coal Centre.(2002), 'Bubbling fluidised bed combustion (BFBC) at atmospheric pressure', As accessed from: http://www.iea-coal.org.uk on 10-November-2004

50. Armesto, L., Bahillo, A, Cabanillas, A., Veijonen, K. Otero, J., Plumed, A and Salvador, L, 'Co-combustion of coal and olive oil industry residues in fluidised bed', Fuel, 82, 2003, pp. 993-1000.

51. Suksankraisorn,K, Patumsawad, S., Vallikul, P., Fungtammasan, B. and Accary, A., 'Co-combustion of municipal solid waste and Thai lignite in a fluidized bed', Energy Conversion and Management, 45, 2004, pp. 947–962

52. Cliffe, K. R., and Sathum, P., 'Co-combustion of waste from olive production with coal in a fluidised bed', *Waste management*, 2001, 21, pp.49-53

53. Saxena, S.C., and Jotshi, C. K., 'Fluidised bed incineration of waste material', *Progress in energy and combustion science,* 1994, 20, pp. 281-324

54. Leckner, B., Amand, L. E. Lucke, K. and wether, J., 'Gaseous emissions from –co-combustion of sewage sludge and coal/wood in a fluidised bed', Fuel, 3, 2004, pp. 477-486

55. Saxena, S.C. and Rao, N. S., 'Fluidised bed incineration of refused derived fuel pellets', Energy and Fuels, 7(2), 1993, pp. 273-278

56. Scale, F., Chirone, R., and Salatino, P., 'Fluidised bed combustion of tyre derived fuel', Experimental thermal and fluid science, 27 (4), 2003, pp. 465-471

57. Fahlstedt I, Lindman E, Lindberg T, Anderson J. Co-firing of biomass and coal in a fluidised bed combined cycle. Results of pilot plant studies. In: Proceedings of the 14th International Conference on Fluidized Bed Combustion in Vancouver, Canada, vol. 1, 1997. pp. 295–299.

58. Van Doorn J, Bruyn P, Vermeij P. Combined combustion of biomass, municiple sewage sludge and coal in an atmospheric fluidised bed installation. In: Biomass for energy and the environment, Proceedings of the 9th European Bioenergy Conference, Copenhagen, Denmark, vol. 2, 24–27 June, 1996. pp. 1007–1012.

59. Desroches Durcane, E., Marty, E., Martin, G and Delfosse, L., 'Co-combustion of coal and municipal solid waste in a circulating fluidised bed', Fuel, 77 (12), 1998, pp. 1311-1314

60. Latva-Somppi, J., Kurkela, J., Tapper, U., Kauppinen, E.I., Jokiniemi, J.K and Johansson, B. (1998). Ash deposition on bed material particles during fluidized bed combustion of wood-based fuels. Proceedings of the ABC'98 International Conference on Ash Behaviour Control in Energy Conversion Systems, Yokohama, Japan, March,18-19, 1998, pp. 110-118.

61. Skrifvars, B-J., Backman, R., Laurén, T., Hupa, M., Binderup-Hansen, F.: The role of Cl and S in post cyclone deposits from CFB boilers firing biomass, in Proc. of The Engineering Foundation Conference, Kona, Hawaii, November 1997.

62. Bapat DW, Kulkarni SV, Bhandarkar VP. Design and operating experience on fluidized bed boiler burning biomass fuels with high alkali ash. In: Preto FDS, editor. Proceedings of the14th International Conference on Fluidized Bed Combustion,Vancouver, New York, NY: ASME, 1997. pp. 165–74.

63. Liu H, Lin Z, Liu D, Wu W. Combustion characteristics of ricehusk in fluidized beds. In: Heinschel KJ, editor. Proceedings of the 13th International Conference on Fluidized Bed Combustion, Orlando, FL, New York, NY: ASME, 1995. pp. 615–618

64. Miles, T. R. , Jr. Baxter, L. L., Bryers, R. W. , Jenkins B. M. , Oden, L. L. Alkali deposits found in biomass power plant: a preliminary investigation of their extent and nature, National Renewable Energy Laboratory, Golden, CO, USA, 1995.

65. Ergudenler, A. and Ghaly, E. 'Agglomeration of silica sand in a fluidized bed gasifier operating on wheat straw,' Biomass Bioenergy, 4, 1993, pp. 135–147.

66. Muthukrishnan M, Sundararajan S, Viswanathan G, SarajamS, Kamalanathan N, Ramakrishnan P. Salient features andoperating experience with world's first rice straw fired fluidizedbed boiler in a 10 MW power plant. In: Heinschel KJ,editor. Proceedings of the 13th International Conference onFluidized Bed Combustion, Orlando, FL, New York, NY:ASME, 1995. pp. 609–614

67. Baxter, L. L., 'The behaviour of inorganic material in biomass-fired power boilers: field & laboratory experiences', Fuel processing technology, 54 (1-3), 1998, pp. 47-48

68. Manno, V. P. and Reitsma, S. H. , 'An annoted bibliography of fluidised bed combustion modelling information', Powder Technology, 63(1), 1990, pp. 23-24

69. Adanez, J. and Abanades, J. C., 'Modelling of lignite combustion in atmospheric fluidised bed combustors. 1. Selection of submodels and sensivity analysis', Industrial & Engineering Chemistry research, 31(10), 1992, pp. 2286-2296

70. Scala, F. and Salatino, P. Modelling fluidized bed combustion of high volatile solid fuels, Chem.Eng.Sci.57 (2002), pp.1175–1196.

71. Marias, F., Puiggali, J. R., and Flamant, G. 'Modelling for simulation Fluidised bed incineration process', AIChE Journal, 47(6), 2001, pp. 1438-1460

72. Olcay, O., Nevin, S and Isik, O, 'Testing of a mathematical model for the combustion of lignites in an AFBC', Fuel,72, 1993, pp. 261-266

73. Perry. R. and Chilton, C. H., Chemical Engineer's Handbook, McGraw Hill,1973

74. Speight, J.G.: The Chemistry and Technology of Coal, Dekker, 1983

75. Sulaiman, M. R., Fluidised bed incineration of EVA Co-polymer waste and its potential to remove sulphur from coal. PhD. Thesis. The University of Sheffield. 1997.

76. Kunii and Levenspiel, Fluidisation Engineering, John Wiley & Sons, Inc: New York, 1969

77. Geldart, D., Gas fluidisation technology, John Wiley & Sons, Inc.: New York, 1986

78. Holman, J. P. Heat transfer. McGraw Hill publishing company, 1990.

79. Strauss, W. Industrial gas cleaning. Volume 8, Pergamon Press, 1996.

APPENDIX A

DESIGN PARAMETERS OF COMBUSTION UNIT

A-1 Fluidised bed combustion unit

Various operating parameters were taken into consideration in the calculations to establish the size of column, such as excess air (0-100%), bed temperatures(700-900°C), fluidising velocities (0.4 – 1.2 m/s) and coal mass flow rates (1 – 1.4 kg/hr).

A coal feed rate for a laboratory coal fired fluidised bed combustor to give reasonable dimensions of the combustor is between 1 - 1.4 kg/hr. Using this range of flow rates the adiabatic flame temperatures and the quantities of the flue gas produced at percentages of excess air between 20-80% were calculated based on complete combustion.

Normally, the range of bed temperatures in a fluidised bed combustor are between 800-950°C, the upper temperature being limited by the material of construction of the fluidised bed (306 stainless steel). The percentages of excess air at 60 and 80 % were selected for burning coal at a feed rate of 1-1.4 kg/hr to limit the maximum bed temperature at 950°C.

The gas flow rate is limited by the minimum fluidisation velocity, u_{mf}, and to ensure uniform fluidisation suspension of the bed material the normal operating flow rate is 5 times u_{mf}. The minimum fluidisation velocities were calculated using Eq. A-1. The sand average size 850 μm was selected as this is a common size used in many studies [44]. The value of minimum fluidisation velocity, u_{mf}, and 5 x u_{mf} are 0.27 and 1.35 m/s respectively.

Knowing the amount of gas flow rate and gas velocity, the cross-sectional area of the combustor and the diameter of the circular combustor can be calculated.

$$dt = (4Q/3600\pi u)^{1/2} \qquad \text{(A-1)}$$

where dt = diameter of column, m

Q = flue gas quantity, 68.18 m^3/hr@900°C
(coal feed rate of 1.2 kg/hr and excess air of 60%)

u = fluidising gas velocity, 1.35 m/s

The diameter of the combustor for operation at 1.2 kg/hr of coal feed rate, 60% excess air and 850 μm of particle size was 0.13 m. This is a non-standard pipe size so the next largest standard diameter pipe (i.e. 0.15 m) as selected for construction of the combustor.

For the design of the Freeboard (FB), the graphical correlation of Zein and Weil [77] was chosen to estimate the transport disengaging height (TDH) as follows:

$$TDH = 1200 H_s Re_p^{1.55} Ar^{-1.1} \qquad \text{(A-2)}$$

For $15 < Re_p < 3000$ $19.5 < Ar < 650000$

$H_s < 0.5$m, settled bed height: $d_p = 0.7 - 2.5$ mm

From Eqn. A-2 and also comparing the size of experimental rigs constructed by other researchers, the TDH was found to be 2 m. Hence the actual freeboard height (H_{FB}) for the present combustor was given as 2.10 m, allowing 0.10 m for the dilute phase transport [76]. Loss of heat radially was minimised by surrounding the combustor of 0.15 m Kaowool blanket insulation with loss thermal conductivity. Under the present operating temperatures, such heat losses represented between 1 and 2 % of the total energy input for all the experiments performed in this study. Whereas the loss of heat axially was reduced by designing a longer freeboard than the length of the control volume (the bed section).

A-2 Cyclone design

The cyclone was constructed from stainless steel and as 0.10 m diameter and 0.40 m high. The cut-size, D_{pc} is the particle size corresponding to a fractional efficiency of 50% and the value calculated using equation A-3 [73].

$$D_{pc} = [9\ \mu B_c / V_i(\rho_s - \rho_a)]^{1/2} \qquad \text{(A-3)}$$

where μ = viscosity of air, $3.482*10^{-5}$ kg/m.s@500°C

B_c = (flue gas quantity)/(cyclone inlet area)

V_i = cyclone inlet velocity, 9.98 m/s

ρs = particle density, 2500 kg/m^3

ρa = air density, 0.47 kg/m^3 @500°C

The performance of the cyclone can be analysed by comparing the collection efficiency of the cyclone at any particle size by referring to Figure A-1 and particle collection efficiency of 70% as shown in Table C-1 – C-18. The particle size of the material in the catchpot was determined using a Malvern particle size analyser.

A-3 Pressure drop in cyclone

The pressure drop can be characterised by a pressure loss coefficient or Euler's number [78]. It was considered that both the collection efficiency and pressure drop of the cyclone are acceptable and so it was used in this project.

$$Const. = \Delta P/(1/2*\rho_a Vi^2) = ab/D_x^2 \qquad \text{(A-4)}$$

Where a = $D/2$

b = $D/4$

Dx = $D/2$

D = diameter of cyclone, 0.1 m

ΔP = $(ab/D_x^2)(1/2*\rho_a Vi^2)$ = 187.49 Pa or 1.9 cmH_20

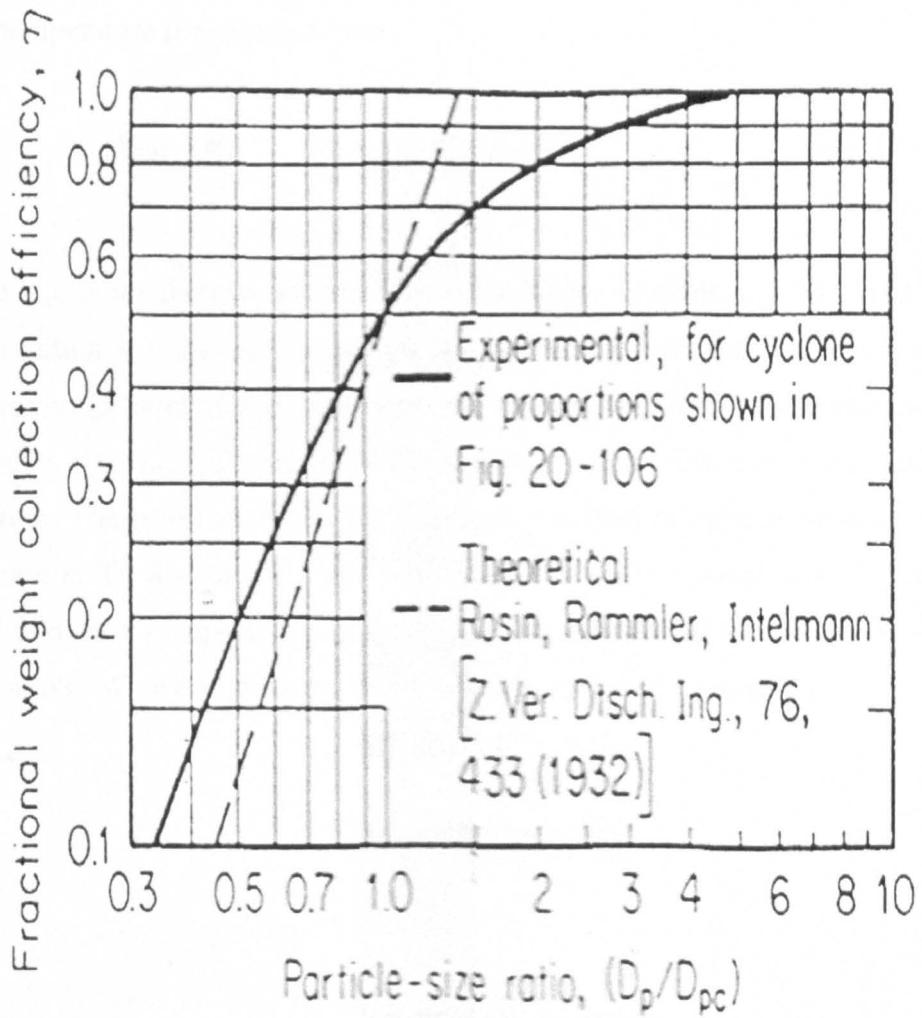

Figure A-1 Collection efficiency of cyclones [73]

A-4 Heat losses to surroundings

The heat lost radially from the fluidised combustor was calculated by applying the Critical Insulation Thickness suggested by Holman, 1990 [79]. Thus, heat flow transferred through the combustor walls and exposed to a convection environment at room temperature is estimated from

$$Q_{rad}\ (W) = \frac{2\pi L_c(T_b-T_o)}{\ln(R_o/R_i)/K_{kw} + 1/R_o h_o} \qquad (A\text{-}5)$$

Where K_{kw} is the thermal conductivity of the Kaowool blanket (0.081 W/m°C) used as the insulation material; ho stands for the convective heat transfer of the air at room temperature (3 $W/m^2°C$); L_c represents the length of fluidised bed combustor from the distributor plate (2.3 m); and R_o (0.225 m) are the respective inside and outer radius of insulation. The heat loss to the surroundings was thus calculated by using an average temperature, Tb due to the lower temperature in the freeboard area. T_b and T_o were 700°C and 40°C, respectively (safe outside temperature of the combustor) giving the heat loss 633 W or 6% of energy input which is considered acceptable.

APPENDIX B

COMBUSTION CALCULATIONS

B-1 Combustion Characteristics of Solid Wastes

Combustion characteristics solid wastes were determined by analysis of the constituents of solid waste. Questions that are pertinent to the combustion of solid wastes are; What volume reduction is attainable? How much air must be supplied for efficient combustion? What are the emissions leaving the furnace? How much the energy can be recovered from the combustion gases?.

B-2 Complete Combustion

Complete combustion is achieved when all carbon and hydrogen elements in a combustion system fully oxidised and become only carbon dioxide and water. However, complete combustion is solely a theoretical concept. In actual practice, partially oxidised products incomplete combustions were formed. These may include carbon monoxide, soot and organic matters.

B-3 Composition of Fuel as a Function of Moisture Content

Let C, H, O, N, S, and A be the mass fractions of each components; carbon, hydrogen, oxygen, nitrogen, sulphur, and ash, respectively, in the fuel on dry basis and W be the fraction of moisture content in the fuel.

At dry basis; $C + H + O + N + S + A = 100\%$ (B-3.0)

At any percentage of moisture content;

$$C = [(100 - W)/100] \times C_{dry\ basis} \quad \text{(B-3.1)}$$

$$H = [(100 - W)/100] \times H_{dry\ basis} \quad \text{(B-3.2)}$$

$$O = [(100 - W)/100] \times O_{dry\ basis} \quad \text{(B-3.3)}$$

$$N = [(100 - W)/100] \times N_{dry\ basis} \quad \text{(B-3.4)}$$

$$S = [(100 - W)/100] \times S_{dry\ basis} \quad \text{(B-3.5)}$$

$$A = [(100 - W)/100] \times A_{dry\ basis} \quad \text{(B-3.6)}$$

B-4 Correction Factor (CF)

The correction factor (CF) for oxygen is defined as:

$$CF = (21 - \text{desired } O_2)/(21 - \text{measured } O_2) \quad \text{(B-4)}$$

B-5 Calculations of Combustion Stoichiometry, Excess air and Flue gas Composition

Calculations based on the mass fractions of carbon (C) , Hydrogen (H), oxygen (O), Nitrogen (N), sulphur (S), ash (A) and moisture (W)content. Assuming that C,H,N,and S present in the fuel are completely converted to CO_2, H_2O, NO and SO_2 respectively.

$C + O_2 \rightarrow CO_2$; O_2 required for $CO_2 = (32/12)x\ C$

$H_2 + 0.5O_2 \rightarrow H_2O$; O_2 required for $H_2O = (9/16)xH$

$N_2 + O_2 \rightarrow 2NO$; O_2 required for $NO = (16/14) \times N$

$S + O_2 \rightarrow SO_2$; O_2 required for $SO_2 = (32/32) \times S$

The total amount of oxygen consumed during the combustion of the fuel:

$X1 = (32/12)C + (16/2)H + (16/14)N + (32/32)S$ (kg/kg fuel) (B-5.0)

The total amount of oxygen required for stoichiometric combustion of 1 kg of the fuel:

$X_2 = (32/12)C + (16/2)H + (16/14)N+(32/32)S - O$ (kg/kg fuel) (B-5.1)

Stoichiometric air requirement $(A/F)s = 4.29\ X_2$ (kg/kg fuel) (B-5.2)

Let : $Ø = (A/F)_{actual}/(A/F)_{stoichiometric}$ (B-5.3)

Therefore,

O_2 supplied = $ØX_2$ (B-5.4)

Mass air supplied $=(4.29)\ ØX_2$ (B-5.5)

or volumetric $(4.29)\ ØX_2 \times 0.78 m^3$ at STP

Mass of CO_2 in the flue gas = (44/12)C or (22.4/12)C m^3 at STP (B-5.6)

Mass of H_2O in the flue gas = (18/2)H or (22.4/2)C m^3 at STP (B-5.7)

(In the fuel)

Mass of SO_2 in the flue gas = (64/32)S or (22.4/32)C m^3 at STP (B-5.8)

Mass of NO in the flue gas = (30/14)N or (22.4/14)C m^3 at STP (B-5.9)

Mass of O_2 in the flue gas = (Ø-1) X_2 or (Ø-1) X_2 (22.4/32) m^3 at STP (from excess oxygen in air supplied) (B-5.10)

Mass of N_2 in the flue gas = $(3.29)ØX_2$ or $(3.29)ØX_2(22.4/28)$ m^3 at STP (from nitrogen in air supplied) (B-5.11)

Mass of H_2O in the flue gas = W or (22.4/14)W m^3 at STP (from moisture content in the fuel) (B-5.12)

mass (kg) of the wet flue gas ; Mw

= (44/12)C + (18/2)H + (64/32)S + (30/14)N + (Ø-1) X_2 + moisture (W) (B-5.13)

or volumetric (m^3 at STP) ; Vw

$= [C/12 + H/2 + S/32 + N/14 + \{(Ø-1)\ X_2\}/32 + \{3.29\ ØX_2\}/28 + W/18] \times 22.4$ (B-5.14)

Mass of the dry flue gas ; M_d

$= (44/12)C + (64/32)S + (30/14)N + (Ø-1)\ X_2 + 3.29\ ØX_2$ (B-5.15)

or m^3 at STP ; V_d

$= [C/12 + S/32 + N/14 + \{(Ø-1)\ X_2\}/32 + \{3.29\ ØX_2\}/28] \times 22.4$ (B-5.16)

The flue gas flow rate and composition are not appreciably influenced if we neglect the presence of SO_2 and NO in the flue gas.

Theoretical flue gas composition (% dry by volume)

$$CO_2 = (100/Vd)x(22.4/12) \times C \quad \text{(B-5.17)}$$

$$O_2 = (100/Vd)x(22.4/32) \times (Ø-1) X_2 \quad \text{(B-5.18)}$$

$$N_2 = (100/Vd)x(22.4/28)x3.29xØX_2 \quad \text{(B-5.19)}$$

$$SO_2 = (100/Vd)x(22.4/32)x S \quad \text{(B-5.20)}$$

$$NO = (100/Vd)x(22.4/14) \times N \quad \text{(B-5.21)}$$

B-6 Calculation of Carbon Combustion Efficiency

A) CO efficiency

A very commonly employed method for the computation of percentage carbon utilisation or combustion efficiency is

$$\mathbf{E1} = \frac{[CO_2]}{[CO_2] + [CO]} \times 100\% \quad \text{(B-6.0)}$$

where : $[CO_2]$ is the percentage of CO_2 in the flue gas

[CO] is the percentage of CO in the flue gas

It assumes that all the carbon feed present in the waste is converted completely to carbon monoxide and carbon dioxide only. However, the carbon fed to the incinerator must be balanced against all losses in different streams as well as by possible chemical reactions. The carbon losses can be estimated by equating the amount of carbon feed to the amount of CO and CO_2 in the flue gas and any unburned carbon.

B) Carbon Utilisation Efficiency

This method is particularly appropriate for solid fuels and is described as follows:

Let C, H, O, N, and S be the mass fractions of carbon, hydrogen, oxygen, nitrogen and sulphur, respectively, in the feed. Further, let A and B be the mass fractions of unburned and burnt carbon, respectively, in the fuel. Then,

$$A + B = C \qquad \text{(B-6.1)}$$

Further define

$$P = \frac{\text{C converted to CO}}{\text{C converted to CO} + CO_2} = \frac{\text{C converted to CO}}{B} \qquad \text{(B-6.2)}$$

$$\text{C converted to CO} = PB \qquad \text{(B-6.3)}$$

$$\text{C converted to } CO_2 = (1\text{-}P)B \qquad \text{(B-6.4)}$$

$$\text{Mass of } CO_2 \text{ in the flue gas} = (44/12)(1\text{-}P)B \qquad \text{(B-6.5)}$$

$$\text{Mass of CO in the flue gas} = (28/12)PB \qquad \text{(B-6.6)}$$

$$O_2 \text{ consumed to produced } CO_2 + CO = (32\text{-}16P)B/12 \qquad \text{(B-6.7)}$$

Assuming that H, N, and S present in the fuel are completely converted to H_2O, NO and SO_2 respectively,

$$O_2 \text{ consumed} = (16/2)H + (16/14)N + (32/32)S = X_1 \qquad \text{(B-6.8)}$$

$$SO_2 \text{ produced} = (64/32)S \qquad \text{(B-6.9)}$$

$$\text{NO produced} = (30/14)N \qquad \text{(B-6.10)}$$

Therefore, total O_2 required for stoichiometric combustion of fuel

$$(32/12)C + (16/2)H + (16/14)N + (32/32)S - O = X_2 \qquad \text{(B-6.11)}$$

Let Z be the fractional excess air supplied, which is defined as the excess air divided by the stoichiometric air. Therefore,

$$O_2 \text{ supplied} = X_2(1+Z) \qquad \text{(B-6.12)}$$

$$\text{Mass of } N_2 \text{ in the flue gas} = (79/12)(28/32)\,X_2(1+Z) \qquad \text{(B-6.13)}$$

$$O_2 \text{ consumed during combustion} = \text{(B-7.7)}+\text{(B-7.8)} = (32\text{-}16P)B/12 + X_1 \qquad \text{(B-6.14)}$$

$$\text{Mass of } O_2 \text{ in the flue gas} = \text{(B-7.12)}-\text{(B-7.14)} = X_2(1+Z)-(32\text{-}16P)B/12+X_1 \qquad \text{(B-6.15)}$$

Let F be the mass of dry flue gas can also be estimated from the flue gas composition. The flue gas flow rate and composition are not appreciably influenced by neglecting the presence of SO_2 and NO in the flue gas. Hence the flue gas may be taken as consisting of CO, CO_2, N_2 and O_2. Let Y be the mass of dry flue gas per unit mass of C burnt in the fuel. Then,

$$Y = \{44[CO_2] + 32[O_2] + 28[N_2]\}/12\{[CO] + [CO_2]\} \qquad \text{(B-6.17)}$$

The square brackets represent the volume fraction of the particular chemical species in the flue gas and Y can be simplified to

$$Y = \{4[CO_2] + [O_2] + 7\}/3\{[CO] + [CO_2]\} \qquad \text{(B-6.18)}$$

By substituting

$$[CO] + [N_2] + [CO_2] + [O_2] = 1$$

mass of dry flue gas per unit mass of the fuel is = F = YB (B-6.19)

Substituting F in (A-6.19) into (A-6.18), then the fraction of C burnt, B, can be written as follows:

$$B = [4.29(1+Z)[(32/12)C + (16/2)H + (16/4)N + (32/32)S - O] - 8H + N + S]/(Y-1) \qquad \text{(B-6.20)}$$

In the absence of complete combustion, a certain amount of thermal energy is lost which corresponds to the values associated with the conversion of carbon to CO and CO2 and the unburned carbon in ash. Thermal efficiency is defined as the ratio of rate of energy release to rate of energy supply:

E2 = (B (B-6.20) + Unburned carbon in ash) / C x 100% (B-6.21)

APPENDIX C

PARTICLE SIZE OF DISTRIBUTION

Table C -1 Particle size distribution of carryover from run of 100% coal combustion

AVERAGE SIZE (μm)	SIZE INTERVAL (μm)	WEIGHT IN BAND (%)	WEIGHT % UNDER
			100.0
171.737	222.8 - 120.67	8.8	91.2
98.495	120.67 - 76.32	10.8	80.4
62.295	76.32 – 48.27	10.2	70.2
39.400	48.27 – 30.53	10.1	60.1
24.920	30.53 – 19.31	9.5	50.6
15.760	19.31 – 12.21	8.3	42.3
9.965	12.21 – 7.72	8.0	34.3
6.300	7.72 – 4.88	9.2	25.1
3.985	4.88 – 3.09	8.8	16.3
2.515	3.09 – 1.95	6.3	10.0
1.595	1.95 – 1.24	4.3	5.7
1.010	1.24 – 0.78	3.6	2.1
0.635	0.78 – 0.49	2.0	0.01
D(50%)	UM : 18.66	D (90%)	UM : 114.28
D(10%)	UM : 1.96	AVG	UM : 39.79

Table C-2 Particle size distribution of carryover from run of MSW(100%)

AVERAGE SIZE (μm)	SIZE INTERVAL (μm)	WEIGHT IN BAND (%)	WEIGHT % UNDER
			100.0
171.737	222.8 - 120.67	10.5	89.5
98.495	120.67 - 76.32	11.8	77.7
62.295	76.32 – 48.27	10.3	67.4
39.400	48.27 – 30.53	10.2	57.2
24.920	30.53 – 19.31	10.2	47.0
15.760	19.31 – 12.21	9.4	37.6
9.965	12.21 – 7.72	8.5	29.1
6.300	7.72 – 4.88	8.0	21.1
3.985	4.88 – 3.09	6.8	14.3
2.515	3.09 – 1.95	4.8	9.5
1.595	1.95 – 1.24	3.8	5.7
1.010	1.24 – 0.78	3.6	2.1
0.635	0.78 – 0.49	2.0	0.1
D(50%)	UM : 22.07	D (90%)	UM : 122.80
D(10%)	UM : 2.05	AVG	UM : 43.77

Table C-3 Particle size distribution of carryover from run of Coal (70%)/MSW(30%)

AVERAGE SIZE (μm)	SIZE INTERVAL (μm)	WEIGHT IN BAND (%)	WEIGHT % UNDER
			100.0
171.737	222.8 - 120.67	10.7	89.3
98.495	120.67 - 76.32	12.2	77.1
62.295	76.32 – 48.27	10.8	66.3
39.400	48.27 – 30.53	10.3	56.0
24.920	30.53 – 19.31	9.4	46.6
15.760	19.31 – 12.21	7.9	38.7
9.965	12.21 – 7.72	6.9	31.8
6.300	7.72 – 4.88	7.3	24.5
3.985	4.88 – 3.09	7.0	17.5
2.515	3.09 – 1.95	5.6	11.9
1.595	1.95 – 1.24	4.8	7.1
1.010	1.24 – 0.78	4.6	2.5
0.635	0.78 – 0.49	2.4	0.1
D(50%)	UM : 22.91	D (90%)	UM : 123.86
D(10%)	UM : 1.59	AVG	UM : 44.25

Table C-4 Particle size distribution of carryover from run of Coal (50%)/MSW(50%)

AVERAGE SIZE (μm)	SIZE INTERVAL (μm)	WEIGHT IN BAND (%)	WEIGHT % UNDER
			100.0
171.737	222.8 - 120.67	7.7	92.3
98.495	120.67 - 76.32	9.8	82.5
62.295	76.32 – 48.27	9.4	73.1
39.400	48.27 – 30.53	9.7	63.4
24.920	30.53 – 19.31	9.7	53.7
15.760	19.31 – 12.21	8.5	45.2
9.965	12.21 – 7.72	8.0	37.2
6.300	7.72 – 4.88	8.7	28.5
3.985	4.88 – 3.09	8.5	20.0
2.515	3.09 – 1.95	6.6	13.4
1.595	1.95 – 1.24	5.3	8.1
1.010	1.24 – 0.78	4.9	3.2
0.635	0.78 – 0.49	3.1	0.1
D(50%)	UM : 15.93	D (90%)	UM : 108.00
D(10%)	UM : 1.47	AVG	UM : 36.57

Table C-5 Particle size distribution of carryover from run of Coal (30%)/MSW(70%)

AVERAGE SIZE (μm)	SIZE INTERVAL (μm)	WEIGHT IN BAND (%)	WEIGHT % UNDER
			100.0
171.737	222.8 - 120.67	6.7	93.3
98.495	120.67 - 76.32	11.8	81.5
62.295	76.32 – 48.27	13.1	68.4
39.400	48.27 – 30.53	13.2	55.2
24.920	30.53 – 19.31	12.9	42.3
15.760	19.31 – 12.21	11.5	30.8
9.965	12.21 – 7.72	9.4	21.4
6.300	7.72 – 4.88	7.3	14.1
3.985	4.88 – 3.09	3.6	10.5
2.515	3.09 – 1.95	3.0	7.5
1.595	1.95 – 1.24	2.3	5.2
1.010	1.24 – 0.78	2.2	3
0.635	0.78 – 0.49	1.5	1.5
D(50%)	UM : 25.47	D (90%)	UM : 104.52
D(10%)	UM : 3.45	AVG	UM : 41.30

Table C-6 Particle size distribution of carryover from run of Coal (90%)/Palm Fibre(10%)

AVERAGE SIZE (μm)	SIZE INTERVAL (μm)	WEIGHT IN BAND (%)	WEIGHT % UNDER
			100.0
171.737	222.8 - 120.67	6.8	93.2
98.495	120.67 - 76.32	9.2	84.0
62.295	76.32 – 48.27	11.5	72.5
39.400	48.27 – 30.53	15.9	56.6
24.920	30.53 – 19.31	17.7	38.9
15.760	19.31 – 12.21	14.5	24.4
9.965	12.21 – 7.72	9.4	15.0
6.300	7.72 – 4.88	5.7	9.3
3.985	4.88 – 3.09	3.5	5.8
2.515	3.09 – 1.95	2.1	3.7
1.595	1.95 – 1.24	1.5	2.2
1.010	1.24 – 0.78	1.5	1.5
0.635	0.78 – 0.49	0.9	1.3
D(50%)	UM : 44.68	D (90%)	UM : 144.52
D(10%)	UM : 6.64	AVG	UM : 61.91

Table C-7 Particle size distribution of carryover from run of Coal (80%)/Palm Fibre(20%)

AVERAGE SIZE (μm)	SIZE INTERVAL (μm)	WEIGHT IN BAND (%)	WEIGHT % UNDER
			100.0
171.737	222.8 - 120.67	10.8	89.2
98.495	120.67 - 76.32	12.2	77.0
62.295	76.32 – 48.27	11.8	65.2
39.400	48.27 – 30.53	14.7	50.5
24.920	30.53 – 19.31	15.8	34.7
15.760	19.31 – 12.21	13.2	21.5
9.965	12.21 – 7.72	8.7	12.8
6.300	7.72 – 4.88	5.2	7.6
3.985	4.88 – 3.09	3.1	4.5
2.515	3.09 – 1.95	1.8	2.7
1.595	1.95 – 1.24	1.3	1.4
1.010	1.24 – 0.78	1.2	0.2
0.635	0.78 – 0.49	0.1	0.1
D(50%)	UM : 29.81	D (90%)	UM : 124.59
D(10%)	UM : 6.00	AVG	UM : 48.75

Table C-8 Particle size distribution of carryover from run of Coal (70%)/Palm Fibre(30%)

AVERAGE SIZE (μm)	SIZE INTERVAL (μm)	WEIGHT IN BAND (%)	WEIGHT % UNDER
			100.0
171.737	222.8 - 120.67	7.7	92.3
98.495	120.67 - 76.32	10.3	82.0
62.295	76.32 – 48.27	12.5	69.5
39.400	48.27 – 30.53	16.4	53.1
24.920	30.53 – 19.31	17.5	35.6
15.760	19.31 – 12.21	13.8	21.8
9.965	12.21 – 7.72	8.6	13.2
6.300	7.72 – 4.88	5.1	8.1
3.985	4.88 – 3.09	3.1	5.0
2.515	3.09 – 1.95	1.8	3.2
1.595	1.95 – 1.24	1.3	1.9
1.010	1.24 – 0.78	1.2	0.7
0.635	0.78 – 0.49	0.6	0.1
D(50%)	UM : 28.18	D (90%)	UM : 107.93
D(10%)	UM : 5.92	AVG	UM : 43.55

Table C-9 Particle size distribution of carryover from run of Coal (70%)/RDF(70%)

AVERAGE SIZE (μm)	SIZE INTERVAL (μm)	WEIGHT IN BAND (%)	WEIGHT % UNDER
			100.0
171.737	222.8 - 120.67	15.4	84.6
98.495	120.67 - 76.32	15.7	68.9
62.295	76.32 – 48.27	13.1	55.8
39.400	48.27 – 30.53	12.2	43.6
24.920	30.53 – 19.31	11.9	31.7
15.760	19.31 – 12.21	10.0	21.7
9.965	12.21 – 7.72	7.3	14.4
6.300	7.72 – 4.88	5.2	9.2
3.985	4.88 – 3.09	3.5	5.7
2.515	3.09 – 1.95	2.1	3.6
1.595	1.95 – 1.24	1.5	1.4
1.010	1.24 – 0.78	1.4	0.7
0.635	0.78 – 0.49	0.69	0.01
D(50%)	UM : 38.67	D (90%)	UM : 141.10
D(10%)	UM : 5.20	AVG	UM : 57.88

Table C-10 Particle size distribution of carryover from run of Coal (50%)/RDF(50%)

AVERAGE SIZE (μm)	SIZE INTERVAL (μm)	WEIGHT IN BAND (%)	WEIGHT % UNDER
			100.0
171.737	222.8 - 120.67	19.5	80.5
98.495	120.67 - 76.32	19.5	61.0
62.295	76.32 – 48.27	14.3	44.0
39.400	48.27 – 30.53	11.1	32.9
24.920	30.53 – 19.31	9.8	23.1
15.760	19.31 – 12.21	8.1	15.0
9.965	12.21 – 7.72	6.0	9.0
6.300	7.72 – 4.88	4.3	4.7
3.985	4.88 – 3.09	2.8	1.9
2.515	3.09 – 1.95	1.7	0.2
1.595	1.95 – 1.24	1.2	-
1.010	1.24 – 0.78	1.2	-
0.635	0.78 – 0.49	0.8	-
D(50%)	UM : 54.01	D (90%)	UM : 150.89
D(10%)	UM : 6.46	AVG	UM : 54.01

Table C-11 Particle size distribution of carryover from run of Coal (30%)/RDF(70%)

AVERAGE SIZE (μm)	SIZE INTERVAL (μm)	WEIGHT IN BAND (%)	WEIGHT % UNDER
			100.0
171.737	222.8 - 120.67	15.2	84.8
98.495	120.67 - 76.32	16.2	68.6
62.295	76.32 – 48.27	13.3	55.3
39.400	48.27 – 30.53	11.9	43.4
24.920	30.53 – 19.31	11.5	31.9
15.760	19.31 – 12.21	9.8	22.1
9.965	12.21 – 7.72	7.3	14.8
6.300	7.72 – 4.88	5.3	9.5
3.985	4.88 – 3.09	3.6	5.9
2.515	3.09 – 1.95	2.1	3.8
1.595	1.95 – 1.24	1.5	2.3
1.010	1.24 – 0.78	1.4	0.9
0.635	0.78 – 0.49	0.9	0
D(50%)	UM : 39.25	D (90%)	UM : 140.01
D(10%)	UM : 5.12	AVG	UM : 57.85

Table C -12 Particle size distribution of carryover from run of Rice husk (100%)

AVERAGE SIZE (μm)	SIZE INTERVAL (μm)	WEIGHT IN BAND (%)	WEIGHT % UNDER
			100.0
171.737	222.8 - 120.67	6.94	93.1
98.495	120.67 - 76.32	13.8	79.3
62.295	76.32 – 48.27	17.9	61.4
39.400	48.27 – 30.53	17.4	44.0
24.920	30.53 – 19.31	14.7	29.3
15.760	19.31 – 12.21	10.8	18.5
9.965	12.21 – 7.72	7.3	11.2
6.300	7.72 – 4.88	4.6	6.6
3.985	4.88 – 3.09	2.4	4.2
2.515	3.09 – 1.95	1.5	2.7
1.595	1.95 – 1.24	1.4	1.3
1.010	1.24 – 0.78	0.9	0.4
0.635	0.78 – 0.49	0.3	0.1
D(50%)	UM : 36.05	D (90%)	UM : 106.44
D(10%)	UM : 7.02	AVG	UM : 47.81

Table C-13 Particle size distribution of carryover from run of Coal (50%)/RH(50%)

AVERAGE SIZE (μm)	SIZE INTERVAL (μm)	WEIGHT IN BAND (%)	WEIGHT % UNDER
			100.0
171.737	222.8 - 120.67	5.6	94.4
98.495	120.67 - 76.32	12.2	82.2
62.295	76.32 – 48.27	16.7	65.5
39.400	48.27 – 30.53	17.1	48.4
24.920	30.53 – 19.31	14.9	33.5
15.760	19.31 – 12.21	11.3	22.2
9.965	12.21 – 7.72	8.1	14.1
6.300	7.72 – 4.88	5.6	8.5
3.985	4.88 – 3.09	3.4	5.1
2.515	3.09 – 1.95	1.9	3.2
1.595	1.95 – 1.24	1.4	1.8
1.010	1.24 – 0.78	1.2	0.6
0.635	0.78 – 0.49	0.6	0
D(50%)	UM : 31.96	D (90%)	UM : 99.42
D(10%)	UM : 5.69	AVG	UM : 43.60

Table C-14 Particle size distribution of carryover from run of Wood pellet (100%)

AVERAGE SIZE (μm)	SIZE INTERVAL (μm)	WEIGHT IN BAND (%)	WEIGHT % UNDER
			100.0
171.737	222.8 - 120.67	8.6	91.4
98.495	120.67 - 76.32	11.0	80.4
62.295	76.32 – 48.27	10.8	69.6
39.400	48.27 – 30.53	13.7	55.9
24.920	30.53 – 19.31	16.1	39.8
15.760	19.31 – 12.21	14.6	25.2
9.965	12.21 – 7.72	12.0	13.2
6.300	7.72 – 4.88	7.8	5.4
3.985	4.88 – 3.09	2.3	3.1
2.515	3.09 – 1.95	2.0	1.1
1.595	1.95 – 1.24	1.1	0
1.010	1.24 – 0.78	0.7	0
0.635	0.78 – 0.49	0.4	0
D(50%)	UM : 25.69	D (90%)	UM : 113.34
D(10%)	UM : 5.73	AVG	UM : 43.63

Table C-15 Particle size distribution of carryover from run of Coal (30%) / Wood(70%)

AVERAGE SIZE (μm)	SIZE INTERVAL (μm)	WEIGHT IN BAND (%)	WEIGHT % UNDER
			100.0
171.737	222.8 - 120.67	18.1	81.9
98.495	120.67 - 76.32	16.9	65.0
62.295	76.32 – 48.27	13.6	51.4
39.400	48.27 – 30.53	12.3	39.1
24.920	30.53 – 19.31	11.7	27.4
15.760	19.31 – 12.21	9.7	17.7
9.965	12.21 – 7.72	7.9	9.8
6.300	7.72 – 4.88	4.6	5.2
3.985	4.88 – 3.09	2.8	2.4
2.515	3.09 – 1.95	1.6	0.8
1.595	1.95 – 1.24	0.9	0
1.010	1.24 – 0.78	0.6	0
0.635	0.78 – 0.49	0.3	0
D(50%)	UM : 45.83	D (90%)	UM : 148.63
D(10%)	UM : 7.27	AVG	UM : 63.63

Table C-16 Particle size distribution of carryover from run of Coal (50%)/Wood Pellet (50%)

AVERAGE SIZ E (μm)	SIZE INTERVAL (μm)	WEIGHT IN BAND (%)	WEIGHT % UNDER
			100.0
171.737	222.8 - 120.67	12.5	87.5
98.495	120.67 - 76.32	12.6	74.9
62.295	76.32 – 48.27	11.2	63.7
39.400	48.27 – 30.53	12.9	50.8
24.920	30.53 – 19.31	14.8	36.0
15.760	19.31 – 12.21	13.1	22.9
9.965	12.21 – 7.72	9.1	13.8
6.300	7.72 – 4.88	5.7	8.1
3.985	4.88 – 3.09	3.5	4.6
2.515	3.09 – 1.95	2.1	2.5
1.595	1.95 – 1.24	1.2	1.3
1.010	1.24 – 0.78	0.8	0.5
0.635	0.78 – 0.49	0.4	0.1
D(50%)	UM : 32.98	D (90%)	UM : 147.68
D(10%)	UM : 6.64	AVG	UM : 56.95

Table C-17 Particle size distribution of carryover from run of Coal (70%)/Wood pellet (30%)

AVERAGE SIZE (μm)	SIZE INTERVAL (μm)	WEIGHT IN BAND (%)	WEIGHT % UNDER
			100.0
171.737	222.8 - 120.67	16.6	83.4
98.495	120.67 - 76.32	12.4	71.0
62.295	76.32 – 48.27	10.4	60.6
39.400	48.27 – 30.53	13.0	47.6
24.920	30.53 – 19.31	15.1	32.5
15.760	19.31 – 12.21	12.5	20.0
9.965	12.21 – 7.72	8.1	11.9
6.300	7.72 – 4.88	4.9	7.0
3.985	4.88 – 3.09	3.1	3.9
2.515	3.09 – 1.95	1.8	2.1
1.595	1.95 – 1.24	1.0	1.1
1.010	1.24 – 0.78	0.7	0.4
0.635	0.78 – 0.49	0.4	0
D(50%)	UM : 29.78	D (90%)	UM : 131.54
D(10%)	UM : 5.83	AVG	UM : 50.76

APPENDIX D

COMBUSTION TESTS RESULTS

D-1 Co-combustion of coal with chicken waste

Substance	coal(30%)	CW(70%)	mixture	O2 require kg/kg fuel	(A/F)s kg/kg fuel	coal(50%)	CW(50%)	mixture	kg/kg fuel	coal(70%)	CW(30%)	mixture	kg/kg fuel
C	22.62%	24.28%	46.90%	1.25		37.70%	17.34%	55.04%	1.47	52.78%	10.40%	63.18%	1.68
H	2%	2.99%	4.49%	0.36		3%	2.14%	4.64%	0.37	4%	1.28%	4.78%	0.38
O	2.79%	20.62%	23.41%	-0.23		4.65%	14.73%	19.38%	-0.19	6.51%	8.84%	15.35%	-0.15
N	0.27%	1.33%	1.60%	0.02		0.45%	0.95%	1.40%	0.02	0.63%	0.57%	1.20%	0.01
S	0.21%	0%	0.21%	0.00		0.35%	0%	0.35%	0.00	0.49%	0%	0.49%	0.00
Ash	0.84%	17.29%	18.13%			1.40%	12.35%	13.75%		1.96%	7.41%	9.37%	
Moisture	1.77%	4%	5.27%			2.95%	3%	5.45%		4.13%	2%	5.63%	
				1.40					1.66				1.93
air needed				6.645035					7.921989				9.198943
volatile matter													
CV(MJ/kg)	31.1	12.92	18.374					22.01				25.646	

Coal (%)		0	0	0	30	30	30	50	50	50	70	70	70
Feedrate (kg/hr)		3	3	3	2.47	2.47	2.47	2.1	2.1	2.1	1.74	1.74	1.74
Main air (l/min)		190	230	270	230	275	300	210	250	300	205	250	290
Feeder air (l/min)		65	65	65	65	65	65	65	65	65	65	65	65
avg (l/min)		255	295	335	295	340	365	275	315	365	270	315	355
avg (kg/hr)		18.513	21.417	24.321	21.417	24.684	28.35268	21.36161	24.46875	28.35268	20.97321	24.46875	27.57589
xcess air (%)		30.42385	50.88249	71.34114	30.48615	50.39082	72.74277	28.40455	47.08158	70.42786	31.03214	52.87083	72.283
Results													
CO2 (%)		13	11.5	10	12.5	11.5	9.5	13	12	10	13	11.5	10
CO(ppm)		504	354	295	405.4	425.4	306.9	328.3	304.2	365	214	331	352
O2 (%)		4	5.1	6.7	6	6.5	8.1	6.5	7.3	8.2	4.5	5	6.9
To	195	192.7	206.7	214.5	193	217.5	272.3	238.8	290.1	220.1	315.3	292.1	275.1
T1	155	193.6	210.2	223	200	217.3	276.3	242.7	294.8	224.4	312.3	290.6	276.5
T2	115	590.9	616.6	676.8	703	689.3	685.8	644.7	694.5	614.2	710.6	672.7	667.7
T3	75	816.8	827.6	830.5	860	858.9	983.3	879.1	985.4	856.5	899.2	877.7	853.5
T4	40	841.6	836.5	845.8	880	857.3	903.3	893.1	904.2	866.9	895.7	879.2	854
T5	30	839.2	834.8	829.7	875	857.8	903.8	894.6	904.6	867.3	895.5	879.7	854.7
T6	20	834.4	837.9	833	860	855.3	900	891.8	904.7	865.8	890.9	876.7	851.8
T7	10	831.3	834.5	830.1	870	756.3	898.7	889.3	899.9	865.3	888.5	875.2	851.5
Ash (kg)			722.96			475			398.3			218.2	
Unburnt C (wt%)			6			8			9			10.7	
Y		19.30975	21.7042	24.88326	20.09483	21.73121	26.09465	19.39973	20.9275	24.8493	19.36556	21.70564	24.80934
B		0.286014	0.295057	0.292297	0.391398	0.418005	0.398666	0.479056	0.509246	0.495397	0.571604	0.594446	0.584552
carbon eff.(%)		82.47245	85.07994	84.28391	83.46082	89.13445	85.01068	87.03776	92.52282	90.00668	90.46659	94.08181	92.51578
CO eff. (%)		99.6138	99.69312	99.70587	99.96829	99.63145	99.67799	99.7481	99.74714	99.63633	99.83566	99.713	99.64923
efficiency (%)		80.74234	83.34984	82.55381	80.18024	85.85387	81.73009	83.93638	89.42144	86.9053	88.34294	91.95816	90.39214
fluidising velocity(m/s)		0.668714	0.806293	0.942161	0.835552	0.984062	1.117192	0.77592	0.931626	1.082541	0.75803	0.911927	1.034893
fludising number		2.476718	2.986271	3.489484	3.094637	3.644672	4.137747	2.873779	3.450467	4.009409	2.807518	3.377507	3.832936

D-2 Co-combustion of coal with rice husk

Substance	coal(30%)	RH(70%)	mixture	O2 require kg/kg fuel	(A/F)s kg/kg fuel	coal(50%)	RH(50%)	mixture	kg/kg fuel	coal(70%)	RH(30%)	mixture	kg/kg fuel
C	22.62%	24.46%	47.08%	1.26		37.70%	17.47%	55.17%	1.47	52.78%	10.48%	63.26%	1.69
H	2%	3.82%	5.32%	0.43		3%	2.73%	5.23%	0.42	4%	1.64%	5.14%	0.41
O	2.79%	27.20%	29.99%	-0.30		4.65%	19.43%	24.08%	-0.24	6.51%	11.66%	18.17%	-0.18
N	0.27%	0.08%	0.35%	0.00		0.45%	0.06%	0.51%	0.01	0.63%	0.03%	0.66%	0.01
S	0.21%	0%	0.21%	0.00		0.35%	0%	0.35%	0.00	0.49%	0%	0.49%	0.00
Ash	0.84%	14.43%	15.27%			1.40%	10.31%	11.71%		1.96%	6.18%	8.14%	
Moisture	1.77%	3%	4.35%			2.95%	2%	4.80%		4.13%	1%	5.24%	
				1.39	6.60				1.66				1.93
air needed				6.603639					7.89242				9.181201
volatile matter													
CV(MJ/kg)	31.1	13.52	18.794		34.94			22.31				25.826	

Coal (%)		0	0	0	30	30	30	50	50	50	70	70	70
Feedrate (kg/hr)		2.97	2.97	2.97	2.44	2.44	2.44	2.1	2.1	2.1	1.73	1.73	1.73
Main air (l/min)		185	225	265	225	275	315	235	275	325	225	265	305
Feeder air (l/min)		65	65	65	65	65	65	65	65	65	65	65	65
avg (l/min)		250	290	330	290	340	380	300	340	390	290	330	370
avg (kg/hr)		18.15	21.054	23.958	21.054	24.684	27.588	21.78	24.684	28.314	21.054	23.958	26.862
xcess air (%)		30.84584	51.78117	72.7165	30.66567	53.19423	71.21708	31.40999	48.93133	70.83299	32.55283	50.83598	69.11913
Results													
CO2 (%)		11.5	10.5	9.5	12.5	11	10	13	12	10	13	12	10
CO(ppm)		542.8	685.3	768.3	406	395.7	452	333.3	269.6	269.6	220.1	629.8	429.8
O2 (%)		5.3	7.1	8.4	7.3	9.3	10.3	6.5	8.3	9.1	5.4	6.7	7.5
To	195	395.8	379.15	354.2	571.6	571.6	436	464.6	470.5	470.5	445.7	459.6	459.6
T1	155	444.3	430.2	415.6	534.5	534.5	482.5	535.3	512.2	512.2	490.4	508.9	508.9
T2	115	732.6	721.35	700.3	845.1	825.5	751.1	802.6	806.4	810	760.8	787.6	800
T3	75	726.9	703.55	655.4	851.9	851.9	739.5	821.4	892.2	892.2	816.8	846.7	846.7
T4	40	703.9	691.35	653.2	880.2	880.2	764.6	865.3	883.4	883.4	863.8	893.5	893.5
T5	30	681.8	674.25	621.4	896	876	765.1	872	888.1	888.1	870.2	893.5	860
T6	20	673.7	678.55	600	869.5	869.5	766.7	867.3	884.6	865	864.8	898.4	898.4
T7	10	673.4	673.6	578	868	868	766.9	866.3	880.5	880.5	864.8	893.9	893.9
Ash (kg)			638.57			348.32			195.6			175.65	
Unburnt C (wt%)			26.2			20.97			28.5			26.63	
Y		21.67451	23.62675	25.97937	20.12929	22.74545	24.89746	19.39898	20.96124	24.90286	19.38769	20.85444	24.81003
B		0.245326	0.263106	0.273605	0.384568	0.39996	0.408828	0.485761	0.51018	0.491226	0.574418	0.60818	0.570682
carbon eff.(%)		70.21363	75.30226	78.30696	81.68735	84.95693	86.84066	88.04804	92.47415	89.03868	90.79981	96.13678	90.20923
CO eff. (%)		99.53022	99.35157	99.19775	99.67625	99.64156	99.55003	99.74427	99.77584	99.73112	99.83098	99.47791	99.57204
efficiency (%)		66.0705	71.15914	74.16383	75.32864	78.59822	80.48195	83.23642	87.66253	84.22706	86.06782	91.40479	85.47724
fluidising velocity(m		0.558969	0.674452	0.750035	0.83234	0.9999	1.034793	0.851485	1.01043	1.194144	0.81397	0.978215	1.093537
fludising number		2.070256	2.49797	2.777907	3.082741	3.703333	3.832567	3.153649	3.742332	4.422756	3.014704	3.623019	4.050137

D-3 Co-combustion of coal with palm kernel shell

Substance	coal(30%)	pks(70%)	mixture	O2 require kg/kg fuel	(A/F)s kg/kg fuel	coal(50%)	pks(50%)	mixture	kg/kg fuel	coal(70%)	pks(30%)	mixture	kg/kg fuel
C	22.62%	31.93%	54.55%	1.45		37.70%	22.81%	60.51%	1.61	52.78%	13.68%	66.46%	1.77
H	2%	4.36%	5.86%	0.47		3%	3.12%	5.62%	0.45	4%	1.87%	5.37%	0.43
O	2.79%	26.26%	29.05%	-0.29		4.65%	18.73%	23.38%	-0.23	6.51%	11.24%	17.75%	-0.18
N	0.27%	1.21%	1.48%	0.02		0.45%	0.87%	1.32%	0.02	0.63%	0.52%	1.15%	0.01
S	0.21%	0%	0.21%	0.00		0.35%	0%	0.35%	0.00	0.49%	0%	0.49%	0.00
Ash	0.84%	0.71%	1.55%			1.40%	0.51%	1.91%		1.96%	0.30%	2.26%	
Moisture	1.77%	6%	7.34%			2.95%	4%	6.93%		4.13%	2%	6.41%	
				1.65					1.85				2.04
air needed				7.863627					8.793601				9.72191
volatile matter													
CV(MJ/kg)	31.1	18	21.93					24.55				27.17	

Coal (%)		0	0	0	30	30	30	50	50	50
Feedrate (kg/hr)		2	2	2	1.74	1.74	1.74	1.59	1.59	1.59
Main air (l/min)		175	205	245	210	250	295	189	229	265
Feeder air (l/min)		65	65	65	65	65	65	65	65	65
avg (l/min)		240	270	310	275	315	360	254	294	330
avg (kg/hr)		17.424	19.602	22.506	19.965	22.869	26.136	18.4404	21.3444	23.958
xcess air (%)		34.65224	51.48377	73.92581	30.48281	49.46213	70.81386	31.88835	52.65817	71.35101
Results										
CO2 (%)		12	11.5	9.5	12	11.5	9.5	13	12	10
CO(ppm)		495.6	570.8	678.7	430.9	479.2	542.9	516.1	608.4	868.1
O2 (%)		10.5	9.4	10.3	6.2	7.9	9	5.9	6.4	7.2
To	195	390.4	393.2	394.1	427.8	428.2	430.9	411.5	413.2	418.5
T1	155	380.4	385.8	388.7	432.7	435.1	435.6	420.5	422	427.5
T2	115	640.4	653.4	656.8	714.5	710.5	688.8	674	670.7	671.8
T3	75	686.2	704.5	701.7	761.6	763.9	741.1	717.6	720.9	741
T4	40	791.1	782.2	777.3	832.2	829.5	825.6	811.4	803.9	744.3
T5	30	795.2	777.5	773.2	833.9	832.1	827.3	812.8	807.7	737.6
T6	20	800.3	774.1	760.1	830.6	826.9	822.7	817.1	801.5	734
T7	10	803.1	775.1	760.8	827.9	824.1	829.7	816.5	800.3	733.6
Ash (kg)			27.96			30.42			31.27	
Unburnt C (wt%)			6.7			11.66			14.9	
Y		20.98279	21.78751	26.06989	20.87504	21.76149	26.06159	20.85199	21.69393	24.69231
B		0.368879	0.401817	0.385382	0.442544	0.488437	0.465011	0.504737	0.563745	0.55493
carbon eff.(%)		80.87675	88.09837	84.4951	81.13073	89.54417	85.24955	83.42071	93.17337	91.71639
CO eff. (%)		99.5887	99.5061	99.29065	99.6422	99.58503	99.43177	99.57176	99.47374	99.13937
efficiency (%)		80.66826	87.88988	84.28661	80.73423	89.14767	84.85305	83.06316	92.81583	91.35884
fluidising velocity(m		0.591554	0.681481	0.811119	0.735583	0.87427	1.027157	0.649405	0.783149	0.847479
fludising number		2.190941	2.524003	3.004144	2.72438	3.238035	3.804286	2.405203	2.900552	3.138811

D-4 Co-combustion of coal with refuse derived fuel

Substance	coal(30%)	RDF(70%)	mixture	O2 required kg/kg fuel	(A/F)s kg/kg fuel	coal(50%)	RDF(50%)	mixture	kg/kg fuel	coal(70%)	rdf(30%)	mixture	kg/kg fuel
C	22.62%	27.79%	50.41%	1.34		37.70%	19.85%	57.55%	1.53	52.78%	11.91%	64.69%	1.73
H	2%	4.05%	5.55%	0.12		3%	2.89%	5.39%	0.20	4%	1.73%	5.23%	0.28
O	2.79%	19.07%	21.86%	-0.03		4.65%	13.62%	18.27%	-0.05	6.51%	8.17%	14.68%	-0.07
N	0.27%	0.56%	0.83%	0.00		0.45%	0.40%	0.85%	0.01	0.63%	0.24%	0.87%	0.01
S	0.21%	0%	0.46%	0.00		0.35%	0%	0.53%	0.00	0.49%	0%	0.60%	0.00
Ash	0.84%	13.24%	14.08%			1.40%	9.46%	10.86%		1.96%	5.68%	7.64%	
Moisture	1.77%	2%	4.06%			2.95%	2%	4.59%		4.13%	1%	5.11%	
				1.44	6.86				1.70				1.95
air needed				6.861789					8.076813				9.291837
volatile matter													
CV(MJ/kg)	31.1	18	21.93					24.55				27.17	

Coal (%)		0	0	0	30	30	30	50	50	50	70	70	70
Feedrate (kg/hr)		2.74	2.74	2.74	2.34	2.34	2.34	2.1	2.1	2.1	1.69	1.69	1.69
Main air (l/min)		335	395	455	275	325	385	240	290	335	220	260	305
Feeder air (l/min)		65	65	65	65	65	65	65	65	65	65	65	65
avg (l/min)		400	460	520	340	390	450	305	355	400	285	325	370
avg (kg/hr)		29.04	33.396	37.752	24.684	28.314	32.67	22.143	25.773	29.04	20.691	23.595	26.862
xcess air (%)		31.2218	50.90507	70.58834	30.60495	49.81156	72.85949	30.55007	51.95172	71.21321	31.76291	50.25595	71.06062
Results													
CO2 (%)		10	9.5	9	12	11	9	12	10	9.5	12.5	11.5	9.5
CO(ppm)		720	496	535	997.1	1105.8	1762.5	716.1	1346.2	1577.6	1319.6	1559.8	2436.5
O2 (%)		5.8	6.1	6.8	6.8	7.1	8.3	7.3	9.2	11.1	8.9	10.6	11
To	195	474.7	474.7	474.7	474.7	487.1	490.3	453.1	502.1	499.2	463	469.8	481.4
T1	155	465.4	465.4	465.4	465.4	479.8	485.6	472.3	518.8	501.2	476.3	471.5	481.3
T2	115	659.5	659.5	659.5	659.5	682	666.6	764.9	732	725.8	809.2	789.1	815.4
T3	75	720.2	720.2	720.2	720.2	735.3	700.5	799.9	763.9	759.2	825.6	810.7	831.8
T4	40	797.8	797.8	797.8	797.8	789.5	770.6	817.5	801.7	800.6	845.6	847.6	857.4
T5	30	845.4	845.4	845.4	845.4	815.8	795.8	844.3	845.4	819.4	858.6	865.1	870.4
T6	20	836.6	836.6	836.6	836.6	807.3	787.4	838.2	838.7	811.1	845.6	851.6	865.2
T7	10	830.1	830.1	830.1	830.1	806.3	782.1	837.6	836.8	807.6	842.5	850.9	863.5
Ash (kg)			54			300			228.6			129.6	
Unburnt C (wt%)			11.35			14.845			17.175			19.505	
Y		24.68229	25.97316	27.34854	20.79389	22.53408	27.03719	20.8561	24.64161	25.85486	20.02592	21.63696	25.62353
B		0.35711	0.392036	0.422171	0.425152	0.451207	0.433127	0.486156	0.478143	0.514584	0.576786	0.609139	0.583479
carbon eff.(%)		70.84114	77.76956	83.74748	84.33876	89.50739	85.92094	84.4754	83.08312	89.41508	89.16147	94.16281	90.19611
CO eff. (%)		99.28515	99.48061	99.40907	99.17593	99.00473	98.07928	99.40679	98.67168	98.36649	98.95535	98.6618	97.4994
efficiency (%)		70.3974	77.32583	83.30375	80.56331	85.73194	82.14549	81.22671	79.83443	86.16639	86.84926	91.8506	87.8839
fluidising velocity(m		1.185621	1.397971	1.610321	0.973271	1.119787	1.30215	0.848564	1.026358	1.158058	0.787806	0.936392	1.103575
fludising number		4.391187	5.177669	5.96415	3.604706	4.147358	4.822777	3.142831	3.801326	4.289103	2.917801	3.468117	4.087314

D-5 Co-combustion of coal with palm fibre

Substance	coal(90%)	PF(10%)	mixture	O2 required (A/F)s kg/kg fuel	kg/kg fuel	coal(80%)	PF(20%)	mixture	kg/kg fuel	coal(70%)	PF(30%)	mixture	kg/kg fuel
C	67.86%	4.72%	72.58%	1.94		60.32%	9.44%	69.76%	1.86	52.78%	14.16%	66.94%	1.79
H	5%	0.60%	5.10%	0.36		4%	1.20%	5.20%	0.32	4%	1.80%	5.30%	0.28
O	8.37%	3.55%	11.92%	-0.08		7.44%	7.10%	14.54%	-0.07	6.51%	10.65%	17.16%	-0.07
N	0.81%	0.14%	0.95%	0.01		0.72%	12.28%	13.00%	0.01	0.63%	0.42%	1.05%	0.01
S	0.63%	0%	0.66%	0.01		0.56%	0%	0.62%	0.01	0.49%	0%	0.58%	0.00
Ash	2.52%	0.84%	3.36%			2.24%	1.68%	3.92%		1.96%	2.52%	4.48%	
Moisture	5.31%	0%	5.43%			4.72%	0%	4.96%		4.13%	0%	4.49%	
				2.23	10.60				2.12				2.01
air needed				10.60206					10.08975				9.577437
volatile matter													
CV(MJ/kg)	31.1	14.25	29.415					27.73				26.045	

Coal(%)		10	10	10	20	20	20	30	30	30
Feedrate (kg/hr)		1.44	1.44	1.44	1.36	1.36	1.36	1.29	1.29	1.29
Main air (l/min)		210	250	295	183	220	255	160	190	225
Feeder air (l/min)		65	65	65	65	65	65	65	65	65
avg (l/min)		275	315	360	248	285	320	225	255	290
avg (kg/hr)		19.965	22.869	26.136	18.0048	20.691	23.232	16.335	18.513	21.054
xcess air (%)		30.77253	49.79398	71.19312	31.21063	50.78641	69.30404	32.21481	49.84345	70.4102
Results										
CO2 (%)		12.5	12	10	11	10.5	9	10	9	8.5
CO(ppm)		961.2	1102	1223.8	639.2	650.9	742.8	1128	1299.6	1257.1
O2 (%)		6.6	7.6	8.4	6.1	6.5	7	6.4	6.6	6.9
To	195	366.5	370	370.5	372.1	380.1	381.6	433.9	442.7	442.1
T1	155	369.5	372.6	374.7	376.2	382.3	385.4	441.7	442.4	442.8
T2	115	627.5	620.7	620.3	673.4	686.4	699.8	689.6	692.1	704
T3	75	699.7	722.7	725.4	743.9	769.5	789.8	710.7	721.2	738.2
T4	40	806.1	832.7	811.3	790.8	784.5	773.6	715.5	721.6	722.5
T5	30	835.9	836.9	821	799.4	792.3	779.9	714.1	702.8	696.8
T6	20	831.2	830.7	813.7	795.5	786.2	772.5	708.4	698.3	684.3
T7	10	830.3	839.5	812.7	796	785.3	770.5	708.9	697.6	681
Ash (kg)			48.12			54.12			57.7	
Unburnt C (wt%)			21.9			25			27	
Y		20.02204	20.79789	24.64506	22.59898	23.61551	27.29326	24.60248	27.1122	28.63146
B		0.584724	0.646522	0.621126	0.51675	0.569842	0.552233	0.476636	0.490351	0.529018
carbon eff.(%)		80.56265	89.07717	85.5781	74.07534	81.68614	79.16179	71.20353	73.25228	79.02862
CO eff. (%)		99.23691	99.09002	98.791	99.42227	99.38391	99.18142	98.88458	98.57655	98.54261
efficiency (%)		79.55434	88.06887	84.5698	72.95546	80.56626	78.04192	69.7348	71.78355	77.55989
fluidising velocity(m		0.736912	0.878067	1.021276	0.621029	0.741649	0.849632	0.499787	0.586703	0.690508
fludising number		2.729303	3.2521	3.782504	2.300106	2.746848	3.146787	1.851063	2.172973	2.557436

D-6 Co-combustion of Coal with wood pellets

Substance	coal(30%)	wood(70%)	mixture	kg/kg fuel	kg/kg fuel	coal(50%)	wood(50%)	mixture	kg/kg fuel	coal(70%)	wood(30%)	mixture	kg/kg fuel
C	22.62%	31.93%	54.55%	1.45		37.70%	22.81%	60.51%	1.61	52.78%	13.68%	66.46%	1.77
H	2%	4.36%	5.86%	0.47		3%	3.12%	5.62%	0.45	4%	1.87%	5.37%	0.43
O	2.79%	26.26%	29.05%	-0.29		4.65%	0.00%	4.65%	-0.05	6.51%	11.25%	17.76%	-0.18
N	0.27%	1.21%	1.48%	0.02		0.45%	0.87%	1.32%	0.02	0.63%	0.52%	1.15%	0.01
S	0.21%	0%	0.21%	0.00		0.35%	0%	0.35%	0.00	0.49%	0%	0.49%	0.00
Ash	0.84%	0.71%	1.55%			1.40%	0.51%	1.91%		1.96%	0.30%	2.26%	
Moisture	1.77%	5.57%	7.34%			2.95%	3.98%	6.93%		4.13%	2.39%	6.52%	
				1.65					2.03				2.04
air needed				7.863627					9.685149				9.721196
volatile matter													
CV(MJ/kg)	31.1	17.2	21.37					24.15				26.93	

Date :
Fuel : Coal/wood waste
Particle Size :

Coal (%)		0	0	0	30	30	30	50	50	50	70	70	70
Feedrate (kg/hr)		1.91	1.91	1.91	1.68	1.68	1.68	1.55	1.55	1.55	1.33	1.33	1.33
Main air (l/min)		160	190	225	175	210	245	180	215	255	170	205	240
Feeder air (l/min)		65	65	65	65	65	65	65	65	65	65	65	65
avg (l/min)		225	255	290	240	275	310	245	280	320	235	270	305
avg (kg/hr)		16.335	18.513	21.054	17.424	19.965	22.506	17.787	20.328	23.232	17.061	19.602	22.143
xcess air (%)		32.17561	49.79903	70.35968	31.89116	51.12529	70.35942	30.51578	49.16089	70.46958	31.95721	51.61042	71.26362
Results													
CO2 (%)		12.5	11	10	11	10	9	12.5	11.5	10	11.5	11	10
CO(ppm)		287	256	221	189.1	188.1	180.8	183	183.7	178.2	196	193.8	192.4
O2 (%)		5	7.6	8.2	6.2	6.8	7.2	5.8	6.2	7	10.2	10.1	11.1
NOx (ppm)													
To	195	459.4	471.6	445	506.9	514.6	519.6	437.3	437.8	446.3	450.4	454.1	459.1
T1	155	455.7	473.7	455.3	510.2	518.6	521.9	439.7	441.8	448.9	462.9	466.7	471.1
T2	115	820.2	772.6	720.3	793.3	797.2	797.7	775.4	759.2	766.7	764.4	763.7	762.9
T3	75	868.4	804.8	745.8	824.4	840.1	842.8	823.5	818.1	830.3	817.9	816.1	822.9
T4	40	835.7	816.3	773.3	851.7	859.4	856.9	851.5	853.1	853.3	874.8	878.7	874.5
T5	30	820	818.6	785.9	867.1	865.6	862.9	861.2	861.3	857.3	897.4	897.1	892.7
T6	20	814.4	814.2	779.9	863.9	861.4	860.6	859.7	857.8	853.9	895.4	892.4	887.7
T7	10	812.2	809.1	777.7	863.6	859.6	857.7	858.2	855.5	849.1	893.6	890.2	881.8
Ash (kg)			17.96			20.42			29.5275			30.02	
Unburnt C (wt%)			3			6			10			11.66	
deposit (g)													
Y		20.08721	22.72288	24.885	22.69432	24.8466	27.47074	20.1252	21.76813	24.85571	21.88155	22.81133	24.98859
B		0.37862	0.379992	0.395793	0.510734	0.535042	0.545427	0.573064	0.606096	0.605619	0.533872	0.590059	0.608283
carbon eff.(%)		83.0125	83.31333	86.77777	84.41183	88.42944	90.14577	94.71351	100.1728	100.0941	80.32623	88.78	91.52199
CO eff. (%)		99.77093	99.76781	99.77949	99.82839	99.81225	99.79951	99.85381	99.84052	99.82212	99.82986	99.82413	99.80797
fluidising velocity(m/s)		0.553406	0.656328	0.753948	0.631371	0.756649	0.880663	0.64605	0.771739	0.91209	0.629632	0.759068	0.885323
fludising number		2.049652	2.430844	2.792399	2.338412	2.802402	3.261716	2.392777	2.858291	3.378111	2.331972	2.811363	3.278975

D-7 Co-combustion of Coal with Wood powder

Substance	coal(30%)	wood(70%)	mixture	kg/kg fuel	kg/kg fuel	coal(50%)	wood(50%)	mixture	kg/kg fuel	coal(70%)	wood(30%)	mixture	kg/kg fuel
C	22.62%	31.93%	54.55%	1.45		37.70%	22.81%	60.51%	1.61	52.78%	13.68%	66.46%	1.77
H	2%	4.36%	5.86%	0.47		3%	3.12%	5.62%	0.45	4%	1.87%	5.37%	0.43
O	2.79%	26.26%	29.05%	-0.29		4.65%	0.00%	4.65%	-0.05	6.51%	11.25%	17.76%	-0.18
N	0.27%	1.21%	1.48%	0.02		0.45%	0.87%	1.32%	0.02	0.63%	0.52%	1.15%	0.01
S	0.21%	0%	0.21%	0.00		0.35%	0%	0.35%	0.00	0.49%	0%	0.49%	0.00
Ash	0.84%	0.71%	1.55%			1.40%	0.51%	1.91%		1.96%	0.30%	2.26%	
Moisture	1.77%	5.57%	7.34%			2.95%	3.98%	6.93%		4.13%	2.39%	6.52%	
				1.65					2.03				2.04
air needed				7.863627					9.685149				9.721196

Coal (%)		0	0	0	50	50	50
Feedrate (kg/hr)		2.91	2.91	2.91	2.51	2.51	2.51
Main air (l/min)		275	325	375	375	440	510
Feeder air (l/min)		65	65	65	65	65	65
avg (l/min)		340	390	440	440	505	575
avg (kg/hr)		24.684	28.314	31.944	31.944	36.663	41.745
xcess air (%)		31.0956	50.37436	69.65313	30.91695	50.25695	71.08465
Results							
CO2 (%)		12	11.5	9.5	11	10.5	9
CO(ppm)		513.2	310.5	340.3	211.4	221.4	230.9
O2 (%)		9.2	9.4	11.5	6	8.4	9.4
NOx (ppm)							
To	195	471.3	473.7	476.7	506.8	508.8	512.9
T1	155	477.1	480.3	487.1	511.4	508.7	521.6
T2	115	780.6	761.6	762.1	806.2	776.1	840.1
T3	75	804.6	773.9	784.4	849.2	819.4	871.7
T4	40	813.9	807.8	793.1	845.9	847.7	850.6
T5	30	811.1	807.3	790.7	854.8	852.9	862.3
T6	20	807.3	803.4	787.1	851.3	848.3	859.8
T7	10	805.4	801.7	785.6	850.1	844.7	857.1
Ash (kg)			27.96			40.51	
Unburnt C (wt%)			3			15.4	
deposit (g)							
Y		20.94376	21.83669	26.20438	22.68368	23.7721	27.53676
B		0.359201	0.397763	0.37344	0.507063	0.55696	0.546456
carbon eff.(%)		78.75487	87.20967	81.87679	76.29248	83.79998	82.21951
CO eff. (%)		99.57415	99.73073	99.64307	99.99972	99.99962	99.99959
fluidising velocity(m/s)		0.943422	1.111045	1.262276	1.338342	1.567676	1.832249
fludising number		3.494154	4.11498	4.675095	4.956823	5.806207	6.786109

PLATES

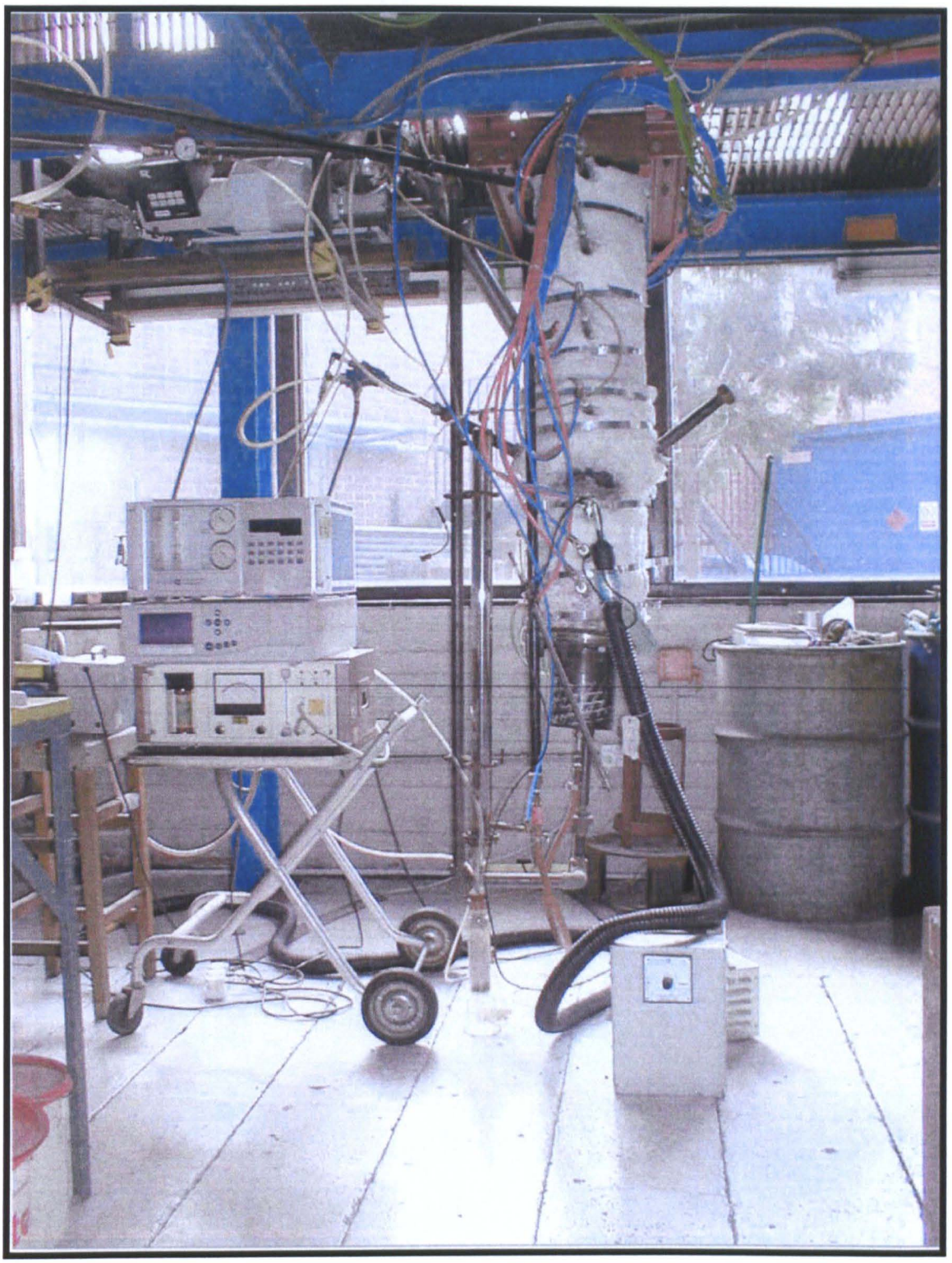

Plate 1 Rig of Fluidised bed combustor

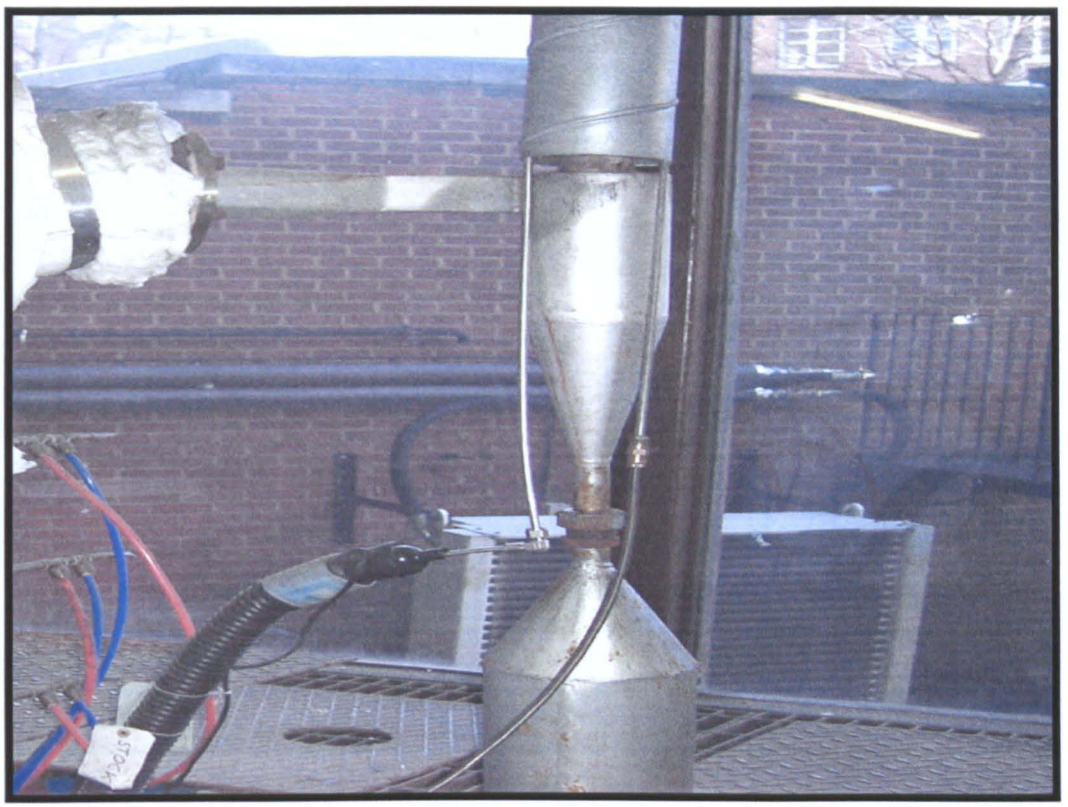

Plate 2 Cyclone and catch-pot

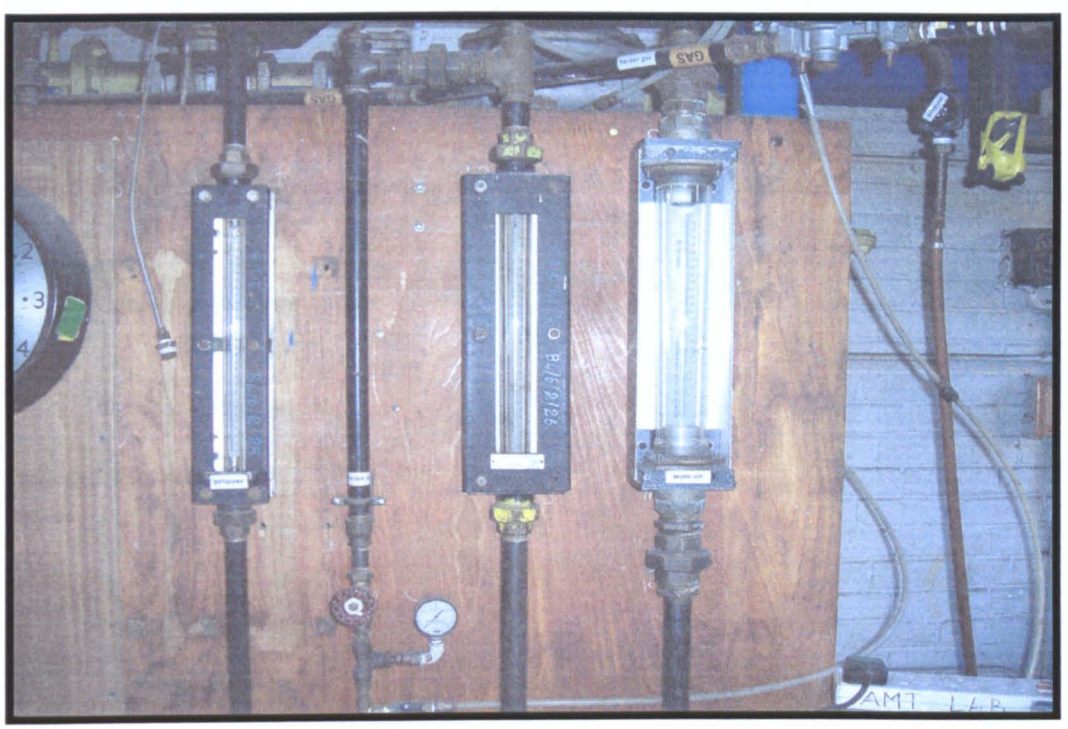

Plate 3 Gas and Air controller

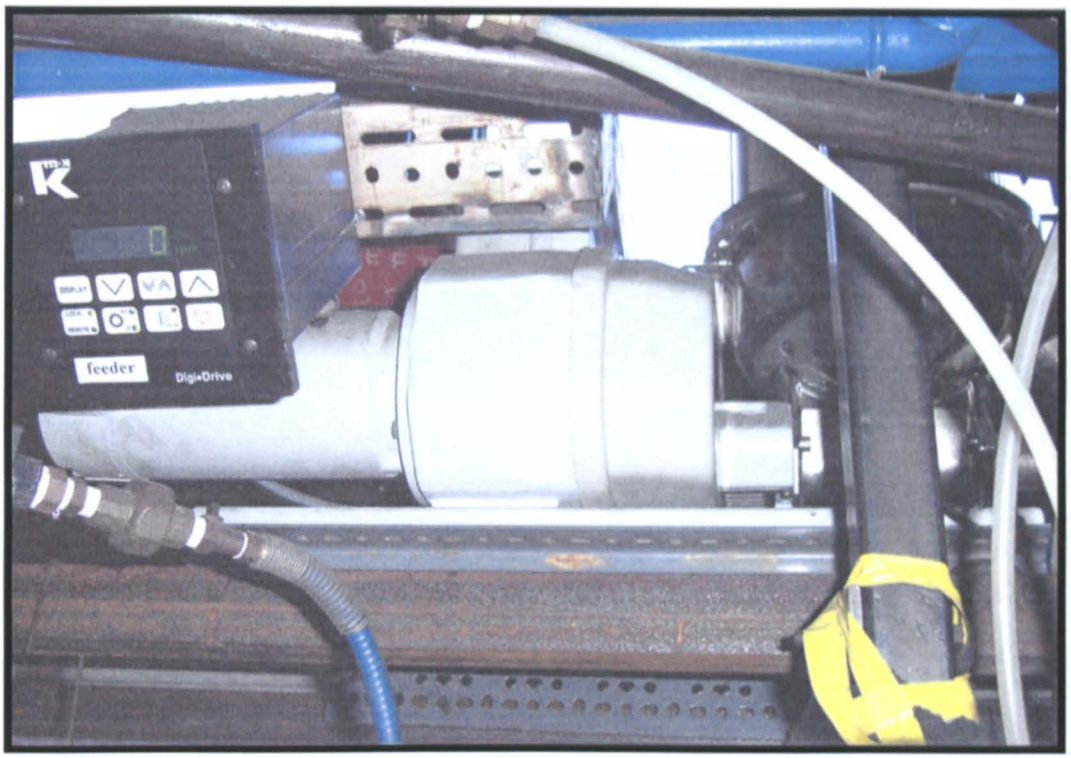

Plate 4 Feeder

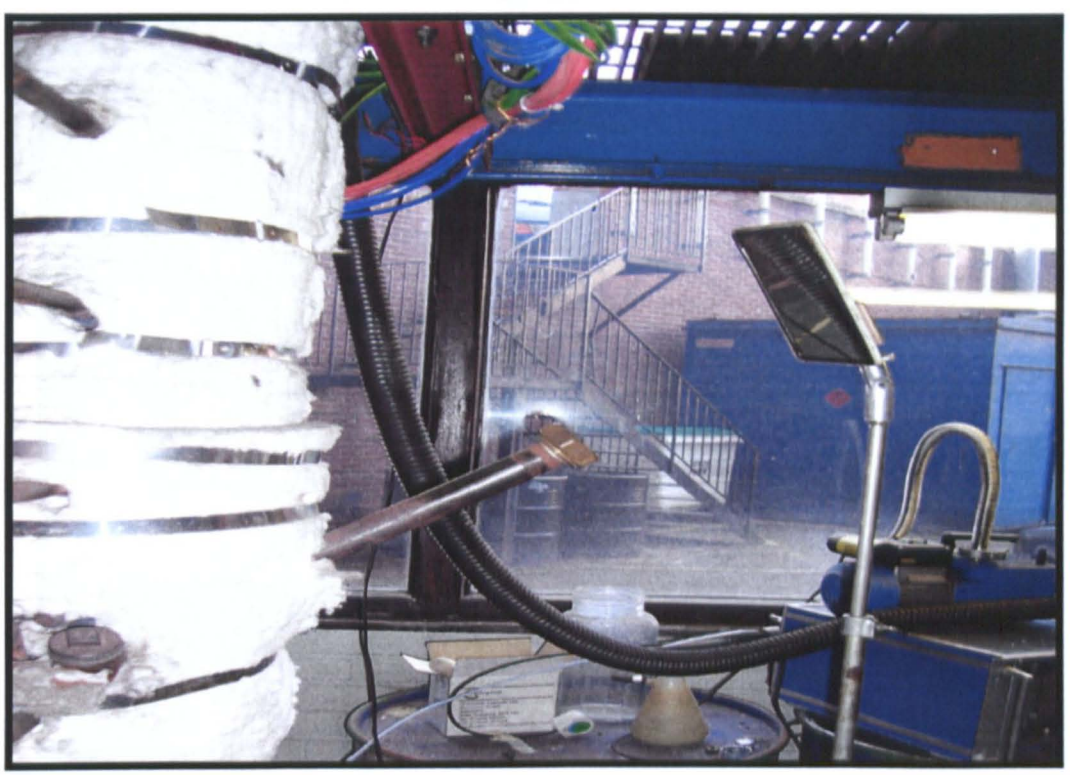

Plate 5 View – point window

Plate 6 Chicken manure pellets

Plate 7 Rice husk

Plate 8 Palm Kernel Shell

Plate 9 Palm Oil Fibre

Plate 10 Wood pellets

Plate 11 Wood Powder

Plate 12 Refuse Derived Fuel

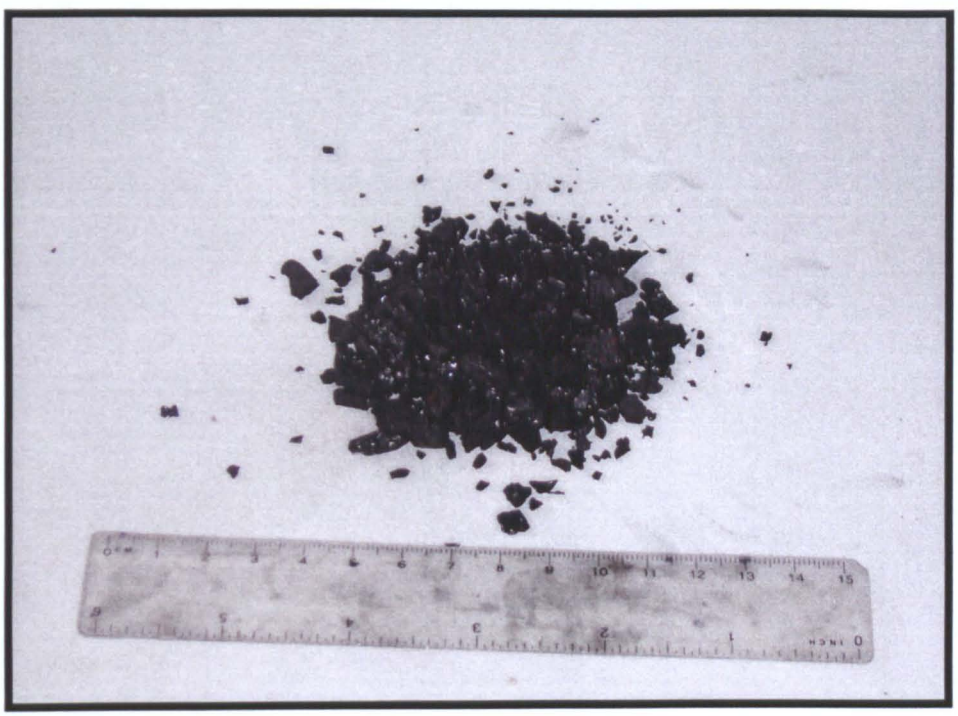

Plate 13 Bituminous Coal